Effect of oocyte glycoproteins on ovarian follicle development and function

Panayiota Ploutarchou
St. Catherine's College
University of Oxford

A thesis submitted for the degree of
Doctor of Philosophy
Extended Trinity Term
2015

Dedicated to the loving memory of
my Grandmother (2012) and Grandfather (2014).
Your memory will be forever in my heart.

~

Σα βγεις στον πηγαιμό για την Ιθάκη,
να εύχεσαι νά'ναι μακρύς ο δρόμος,
γεμάτος περιπέτειες, γεμάτος γνώσεις[..]

As you set out for Ithaka,
hope the voyage is a long one,
full of adventure, full of knowledge[…]

C.P.Cavafy

Acknowledgements

Firstly, I would like to express my sincere gratitude to my supervisor, Dr Suzannah Williams, for trusting me and offering me the opportunity to undertake this DPhil. I will be forever thankful for Dr Williams' never-ending guidance, understanding and support during my time in the group. I could not have wished for a better supervisor.

I would also like to thank my co-supervisor, Dr Christian Becker, for his advice and mentoring during my research.

My experience as a DPhil student would certainly not have been the same without the friendliest and most fun group of fellow students I could ever wish for. Patricia Grasa, Heidy Kaune and Sairah Sheikh – your constant support, advice and simply your presence have made my DPhil an enjoyable and an unforgettable experience.

I would also like to thank my partner, Stelios, for his patience and endless support, especially during the last months of my DPhil.

Last, and certainly not least, I would like to thank my parents and brother for their eternal love and support. Mum and dad – I would not have gotten to this stage without your encouragement, understanding and most of all love. You have always been a constant source of inspiration for me, supporting my every decision in life and always making me believe that I can achieve my dreams - for that, I will be forever thankful.

Abstract

The precise mechanisms that regulate the ovulation rate of species are not entirely understood. The *C1galt1* Mutant mouse, in which oocytes lack core 1-derived *O*-glycans, is characterised by (i) increased fertility, evident from ~40-50% larger litters as a result of increased number of growing follicles and (ii) modified cumulus expansion. Work carried out in this thesis investigated both of these phenotypes and led to the understanding of possible mechanisms involved in increased fertility.

Through detailed analysis of the cumulus complex both prior- and post-ovulation in Control mice, novel characteristics regarding the physiology of cumulus expansion have been found. In addition, the analysis of *C1galt1* Mutants has revealed that a functional cumulus-oocyte-complex requires the essential components to be present above a minimum threshold level, and thus some variation in ECM composition does not adversely affect oocyte development, ovulation or fertilisation. These data have important implications for IVF and the use of cumulus expansion as a criterion for oocyte assessment.

C1galt1 Mutants have (i) altered follicle growth characteristics, (ii) reduction in apoptosis levels and (iii) reduction in AMH levels, all of which could be directly or indirectly contributing to the increased fertility phenotype. These data reveal new and important roles for the oocyte in follicle development and female fertility, providing perspectives for future work in female reproduction.

Abbreviations

C1galt1	Core 1 β1,3-galactosyltransferase
CC	Cumulus cell
CEC	Cumulus-egg complex
COC	Cumulus-oocyte complex
ECM	Extracellular matrix
FSH	Follicle stimulating hormone
GC	Granulosa cell
HA	Hyaluronic acid
HC	Heavy chain
LH	Luteinizing hormone
OSF	Oocyte secreted factor
TGF-β	Transforming growth factor – β

TABLE OF CONTENTS

CHAPTER 1: Introduction

1.1 Follicle development

1.1.1 Basics of follicle development

Follicle development is the progression of a follicle, from primordial to an ovulatory, whereby a mature egg is ovulated. Moreover, many follicles do not complete development and therefore the regulation of follicle development to result in the ovulation of a defined number of eggs is a complex process that we are only beginning to understand.

The pool of primordial follicles in female ovaries forms *in utero* in certain species, for example primates and ruminants (Rabinovici & Jaffe 1990), and in other species, for example rodents and rabbits, formation is not completed until early postnatal life (Borum 1961, Peters 1969). Each primordial follicle consists of a meiotically quiescent oocyte surrounded by a single layer of somatic cells known as the pre-granulosa cells (Pepling & Spradling 2001). Throughout reproductive life primordial follicles leave the dormant pool and begin to grow, progressing through the different stages of development (Peters 1969) (Fig. 1.1). Follicle development culminates in the generation of one or more developmentally competent oocytes depending on whether the mammal is mono- or poly-ovulatory. Oocytes have crucial roles in female fertility and therefore successful oocyte maturation and development is critical to female fertility.

Once the primordial follicle population is established, activation of primordial follicles occurs continuously until the pool is exhausted, otherwise known as menopause in humans (Richardson *et al.* 1987). Initial growth of

primordial follicles involves (i) the growth of the oocyte (Peters 1969, Qvist *et al.* 1990), (ii) the differentiation of the flattened pre-granulosa cells into cuboidal granulosa cells (GCs) (Lintern-Moore & Moore 1979) and (iii) the proliferation of GCs (Lintern-Moore & Moore 1979, Picton 2001). Once GCs have proliferated into a single layer of cells, the follicle is referred to as primary. At the primary follicle stage, the oocyte produces and secretes glycoproteins known as zona pellucida (ZP) proteins (Philpott *et al.* 1987) which form the oocyte's extracellular matrix; the ZP has functions in fertilisation and early embryo development (Shur & Hall 1982). The

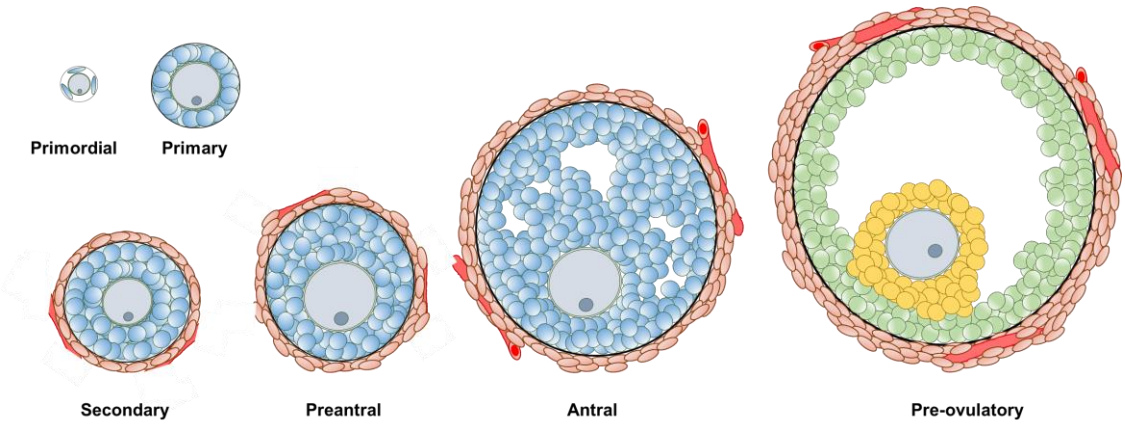

Figure 1.1. Schematic representation of the different stages of follicle development. Primordial follicles consist of an oocyte surrounded by pre-granulosa cells, which are flattened somatic cells. Activation of the primordial follicle results in oocyte growth and granulosa cell (GC) cuboidalisation and proliferation. Primary follicles consist of an oocyte and a complete, cuboidal GC layer (blue). Secondary follicles have two full layers of GCs, and have formed a theca layer (red). Preantral follicles have multiple GC layers and theca. Antral follicles have follicular fluid (antrum) deposited between GCs. In preovulatory follicles, the GC population has differentiated into 2 structurally and functionally distinct types of cells: cumulus cells which immediately surround the oocyte (yellow), and mural GCs (green) which line the follicular basal lamina.

composition of the ZP varies between species; mouse ZP is made up of ZP1, ZP2 and ZP3 (Bleil & Wassarman 1980) while human, rat and hamster ZP is made up of ZP1, ZP2, ZP3 and ZP4 (Lefievre *et al.* 2004, Hoodbhoy *et al.* 2005, Izquierdo-Rico *et al.* 2009).

By the secondary follicle stage an additional GC layer has formed around the oocyte and also a layer of vascularised theca cells is deposited externally to the follicle basal lamina (Peters 1969). As the follicle continues to develop, proliferation of GCs continues creating more cell layers around the oocyte and the follicles are now referred to as preantral. Development of follicles up to the preantral stage is gonadotrophin independent (Kumar *et al.* 1997, Dierich *et al.* 1998, Abel *et al.* 2000). A more detailed description of gonadotrophin action is provided in Section 1.1.2.

Progression of follicles beyond the preantral stage is dependent on gonadotrophin action on the follicle (Kumar *et al.* 1997). Under the influence of follicle stimulating hormone (FSH), preantral follicles form a fluid-filled cavity called the antrum and progress to the antral phase of follicle development. The origins and accumulation of the antrum are not clearly understood, but it is believed that it forms through diffusion of serum components from the vascularized theca via the GCs (Shalgi *et al.* 1972, Gosden *et al.* 1988). During the process of antral follicle development, the antrum is progressively modified by secretions from cells within the follicle (Gosden *et al.* 1988, Rodgers & Irving-Rodgers 2010). Antrum formation facilitates the physical separation and differentiation of GCs into two distinct sub-lineages: the mural GCs, which line the follicle wall, and the cumulus

cells (CCs), which envelope the maturing oocyte. Together, the oocyte and its surrounding CCs are called the cumulus-oocyte complex (COC) and the follicle is known as pre-ovulatory.

Even though the process of follicle development is highly sophisticated and carefully regulated, the vast majority of follicles (and, hence, oocytes) will undergo atresia at various stages of development (Baker 1963, Peters 1969). Follicle atresia occurs via programmed death of follicular cells, a process known as apoptosis. Apoptosis in follicles is thought to result from one or more of the following biological activities: (i) depletion of cell survival factors, including estradiol, FSH and insulin-like growth factor (IGF), (ii) activation of death ligand-receptor systems, for example the FAS ligand and FAS system and (iii) action of members of the B-cell lymphoma 2 (Bcl2) family of proteins (Tsujimoto *et al.* 2001b, van Delft & Huang 2006, Taylor *et al.* 2008). The process and regulation of follicular atresia is revisited in Chapter 6.

1.1.2 Role of pituitary gonadotrophins in follicle development

The hypothalamic-pituitary-gonadal (HPG) axis in females is the reproductive axis that regulates fertility, i.e. differentiation and maturation of the ovary, sex hormone secretion and follicle development. The focus of the discussion here will be on the role of the HPG axis in follicle development.

A vital regulator of the HPG axis is gonadotrophin-releasing hormone (GnRH) which is secreted by the hypothalamus in a pulsatile manner (Antunes *et al.* 1978, Levine & Ramirez 1982). GnRH binds to cognate receptors on the anterior pituitary, stimulating the synthesis and release of gonadotrophins FSH and luteinizing hormone (LH) (Belchetz *et al.* 1978, Collins *et al.* 1981, Clarke *et al.* 1984). FSH and LH are glycoproteins that share a common α-subunit and each have a unique β-subunit (Baenziger & Green 1988). The secretion pattern during the estrous cycle and site of action of FSH and LH are distinct for each gonadotrophin, due to the different roles of each hormone in follicle development.

The estrous cycle refers to the reproductive cycle and in rodents is analogous to the menstrual cycle in women. The duration of the estrous cycle in rodents is 4-5 days (Murr *et al.* 1973) and pituitary gonadotrophin and ovarian steroid secretion follow a distinct pattern through the cycle. The proestrus stage represents the day prior to ovulation and ovulation takes place during estrus. The metestrus stage represents the formation of corpus lutea, while diestrus is characterized by corpus luteum progesterone production (Allen 1935).

1.1.2.1 Follicle stimulating hormone

FSH is constitutively secreted throughout the estrous cycle, with a distinct rise in FSH levels during the proestrus stage (Haisenleder *et al.* 1990) which enables a subpopulation of preantral follicles to continue development. Female mice lacking either FSHβ (Kumar *et al.* 1997) or FSHR (Dierich *et al.* 1998) exhibit arrested follicle development at the preantral stage, highlighting the vital role of FSH in the preantral to antral transition. FSH action on the GCs of late antral follicles induces steroidogenesis by augmenting the activity of the aromatase enzyme (Moon *et al.* 1975, Armstrong & Papkoff 1976) which aromatises androgens produced in theca cells into estrogens.

1.1.2.2 Luteinizing hormone

LH is secreted in a pulsatile manner in response to the pulsatile action of GnRH (Antunes *et al.* 1978) and binds to the cognate LH receptor (LHR) in the ovary. Specifically, LHR is found on (i) theca cells (Camp *et al.* 1991) where LH binding induces androgen production (Fortune & Armstrong 1977), (ii) GCs of pre-ovulatory follicles (Peng *et al.* 1991) where LH initiates ovulation at late proestrus and (iii) luteal cells (Camp *et al.* 1991) where LH regulates progesterone production (Natraj & Richards 1993).

1.1.3 Regulation of follicle development by follicular somatic cells

The process of ovarian follicle development is the result of a highly regulated balance between follicle survival and follicle atresia to ensure the correct number of eggs are ovulated. In particular, granulosa cells (GCs) have been demonstrated to secrete a wide array of proteins that act both on GCs themselves (autocrine) and on neighbouring follicular cells (paracrine) to determine the follicle's fate. Although a plethora of molecules are involved in follicle development (Fig. 1.2), a discussion of the most relevant factors to my thesis work is presented here.

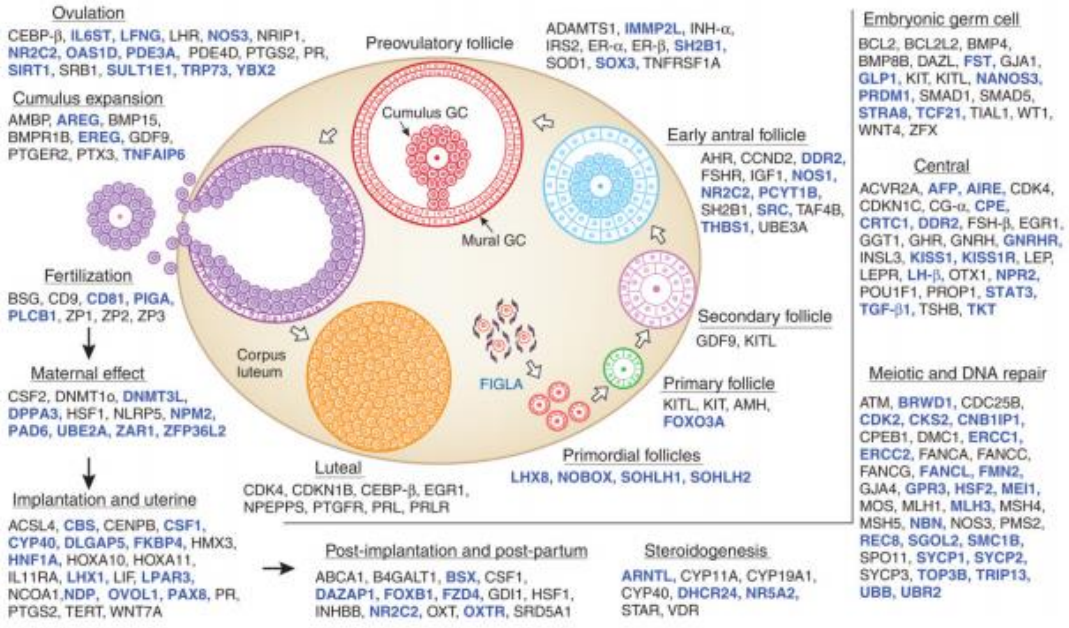

Figure 1.2. Pathways regulating female fertility in mice. Summary of the key regulatory molecules involved in follicle development and ovulation. Molecules in black represent factors identified by 2002, and molecules in blue are additional factors that were identified by 2008. *Adapted from (Matzuk & Lamb 2008).*

Estradiol

Estrogen has been studied extensively for its mitogenic effects on follicular cells. Estrogen increases GC proliferation both *in vivo* (Goldenberg *et al.* 1972) and *in vitro* (Goldenberg *et al.* 1972, Rao *et al.* 1978). In addition, estrogen suppresses follicular apoptosis *in vitro* (Lund *et al.* 1999) and *in vivo* (Billig *et al.* 1993).

GCs synthesise estrogen from thecal androgens, catalysed by the enzyme aromatase (also known as CYP19) (Dorrington *et al.* 1975, Fortune & Armstrong 1977, Hillier & De Zwart 1981). Secretion of estrogen is greatly stimulated by FSH *in vitro* (Dorrington *et al.* 1975, Daniel & Armstrong 1980) and *in vivo* (Erickson & Hsueh 1978). Collectively, research into GC estrogen biosynthesis led to the '2-cell 2-gonadotrophin' model, whereby theca cells produce androgens in response to LH (Fortune & Armstrong 1977) and the androgens then diffuse through the follicle basal lamina into GCs. FSH stimulates aromatase in GCs, and aromatase catalyses the conversion of androgens to estrogens (Dorrington *et al.* 1975).

Transforming growth factor-β family

The transforming growth factor-β (TGF-β) superfamily is a group of proteins with diverse functions throughout the body. The major families within the TGF-β superfamily are: bone morphogenetic proteins (BMPs), growth differentiation factor (GDF), TGF-β, activins and inhibins (Knight & Glister

2006). All TGF-β superfamily members are found in the form of secreted extracellular ligands and exert their actions through binding on serine/threonine kinase receptors (Wrana *et al.* 1994, Heldin *et al.* 1997). TGF-β receptors are subdivided into type-I and type-II receptors; to date, 5 type II receptors and 7 types I receptors have been identified. Each TGF-β acts through binding to a unique heterodimeric combination composed of one type I and one type II receptor (Ebner *et al.* 1993). Ligand binding to this heterodimeric receptor complex causes receptor phosphorylation and activation (Souchelnytskyi *et al.* 1996), recruitment of receptor SMADs (SMAD 1, 2, 3, 5, 8) (Heldin *et al.* 1997) and propagation of the TGF-β signal to the nucleus via other SMADs (SMAD regulation of TGF-β ligands is re-visited in Chapter 3.1).

Oocyte-produced growth differentiation factor 9 (GDF9) and bone morphogenetic protein 15 (BMP15) are glycoproteins with species-specific roles in follicle development and fertility and are discussed in Section 1.1.4.

The glycoprotein anti-mullerian hormone (AMH) is a member of the TGF-β superfamily. Despite its role in mammalian fetal development as an inhibitor of Mullerian duct development (Munsterberg & Lovell-Badge 1991), AMH has central roles in ovarian function and follicle development.

The role of AMH in the mammalian ovary became clear from studies of $AMH^{-/-}$ female mice and *in vitro* studies. AMH-deficient female mice have a severely depleted primordial follicle pool and more growing follicles at 4 months of age (Durlinger *et al.* 1999), indicating a role of AMH in inhibiting

primordial follicle activation. Also, *in vivo* and *in vitro* studies reveal that AMH causes inhibition of the FSH-stimulated growth of preantral follicles to antral follicles (di Clemente *et al.* 1994, Durlinger *et al.* 1999).

Epidermal growth factor-related proteins

Epidermal growth factor (EGF)-related proteins consist of 7 EGF-related ligands and 4 tyrosine kinase receptors; the action of each ligand is through a homo- or hetero-dimeric complex of receptors. EGF-related signalling was originally shown to have central roles in organogenesis and oncogenesis (Burden & Yarden 1997), while subsequently the requirement for EGF-related ligands during the LH-induced ovulation process was appreciated.

Induction of ovulation in mice showed the rapid expression of 3 EGF-related ligands in the ovary *in vivo*: amphiregulin (AR), β-cellulin (BTC) and epiregulin (EPI) (Park *et al.* 2004). The specific ovarian site of AR, BTC and EPI expression are the mural granulosa cells (GCs). *In vitro* treatment of follicles with AR, BTC and EPI mimics the effect of LH treatment, i.e. resumption of meiosis and cumulus expansion (Dekel & Sherizly 1985), but in a shorter period of time (Park *et al.* 2004). In addition, EGF-related ligands have been detected in the follicular fluid of porcine follicles (Hsu *et al.* 1987), and also EGF-receptor (EGF-R) activity has been shown in cumulus cells following ovulation induction (Panigone *et al.* 2008). Collectively, these

results demonstrate the communication of the ovulatory LH signal to the oocyte, through the EGF signalling network (Revisited in Chapter 4).

1.1.4 Role of the oocyte in follicle development

For many decades it was believed the oocyte was a passive entity in the follicle, whereby the surrounding follicular somatic cells were solely responsible for the endocrine and local ovarian signals required for oocyte growth and function. However, ground-breaking studies in the 1990s revealed that GCs are subject to paracrine signalling from the oocyte in the form of soluble oocyte-secreted factors (OSFs) which regulate follicular growth (Buccione *et al.* 1990, Salustri *et al.* 1990, Vanderhyden *et al.* 1990). Therefore, by regulating the development of surrounding somatic cells, the oocyte indirectly regulates its own microenvironment. In this section, an overview is provided of oocyte-produced molecules (both secreted and non-secreted) that have roles in determining female fertility.

C1galt1

A role for oocyte glycans has been described in mice. Oocytes lacking core 1-derived *O*-glycans, due to deletion of core 1 β1,3-galactosyltransferase (*C1galt1*) have increased fertility with a ~40% increase in litter size compared to Controls, until at least 6 months of age (Williams *et al.* 2007, Williams & Stanley 2008). Further research has shown that the increased fertility in *C1galt1* Mutant mice arises from more, healthy growing follicles compared to Controls leading to an increased ovulation rate (Grasa

et al. 2015). Understanding the increase in fertility in *C1galt1* Mutant mice is one of the aims of this thesis and will be discussed further in Section 1.3.

FOXO3a

Increased fertility has also been observed in female mice with constitutively active Forkhead Box O3a (FOXO3a) in oocytes of primordial and primary follicles (Pelosi *et al.* 2013). FOXO3a is a member of the forkhead family of transcription factors, and the increased fertility in transgenic females is thought to arise from prolonged maintenance of the primordial follicle reserve. Maintenance of the primordial follicle reserve could be due to (i) decreased rate of activation of primordial follicles or (ii) decrease primordial follicle apoptosis, or both. However, the results of the study presented are inconclusive with regards to the biological explanation of the maintenance of primordial population.

DAZL

Deleted in AZoospermia-Like (DAZL), which is an RNA binding protein expressed in male and female germ cells, has also been shown to have central roles in fertility. The litter size of $DAZL^{+/-}$ females is increased by 50% until at least 6 months of age. This phenotype is believed to be the result of increased sensitivity of growing follicles to FSH, reducing the rate of follicle atresia and resulting in increased ovulation rate (McNeilly *et al.* 2011).

GPR149

The G protein-coupled receptor (GPR) 149 is highly expressed in mouse oocytes (Edson *et al.* 2010). GPR149$^{-/-}$ female mice show increased fertility, evident from larger litter size maintained up to at least 6 months of age (Edson *et al.* 2010). In addition, GPR149$^{-/-}$ mutant females have increased numbers of healthy growing follicles which then leads to increased ovulation rate, contributing to the increased fertility phenotype.

ZP3

At the primary follicle stage, the oocyte produces and secretes glycoproteins known as zona pellucida (ZP) proteins (Philpott *et al.* 1987) which form the oocyte's extracellular matrix. ZP3$^{-/-}$ female mice lack a ZP matrix around the oocyte, and females are infertile due to an inability of the oocytes to be fertilised (Rankin *et al.* 1996). These results highlight the central role of the ZP3 component in ZP assembly and the importance of the ZP during mouse fertilisation.

GDF9

Oocyte-produced TGF-β superfamily proteins have been recognised as vital players in regulating ovarian follicle development. Growth differentiation factor 9 (GDF9) is a TGF-β member that is synthesised in oocytes from the primary follicle stage onward (McPherron & Lee 1993). GDF9 mediates its signal via the activation of intracellular SMAD2/3 pathway (Kaivo-Oja *et al.* 2003, Roh *et al.* 2003). GDF9 is an *N*-glycosylated protein,

while *O*-glycosylation sites have not been identified (Hayashi *et al.* 1999, Hashimoto *et al.* 2012).

GDF9-deficient female mice are infertile due to a block in follicle development at the primary follicle stage (Dong *et al.* 1996). Interestingly, even though follicles in GDF9$^{-/-}$ mice never exceed the primary stage with respect to GC layers, the growth of the oocyte itself in GDF9 mutant females exceeds the size of control oocytes in antral follicles (Carabatsos *et al.* 1998). These observations highlight not only the central role of GDF9 in somatic cell development beyond the primary stage, but also the role of GCs in regulating and controlling oocyte growth, further exemplifying the importance of correct two-way communication. Subsequent research revealed that the deletion of GDF9 results in upregulation of Inhibin A from GCs (Elvin *et al.* 1999) which seems to be the cause of the primary follicle block in GDF9$^{-/-}$ mice, as GDF9$^{-/-}$InhibinA$^{-/-}$ mice overcome this block and follicles develop beyond the primary stage (Wu *et al.* 2004).

BMP15

Another oocyte-produced TGF-β protein is bone morphogenetic protein 15 (BMP15, also known as GDF9B); *BMP15* is located on the X chromosome and is expressed in oocytes from the primary follicle stage onward (Dube *et al.* 1998). Recombinant human BMP15 is *O*-glycosylated (Saito *et al.* 2008), however, no work has been published describing if this is also the case for native mouse BMP15 protein. BMP15 signals through the SMAD 1/5/8 pathway (Moore *et al.* 2003). Studies of experimental and

naturally occurring mutations reveal different roles of BMP15 in different species depending on whether the species is mono- or poly-ovulatory.

In contrast to GDF9$^{-/-}$ female mice which are sterile, BMP15$^{-/-}$ null mice are subfertile with reduced litter size compared to both BMP15$^{+/-}$ mice and control mice (Yan *et al.* 2001). BMP15$^{-/-}$ mice contain follicles at all stages of development and also have denuded oocytes (i.e. not associated with cumulus cells) in preovulatory follicles (Yan *et al.* 2001). The authors propose that the subfertility in BMP15$^{-/-}$ is due to compromised cumulus expansion in some follicles which results in less ovulations. However, quantification of growing follicles was not carried out, therefore the possibility that reduced ovulation is due to less growing follicles cannot be excluded.

Mutations of BMP15 in ewes reveals a different phenotype compared to mice highlighting the different molecular regulation of fertility in poly- and mono-ovulatory species. Heterozygous ewes with mutations in BMP15 (BMP15$^{+/-}$), for instance Inverdale and Hanna sheep, have increased fertility due to increased ovulation rates (Galloway *et al.* 2000). In contrast, BMP15$^{-/-}$ sheep are infertile (Davis *et al.* 1992) with follicle development arrested at the primary follicle stage (Braw-Tal *et al.* 1993). Mutation of the *BMP15* gene has also been reported in rare cases of infertile women (Di Pasquale *et al.* 2004).

Heterodimeric GDF9:BMP15 complexes are reported to be more active ligands in cumulus expansion compared to the individual proteins (Peng *et al.* 2013). However, the purity of the heterodimeric complexes and indeed the biological existence of GDF9:BMP15 heterodimers at all is still in

question (Mottershead *et al.* 2013). Interestingly, the ratio of mRNA levels of *GDF9* and *BMP15* has been shown to be highly correlated within various species studied (sheep, pig, cow, rat, mouse, deer) and the ratio differs between species (Crawford & McNatty 2012). Poly-ovulatory animals have an increased GDF9:BMP15 ratio compared to mono-ovulatory animals.

1.2 Cumulus expansion

1.2.1 Importance of cumulus expansion

Following the ovulatory LH surge, an extracellular matrix (ECM) is assembled between the CCs leading to expansion of the cumulus mass that surrounds the oocyte. CCs and expansion of the cumulus complex have been recognised as vital components in the oocyte's developmental journey leading to successful fertilisation.

Prior to ovulation, the CCs have a vital role in maintaining the oocyte at meiotic arrest (Tanghe *et al.* 2002) by production and transfer of cyclic adenosine monophosphate (cAMP) (Eppig & Downs 1984, Eppig 1991) to the oocyte via gap junctions (Dekel 1988). Expansion of the cumulus complex is necessary for ovulation of the COC and the expanded cumulus mass is believed to facilitate efficient capture of an ovulated egg by the oviductal fimbriae and transport into the oviduct (Chen *et al.* 1993, Tanghe *et al.* 2002). Furthermore, oocyte quality and fertilizability have been linked to the degree of cumulus expansion in humans (Ng *et al.* 1999), rats and mice (Vanderhyden & Armstrong 1989, Chen *et al.* 1993) and bovine *in vitro* fertilisation protocols (Ball *et al.* 1983).

Several lines of evidence show that the cumulus oophorus facilitates the process of fertilisation in the oviduct. Following ovulation, the rat oviduct was shown to have sperm predominantly distributed within the cumulus complex and not in the rest of the ampullary fluid (Bedford & Kim 1993). The

fertilisation rate of bovine oocytes *in vitro* is higher in cumulus-oocyte complexes (COCs) compared to cumulus-free oocytes (Chian *et al.* 1995), suggesting that cumulus oophorus acts as a chemoattractant to sperm, guiding sperm to the oocyte membrane.

1.2.2 The process of cumulus expansion

Ovulation is stimulated by the release of luteinising hormone (LH), which initiates two signalling events. First, mGCs secrete epidermal growth factor-like (EGF-L) peptides that bind to EGF receptors on CCs (Park *et al.* 2004). Secondly, the oocyte produces soluble growth factors termed oocyte-secreted factors (OSFs) also acting on CCs, which are required for cumulus expansion in mice. OSFs include members of the transforming growth factor beta (TGF-β) superfamily (e.g. GDF9 and BMP15) (Su *et al.* 2004, Dragovic *et al.* 2005, Peng *et al.* 2013). Binding of TGF-β ligands to cognate receptors on CCs results in the activation of signal transduction pathways mediated via either SMAD2/3 or SMAD1/5/8 (Moore *et al.* 2003, Dragovic *et al.* 2007). Although OSFs have a central role in cumulus expansion in mice, a similar role has not been shown in mono-ovulatory species. Cow and ovine cumulus–oocyte complexes (COCs) undergo follicle-stimulating hormone-induced cumulus expansion *in vitro* in the absence of the oocyte, suggesting that OSFs are not vital for cumulus expansion in all species (Gilchrist *et al.* 2008, Varnosfaderani Sh *et al.* 2013).

Following the LH surge, the combined action of EGF- and OSF-mediated signalling pathways induces CCs to express hyaluronan synthase 2 (HAS2) which synthesises the glycosaminoglycan hyaluronan (HA) (Fulop *et al.* 1997b), the major structural component of the viscoelastic cumulus ECM (Salustri *et al.* 1989). The organisation and stability of the cumulus matrix are dependent on cross linking of the HA polysaccharide (Fig. 1.2), which is mediated by several proteins, including pentraxin-3 (PTX3), TSG-6 (which is the secreted protein product of TNFAIP6, hereafter referred to as TSG-6) and the heavy chains of inter-α-inhibitor (IαI) and pre-α-inhibitor (PαI) (Sato *et al.* 2001, Zhuo *et al.* 2001, Fulop *et al.* 2003, Salustri *et al.* 2004, Scarchilli *et al.* 2007). The roles of cumulus ECM molecules will be revisited in more depth in Chapter 3.

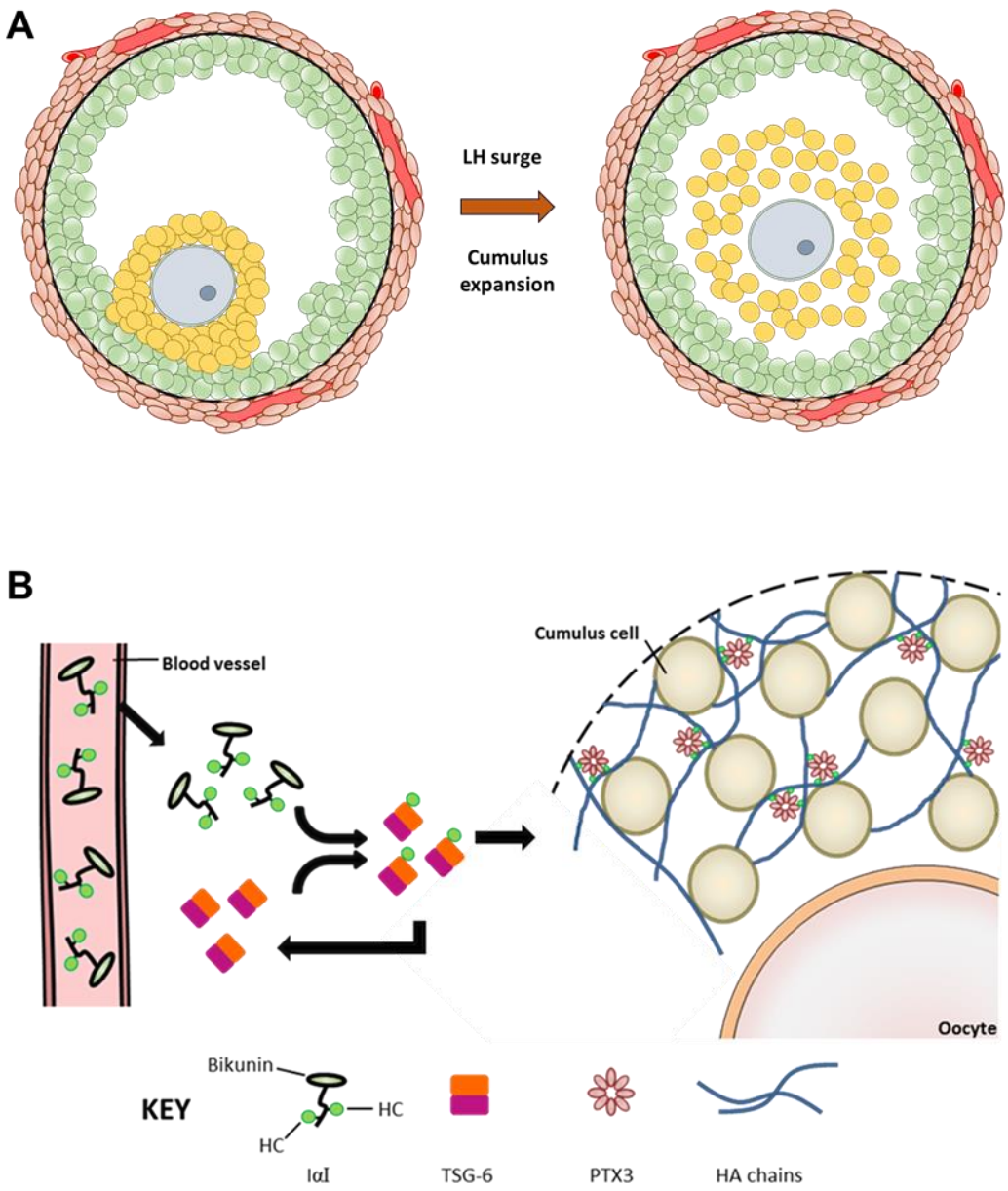

Figure 1.3. Cumulus expansion. (A) Following the ovulatory LH surge, cumulus cells (CCs) are induced to secrete a hyaluronic acid-rich extracellular matrix (ECM) which causes cumulus expansion. (B) Detailed schematic of cumulus ECM assembly. IαI family proteins are serum-transported and following the ovulatory LH surge they diffuse into the preovulatory follicle. TSG-6 molecules, secreted by cumulus cells, act as catalysts in the transfer of the heavy chains (HCs) of IαI onto HA chains. HA is the structural backbone of cumulus ECM and interactions with the multimeric PTX3 and HC enable HA chain cross linking. (B) is from (Ploutarchou *et al.* 2015).

1.3 The *C1galt1* Mutant mouse model

Follicle development is a highly regulated and complex process which, as abovementioned, involves endocrine and paracrine cross-talk between different follicular compartments. In this thesis, the role of oocyte-produced core 1-derived *O*-glycans in follicle development from the primary follicle stage onward is investigated, using the *C1galt1* Mutant mouse as a model.

1.3.1 Genetics of the *C1galt1* Mutant mouse

The C1galt1 enzyme is central in the process of *O*-glycosylation (discussed further in Section 1.3.3). *C1galt1*$^{-/-}$ embryos die by embryonic day 14 due to spinal cord and brain hemorrhages (Xia *et al.* 2004, Williams *et al.* 2007). Therefore, to assess the potential role(s) of core 1-derived *O*-glycans in female fertility, a mouse model was generated in 2007 in which *C1galt1* is specifically deleted in oocytes from the primary follicle stage onward (Williams *et al.* 2007).

The oocyte-specific deletion of *C1galt1* utilizes Cre/loxP technology (Fig. 1.4). Exons 1 and 2 of *C1galt1* are flanked by loxP sites, and a ZP3*Cre* transgene enables the expression of Cre recombinase when the ZP3 promoter is activated, i.e. only in oocytes at the primary follicle stage (Philpott *et al.* 1987). Therefore, in the *C1galt1* Mutant mouse the oocyte proteins destined for core 1-derived *O*-glycosylation lack this post-translational modification. Herein, *C1galt1* Mutant mice are referred to as 'Mutant'.

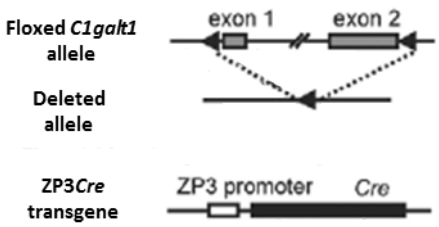

Figure 1.4. Oocyte-specific deletion of *C1galt1*. Diagram of *C1galt1* floxed and deleted alleles, and the ZP3*Cre* transgene. Adapted from Williams et al, 2007.

1.3.2 Phenotype of the *C1galt1* Mutant mouse

The oocyte-specific mutation of *C1galt1* in this Mutant mouse leads to 2 interesting phenotypes: (i) sustained increased fertility (Williams & Stanley 2008), and (ii) modified cumulus expansion (Williams *et al.* 2007).

The increased fertility aspect of this Mutant was first reported in 2007 where Mutant female mice gave birth to ~40% bigger litters compared to Controls (Williams *et al.* 2007, Williams & Stanley 2008). Further investigation revealed that this increase in litter size is maintained until at least 6 months of age in the Mutant (Williams & Stanley 2008). The increase in fertility arises due to more, healthy growing follicles in the Mutant ovary (Williams & Stanley 2008, Grasa *et al.* 2015). When this mouse model was first described it was the only mouse model with sustained increased fertility. However, since then other mutant mice have been reported with sustained increased fertility (described previously in Sections 1.1.3 and 1.1.4).

Superovulated *C1galt1* Mutant cumulus-egg-complexes (CECs) collected from oviducts have altered cumulus mass morphology. Mutant eggs have a less expanded cumulus matrix compared with Controls and exhibit an increased resistance to hyaluronidase digestion (Williams *et al.* 2007).

Therefore, both of these phenotypes make the *C1galt1* Mutant a unique model for studying the effects of oocyte-derived *C1galt1* on female fertility and to explore the altered mechanisms that lead to increased fertility. Furthermore, the *C1galt1* Mutant is an important animal model for the study of cumulus expansion, as the modified cumulus expansion displayed by this Mutant does not negatively impact fertility, as opposed to other mouse models in which irregular cumulus expansion is accompanied by compromised fertility (more details in Chapter 3.1).

1.3.3 Core 1 derived *O*-glycans

Protein glycosylation is a common post-translational modification which aids the attachment of oligosaccharide chains on recently translated proteins. The majority of proteins in biological systems are glycosylated, and glycosylation has important implications in determining the structure and function of glycoproteins (Moremen *et al.* 2012)

One of the main types of glycans are *O*-linked glycans (Fig. 1.5). A serine or threonine residue of the newly translated protein is covalently modified through an α-linkage to aid in the addition of an *N*-

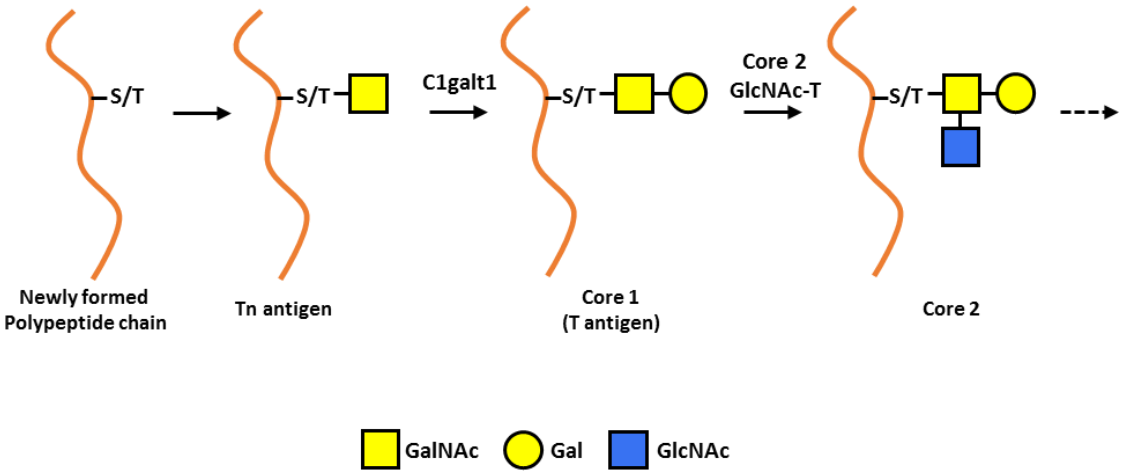

Figure 1.5. Action of C1galt1 in *O*-glycosylation. A newly translated protein is covalently modified through the addition of an *N*-acetylgalactosamine (GalNAc) sugar molecule on a serine or threoning residue. Core 1 β1,3-galactosyltransferase 1 (C1galt1) catalyses the addition of a galactose molecule to the Tn-antigen (N-Acetylgalactosamine – Serine/Threonine) to form Core 1 *O*-glycans which are precursors to more complex *O*-glycans. Core 2 GlcNAc-T (beta-1,6-N-acetylglucosaminyltransferase) extends Core 1 *O*-glycans by the addition of N-Acetylglucosamine to form Core 2 *O*-glycans.

acetylgalactosamine (GalNAc) sugar molecule to initiate *O*-glycosylation (Young *et al.* 1979). This first step in *O*-glycosylation occurs in the *cis*-Golgi network (Rottger *et al.* 1998). Core 1 β1-3 galactosyltransferase enzyme, termed C1galt1, also known as T synthase, catalyses the further addition of a galactose molecule onto the GalNAc in *trans*-Golgi vesicles creating a core 1 *O*-glycan. Core 1-*O* glycans provide the core structure onto which more complex *O*-glycosylations can be built (Ju *et al.* 2002). Any subsequent additions to a core 1 *O*-glycan are termed herein core 1-derived *O*-glycan.

O-glycans have been shown to be important in modulating protein half-life (Sola & Griebenow 2010), receptor signalling (Stanley 2011), cell-cell

interaction (Yago *et al.* 2010), cell-matrix interaction (Tian *et al.* 2012) and can provide protective roles for glycoproteins against proteolytic degradation (Pan *et al.* 2014).

1.4 Aims of thesis

1.4.1 Altered cumulus expansion in *C1galt1* Mutants.

- To investigate the altered cumulus expansion phenotype in *C1galt1* Mutant mice by assessment of structural and molecular changes of the cumulus complex.

- To determine whether the altered cumulus expansion in the Mutant is rescued in the oviduct post-ovulation compared to prior-ovulation by analysis of the cumulus in post-ovulatory complexes.

- To investigate the mechanism of altered expansion in the Mutant by attempting to rescue cumulus expansion *in vitro*.

1.4.2 Increased fertility in *C1galt1* Mutants.

- To assess the effect of oocyte deletion of *C1galt1* in the Mutant on follicle development by characterising morphological changes in follicle development.

- To explore apoptosis and mediators of apoptosis in Mutant ovaries by detection of DNA fragmentation, Bcl2 and Bax levels.

- To assess functional differences in Mutant follicles by assessment of AMH and aromatase levels of follicles.

CHAPTER 2: Materials and Methods

2.1 Generation of transgenic mice

Generation of mice (*Mus musculus*) carrying the floxed *C1galt1* allele and the ZP3*Cre* transgene was as described in (Williams *et al.* 2007). *C1galt1*$^{F/F}$:ZP3*Cre* male mice were mated with *C1galt1*$^{F/F}$ female mice to generate *C1galt1*$^{F/F}$:ZP3*Cre* (Mutant) and *C1galt1*$^{F/F}$ (Control) female mice in a mixed 129/Sv1mJ and C57BL/6J genetic background (Williams *et al.* 2007). The ZP3*Cre* transgene does not affect fertility (Williams *et al.* 2007). Mice were kept in a 12 h : 12 h light-dark cycle with lights on at 07:00 h. All tissue collection details are provided in the Materials and Methods section of subsequent chapters. All experiments were approved by the Home Office and the Clinical Medical Local Ethical Review Committee.

2.2 Hormone treatments

For superovulation mice were injected intraperitoneally with 5 IU of pregnant mare serum gonadotrophin (PMSG, Biosupply, Bradford, UK) at 16:00 and, 48 h later, with 5 IU of human chorionic gonadotrophin (hCG; Chorulon, Biosupply). Details of the procedures following hCG injection are included in the Materials and Methods section of subsequent chapters.

2.3 Genotyping

Tissue was obtained from mice via ear biopsy for DNA analysis. For DNA extraction, ear biopsies were incubated with 3% Proteinase K (Roche

diagnostics, Mannheim, Germany) buffer solution for 8 h at 55^{o}C. The digested samples were then centrifuged at 13,200 rpm for 8 min. The supernatant (40µl) was then boiled at 99^{o}C for 10 min. The samples were then diluted with 100µl of distilled water and stored at 4^{o}C.

Mice samples were genotyped using protocols adapted from (Williams *et al.* 2007). Each 25 µl Polymerase Chain Reaction (PCR) contained 2.5 µl of 10x PCR buffer (Bioline, London, UK), 0.75 µl of 50 mM $MgCl_2$ solution (Bioline), 0.5 µl of 10 mM DNTP (Roche, Mannheim, Germany), 0.5 µl of each primer (Eurogentec, Liege Science Park, Belgium), 1 µl of genomic DNA (ear) and 0.15 µl of Taq polymerase (Bioline) for the detection of floxed *C1galt1* or 0.5 µl of Taq polymerase for the detection of the *Cre* transgene. The primers used to detect the *C1galt1* floxed allele were FB33 and FB34 (Batista *et al.* 2012) and the *Cre* transgene was detected using primers PS502 and PS607 (Shi *et al.* 2004).

PCR reactions to detect the ZP3*Cre* transgene were performed as follows: preheating at 94^{o}C for 2 min followed by 35 cycles of 94^{o}C for 30 sec, 56^{o}C for 30 sec and 72^{o}C for 1 min. Subsequently, there was a final cycle of 72^{o}C for 5 min. PCR reactions for detecting the floxed *C1galt1* allele was as described above, but with an annealing temperature of 66^{o}C.

For DNA electrophoresis, an agarose gel was prepared using a 1.5% weight/volume solution (3g agarose, #438794L Agarose, VWR, Leicestershire, UK with 200ml TAE buffer, made of Trizma base, T1503, Sigma-Aldrich, Dorset, UK, Na_2EDTA, Fisher Scientific, Loughborough, UK

and acetic acid glacial, Fisher Scientific). The agarose/buffer mixture was heated in a microwave to ensure agarose was dissolved and then ethidium bromide was added (0.01%, Ethidium Bromide, Fisher Scientific) to stain DNA and visualise during electrophoresis. A gel comb is positioned into the agarose mixture to create wells and then the mixture is left to cool. Following PCR, DNA samples were mixed with gel loading dye (R0631, Life technologies, Paisley, UK) and were loaded onto the agarose gel along with DNA ladder (N3231L, New England Biolabs, Hitchin, UK). The power supply of the electrophoresis tank was programmed at 100V and 250mA and the gel was run until satisfactory separation of DNA fragments. When DNA electrophoresis was completed, the gel was visualised under UV light and imaged for assessment of results.

2.4 Histochemistry and Immunohistochemistry

For use of the antibodies and binding proteins presented in this thesis, extensive troubleshooting and optimisation was required. Below, the general protocol for Histochemistry (HCh, for binding proteins) and Immunohistochemistry (IHC, for antibodies) is provided, along with the different elements of the protocol that require optimisation for each new antibody/binding protein. Specific conditions for each antibody/binding protein are provided in the Materials and Methods section of the relevant chapters.

(1) Sections are deparaffinised in Xylene (X/0250/17, Fisher Scientific), 3 washes x 3 min, and rehydrated by successive washes in 100% ethanol (Ethanol, #32221, Sigma-Aldrich) 90% ethanol, 70% ethanol, 50% ethanol, 1 min each, and subsequently in distilled water, 3 washes x 1 min.

(2) Antigen retrieval performed. Methods tested are presented in Table 2.1.

Table 2.1. Antigen retrieval methods tested for HCh and IHC.

Antigen Retrieval methods	Notes
Low pH Heat-Induced Epitome Retrieval	Citrate Buffer* (pH 6). Microwave set to full power for 1 min, and then medium power for 9 min. Slides left to cool for 20 min.
High pH Heat-Induced Epitome Retrieval	High pH solution* Process as for Citrate Buffer.
Enzymatic retrieval	20µg/ml Proteinase K* solution, 15 min at room temperature.
No treatment	Go straight to next step.

*Citrate buffer: Sodium citrate tribasic dehydrate, #S4641, Sigma-Aldrich.

*High pH solution, H-3301, Vector Lab.

*Proteinase K, Roche, Welwyn Garden City, UK.

(3) Wash in distilled water, 2 washes x 2 min.

(4) Block endogenous peroxidase by incubation in 30% H_2O_2 (#10687022, Fischer Scientific) for 5 min.

(5) Wash in distilled water, 2 washes x 2 min.

(6) Block non-specific secondary antibody binding. The different blocks tested are presented in Table 2.1.

Table 2.2. Antigen retrieval methods tested for HCh and IHC.

Block options	Notes
Normal Goat Serum (NGS)*	Tested various concentrations, with range 1.5%-10%.
Fetal Calf Serum (FCS)*	Tested various concentrations, with range 2%-5%.
Bovine Serum Albumine (BSA)*	Tested various concentrations, with range 5%-20%.
Dried milk*	Used at 5% concentration.

*NGS, Vectastain ABC Elite kit, PK-6101, Vector Labs.

*FCS, Fisher Scientific.

*BSA, BPE1600-100, Fisher Scientific.

*Dried milk, Alcafe, Reading, UK.

(7) Primary antibody binding: For this step, both primary antibody (i) dilution and (ii) incubation time were tested for optimum conditions for each individual antibody.

(8) Wash in PBS, 3 washes x 3 min.

(9) Secondary antibody binding: Biotin-labelled secondary antibody used at 1:200 dilution, for 60 min at RT. Wash in PBS, 3 washes x 3 min.

(10) Wash in PBS, 3 washes x 3 min.

(11) For antigen signal amplification, an avidin-biotin-peroxidase complex (ABC) is used (Vectastain ABC Elite Kit, Vector Labs) for 30 min at RT.

(12) Wash in PBS, 3 washes x 5 min.

(13) Antigen-specific detection was revealed using a DAB Kit (Vector Labs). The slides were then dehydrated and mounted with Depex (VWR, Leicestershire, UK)

2.5 Hematoxylin staining

For histological analysis of paraffin-embedded ovary sections, hematoxylin staining was performed. Hematoxylin staining was also carried out on some section following DAB staining, after removing the coverslips by extended immersion in Xylene.

Slides were incubated with xylene (Fisher Scientific), 1 wash x 8 min followed by 2 washes x 4 min, and then incubated in 100% ethanol (Sigma-Aldrich), 2 washes x 3 min, followed by 90% ethanol for 2 min, 70% ethanol for 3 min, 50% ethanol for 3 mins and tap water for 3 min. The slides were then stained with Hematoxylin (Shandon Gill 2 Hematoxylin, Fisher Scientific) for 2 min and then washed under running water for 5 min. Slides were then dehydrated by immersion through an increasing alcohol gradient: 80% ethanol for 1 min, 95% ethanol for 30 sec, 100% ethanol for 45 sec, 100% ethanol for 1 min, 100% ethanol for 2 min and finally 2 washes in

xylene for 8 min each. Glass slides were mounted with Depex (VWR) and left to dry before imaging.

2.6 Statistics

Statistical comparisons and tests used are described in detail in subsequent experimental chapters. The sample size (n) used for statistical analysis of experiments is the number of follicles or oocytes, depending on the nature of the experiment. For all statistical analyses, the sample size was derived from at least 3 mice (precise number is given under each figure legend).

CHAPTER 3: Molecular and structural changes in cumulus ECM of *C1galt1* Mutants

3.1 INTRODUCTION

The signal for ovulation, which is received by pre-ovulatory follicles in the form of the LH surge, causes the secretion of an extracellular matrix (ECM) by the cumulus cells (CCs) leading to expansion of the cumulus mass that surrounds the oocyte. The organisation and stability of the cumulus ECM is dependent on the crosslinking of Hyaluronic Acid (HA) by several proteins, including the Heavy Chains (HCs) of inter-α-inhibitor (IαI) and pre-α-inhibitor

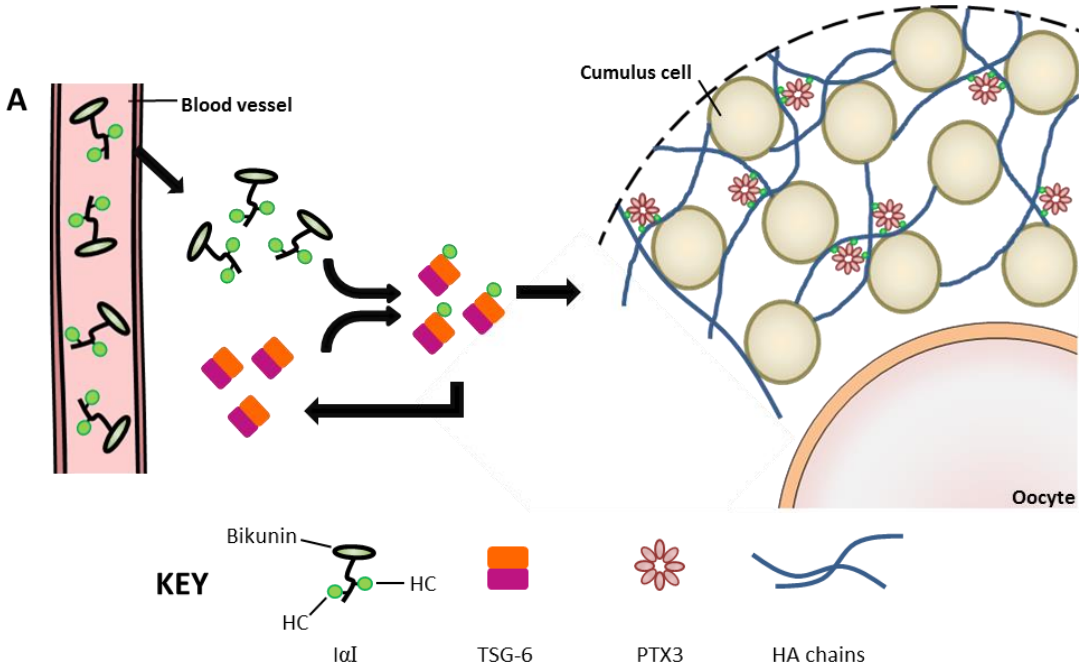

Figure 3.1. Assembly of cumulus extracellular matrix (ECM). Schematic model of the interactions between HA and HA-binding proteins in ECM. IαI family proteins are transported by blood and following the ovulatory LH surge the follicle basal lamina is broken down and IαI proteins diffuse into the pre-ovulatory follicle. TSG-6 molecules secreted by cumulus cells (CCs) act as catalysts in the transfer of the heavy chains (HCs) components of IαI onto HA chains. HA is the structural backbone of cumulus ECM and interactions with the multimeric PTX3 and HC enable HA chain cross linking. Generated by author. (Ploutarchou *et al.* 2015)

(PαI), TNF-stimulated gene-6 (TSG-6) and pentraxin-3 (PTX3) (Fig. 3.1).

IαI and PαI are circulating glycoproteins composed of a light chain, referred to as Bikunin, and one or two heavy chains (HCs). IαI and PαI are synthesised in the liver and transported in serum, but their size and charge cause them to be excluded from the follicle by the basal lamina (Hess *et al.* 1998). At ovulation, the LH surge initiates the breakdown of the blood–follicle barrier (McClure *et al.* 1994, Irving-Rodgers *et al.* 2002), allowing IaI and PaI to diffuse into pre-ovulatory follicles where the HC components are incorporated into the cumulus ECM (Chen *et al.* 1996). During cumulus expansion, the HCs are transferred from IαI and PαI onto HA to form covalent HC•HA complexes; this process is catalysed by TSG-6 and occurs via TSG-6•HC intermediates (Rugg *et al.* 2005, Sanggaard *et al.* 2008). Mice that are deficient in the expression of either bikunin or TSG-6, fail to support COC expansion (Sato *et al.* 2001, Zhuo *et al.* 2001, Fulop *et al.* 2003) indicating that the covalent modification of HA with HCs is essential for the assembly and cross-linking of a stable cumulus ECM. Naturally ovulated oocytes from Bikunin$^{-/-}$ females are completely devoid of CCs which prevents *in vivo* fertilisation (Zhuo *et al.* 2001).

TSG-6 participates in multiple ECM remodelling processes (Milner & Day 2003, Milner *et al.* 2006) and is secreted by CCs and mural granulosa cells (GCs) in response to ovulatory stimuli (Yoshioka *et al.* 2000, Carrette *et al.* 2001, Mukhopadhyay *et al.* 2001). As noted above, TSG-6 binds covalently to HCs during the catalysis of HC•HA formation (Rugg *et al.* 2005, Sanggaard *et al.* 2005, Sanggaard *et al.* 2008). TSG-6-deficient female mice

lack HC•HA complexes and are severely sub-fertile, which has been attributed to an unstable cumulus ECM leading to an absence of cumulus expansion (Fulop *et al.* 2003). Although TSG-6 contains a Link module domain (in common with most other HA-binding proteins (Day & Prestwich 2002, Higman *et al.* 2014) and binds directly to HA (Kohda *et al.* 1996), it is unclear whether TSG-6 is incorporated into the cumulus ECM.

PTX3, which is also secreted by CCs and required for ECM formation, is a multimeric protein, belonging to the pentraxin superfamily (Garlanda *et al.* 2005, Inforzato *et al.* 2010). PTX3 has been found to interact with HCs (Scarchilli *et al.* 2007, Ievoli *et al.* 2011) and to play a key role in the organisation and cross-linking of HC•HA (Baranova *et al.* 2014). PTX3-deficient female mice are severely subfertile, with reduced frequency of litters and reduced litter size (Varani *et al.* 2002). $PTX3^{-/-}$ females ovulate eggs normally, however CCs are unable to undergo cumulus expansion and the ovulated eggs are denuded. Interestingly, oocytes from $PTX3^{-/-}$ females can successfully undergo *in vitro* fertilisation (Salustri *et al.* 2004). Therefore, it is believed that *in vivo*, the absence of CCs and cumulus ECM around the oocyte prevent fertilisation, even though oocytes have full fertilisation potential.

As described above, compromised COC expansion negatively affects female fertility in mice and the degree of cumulus expansion in human IVF has been shown to be positively correlated with oocyte quality and thus fertilization and implantation rates (Ng *et al.* 1999). The *C1galt1* mouse model is unique since it exhibits defective cumulus expansion but fertility is

not compromised (Williams & Stanley 2008, Grasa *et al.* 2015). These observations suggest that some aspects of cumulus expansion are redundant to successful fertilisation and the aim of this study was to identify these aspect(s).

Eggs ovulated from *C1galt1* Mutant mice are surrounded by a cumulus mass that is denser and more resistant to hyaluronidase treatment compared with Control, indicating altered structure and function (Williams & Stanley 2008). The effects of oocyte-generated core 1-derived *O*-glycans, including those of oocyte secreted factors (OSFs, e.g. GDF9, BMP15) on surrounding CCs have not been investigated and therefore the *C1galt1* Mutant mouse provides a good model to investigate the role of these glycans on cumulus function.

Therefore, on the basis that the cumulus expansion defect in *C1galt1* Mutant mice does not lead to a compromise in subsequent fertility (as opposed to other mouse models with cumulus defects) we hypothesised that the altered cumulus mass was due to structural and molecular changes of the cumulus ECM. Changes in any of the cumulus molecules would indicate either redundancy or plasticity in the function of the cumulus complex. In addition, considering the importance of the different cumulus ECM molecules, a novel intra-follicular approach comparing the levels of ECM molecules within individual COCs, enabled the analysis of correlations between these molecules in Control and Mutant cumulus complexes.

3.2 AIMS

- To investigate the modified cumulus expansion of *C1galt1* Mutant mice by assessment of structural characteristics and changes in ECM molecules.

- To assess the presence, if any, of intrafollicular molecule relationships by correlating the levels of cumulus ECM molecules within individual cumulus complexes.

3.3 MATERIALS AND METHODS

3.3.1 Ovary collection and histology

Ovaries from 8- to 9-week-old Control and Mutant mice were dissected 9 h post-hCG, fixed in 10% buffered formalin (Sigma-Aldrich, Dorset, UK) for 8 h, and washed in 70% ethanol. Ovaries were embedded in paraffin, sectioned at 5 µm and mounted on glass slides.

3.3.2 Histochemistry and Immunohistochemistry

The general protocol for Histochemistry (HCh) and Immunohistochemistry (IHC) was followed as described in Chapter 2.3, with additional specific details provided in Table 3.1 for Hyaluronan, TSG-6, PTX3 and Heavy Chains (HCs) and Table 3.2 for pSMAD2, pSMAD1/5/8 and Ki67.

Table 3.1. Specific details of HCh and IHC protocol used for detection of Hyaluronan, TSG-6, PTX3 and Heavy Chains (HCs) to complement the basic method described in Chapter 2.3.

	Molecule detected			
	Hyaluronan	**TSG-6**	**PTX3**	**Heavy Chains**
Antigen retrieval	None	Low pH Heat-Induced Epitome Retrieval	None	None
Block agent	2% FCS, 1 h	1.5% NGS, 1 h	10% dried milk, 2 h	5% dried milk, 2 h
Primary antibody/binding protein	Hyaluronan binding protein (Seikagaku, Tokyo, Japan) at 1:50, 2h at RT	rabbit anti-mouse TSG-6 polyclonal anti-sera (Carrette et al. 2001) at 1:150, 4^{o}C overnight	rabbit anti-human PTX3 polyclonal antibody (Scarchilli et al. 2007, generously supplied by Dr Antonio Inforzato) at 1:200, 4^{o}C overnight	rabbit anti-human Ial/Pal polyclonal (Carrette et al. 2001, Mukhopadhyay et al. 2001) at 1:100, 4^{o}C overnight
Secondary antibody	anti-rabbit IgG (Vectastain ABC Elite Kit, Vector Laboratories), 1 h at RT			

Table 3.2. Specific details of HCh and IHC protocol used for detection of pSMAD2, pSMAD1/5/8 and Ki67 to complement the basic method described in Chapter 2.3.

	Molecule detected		
	pSMAD2	**pSMAD1/5/8**	**Ki67**
Antigen retrieval	Low pH Heat-Induced Epitome Retrieval	Low pH Heat-Induced Epitome Retrieval	Low pH Heat-Induced Epitome Retrieval
Block agent	1.5% NGS, 1 h	5% BSA, 1h	1.5% NGS, 1 h
Primary antibody	rabbit anti-pSMAD2 polyclonal (Life technologies, Invitrogen, Paisley, UK) at 1:100, 2 h at RT	anti-pSMAD1/5/8 polyclonal (Cell Signalling, Beverly, Massachusetts, USA) at 1:250, 4^{o}C overnight	rabbit anti-Ki67 (Abcam, Cambridge, UK) at 1:100, 2 h at RT
Secondary antibody	anti-rabbit IgG (Vectastain ABC Elite Kit, Vector Laboratories), 1 h at RT		

Note: Immunohistochemical detection of pSMDA2, pSMAD1/5/8 and Ki67 were not performed by author. Data collection and analysis were performed by author.

3.3.3 Characterization of cumulus complex

Molecules detected in CCs and cumulus ECM were quantified using ImageJ software (National Institutes of Health, Bethesda, Maryland, USA). In ImageJ, each pixel is given an intensity value from 0 (black) to 255 (white), and based on this, total pixel intensity and mean pixel intensity were calculated. The values for total pixel intensity, number of pixels and mean pixel intensity for each cumulus complex were all calculated and exported from ImageJ. The pixel values were then inverted so that 0=white, and

255=black to facilitate data interpretation. Finally, mean pixel intensity was expressed as a percentage (i.e. scale 0 to 100). To normalise to CC numbers, the value of total pixel intensity was divided by the number of CCs.

To analyse the size of cumulus complexes, the section closest to the centre of the oocyte were used. Cumulus area was quantified by selecting the space occupied by CCs (Fig. 3.2A), and average cumulus diameter was determined by averaging the two largest perpendicular diameters in the cumulus complex (Fig. 3.2B). To count the total number of CCs in each COC and the number of CCs in the corona radiata, the centremost section of the COC was counterstained with hematoxylin (protocol in Chapter 2.4) and the number of CCs was determined using the count tool in ImageJ. To measure the distance between each corona radiata CC and the distance between corona radiata CCs and the oocyte, the straight-line tool in Image J was used. The numbers of complexes analysed are given in respective Figure legends.

3.3.4 Statistics

A minimum of 3 IHC experiments were done for all antigenic reactions presented (i.e. HABP, TSG6, PTX3, HCs, pSMAD2, pSMAD1/5/8 and Ki67). Data are presented as mean ± SD. Statistical comparisons were performed using Prism GraphPad software version 6.0 (GraphPad Software, La Jolla, CA, USA). An unpaired *t*-test was used for normally-distributed data. A

Mann-Whitney test was used for not normally-distributed data. Differences were considered significant when $p<0.05$.

For correlations of ECM molecules and cumulus expansion, the coefficient of determination (r^2) was calculated (GraphPad Prism) to establish the degree of association between the variables. An r^2 value of >0.8 was considered to indicate a strong association.

3.4 RESULTS

3.4.1 Cumulus expansion in the *C1galt1* Mutant is reduced

Eggs from superovulated *C1galt1* Mutant female mice are surrounded by a modified cumulus mass compared to Controls (Williams & Stanley 2008). To characterize and quantify the Mutant phenotype in expanded COCs, *C1galt1* Mutant and Control females were induced to ovulate using exogenous gonadotrophins. Ovaries were collected 9 h post-hCG and sections through the centre of each oocyte were used for subsequent analysis (oocyte diameter did not differ between Control and Mutant follicles, data not shown). Analysis of these sections revealed that cumulus mass area (Fig. 3.2A) and diameter (Fig. 3.2B) were both significantly decreased in Mutant follicles (~32% decrease; Fig. 3.2C and ~16% decrease; 3.2D, respectively). Cumulus cell (CC) counts revealed that the reduced cumulus mass area contained a smaller number of CCs in the Mutant (~24% fewer) compared to Controls (Fig. 2E). Therefore, although the amount of space occupied by each CC (i.e. density) did not differ in Controls and Mutants there was a ~13% decrease in average area per CC in the Mutant (Fig. 2F) reflecting a non-significant increase in density.

The innermost layer of the cumulus mass is known as the corona radiata. The number of CCs in the corona radiata was equivalent in Mutant and Control (Fig. 2G). However, the distance between each corona radiata CC, as well as the distance between corona radiata CCs and the oocyte centre, were both decreased in the Mutant (Fig. 2H and 2I respectively).

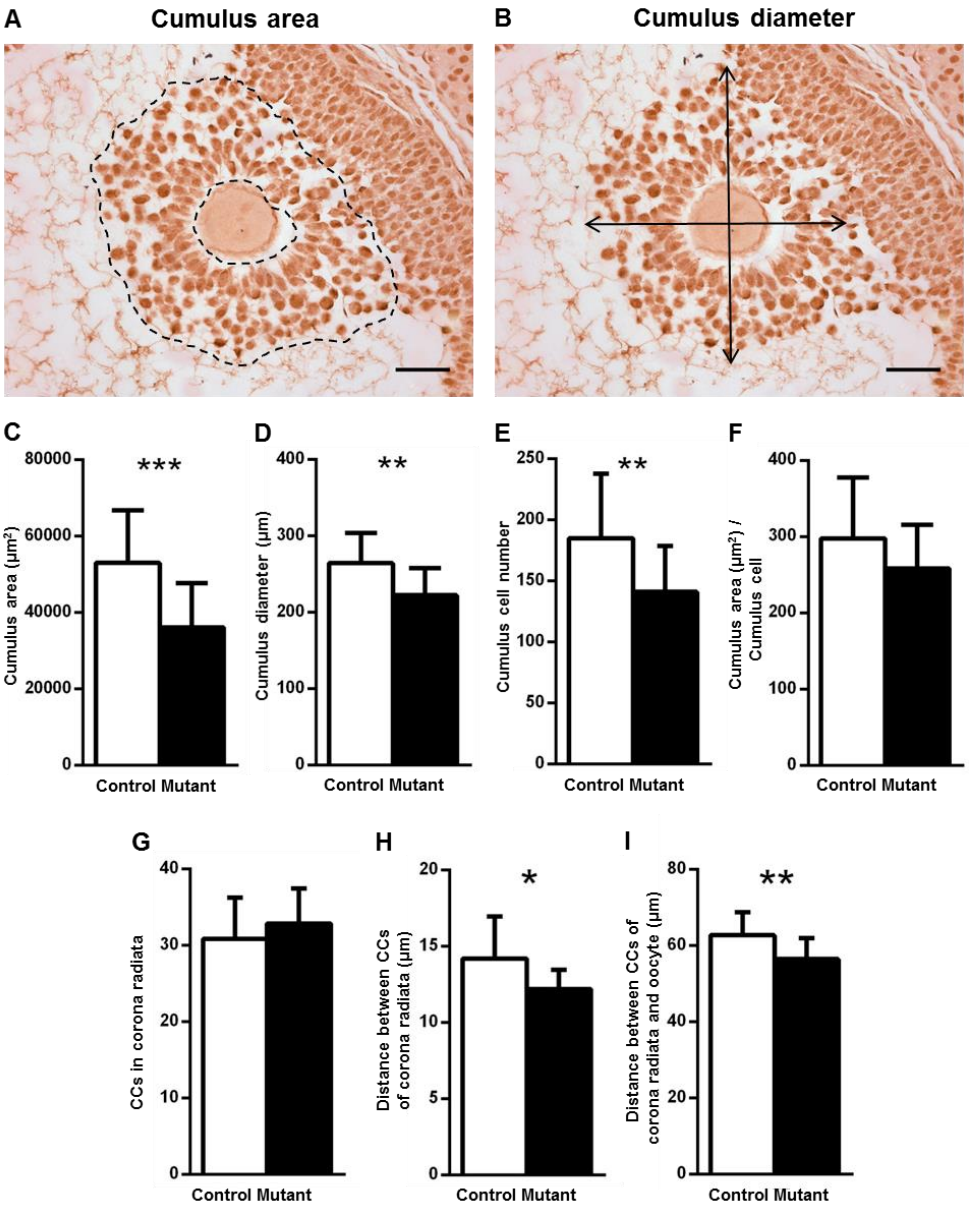

Figure 3.2. Effect of oocyte-derived *O*-glycans on cumulus expansion. The central section through each oocyte was used and the size of the cumulus complex assessed by determining the area occupied by the CCs (A) and by averaging the two largest perpendicular diameters of the COC (B). The following values were determined for Control and Mutant COCs: size of the cumulus area in COCs (C), average diameter of COCs (D), total CC number making up the cumulus complex (E), density of CC distribution in COCs (F), number of CCs making up corona radiata (G), average distance between adjacent CCs in the corona radiata (H) and average distance between corona radiata CCs and the centre of the oocyte (I). (C-F): n=16 Control and n=22 Mutant COCs. (G-I): n=13 Control and n=29 Mutant COCs. *p<0.05; **p<0.01; ***p<0.001. Scale bar: 50 µm. (Ploutarchou *et al.* 2015)

3.4.2 Cumulus ECM composition is altered in the *C1galt1* Mutant

Having determined that *C1galt1* Mutant COCs have smaller cumulus masses, the molecular origin of this phenotype was investigated by analysis of cumulus ECM composition. HA was detected throughout the cumulus ECM and also around the peripheral mural GCs closest to the CCs (Fig. 3.3Ai). Quantification revealed that even though the mean intensity of HA staining in the COC was increased in the Mutant (Fig. 3.3Aii), when normalized to CC number the stain density was similar in Control and Mutant COCs (Fig. 3.3Aiii). PTX-3 was also detected (Fig. 3.3Bi) and although mean staining intensity was increased in the Mutant (Fig. 3.3Bii) intensities per CC were similar in Control and Mutant (Fig. 3.3Biii). TSG-6 was detected surrounding CCs (Fig. 3.3Ci), and the staining intensities were comparable in Controls and Mutants (Fig. 3.3Cii and iii). IαI and PαI enter ovarian follicles from serum and the HC components become covalently attached to HA. The presence of HCs in the cumulus mass was assessed using an antibody which detects bikunin and the heavy chains of IαI and PαI; this analysis is hereafter referred to as HC (Fig. 3.3Di). HC detection revealed a similar pattern to that seen for HA, with an increase in staining intensity in Mutants compared to Controls (Fig. 3.3Dii). However, in contrast to the other matrix components, HCs were found at higher levels in Mutant cumulus ECM compared to Controls (Fig. 3.3Diii).

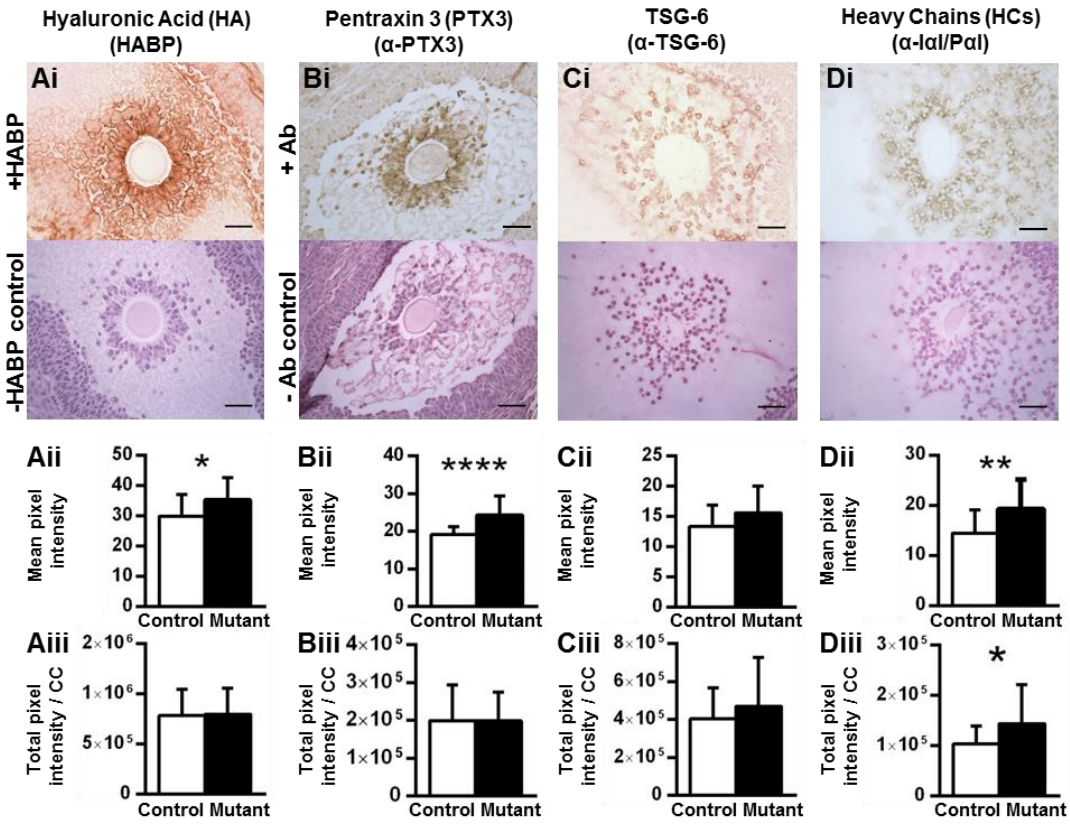

Figure 3.3. Localization and quantification of HA, PTX3, TSG-6 and IαI in preovulatory cumulus masses. Localizations of (Ai) HA, (Bi) PTX3, (Ci) TSG-6, (Di) HCs were determined in preovulatory follicles (molecule used for detection in brackets). Respective mean pixel intensities (Aii), (Bii), (Cii), (Dii) and total pixel intensities normalised to CC number (Aiii), (Biii), (Ciii) and (Diii) were determined for each of the matrix components. The upper panels of (Ai), (Bi), (Ci) and (Di) show representative images from COCs stained with bHABP or a protein-specific antibody; lower panels show sections counterstained with Hematoxylin in the absence of any bHABP or primary antibody (i.e., only secondary detection reagents were applied). Data are presented as mean values ± s.d. (Aii-Aiii): n=17 Control, n=21 Mutant. (Bii-Biii): n=17 Control, n=23 Mutant. (Cii-Ciii): n=20 Control, n=20 Mutant. (Dii-Diii): n=16 Control, n=21 Mutant. *p<0.05; **p<0.01; ****p<0.0001. Scale bar: 50 µm. Ab=antibody. (Ploutarchou *et al.* 2015)

3.4.3 Quantification of cumulus intracellular molecules

Cumulus expansion requires oocyte secreted factors (OSFs) to act on the CCs. Since the *C1galt1* Mutant has an oocyte-specific deletion which affects secreted core 1-derived *O*-glycoproteins, we hypothesized that this mutation might directly or indirectly affect the function of one or more OSFs. To assess the function of the OSF involved in cumulus expansion, we examined intracellular signalling pathways activated in response to TGF-β ligands (key OSFs are members of the TGF-β superfamily); i.e., the SMAD2 and SMAD1/5/8 pathways. Localization of pSMAD2 was cell-associated as expected (Fig. 3.4A) and normalization of the stain to CC numbers revealed similar levels in Controls and Mutants (Fig. 3.4B). Levels of pSMAD1/5/8, which was also cell-associated (Fig. 3.4C) also did not differ between Controls and Mutants (Fig. 3.4D).

Since modified cumulus expansion in the *C1galt1* Mutant is not associated with changes in the ability of CCs to deposit ECM, the proliferative potential of CCs was investigated to determine whether it was altered in the Mutant leading to changes in CC counts. Localization and quantification of Ki67, a nuclear marker of proliferation (Fig. 3.4E), revealed that levels of Ki67 were similar in Control and Mutant CCs (Fig. 3.4F) indicating that cell proliferation was unaltered at 9 h post-hCG.

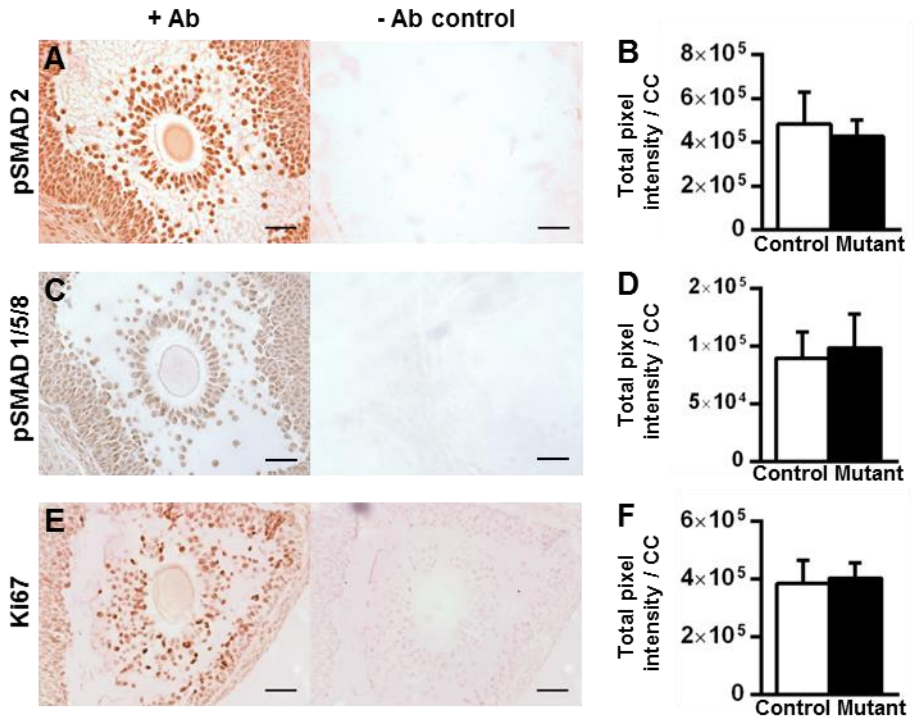

Figure 3.4. Localization and quantification of pSMAD2, pSMAD1/5/8 and Ki67 in pre-ovulatory cumulus masses. Localizations of (A) pSMAD2, (C) pSMAD1/5/8, (E) Ki67 and respective total pixel intensity normalised to CC number (B), (D), and (F) were determined for Mutant and Control preovulatory follicles. Left panels of (A), (C) and (E) show representative images from COCs stained with each of the protein-specific antibodies; right panels show sections without addition of primary antibody, showing no visible DAB staining. Data are presented as mean values ± s.d. (B): n=15 Control and n=18 Mutant COCs. (D): n=19 Control and n=20 Mutant COCs. (F): n=16 Control and n=19 Mutant COCs. Scale bar: 50 μm. (Ploutarchou *et al.* 2015)

3.4.4 Correlations between cumulus expansion and cumulus molecules

Although the requirement for HA, PTX3, TSG-6 and HCs in cumulus expansion and their inter-dependence during ECM deposition is well described, the relationship between the levels these molecules and the extent of expansion has not been analysed in detail. Here, we tested the presence of correlations between the amount of each molecule in the cumulus mass (as determined by staining intensity) and the cumulus area (Fig. 3.5). In Controls, surprisingly, the extent of cumulus expansion did not correlate with the quantity per CC of HA, TSG-6, PTX3 or HCs (Fig. 3.5A-D); nor did levels of OSF-induced pSMAD2 per CC correlate with cumulus size (Fig. 3.5E). Furthermore, in *C1galt1* Mutant mice, the lack of oocyte glycoproteins with core 1-derived *O*-glycans, did not alter the relationship between ECM molecules or pSMAD2 with cumulus size, as no correlations were observed (Fig. 3.5F-J), similar to Controls.

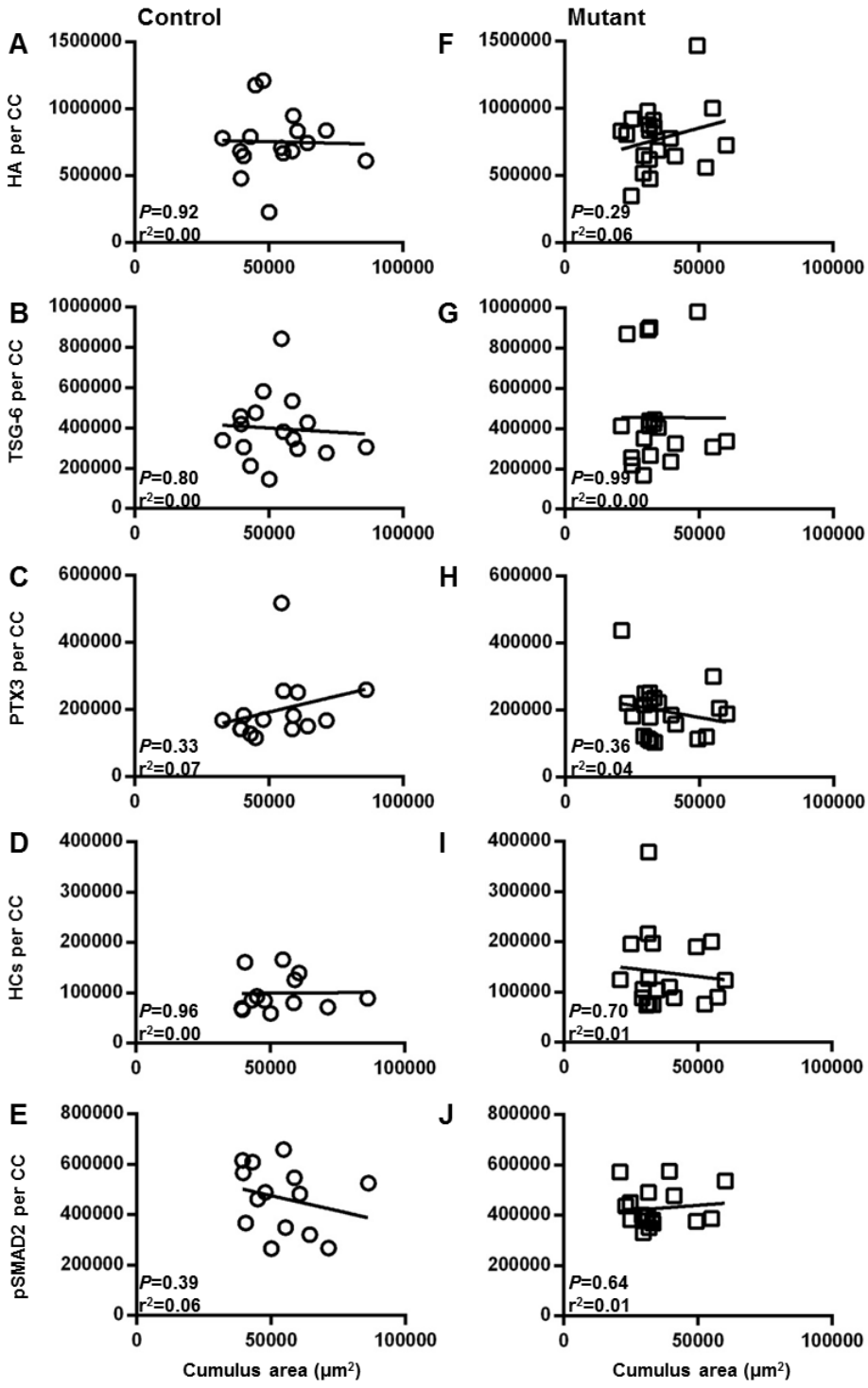

Figure 3.5. Correlation analysis between area of the cumulus complex and levels of cumulus ECM molecules. Correlation analysis between cumulus area and levels (as determined by pixel intensity per CC) of (A,F) HA, (B,G) TSG-6, (C,H) PTX3, (D,I) HCs (determined using an IαI/PαI antibody) and (E,J) pSMAD2 in Controls and Mutants respectively.

3.4.5 Correlations between different cumulus molecules

In light of reported the interdependencies between ECM components during cumulus expansion (Fulop *et al.* 2003, Salustri *et al.* 2004, Scarchilli *et al.* 2007), the relationships between the quantities of these molecules within individual COCs were also investigated (Fig. 3.6). Somewhat surprisingly, no correlation was found between any combination of cumulus ECM proteins in either Control or Mutant revealing unexpected flexibility in the system.

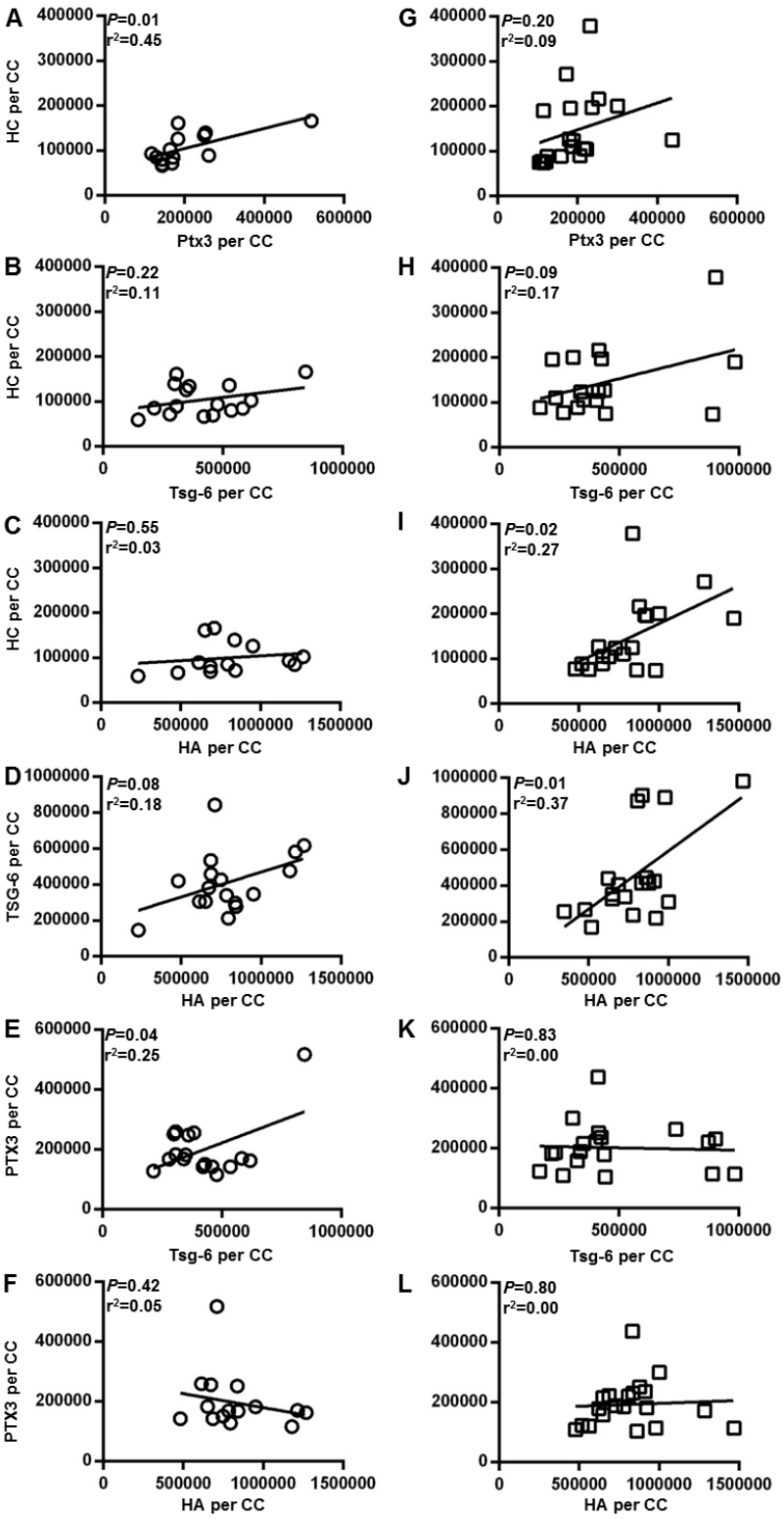

Figure 3.6. Correlation analysis between cumulus ECM molecules. Correlation analysis between pixel intensities per CC of (A,G) PTX3 and HCs (determined using an Iαl/Pαl antibody), (B,H) TSG-6 and HCs, (C,I) HA and HCs, (D,J) HA and TSG-6, (E,K) TSG-6 and PTX3 and (F,L) HA and PTX3 for Controls and Mutants, respectively.

Since activation of the SMAD2/3 pathway in CCs is essential for cumulus expansion, the relationship between the levels of CC-derived ECM components and the levels of pSMAD2 in CCs was also investigated. Again, no correlations were observed in either Controls (Fig. 3.7A-C) or Mutants (Fig. 3.7D-F).

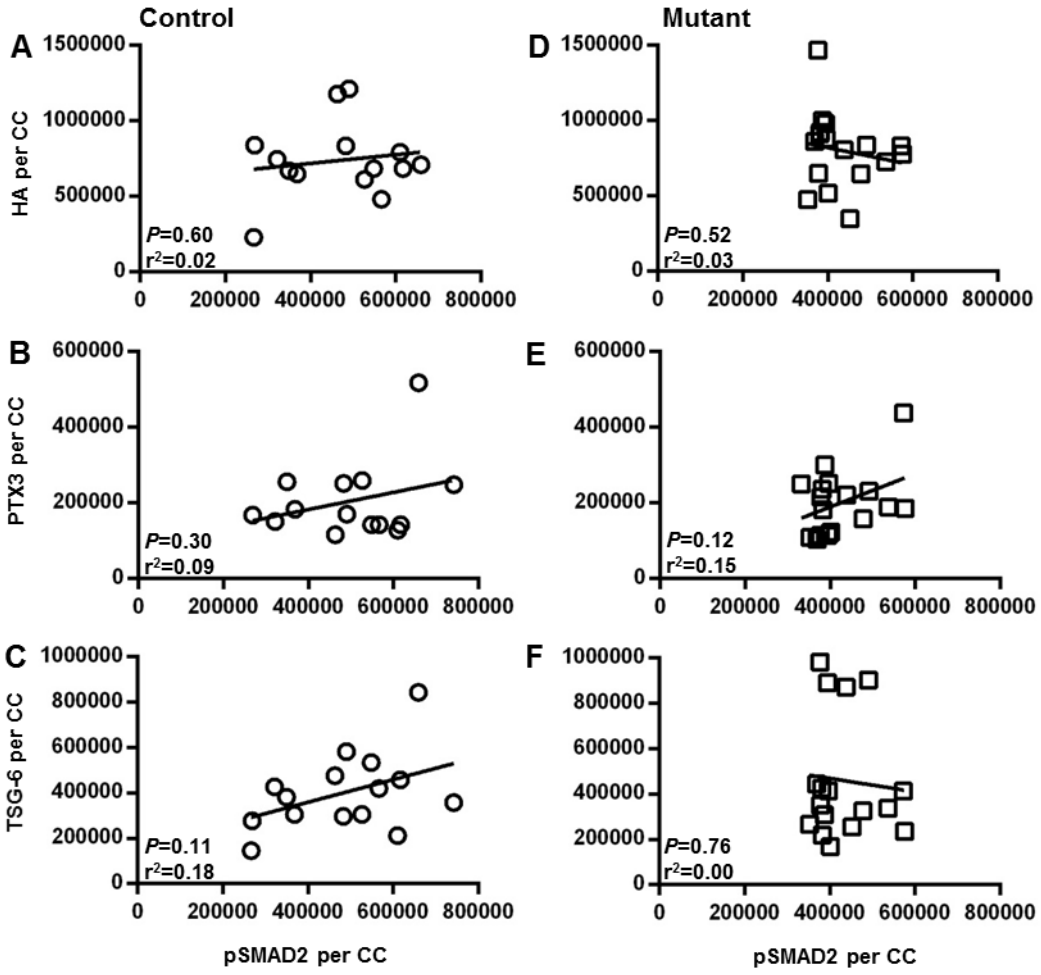

Figure 3.7. Correlation analysis between levels of pSMAD2 and levels of cumulus ECM molecules. Correlation between levels of pSMAD2 and levels of (A,D) HA, (B,E) PTX3 and (C,F) TSG-6 per CC in Controls and Mutants, respectively.

3.5 DISCUSSION

Cumulus mass expansion has important roles in oocyte development, ovulation and is believed to facilitate the transfer of ovulated eggs to the oviduct. Indeed, historically, the numbers of CCs surrounding eggs for human IVF have been thought to be a useful marker of implantation potential (Gregory 1998). On the basis that the observed cumulus expansion defect in *C1galt1* Mutant mice (Williams *et al.* 2007) does not lead to a compromise in subsequent fertility (as opposed to other mouse models with cumulus defects) we investigated the structural and molecular changes of the cumulus ECM.

Our results reveal that reduced cumulus size does not prevent ovulation and subsequent fertilization since these processes are not compromised in the *C1galt1* Mutant despite a ~32% decrease in cumulus size compared to Controls. These data suggest that there is a minimum size of cumulus required, below which ovulation is negatively affected. If this is the case, then the extent of cumulus matrix expansion within *C1galt1* Mutant follicles is sufficient to support ovulation. Novel analysis is presented here of the associations between the different cumulus ECM molecules by determining the levels of essential cumulus matrix molecules (i.e. HA, HCs, TSG-6 and PTX3) within individual COCs. These analyses reveal that there are no strong correlations either between the amount of any one of these ECM molecules and the size of the cumulus mass, or between the relative levels of any of the matrix components in both Control and Mutant COCs. This suggests a highly flexible system whereby the relative amounts of HA,

HCs, TSG-6 and PTX3 can vary quite substantially but they can still form a functional matrix provided that they are all present at, or above, the minimum level required. Furthermore, the degree of cumulus expansion does not predict the respective levels of cumulus ECM molecules.

The role of the cumulus complex in supporting oocyte maturation has been identified as an important factor in determining the success of some human assisted reproductive technology (ART) methods (e.g. *in vitro* maturation; IVM). The low success rate of ART techniques (IVM <35% (Ellenbogen *et al.* 2014), *in vitro* fertilisation (IVF) <40% (Hogue 2002)) is partly attributed to the selection of eggs that, despite possessing a normal complement of chromosomes, have other impairments. Therefore, the development of objective criteria to define oocyte quality is of great importance. It has been suggested that CC assessment can be an informative predictor of oocyte developmental potential, since CC proliferative potential has been positively correlated with pregnancy rates (Gregory 1998, Khurana & Niemann 2000). The results presented in this report indicate that the ~23% decrease in CC number associated with oocytes in *C1galt1* Mutants is not detrimental to fertilization and implantation and therefore a reduction of this magnitude in CC number is not a reliable assessment to predict oocyte developmental potential. As a result, a partially expanded cumulus complex in human ARTs may not be the best indicator of oocyte quality.

To investigate the origin of the reduced cumulus size observed in the *C1galt1* Mutant, two parameters were examined that underlie the formation

of the cumulus matrix during the periovulatory period: (i) the number of CCs that make up the CC complex, and (ii) levels of cumulus ECM molecules. Mutant COCs were shown to occupy ~32% less area compared to the Control, which is accompanied by fewer CCs in the entire complex. Furthermore, the corona radiata CCs in the Mutant were more tightly packed and were also closer to the oocyte compared with Control indicating aberrant expansion. In addition, the area occupied per CC in the Mutant is ~13% less than Controls, making the Mutant COC ~13% more dense. As a result of this, the mean intensity of HA and PTX3 molecules was higher in the Mutant COC although when analysed per CC, the intensity of these two molecules was similar between Control and Mutant indicating that each individual CC in the Mutant functions as Control. Interestingly, the levels of HCs detected, which are the only cumulus ECM component not produced within the follicle, were increased in Mutants compared to Controls. An increased production of IαI, and thus HC, by the liver due to the oocyte modification is unlikely. However, it has been observed that the basal lamina of Mutant follicles is altered during follicle development (Christensen *et al.* 2015). Therefore, in these mice the BL may be permeable to IαI even in the absence of an ovulatory stimulus, such that the intrafollicular presence of IαI, and hence HCs, is elevated compared to Controls during the periovulatory period. Increased levels of HCs could result in more extensive HA cross-linking (Baranova *et al.* 2014), and hence a more compact cumulus matrix.

Therefore, although CCs in *C1galt1* Mutant mice appear functionally normal, as demonstrated by cumulus intracellular signalling pathways and

the ability of CCs to produce ECM components, the combined effects of fewer CCs and more HCs could result in the production of a cumulus matrix with altered organisation in *C1galt1* Mutant mice (see proposed model in Fig. 3.8).

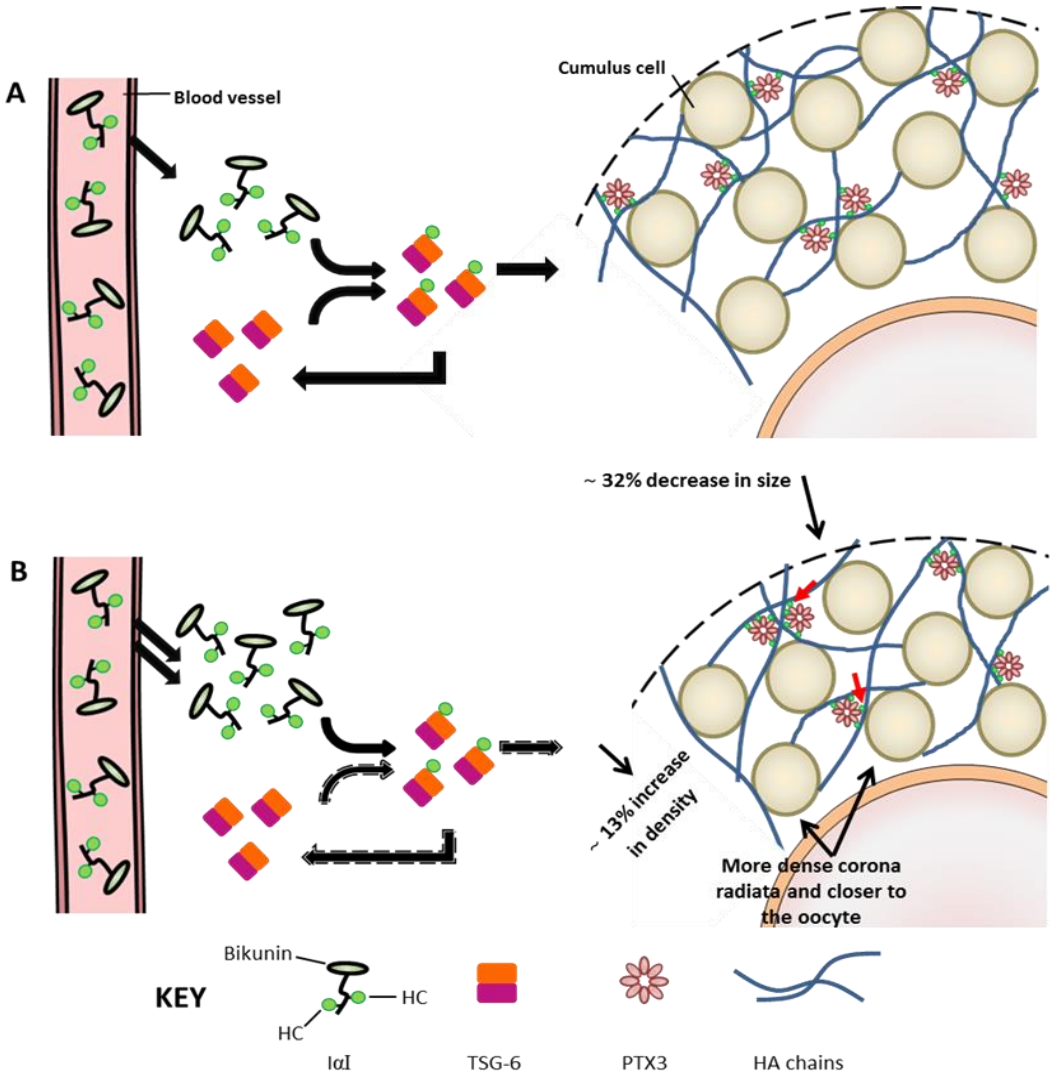

Figure 3.8. Proposed model of modified cumulus expansion in *C1galt1* Mutant mice. (A) Assembly of cumulus ECM in Control COCs. (B) The cumulus mass of Mutant COCs occupies ~32% less area compared with the Control (Fig. 2C), and also contains fewer CCs (Fig. 3.2E). In addition, the area per CC in the Mutant is ~13% less than Controls (Fig. 3.2F). The cumulus ECM of the Mutant contains increased amounts of HCs per CC (red arrows; Fig. 3.3Diii), while levels of HA, PTX3 and TSG-6 per CC remain similar to Controls (Fig. 3.3Aiii, Biii and Ciii). The modified basal lamina of Mutant follicles (Christensen et al. 2014) may allow the influx of more IαI molecules during follicle development and/or the periovulatory period (double arrow from blood vessel); this could result in increased transfer of HCs onto HA (arrows with broken border), resulting in a higher degree of HA chain cross-linking. As a result, the Mutant develops a smaller and denser cumulus mass compared to Controls. The relative sizes of the cells and molecule components are not to scale. (Ploutarchou *et al.* 2015)

The decreased number of CCs in Mutant preovulatory follicles suggests that these cells have an altered proliferative potential, but there was no difference in Ki67 levels between Control and Mutant. However, the reduced CC number in Mutant follicles suggests that: (i) there was altered proliferation of CCs in earlier stages of cumulus expansion, or (ii) there were fewer somatic cells associated with the oocyte from the outset, or (iii) CC apoptosis is elevated in the Mutant resulting in fewer CCs at 9 h post-hCG. The second hypothesis is consistent with characteristics of Booroola sheep that exhibit increased fertility (similar to *C1galt1* Mutant mice) resulting from heterozygosity of a mutation in bone morphogenetic protein receptor 1B (BMPR-1B; a receptor for TGF-β superfamily molecules). In these sheep, the increased number of preovulatory follicles is accompanied by a smaller number of granulosa cells per follicle resulting in fewer cells contributing to the cumulus complex (McNatty & Henderson 1987). However, since SMAD signalling (activated by TGF-β superfamily molecules) was unaltered in *C1galt1* Mutant mice, it is unlikely that TGF-β signalling is modified at this stage by the oocyte-generated core 1-derived *O*-glycans, including those of OSFs. This does not rule out changes in COC signalling at earlier stages of Mutant follicle development which may be the origin of the reduced number of CCs.

In conclusion, the absence of core 1-derived *O*-glycans from oocyte-expressed glycoproteins has effects on the whole follicle that are evident from (i) greater levels of HCs of IαI and Pαl in the follicle and (ii) altered numbers of CCs. This highlights the critical role of the oocyte in follicle

development. The effects of oocyte *C1galt1* deletion on the cumulus mass could be a direct result of changes to the OSFs that determine the proliferative potential of CCs or an indirect outcome relating to the effects of OSFs on EGF-ligands/EGF-receptors, whereby if these are altered, the LH signal is not properly transmitted to CCs. The observation that mouse COCs with reduced CC numbers can function normally without compromising the developmental potential of oocytes is intriguing and raises the question of why do Control COCs have an apparent excess of CCs? In addition, it will be interesting to investigate whether this observed CC redundancy in mouse COCs applies to human COCs, in which case, assessment of the cumulus complex as an indication of oocyte quality for IVF needs to be used with caution. Finally, the lack of strong correlations between the levels of different ECM molecules relative to each other or to the size of the cumulus mass indicates that, providing the minimum requirements for matrix formation are met, this system possesses a high degree of flexibility. It remains to be determined whether the specific expression patterns of individual ECM molecules by human CCs might be predictive of oocyte quality.

Chapter 4: Cumulus expansion dynamics in *C1galt1* Mutant mice

4.1 INTRODUCTION

The ovulatory signal is transmitted to follicles in the form of an LH surge secreted from the anterior pituitary. The LH surge acts on mural granulosa cells (GCs) causing them to release epidermal growth factor (EGF)-like peptides into the follicular antrum (Park *et al.* 2004) (Fig. 4.1). These peptides subsequently bind to EGF receptors on cumulus cell (CCs)

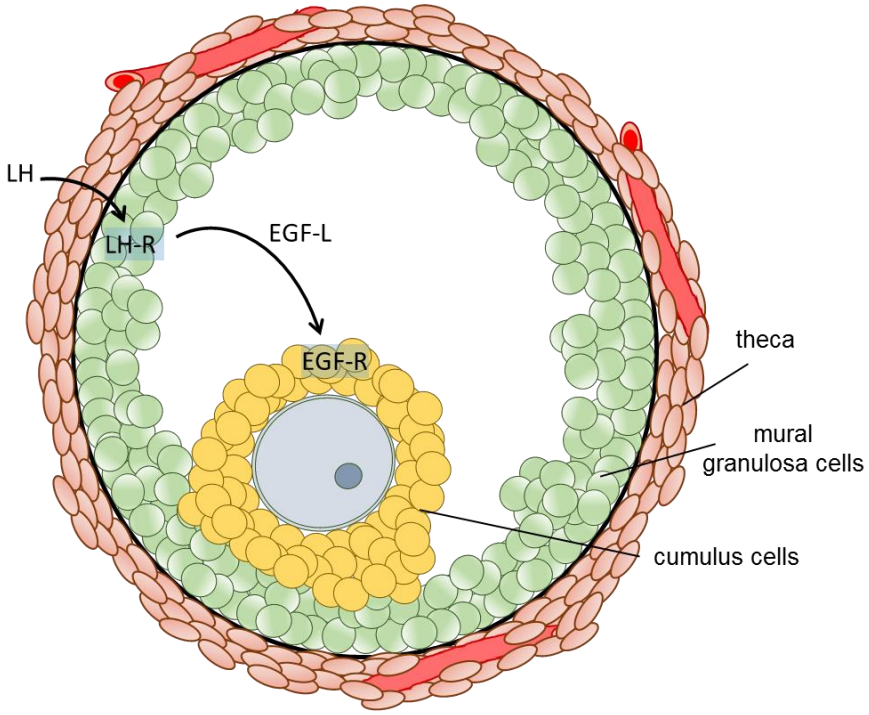

Figure 4.1. Initiation of cumulus expansion. The ovulatory stimulus of LH binds to its cognate receptor LH-R, which is expressed on mGCs during the late stages of follicle development. Mural GCs then express and secrete EGF-like growth factors (amphiregulin, epiregulin and β-cellulin) (Park *et al*, 2004) which traverse the follicular fluid (Hsu *et al.* 1987) and act on CCs to initiate cumulus expansion (Conti *et al.* 2006). Generated by author.

(Panigone *et al.* 2008), the expression of which is dependent on paracrine signals secreted by the oocyte (Diaz *et al.* 2007). The combined action of

EGF-L and oocyte-secreted factors (OSFs) stimulates CCs to produce an extensive extracellular matrix resulting in cumulus expansion. Cumulus expansion can be achieved *in vitro* by treating cumulus-oocyte complexes (COCs) with FSH (Eppig 1979), EGF (Downs 1989) or EGF-like peptides (Park *et al.* 2004). In the mouse, extracellular matrix synthesis activity is upregulated 2-3 h after gonadotrophin stimulation and remains high until just before ovulation at 12 h (Salustri *et al.* 1989, Fulop *et al.* 1997a). Several studies have shown that impaired cumulus expansion leads to female infertility due to defects in ovulation and/or fertilisation (Zhuo *et al.* 2001, Varani *et al.* 2002, Fulop *et al.* 2003). Post-ovulation cumulus expansion in the oviduct has not been extensively studied, however it is thought to be important for fertilisation. Mice deficient in prostaglandin E2 receptor subtype EP2 have compromised fertility which is attributed to defects in oviductal cumulus expansion as ovulation is not severely affected (Hizaki *et al.* 1999).

In summary, cumulus expansion prior to and post ovulation has been shown to play a vital role in fertility and has been linked to the process of meiotic maturation of the oocyte. As the *C1galt1* Mutant mouse has a defect in cumulus expansion at 9 h post-hCG, just prior to ovulation (Chapter 3 and (Ploutarchou *et al.* 2015)), we hypothesise that cumulus expansion in the oviduct is modified to enable successful fertilisation. Also, we hypothesise that the changes in cumulus expansion of Mutant mice, are not an artifact of hormonal injections.

4.2 AIMS

- To assess cumulus expansion following ovulation to determine whether the modified expansion in the Mutant is also present at the time of fertilization.

- To determine whether the altered cumulus expansion in the Mutant is a result of exogenous gonadotrophins by comparison with cumulus expansion in naturally ovulated COCs.

- To investigate the mechanism of the cumulus expansion defect in the Mutant by attempting to rescue expansion *in vitro*.

4.3 MATERIALS AND METHODS

4.3.1 Analysis of cumulus-egg-complexes following hormone-induced and natural ovulation

For assessment of ovulated cumulus-egg-complexes (CECs), Control and Mutant female mice (8-10 week old) were either induced to superovulate (as described in Chapter 2.1) or mated overnight with Control males and checked the following morning for the presence of a vaginal plug, an indication of mating and thus ovulation. The oviducts of hormone-injected and naturally ovulated females were collected (17-18 h post-hCG and at 9-10am, respectively) and dissected in M2 medium (Sigma-Aldrich, Dorset, UK) to release CECs. To visualise the cumulus mass, the medium was transiently removed from the dish enabling the mass to spread out (as previously described, Williams and Stanley 2009). The cumulus mass was then photographed using a MicroPublisher 5.0 RTV camera (Microscope Services, Ltd).

4.3.2 *In vitro* cumulus expansion

To assess the dynamics of cumulus expansion *in vitro*, cumulus-oocyte-complexes (COCs) were collected from 6-8 week old female mice, 48 h after injection of PMSG, prior to any cumulus expansion. Ovaries were collected and COCs released from antral follicles by puncturing with a 29 Gauge needle (Terumo, Somerset, NJ, USA). COCs were transferred into

culture medium (5 COCs per 20µl droplet of medium): α-minimal essential medium (α-MEM) (Fisher Scientific, Loughborough, UK) supplemented with 5% FBS (Sigma-Aldrich), 10µM Milrinone (Sigma-Aldrich) and ±1ng/ml human recombinant Epidermal Growth Factor (EGF) (Sigma-Aldrich). The complexes were incubated at 37^{o}C in 5% CO_2 in air for 16-18hrs. Following incubation, the COCs were imaged to assess the degree of cumulus expansion. For the EGF dose-response experiments, collection of COCs and components of the culture medium were as described above, with EGF at various concentrations (1ng/ml, 0.5ng/ml, 0.25ng/ml and 0.1ng/ml).

4.3.3 Assessment of cumulus expansion *in vitro*

To quantify individual cumulus expansion *in vitro*, one or more of the following methods was used: (i) the radius of cumulus expansion at the 4 compass points was measured of each CEC and the average calculated and (ii) the distance between each egg and its nearest neighbouring egg was measured. Quantification was done using ImageJ software (National Institutes of Health, Bethesda, Maryland, USA).

4.3.4 Statistics

Data are presented as mean ± SD. Statistical comparisons were performed using Prism GraphPad software version 6.0 (GraphPad Software, La Jolla, CA, USA). An unpaired *t*-test was used for normally-distributed data.

A Mann-Whitney test was used for not normally-distributed data. Differences were considered significant when $p<0.05$.

4.4 RESULTS

4.4.1 Cumulus expansion in ovulated CECs is reduced in the *C1galt1* Mutant

Cumulus expansion is modified in Mutant COCs at 9 h post-hCG, before ovulation (Chapter 3; Ploutarchou *et al*. 2015). To investigate whether the oviductal environment rescues the cumulus expansion defect that Mutant COCs exhibit prior to ovulation, ovulated CECs were retrieved from mouse oviducts. Analysis of cumulus expansion in ovulated CECs retrieved from hormone-injected mice revealed that cumulus mass radius (Fig. 4.2A) and minimum distance between eggs (Fig. 4.2B) were both decreased in the Mutant, compared to the Control (Fig. 4.2C and 4.2D respectively).

To ascertain if the differences in expansion were a function of exogenous gonadotrophin administration, we assessed cumulus expansion of naturally ovulated CECs. Cumulus expansion (Fig. 4.2E) and minimum distance between eggs (Fig. 4.2F) were both decreased in naturally ovulated Mutant CECs compared to Controls. Fig. 4.2G shows the comparison of cumulus expansion between superovulated and naturally ovulated complexes from Control mice.

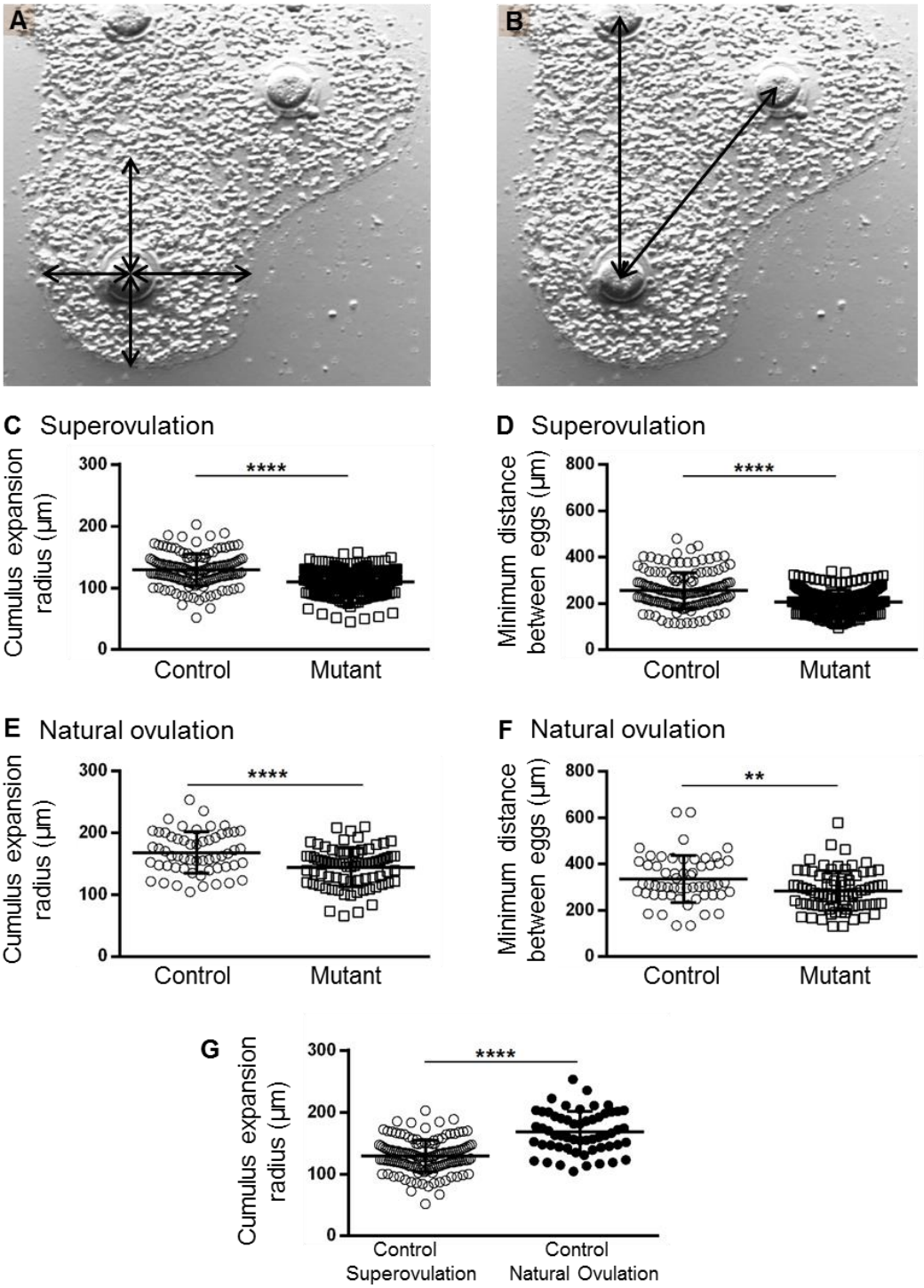

Figure 4.2. *Cumulus* expansion of ovulated CECs. Ovulated complexes were imaged and the size of the cumulus complex was assessed by measuring the radius of cumulus expansion (A) and the minimum distance separating neighbouring eggs (B). (C) Cumulus expansion radius and (D) minimum distance between eggs in superovulated complexes from Control and Mutant mice. (E) Cumulus expansion radius and (F) minimum distance between eggs in naturally ovulated complexes from Control and Mutant mice. (G) Comparison of cumulus expansion radius of superovulated and naturally ovulated complexes from Control mice. (C) and (D): n=142 Control CECs, n=8 mice; n=245 Mutant CECs, n=11 mice. (E) and (F): n=57 Control CECs, n=7 mice; n=76 Mutant CECs, n=9 mice. ** $p<0.01$; **** $p<0.001$.

Our *in vivo* analysis revealed that modified cumulus expansion is a characteristic of Mutant COCs. To determine if Mutant cumulus expansion can be rescued *in vitro*, COCs were obtained 48 h post PMSG, prior to cumulus expansion, and expansion was initiated *in vitro* using EGF (Fig. 4.3).

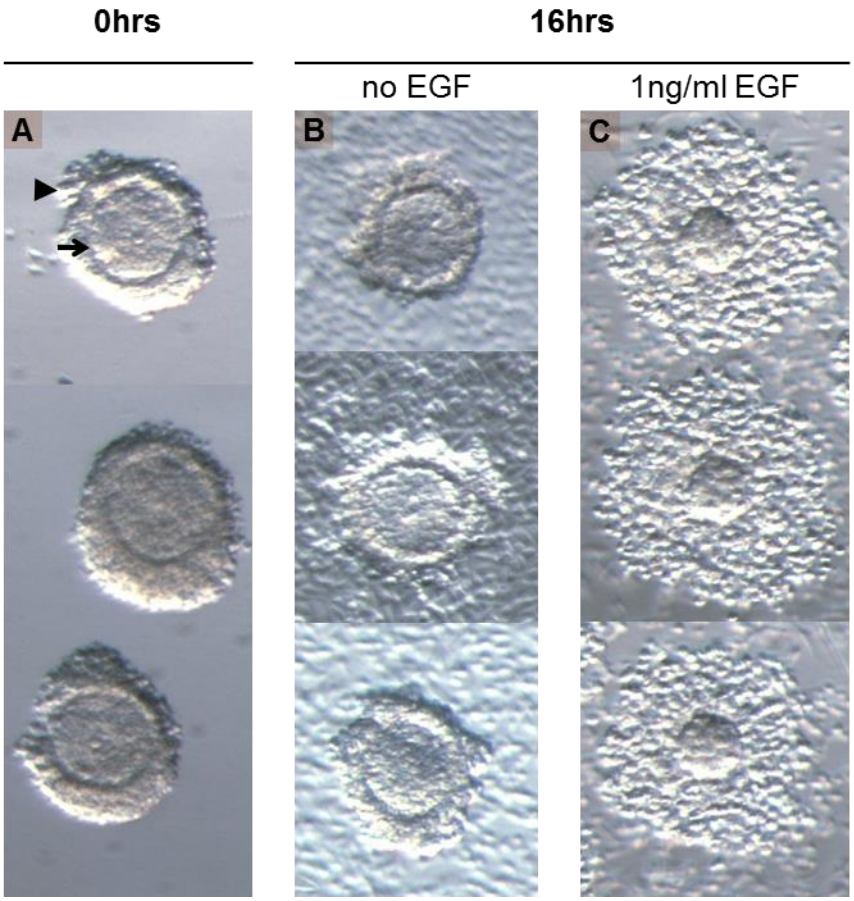

Figure 4.3. *In vitro* cumulus expansion of COCs. (A) COCs collected 48 h post PMSG injection, prior to any cumulus expansion. Oocyte shown by arrow, unexpanded cumulus complex shown by arrowhead. (B) COCs following 16-18 h incubation without EGF. (C) COCs following 16-18 h incubation with 1ng/ml EGF in the culture medium.

Surprisingly, Mutant COCs, following 16-18 h of incubation *in vitro*, had the same degree of cumulus expansion as Controls (Fig. 4.4).

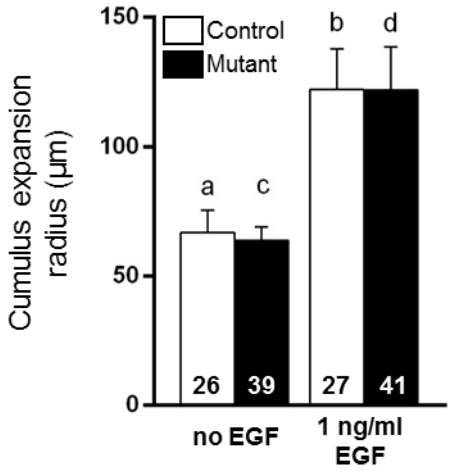

Figure 4.4. Quantification of cumulus expansion of *in vitro*-matured COCs. Size of expanded COCs after 16 h of *in vitro* culture, in 0ng/ml and 1ng/ml EGF. Numbers in columns refer to the number of COCs used. Results presented are from 3 experiments, n=6 Control mice, n=9 Mutant mice. *p* value for *a* versus *b* <0.0001, and for *c* versus *d* <0.0001.

Since Mutant COCs have the potential to expand fully *in vitro*, this begs the question of why, then, do they not expand fully *in vivo*? We hypothesised that this could be due to a compromise of function and/or levels of EGF-R in cumulus cells, which compromises the Mutant COC's ability to undergo normal cumulus expansion. Therefore, the next experimental aim was to induce COCs to expand *in vitro*, in varying EGF concentrations (Fig. 4.5A) to test COCs' responsiveness.

Culture of COCs in decreasing concentrations of EGF resulted in equivalent levels of cumulus expansion between Control and Mutant COCs, in all EGF concentrations used (Fig. 4.5B).

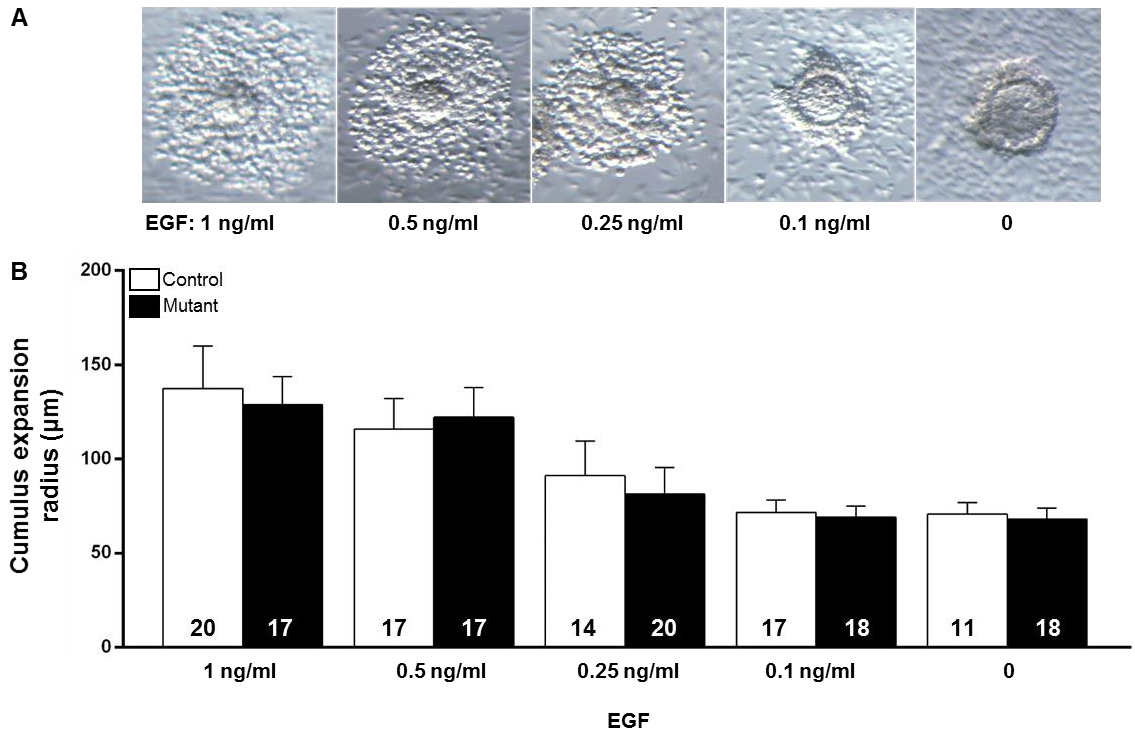

Figure 4.5. *In vitro* cumulus expansion of COCs in varying EGF concentrations. (A) COCs following 16-18 h incubation, in varying concentrations of EGF. (B) Quantification of cumulus expansion *in vitro*, for COCs exposed to various EGF concentrations. Results presented are from 4 experiments, n=11 Control mice and n=9 Mutant mice.

4.5 DISCUSSION

Expansion of the cumulus complex in preovulatory follicles has important implications in successful ovulation and subsequent fertilization. Surprisingly, the *C1galt1* Mutant mouse in which oocyte glycoproteins are deficient in core 1-derived *O*-glycans has altered cumulus expansion at 3h, 6h (Ploutarchou *et al*, manuscript in preparation, to include Fig. 4.2, 4.4 and 4.5) and 9 h post-hCG (Ploutarchou *et al.*, 2015) without negatively affecting fertility. Considering the importance of normal cumulus expansion in fertilisation, we hypothesised that once Mutant COCs leave the ovarian environment and enter the oviduct, they undergo full cumulus expansion which enables successful fertilisation.

In this study, we show that the degree of cumulus expansion in ovulated CECs from *C1galt1* Mutant mice remains altered, as was the case before ovulation, irrespective of the molecular mechanisms utilized to initiate ovulation (i.e. natural and hormonal stimulation). This is quite surprising, as several studies highlight the importance of cumulus cells and an expanded cumulus matrix for successful fertilisation (Zhuo *et al.* 2001, Van Soom *et al.* 2002). Since fertility of *C1galt1* Mutant females is not compromised, then it can be concluded that inability of the cumulus complex to fully expand is not detrimental to either ovulation (Chapter 3) or fertilisation. Moreover, the sole use of cumulus expansion as a marker of oocyte quality in Assisted Reproductive Technologies (ARTs) should be done with caution; the *C1galt1*

Mutant mouse provides evidence that compromised cumulus expansion does not affect fertilisation potential.

Another interesting observation is that obtaining ovulated eggs via administration of exogenous gonadotrophins results in reduced cumulus expansion in both Controls and Mutants compared to ovulated eggs from natural matings. The effect observed through administration of exogenous gonadotrophins could be due to: (i) the accelerated development of less advanced follicles which do not manage to achieve full cumulus expansion potential due to less cellular proliferations, and/or (ii) the ovary having to accommodate a larger number of ovulating follicles, and due to spatial restrictions growth of each follicle (and subsequently cumulus expansion) is compromised. With relation to hypothesis (ii), ovaries from *C1galt1* Mutant mice at 3 weeks of age are significantly heavier than Control ovaries (Williams & Stanley 2008) suggesting that the mouse ovary *does* have the capacity to enlarge and accommodate more follicles. However, administration of exogenous gonadotrophins results in the growth of a very large number of follicles which might be causing the ovary to reach its physical limits in terms of growth and therefore compromising the growth of follicles and thus cumulus expansion.

Cumulus expansion is the result of paracrine signalling acting on CCs, culminating in ECM secretion. Such paracrine signaling is required both from mural GCs in the form of EGF ligands (EGF-L) and from the oocyte via oocyte secreted factors (OSFs). Therefore, in an effort to elucidate the mechanism of altered cumulus expansion in *C1galt1* Mutant mice, we

hypothesised that *C1galt1* Mutant pre-ovulatory follicles have defects in EGF-R in cumulus cells, leading to altered expansion. To test this hypothesis, cumulus expansion of Control and Mutant COCs was induced *in vitro* using EGF. When Mutant COCs are exposed to the same amount of EGF-L as Controls, they expand to the same degree as Controls, and this effect was tested with varying EGF concentrations.

The finding that cumulus expansion in Mutant complexes can be rescued *in vitro*, leads to the proposition of 3 hypotheses.

First, Mutant COCs are not expanding to the same degree as Controls *in vivo* because of decreased expression of EGF-L by the mural GCs compared to Controls. *In vitro*, Mutant COCs are exposed to the same amount of EGFs as Controls, and therefore undergo normal expansion.

An alternative hypothesis to explain the inability of Mutant COCs to undergo normal expansion *in vivo* is that secretion of EGF-L in the Mutant is at normal levels, but expression of less EGF-R on CCs compromises the response to EGF-L and therefore limits the extend of cumulus expansion. Expression of cumulus EGF-R is dependent on OSFs acting through the pSMAD 2/3 pathway (Diaz *et al.* 2007). However, as shown in Chapter 3, pSMAD 2 levels in CCs is similar in Mutant and Controls, indicating there is similar activation of EGF-R in Mutants, as in Controls. Also, the *in vitro* dose-response assays presented in Fig. 4.5 suggest that EGF-R in Mutant COCs are functionally normal compared to Controls as the extent of expansion is

similar between the two groups. Moreover, the possibility that Mutant oocytes prevent normal EGF-R expression *in vivo*, but allow it *in vitro* seems unlikely.

The third hypothesis relates to another potential candidate that could be preventing normal cumulus expansion *in vivo* but is absent from the *in vitro* cumulus expansion system is the antral fluid. The antral fluid is thought to form through diffusion of serum components from the vascularized theca through the basal lamina and granulosa cells (Shalgi *et al.* 1972, Gosden *et al.* 1988). During the process of antral follicle development, the antral fluid is progressively modified by secretions of cells within the follicle (Gosden *et al.* 1988, Rodgers & Irving-Rodgers 2010). *C1galt1* Mutant follicles have been shown to have a modified basal lamina, both in terms of function and structure (Christensen *et al.* 2015). The modifications to the Mutant basal lamina and/or potentially altered cellular secretions in the antral fluid may be changing the properties of the fluid. Structural or molecular modifications of the antral fluid in the Mutant, could be (i) preventing the spatial expansion of the cumulus complex, or (ii) preventing normal EGF-L transport from mural GCs to cumulus cells, therefore resulting in less expansion compared to Controls. The possibility that cumulus expansion is restricted due to the structural and/or molecular properties of the antral fluid could be tested *in vitro*, by inducing cumulus expansion in a variety of different culture media (e.g. different viscosities) and observing the extent of expansion in different conditions.

To conclude, based on *in vivo* and *in vitro* studies presented in this Chapter, the defect of cumulus expansion in *C1galt1* Mutant mice is unlikely

to be due to altered EGF-R levels or function. What is more probable is that in the Mutant, cumulus exposure to lower levels of EGF-L compared to Controls or antrum fluid changes result in a cumulus expansion defect.

Chapter 5: Effect of *C1galt1* mutation on follicle development and follicle growth dynamics

5.1 INTRODUCTION

Following birth, the mouse ovary undergoes remarkable development and supports a plethora of dynamic changes, for instance follicle growth. During the first week of life, only primordial and transitional follicles are present and by two weeks of age follicles of up to the secondary stage (2 full layers of granulosa cells (GC)) are present (Peters 1969). By 3 weeks of age, many different types of follicles (up to mid-antral stage) are present; however, the hormonal regulation does not allow follicles to progress further than the mid-antral stage and therefore follicles undergo apoptosis hereafter (Peters 1969, Da Silva-Buttkus *et al.* 2008).

The oocyte-specific *C1galt1* mutation results in changes throughout the entire structure of the follicle, evident from changes of cumulus cells and cumulus ECM (Ploutarchou *et al.* 2015), the theca cell layer (Christensen *et al.* 2015) and formation of the perivitelline space and trans-zonal processes (Ploutarchou *et al.* in preparation). In addition, *C1galt1* oocyte-deletion results in Mutant mice being more fertile than Controls, with more, healthy growing follicles in adult cycling mice (Grasa *et al.* 2015). As the *C1galt1* Mutant mouse exhibits changes in various aspects of follicle development, we hypothesise that oocyte-produced core 1-derived *O*-glycans have a fundamental impact on the growth characteristics and dynamics of follicle development. Furthermore, the increased fertility phenotype in *C1galt1* Mutant mice has been hypothesised to be due to slower follicle growth which results in follicle accumulation and more available follicles for ovulation

(Williams & Stanley 2008). Work presented in this chapter will address this hypothesis.

The mouse ovary at 3 weeks of age provides a good model to study such developmental changes for 2 important reasons: (i) it allows the study of rates of follicle development (since the time of initiation of follicle growth is soon after birth) and (ii) as the ovary is not under cyclic hormonal regulation (as is the pubertal mouse), it allows direct comparison of follicle characteristics between Control and Mutant.

5.2 AIMS

- To determine the effect of the oocyte *C1galt1* deletion on follicle growth rates by assessment of the follicle population at 3 weeks of age.

- To investigate and quantify the effect of the *C1galt1* deletion on follicle morphology and developmental characteristics (e. g. oocyte size, GC numbers, follicle size etc).

5.3 MATERIALS AND METHODS

5.3.1 Tissue collection

Ovaries from 3-week-old Control and Mutant mice were dissected, fixed in 10% buffered formalin (Sigma-Aldrich, Dorset, UK) for 6 h, and washed in 70% ethanol. Ovaries were embedded in paraffin, sectioned at 5 μm and mounted on glass slides.

5.3.2 Classification of follicles; primordial to Preantral

The ovaries of Control and Mutant mice were serially sectioned at 5µm, stained with Hematoxylin (see Chapter 2.4) and every 40th section was imaged (Leica DM 2500, Microscope services Ltd, Woodstock, UK) and used for follicle counts. Follicles containing an oocyte with a clearly distinguishable nucleus were classified. For classification of resting (primordial) and small growing follicles (transitional to preantral), specific criteria based on GC layers and presence of an antrum were used (Table 5.1). It is noteworthy that 'Primary plus with antrum' follicles were recorded although the presence of an antral cavity at this follicle stage is unusual. What could be done to confirm whether this is indeed antrum, is to stain a consecutive section of a 'Primary plus with antrum' follicle for hyaluronic acid which is normally present in the antral cavity.

Table 5.1. Morphological criteria for classification of primordial and small growing follicles.

		Granulosa cells (GCs)	Antrum
	Primordial	≤ 3, Squamous/flat	Absent
	Transitional	>3, Mixture of squamous and cuboidal	Absent
Primary Inc.	**Primary**	1 complete layer (hereafter all cuboidal)	Absent
Primary Inc.	**Primary plus**	1 complete layer + ≥1 GCs	Absent
Primary Inc.	**Primary plus, with antrum**	1 complete layer + ≥1 GCs	Present
Secondary Inc.	**Secondary**	2 complete layers	Absent
Secondary Inc.	**Secondary plus**	2 complete layers + ≥1 GCs	Absent
Secondary Inc.	**Secondary plus, with antrum**	2 complete layers + ≥1 GCs	Present
	Preantral	>2 complete layers	No

For the purpose of data presentation, Primary and Primary plus follicles were combined and they are hereafter referred to as ‘Primary Inc’. Similarly, secondary, secondary plus and secondary plus with antrum were combined and are hereafter referred to as ‘Secondary Inc’.

5.3.3 Classification of follicles; Early antral and Late antral

The population of antral follicles ranged in size leading to the creation of 2 sub-categories; Early antral and Late antral follicles. These 2 sub-categories were based on the two key characteristics that are correlated with the advancement of antral follicles; the number of GCs and size of the antrum. Therefore, the relationship of these 2 variables was explored in all Control antral follicles (Fig. 5.1).

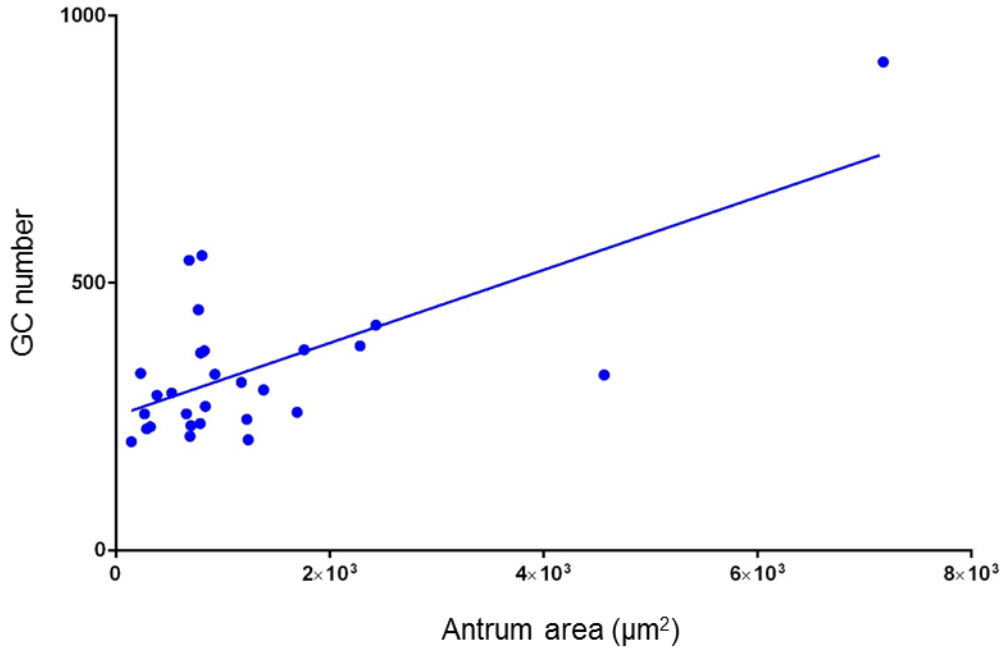

Figure 5.1. Correlation of granulosa cell (GC) number and size of antrum in Control antral follicles. Sections of Control antral follicles through the oocyte nucleus were used to gather data on GC number and antrum size (μm^2). Note: Half of the data on this figure were collected by Miranda Stoddart (FHS student supervised by author, Williams Lab, 2015).

The 2 sub-categories of antral follicles were derived from the correlation analysis of the 2 variables, i.e. perpendicular to the linear regression line ($Line_{perp}$) which describes the relationship between GC number and antrum size (Fig. 5.2).

The decision for the position of the perpendicular line ($Line_{perp}$) was based on morphological assessment of the whole antral follicle population and, thus, all follicles that fall on the left of $Line_{perp}$ (i.e. Early antral) are morphologically less developed than follicles on the right of $Line_{perp}$ (i.e. Late antral). Mutant antral follicles were classified as either Early antral or Late antral, depending on their relative position on the graph in Fig. 5.2.

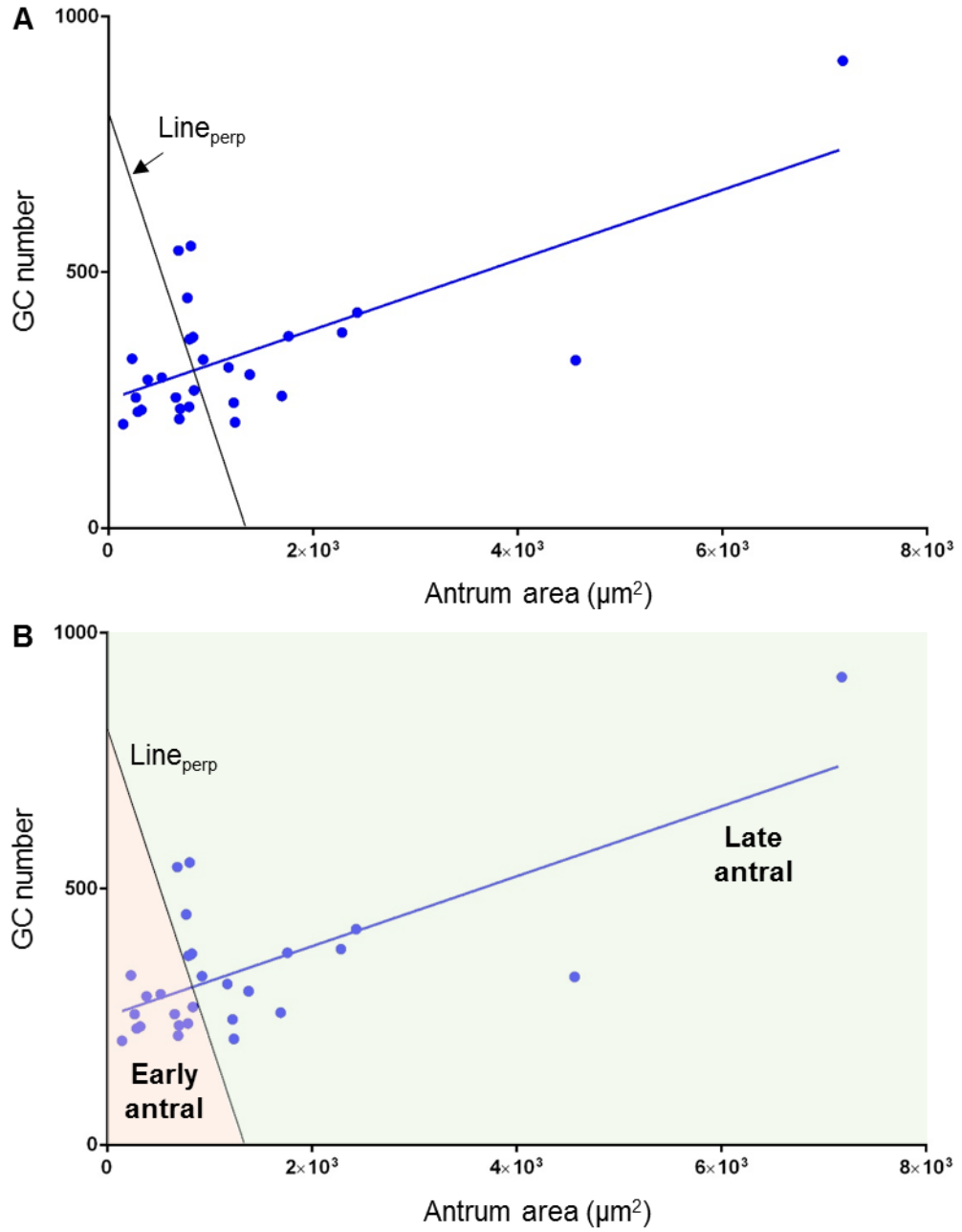

Figure 5.2. Determination of Early antral and Late antral sub-categories. (A) Division of the whole antral follicle population was done using a perpendicular line ($Line_{perp}$). The decision for the position of the perpendicular line ($Line_{perp}$) was based on morphological assessment of the whole antral follicle population and, thus, all follicles that fall on the left of $Line_{perp}$ (i.e. Early antral) are morphologically less developed than follicles on the right of $Line_{perp}$ (i.e. Late antral). (B) Follicles on the left of $Line_{perp}$ are classified as Early antral, and on the right as Late antral.

5.3.4 Estimation of total follicle number per ovary

To determine the total number of follicles in 3-week old ovaries, the number of each type of follicle obtained from the 40th sections was multiplied by the total number of sections in that ovary, and then counts were corrected for section thickness (5 µm) and nucleus diameter using Abercrombie's model (Abercrombie 1946). Oocyte nucleus diameter was measured in follicles at different stages and revealed large variability in nuclei size within each follicle stage (Fig. 5.3). This is because not all sections went through the centre of the nucleus.

Based on the assumption that the nucleus has a spherical shape, the true diameter of a nucleus is found in a section that passes through the nucleus centre. Therefore, of all the nuclei values collected for each follicle stage, the average of the top 10% of the values (black dotted lines, Fig. 5.3) was considered to represent the correct nucleus diameter of that follicle stage. A summary of all calculated nuclei diameter is presented in Table 5.2.

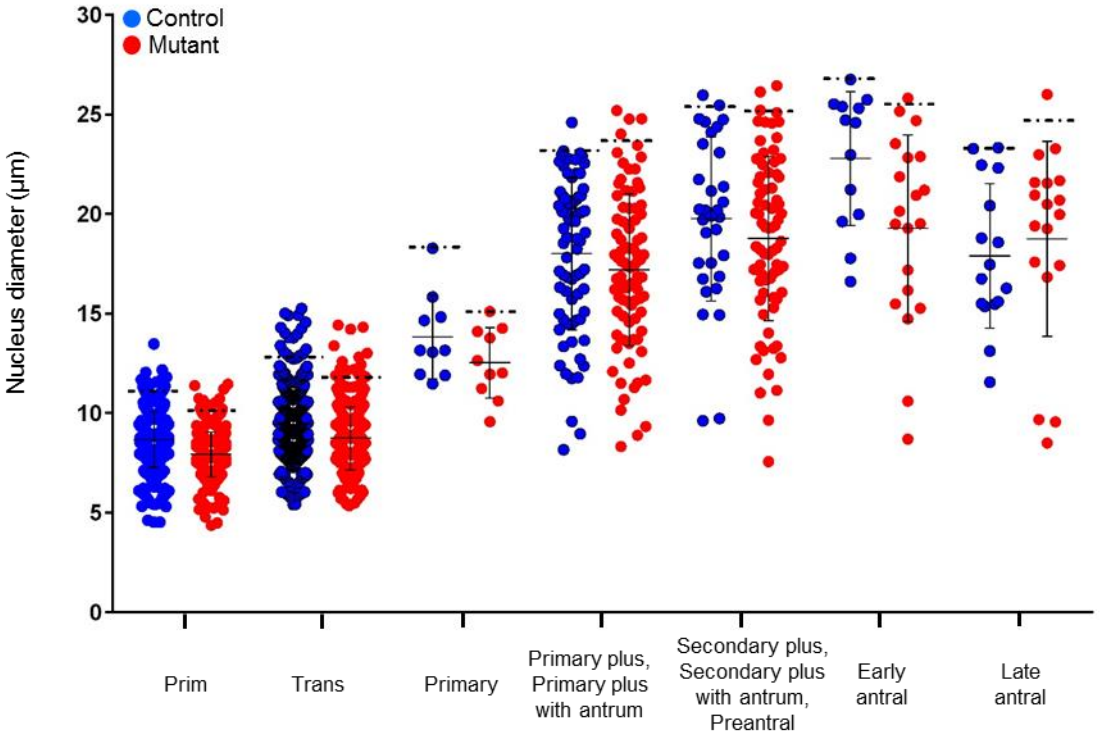

Figure 5.3. Nucleus diameter (µm) at different follicle stages. Each point on the graph represents the nucleus size of an oocyte. Data are presented as mean ± S.D. The dotted black lines represent the mean nucleus diameter of the top 10% of the values for each follicle stage. For a summary of all calculated nuclei diameter see Table 5.2. Prim; primordial, Trans; transitional. N=4 mice for Controls (blue), n=4 mice for Mutants (red).

Table 5.2. Mean nuclei diameter for largest 10% of values for each follicle class.

Stage	Control	Mutant
Primordial	11.1	10.1
Transitional	12.8	11.8
Primary	18.3	15.1
Primary plus, Primary plus with antrum	23.2	23.7
Secondary plus, Secondary plus with antrum, Preantral	25.4	25.2
Early antral	26.8	25.5
Late antral	23.3	24.7

5.3.5 Histological analysis of follicles

All follicles used to determine the total follicle population were analysed to assess follicle development. Oocyte area, oocyte nuclei area, theca layer area, GC number, GC area and antrum area were measured using ImageJ software (National Institutes of Health, Bethesda, MD, USA). The oocyte diameter was calculated from oocyte area measurements. The follicle area included the theca cell layer in any follicle with a visible theca layer. In all other follicles, the basement membrane was taken as the external follicle boundary.

5.3.6 Statistics

Data are presented as mean ± SD. Statistical comparisons were performed using Prism GraphPad software version 6.0 (GraphPad Software, La Jolla, CA, USA). An unpaired *t*-test was used for normally-distributed data. A Mann-Whitney test was used for not normally-distributed data. Differences were considered significant when $p<0.05$.

For correlation analysis of GC number and follicle area, the coefficient of determination (r^2) was calculated (GraphPad Prism) to establish the degree of association between the variables. An r^2 value of >0.8 was considered to indicate a strong association.

5.4 RESULTS

5.4.1 Pre-pubertal *C1galt1* Mutant mice have an altered follicle population compared to Controls.

To determine whether depletion of core 1-derived *O*-glycans from oocytes affects the variety and numbers of follicles, follicle counts were done and follicles classified according to morphology (criteria presented in Section 5.3.1). In both Control and Mutant 3 week-old mice, follicles at most stages of development are present (Fig. 5.4).

Assessment of total follicle populations within each ovary shows that for both Control and Mutant 3-week old mice the majority of follicles are at the primordial stage (Fig. 5.5A). Interestingly, Mutant ovaries contain increased numbers of both Secondary Inc. and Preantral follicle categories, compared to Controls (Fig. 5.5B). Numbers of all other follicle stages were comparable between Control and Mutant.

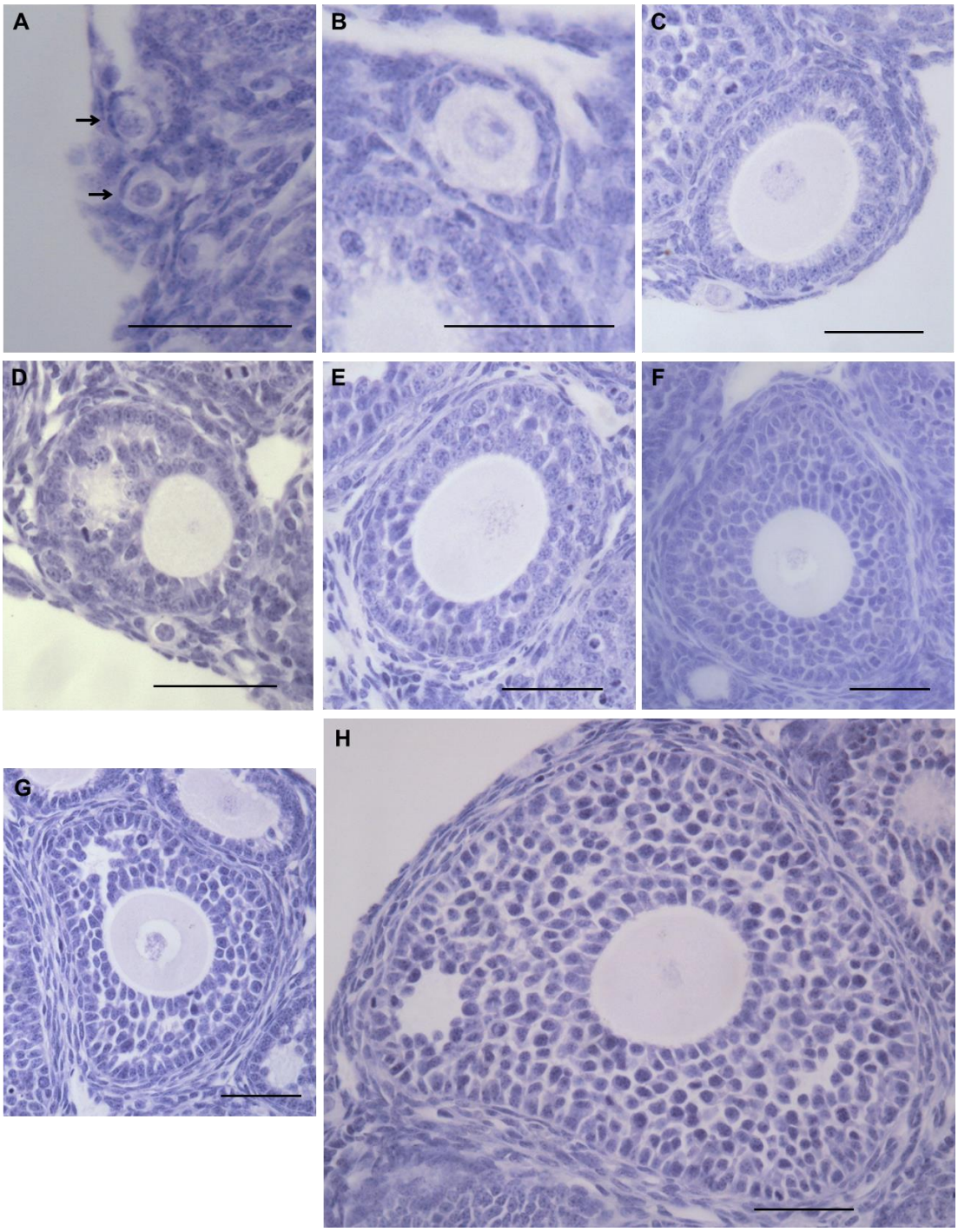

Figure 5.4. Follicles from 3-week old mice at different stages. (A) Primordial follicles (arrows); oocyte surrounded by 2-3 pre-granulosa cells (GCs). (B) Transitional; GCs are undergoing cuboidalisation and proliferation. (C) Primary plus; the follicle has 1 full layer of GCs plus additional cells in the process of creating a 2nd layer. (D) Primary plus with antrum. (E) Secondary plus; the follicle has 2 full GC layers plus additional cells forming subsequent layers. (F) Preantral; multiple layers of GCs. (G) Early antral; the follicle has at least 3 layers of GCs with antrum forming. (H) Late antral; the follicle has >5 GC layers with large antrum area. Scale bar for (A) to (G) is 50μm.

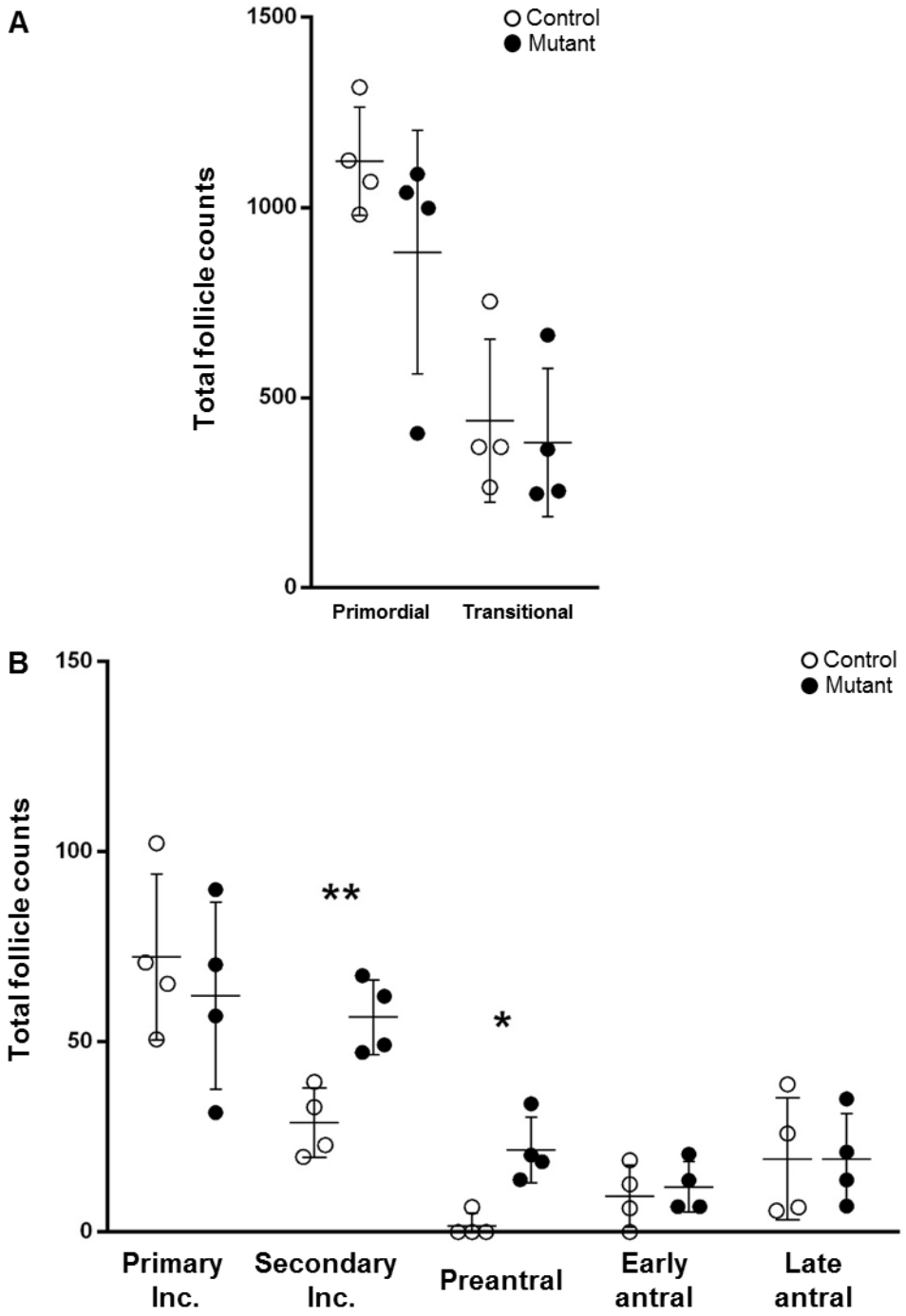

Figure 5.5. Total follicle numbers in Control and Mutant ovaries. (A) Total follicle numbers for quiescent and small growing follicles, in Control and Mutant ovaries. (B) Total follicle number estimates for growing follicles, in Control and Mutant ovaries. Primary Inc.; primary and primary plus, secondary Inc.; secondary, secondary plus and secondary plus with antrum. For (A) and (B) n=4 Control ovaries and n=4 Mutant ovaries. *p<0.05; **p<0.01.

5.4.2 Follicles from Mutant ovaries have stage-specific differences in overall size compared to Controls.

To begin exploring whether the oocyte-specific *C1galt1* deletion affects follicle growth, the size of the entire follicle was measured at all growing follicle stages. Interestingly, transitional follicles in Mutant ovaries are smaller in size compared to Controls (Fig. 5.6), while Late antral follicles in the Mutant are larger than Controls. All other growing follicles are of a similar size in Mutant and Controls.

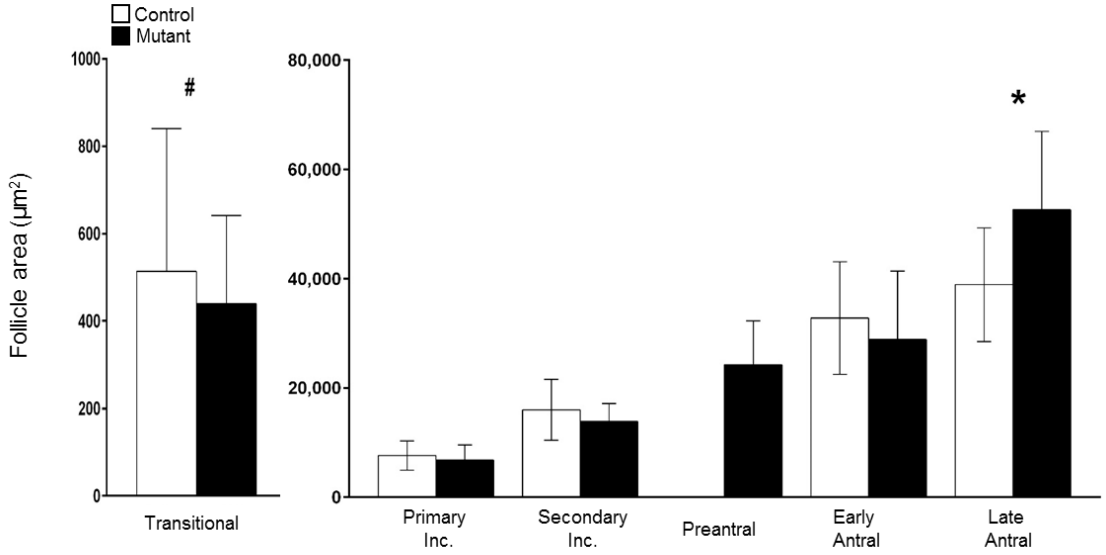

Figure 5.6. Size of growing follicles in 3 week-old ovaries. Measurement of follicle area at all stages of development. For Control, n=4 ovaries, n=160 transitional, n=41 Primary Inc., n=18 Secondary Inc., n=6 Early antral and n=12 Late antral follicles. For Mutant, n=4 ovaries, n=134 transitional, n=37 Primary Inc., n=35 Secondary Inc., n=13 Preantral, n=7 Early antral and n=11 Late antral follicles. *$p<0.05$; $^{\#}p=0.059$.

5.4.3 Small growing follicles from Mutant ovaries have smaller oocytes compared to Controls.

The finding that certain follicle stages in the 3 week Mutant (transitional and Late antral, Fig. 5.6) have a different overall size compared to Controls, prompted an investigation to determine which component of follicles contributes to this phenotype. To assess whether the oocyte-specific *C1galt1* deletion affects oocyte growth relative to the stage of the follicle, oocyte diameter was measured in follicles at all stages. In both Control and Mutant ovaries, there was significant oocyte growth from transitional follicles onwards, accompanying the progression through follicle stages (Fig. 5.7). Surprisingly, the oocyte diameter of Mutant follicles at the transitional, Primary Inc. and Secondary Inc. stages was smaller than Control follicles, whereas oocyte diameter of antral follicles was similar between Mutant and Controls (Fig. 5.7).

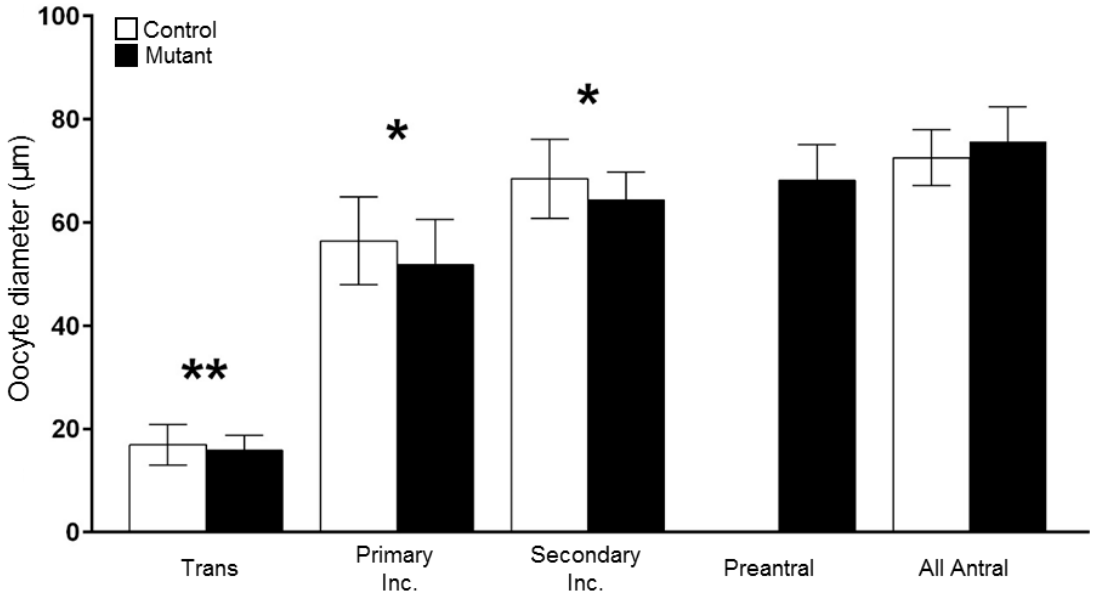

Figure 5.7. Oocyte diameter in growing follicles in 3 week-old ovaries. Oocyte diameters were calculated from oocyte area measurements at all stages of development. Trans; transitional, Primary Inc; primary, primary plus and primary plus with antrum; Secondary Inc; secondary, secondary plus and secondary plus with antrum. For Control, n=4 ovaries, n=160 transitional, n=41 Primary Inc., n=18 Secondary Inc., n=18 antral follicles. For Mutant, n=4 ovaries, n=134 transitional, n=37 Primary Inc., n=35 Secondary Inc., n=13 Preantral, n=18 antral follicles. *p<0.05; **p<0.01.

5.4.4 Large growing follicles from Mutant ovaries have more granulosa cells (GCs) compared to Controls

The observed change in the relationship between oocyte size and stage of the follicle, suggested altered follicle dynamics in the development of Mutant follicles. As follicle development progresses, there is substantial GC proliferation taking place as part of follicle growth. The *C1galt1* mutation in our Mouse model has been shown to have substantial effects on surrounding somatic cells (Ploutarchou *et al*. 2015; Christensen *et al*. 2015), therefore the next aim was to investigate the effect of the oocyte mutation on the number of surrounding GCs.

Assessment of the correlation between GC number and follicle size of all growing follicles revealed an altered relationship between these two variables in Mutant follicles, compared to Controls (Fig. 5.8A). To explore this relationship in more depth, GC number at each follicle stage were compared (Fig. 5.8B). Small and medium-sized growing follicles have similar GC numbers in Controls and Mutants. However, at the late antral stage, Mutant follicles have more GCs compared to Controls.

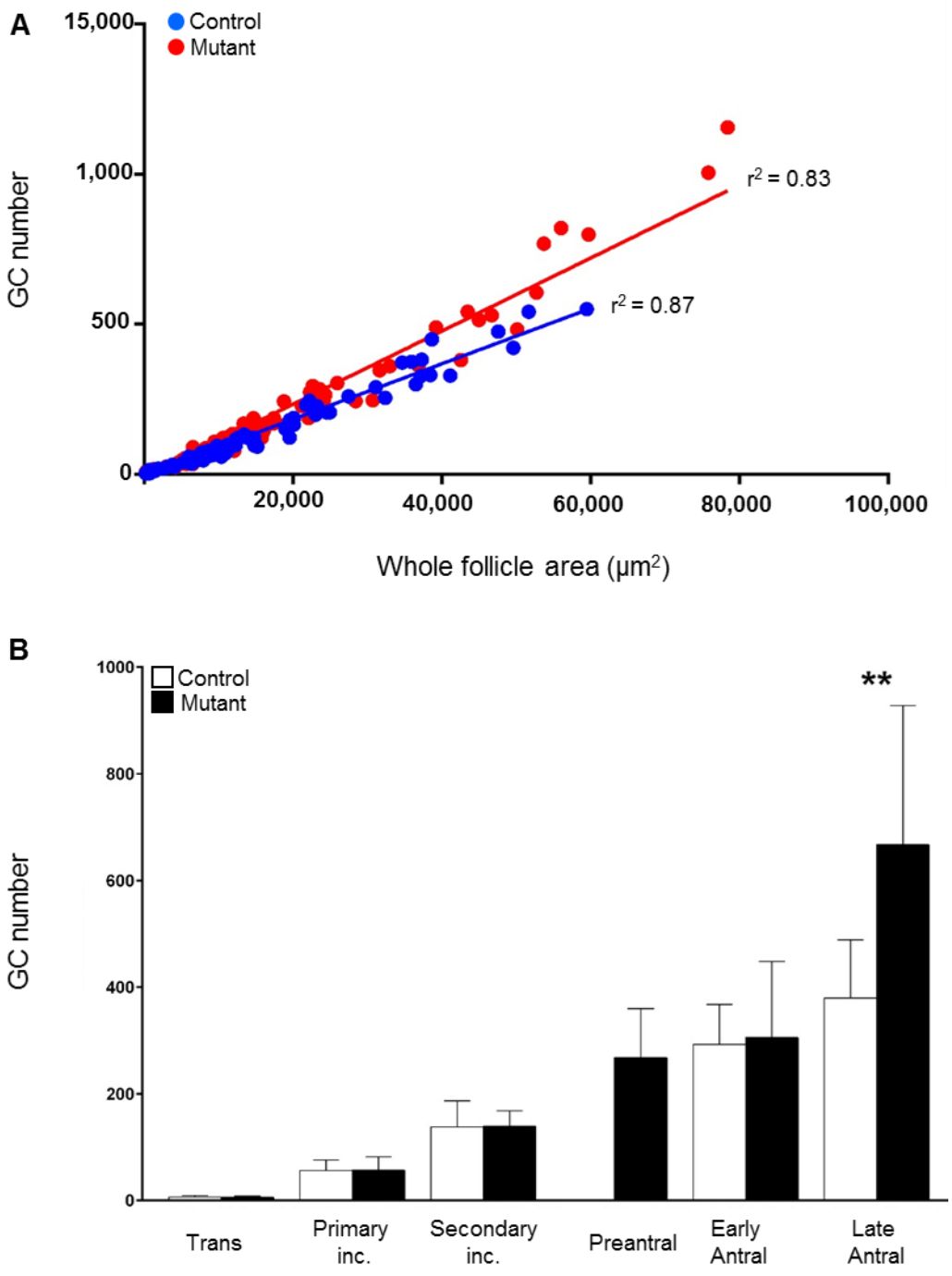

Figure 5.8. GC numbers in growing follicles in 3 week-old ovaries. (A) Correlation between GC numbers and size of follicles. (B) GC numbers of follicles at each growing follicle stage. Trans; transitional, primary Inc; primary and primary plus, secondary Inc; secondary, secondary plus and secondary plus with antrum. For Control, n=4 ovaries, n=160 transitional, n=41 Primary Inc., n=18 Secondary Inc., n=6 Early antral and n=12 Late antral follicles. For Mutant, n=4 ovaries, n=134 transitional, n=37 Primary Inc., n=35 Secondary Inc., n=13 Preantral, n=7 Early antral and n=11 Late antral follicles. ***p*<0.01.

The differences regarding follicle area and GC number between Control and Mutant follicles suggested differences in the GC density. Therefore, the GC number per unit area occupied by GCs was calculated at all follicle stages. Transitional, Primary Inc., Secondary Inc., and Late antral follicles in Mutant mice had more GC numbers per area compared to Controls, suggesting more compact localisation of GCs in the Mutant (Fig. 5.9)

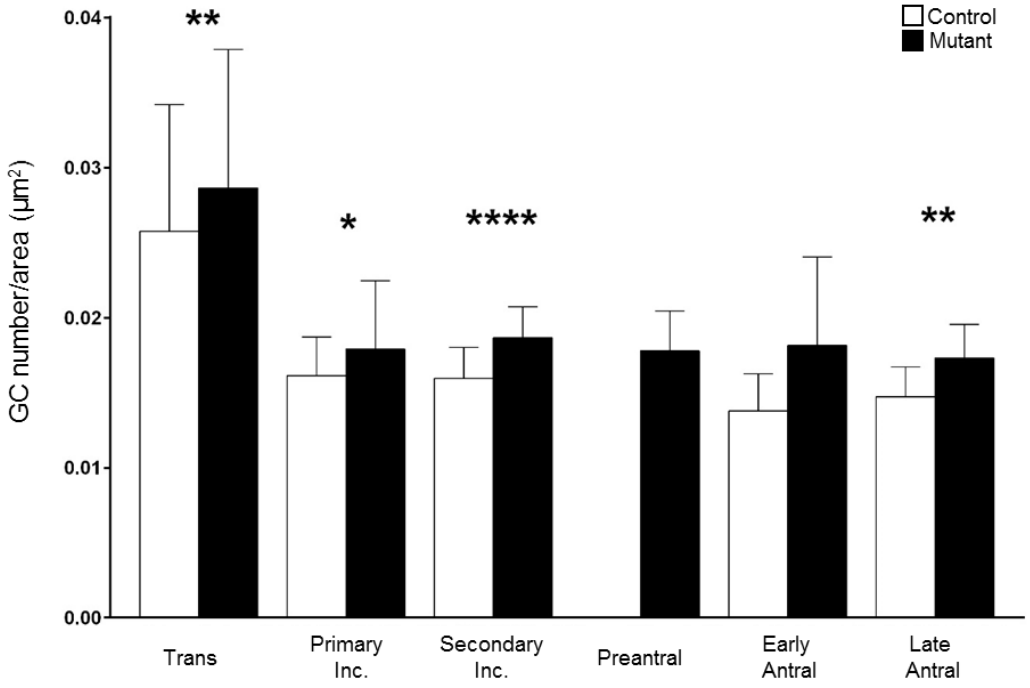

Figure 5.9. GC number per unit area of growing follicles in 3 week-old ovaries. GC numbers of follicles at each growing follicle stage. Trans; transitional, primary Inc; primary and primary plus, secondary Inc; secondary, secondary plus and secondary plus with antrum. For Control, n=4 ovaries, n=160 transitional, n=41 Primary Inc., n=18 Secondary Inc., n=6 Early antral and n=12 Late antral follicles. For Mutant, n=4 ovaries, n=134 transitional, n=37 Primary Inc., n=35 Secondary Inc., n=13 Preantral, n=7 Early antral and n=11 Late antral follicles. *p<0.05, **p<0.01; ****p<0.0001.

5.4.5 Large antral follicles from Mutant ovaries have larger theca cell layer compared to Controls.

Although the origin of the theca cell layer is not entirely understood (Young & McNeilly 2010), several scientific reports support the hypothesis that activated follicles secrete factors that induce theca cell recruitment and differentiation from ovarian stroma. To investigate the role of oocyte-produced core 1-derived *O*-glycans on the theca cell layer, the theca layer was measured in all growing follicles. The earliest stage that the theca layer is observable in both Control and Mutant is the Primary Inc. stage (Fig. 5.10),

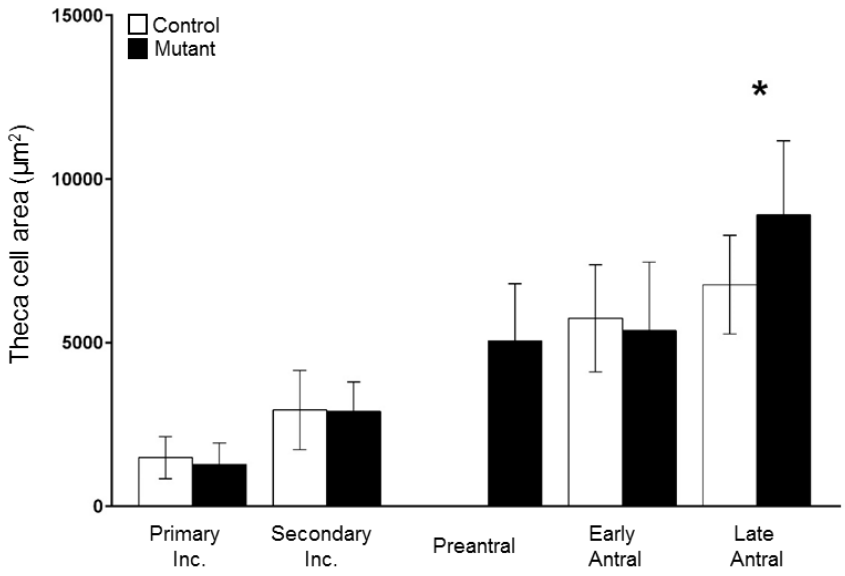

Figure 5.10. Size of the theca layer in growing follicles in 3 week-old ovaries.

Measurement of the area taken up by theca cells in growing follicles. Note that transitional follicles are not plotted, as they have not formed a theca cell layer yet. Primary Inc; primary and primary plus, secondary Inc; secondary, secondary plus and secondary plus with antrum. For Control, n=4 ovaries, n=160 transitional, n=41 Primary Inc., n=18 Secondary Inc., n=6 Early antral and n=12 Late antral follicles. For Mutant, n=4 ovaries, n=134 transitional, n=37 Primary Inc., n=35 Secondary Inc., n=13 Preantral, n=7 Early antral and n=11 Late antral follicles. *p<0.05.

and this is in agreement with other scientific reports (Peters 1969). The size of the theca layer is similar between Control and Mutant follicles in all growing follicle stages, up to Late antral follicles. At the Late antral stage, Mutant follicles have an increased size of theca cell layer compared to Controls.

5.5 DISCUSSION

Activation of primordial follicles and the process of follicle growth are complex developmental processes with a multitude of autocrine and paracrine factors acting on follicles. The role of oocyte-secreted factors (OSF) in regulating follicle development has become increasingly acknowledged and appreciated. In this chapter a detailed study of the role of oocyte-produced core 1-derived *O*-glycans on follicle dynamics and growth is undertaken, with novel findings for the importance of these glycans. In addition, the work undertaken in this Chapter has addressed a proposed hypothesis that the increased fertility phenotype in *C1galt1* Mutant mice is due to slower follicle growth which results in follicle accumulation and more available follicles for ovulation.

Total follicle number in Control and Mutant ovaries

Interestingly, *C1galt1* Mutant ovaries have increased numbers of medium-sized growing follicles (Secondary Inc. and Preantrals) compared to Controls at 3 weeks of age, which could be the result of (i) increased primordial follicle activation or (ii) decreased follicle apoptosis in medium-sized growing follicles. The ZP3 protein is reported to be expressed from the primary follicle stage onward (Philpott *et al.* 1987), therefore the *C1galt1* gene deletion occurs following primordial follicle activation; indeed, numbers of quiescent and small growing follicles at 3-weeks of age are similar between Control and Mutant ovaries. As a result, the observed increase in

medium-sized follicles is likely to be due to decreased follicle apoptosis compared to Controls, and not due to increased primordial follicle activation. Furthermore, according to the proposed model of prolonged follicle development in *C1galt1* Mutants (Williams & Stanley 2008) it would be expected that the Mutant has less Late antral follicles compared to Controls, as they would require longer time to reach that stage. In contrast, data presented in Fig. 5.5 show that the Mutant has similar numbers of Late antral follicles compared to Controls, suggesting that Mutant follicles are not growing slower than Controls.

As detailed in Section 5.3.4, follicle counts were done for every 40th section through mouse ovaries. Sampling at such a frequency could mean that counts of larger follicles (i.e. Antrals) carry a bigger error compared to counts of small follicles and therefore the data do not allow definitive conclusions regarding rates of follicle growth and follicle activation. An improved method of sampling would be to sample sections more frequently through the ovary, for example every 20th section.

Morphological changes in small growing follicles in the Mutant

As the oocyte-specific *C1galt1* deletion affects the whole follicle population, we next aimed to investigate whether follicle morphology is altered in the Mutant. The oocyte diameter in Control follicles are in agreement with other studies that show that oocytes in transitional follicles are ~17μm in diameter, reaching a maximum of ~70μm in antral follicles

(Carabatsos *et al.* 1998, Da Silva-Buttkus *et al.* 2008). Transitional follicles in Mutant mice are smaller than Controls, with smaller oocytes but equivalent GC numbers to Controls. Due to the stage-specific expression of the ZP3*Cre* transgene, *C1galt1* gene deletion is improbable in transitional follicles. Paracrine signalling is common in-between follicles therefore a possible explanation is that growing follicles in Mutant mice exert altered paracrine signalling on neighbouring activated primordial follicles, causing the observed changes in transitional follicles. As the GC number of Mutant transitional follicles is similar with Controls, it appears that potential paracrine signalling either (i) limits the growth of the oocyte relative to GC number, or (ii) induces more GC proliferation relative to oocyte size, compared with Controls. Transgenic female mice deficient in GDF9, an oocyte-secreted glycoprotein member of the TGF-β superfamily, have bigger oocytes with relation to follicle size, which could be due to (i) accelerated oocyte growth relative to GC number, or (ii) retardation of GC proliferation relative to oocyte growth (Dong *et al.* 1996, Carabatsos *et al.* 1998). *C1galt1* Mutant mice present an opposite pattern to GDF9$^{-/-}$ female mice, suggesting a modest elevation in GDF9 production by the oocyte compared to Controls. An increased GDF9:BMP15 ratio has been shown to be correlated with species with increased ovulation rates (Crawford & McNatty 2012). Indeed, *C1galt1* Mutant mice have an increased GDF9:BMP15 ratio (mRNA levels) at diestrus (Grasa *et al*. 2015). The results presented here suggest that a modest elevation of GDF9 causes (i) slower oocyte growth in small growing follicles in the Mutant or (ii) accelerated GC proliferation. To determine the

precise effects of GDF9 on growth of small follicles, small follicles could be cultured *in vitro* with increasing doses of GDF9 and quantification of the effects that GDF9 has on follicle growth with time (e.g. oocyte diameter, GC number etc).

Retardation of Mutant oocyte growth is observable up until the Secondary Inc. follicle stage suggesting that core 1-derived *O*-glycans are required for optimum oocyte growth, at least for the small growing follicles. Surprisingly, even though follicles up to the Secondary Inc. stage in the Mutant have smaller oocytes, the GCs that surround the oocyte are found at similar number as Controls, suggesting a change in the relationship between the oocyte and surrounding somatic cells.

Morphological changes in large growing follicles in the Mutant

Mutant follicles at the Late antral stage are bigger in size compared to Controls. Further investigation into the Mutant Late antral follicles, revealed that their bigger size is the result of both more GCs and larger theca cell layer. These results raise 2 questions, (1) why do Mutant Late antral follicles have a bigger theca layer, and (2) why do Mutant Late antral follicles have more GCs compared to Controls? With relation to question (1), studies performed *in vitro* have shown that GCs have the capability to induce theca cell differentiation and recruitment from ovarian stromal cells (Orisaka *et al.* 2006, Young & McNeilly 2010). Therefore, the presence of a larger theca layer in combination with more GCs in the *C1galt1* Mutant supports the role

of GCs in theca cell recruitment. With relation to question (2), it has been shown that culture of goat preantral follicles with GDF9 improves follicular growth rate to antral follicles, i.e. the diameter of antral follicles treated with GDF9 is bigger than controls (Almeida *et al.* 2011). In *C1galt1* Mutant Late antral follicles a similar improvement in follicle size is observed as in goats. The results presented here provide further evidence of elevated GDF9 levels in Mutant oocytes, as well as showing that GDF9 has potentially similar roles in promoting late follicle growth as in goats.

Conclusion

In conclusion, results presented in this chapter indicate novel roles of oocyte-produced *C1galt1* on inter-follicular communication, evident from the fundamental differences in Mutant transitional follicles. Furthermore, oocyte *C1galt1* plays a significant role in the development of the growing follicle population, as ablation of this gene from oocytes alters follicle numbers at specific stages. A hypothesis was proposed in 2008, suggesting that the increased fertility phenotype in *C1galt1* Mutant mice is due to slower follicle growth; work presented in this chapter provides evidence that the hypothesis is not correct. Lastly, through detailed analysis of follicle characteristics, it has become apparent that oocyte *C1galt1* has a central role in defining key aspects of follicle development (e.g. oocyte size, GC number, theca layer size) throughout the entire growing phase of follicles.

Chapter 6: Investigating the mechanism of increased fertility in C1galt1 Mutant mice: part I

Assessment of apoptosis

6.1 INTRODUCTION

Ovarian follicle development is regulated by a multitude of factors including endocrine, paracrine and autocrine signals. The process of follicle development refers to the growth of a primordial follicle to a pre-ovulatory follicle; however, most ovarian follicles will never complete this developmental process. From the population of both resting and growing follicles, more than 99.9% follicles in humans (Baker 1963) and rats (Beaumont & Mandl 1962) will undergo atresia before successfully ovulating an egg.

The characteristics of atretic follicles suggest that follicle atresia is mediated via apoptosis and not necrosis (Hsueh *et al.* 1994). Apoptosis is programmed cell death and cellular apoptosis is characterised by membrane blebbing, activation of caspases and DNA fragmentation, the latter being the hallmark of apoptosis (Wyllie *et al.* 1980, Duke *et al.* 1983). Apoptosis in follicles is thought to result from depletion of cell survival factors (e.g. steroids, gonadotrophins and local ovarian factors, discussed in Chapter 1.1.3) and exposure to atretogenic factors, such as the FAS ligand and FAS system and members of the B-cell lymphoma 2 (Bcl2) family of proteins (Tsujimoto *et al.* 2001a, van Delft & Huang 2006, Taylor *et al.* 2008).

The Bcl2 protein family comprises a large number of both pro- and anti-apoptotic members, whose interplay with one-another is crucial in regulating mitochondrial cytochrome c release, and subsequent apoptosome assembly (Taylor *et al*. 2008). Two members of this family, Bcl2 and Bax,

were selected for assessment in Control and *C1galt1* Mutant mice as they are the best characterised from the family and their role in ovarian cell survival has been established *in vivo*, using several rodent models.

Bcl2 is an anti-apoptotic protein that promotes cell-survival (Vaux et al, 1988). Bcl2-deficient mice have decreased numbers of healthy primordial follicles compared to controls, and increased numbers of primordial follicles with atretic or absent oocytes (Ratts *et al.* 1995). Bcl2 overexpression in mouse oocytes from primary follicles onward results in more, healthy growing follicles and less atretic growing follicles compared to Controls (Morita et al, 1999). Bcl2 overexpression in mouse granulosa cells (GCs) leads to decreased levels of ovarian apoptotic DNA fragmentation (Hsu *et al.* 1996).

Bcl2–associated X protein (Bax) is a pro-apoptotic molecule (7). Bax-deficient mice have more primordial follicles and more growing follicles at both the start of post-pubertal life and at 20 months of age (Perez *et al.* 1999). The increased number of healthy follicles was accompanied by reduced follicle atresia in Bax-deficient mice compared to Controls, assessed by morphological analysis, highlighting the crucial role of Bax as an apoptosis-inducing molecule.

Bcl2 and Bax can form homodimeric or heterodimeric complexes (Oltvai *et al.* 1993). The varied interactions between the 2 molecules and the ratio of Bcl2 to Bax has been shown to determine cell susceptibility to apoptosis (Raisova *et al.* 2001, Salakou *et al.* 2007); a lower ratio, and thus dominance of Bax over Bcl-2, denotes accelerated apoptosis.

The abovementioned link between increased follicle numbers and decreased levels of follicle atresia prompted us to investigate follicle atresia in the *C1galt1* Mutant, as the oocyte-specific *C1galt1* deletion results in increased numbers of healthy growing follicles (Williams & Stanley 2008).

In an effort to explain the increased numbers of growing follicles in *C1galt1* Mutant mice, previous assessment of 3 week-old Control and Mutant ovaries was done which indicated increased numbers of growing follicles and decreased levels of apoptosis through assessment of DNA fragmentation (Williams & Stanley 2008). However, the results obtained from these pre-pubertal mice should be used with caution when trying to explain the increase in growing follicle numbers. This is because ovarian dynamics and follicle development at 3 weeks of age in mice is not reflective of the dynamics in post-pubertal mice, which is when the increase in follicle numbers is observed.

Assessment of the healthy follicle population in post-pubertal Mutant mice revealed increased numbers of growing follicles compared to Controls (Grasa *et al*. 2015). A link between levels of *O*-glycosylation and cell apoptosis was made in a pancreatic cell line *in vitro*, when general inhibition of *O*-glycosylation led to reduced cell apoptosis, assessed by DNA fragmentation (D'Alessandris *et al.* 2004). Therefore, as *O*-glycosylation *can* modify cell apoptosis, we hypothesise that the growing follicles in the post-pubertal Mutant have lower levels of apoptosis compared to Controls, which enables them to persist in the ovary and ovulate more fertilisable eggs.

The results presented in this chapter are based on raw data generated by the author that have been published in a different format (Appendix B).

6.2 AIMS

- To assess the effect of the oocyte *C1galt1* mutation on follicle apoptosis in post-pubertal mice by detection and quantification of DNA degradation (using TUNEL assay) in a follicle-specific and estrous stage-specific manner.

- To investigate whether the oocyte *C1galt1* mutation affects the mechanism of follicle apoptosis by assessment of Bcl2 and Bax molecules.

6.3 MATERIALS AND METHODS

6.3.1 Tissue collection

Ovaries from 8- to 10-week-old Control and Mutant mice were collected at each stage of the estrous cycle, fixed in 10% buffered formalin (Sigma-Aldrich, Dorset, UK) for 8 h, and washed in 70% ethanol. Ovaries were embedded in paraffin, sectioned at 5 μm and mounted on glass slides.

Estrous cycle evaluation from Grasa *et al*. 2015 (not performed by author)

The estrous cycle of female mice has 4 distinct stages (proestrus, estrus, metestrus, and diestrus) identified by the analysis of the cell types present in the vagina (Nelson *et al.* 1982). Estrus cyclicity was evaluated in 8- to 10-wk-old Control and Mutant females by daily analysis of vaginal smears collected between 8:00 and 10:00 am. Vaginal cell smears were obtained by rinsing the vagina with 100 ml of 0.9% sodium chloride. This was placed on a glass slide, air dried, and stained with Giemsa (Sigma-Aldrich, Dorset, United Kingdom). Cell type was evaluated, and the stage of the estrous cycle was determined. During diestrus, vaginal washes were characterized by high leukocyte content, whereas during proestrus nucleated epithelial cells appear. Estrus was identified by the presence of cornified enucleate epithelial cells, and in metestrus leukocyte infiltration starts.

Smears were used to establish that an animal was having regular cycles, as evidenced by at least 2 complete estrous cycles, before sample collection.

6.3.2 TUNEL assay

Apoptosis was detected using terminal deoxynucleotidyl transferase-mediated nick end labeling (TUNEL) staining (Apoptag kit; Chemicon, Temecula, CA, USA) of ovarian sections. Sections were deparaffinised and rehydrated as described in Chapter 2.3. Antigen retrieval was performed using 20mg/ml of Proteinase K (Roche Diagnostics, Welwyn Garden City, Hertfordshire, United Kingdom) for 15 min at room temperature. Endogenous peroxidase was blocked with 3% H_2O_2 (Thermo Fisher Scientific) in PBS for 5 min. Equilibration buffer (Apoptag kit) was added to the sections for 10 min at room temperature. Sections were then incubated with 30% terminal deoxynucleotidyl transferase enzyme (Apoptag kit) in reaction buffer for 1 h at 37°C. Control sections were incubated with reaction buffer only. All sections were then incubated with Stop/Wash buffer (Apoptag kit) for 10 min at room temperature, and then anti-digoxigenin conjugate (Apoptag kit) was added to the sections for 30 min at room temperature. Antigen-specific detection was revealed using a DAB kit (Vector Laboratories). Slides were then dehydrated, mounted with Depex, and imaged under the same microscope conditions (Leica DM 2500; Microscope Services Ltd.).

6.3.3 Immunohistochemistry (IHC) for Bcl2 and Bax detection

The general protocol for IHC was followed as described in Chapter 2.3, with additional specific details provided in Table 6.1.

Table 6.1. Specific details of IHC protocol used for detection of Bcl2 and Bax to complement the basic method described in Chapter 2.3.

	Molecule detected	
	Bcl2	**Bax**
Antigen retrieval	None	
Block agent	10% dry milk, 1 h	5% BSA, 1 h
Primary antibody	rabbit anti-mouse Bcl2 polyclonal (PRS3335; Sigma-Aldrich) at 1:50, 4^{o}C overnight	rabbit anti-mouse Bax polyclonal (SAB4502549; Sigma-Aldrich) at 1:100, 4^{o}C overnight
Secondary antibody	anti-rabbit IgG (Vectastain ABC Elite Kit, Vector Laboratories), 1 h at RT	

6.3.4 Classification of follicles assessed for apoptosis

Only morphologically healthy follicles sectioned through the oocyte, to enable consistent follicle staging, were analyzed. Slides were counterstained with Hematoxylin (method described in Chapter 2.4) and re-imaged to enable visualization of follicle histology and cell boundaries. The criteria for

classification of follicles up to the Preantral stage are described in Chapter 5.3.2. Classification of Early antral and Late antral follicles is based on the methodology outlined in Chapter 5.3.3.

6.3.5 Quantification of TUNEL, Bcl2 and Bax staining

Assessment of GC staining for DNA fragmentation (TUNEL), Bcl2 and Bax was carried out. To quantify TUNEL assay, Bcl2 and Bax in follicles, mean pixel intensity (MPI) of the GCs of individual follicles (excluding antrum and oocyte) was determined using ImageJ (National Institutes of Health, Bethesda, MD, USA).

6.3.6 Determination of Bcl2/Bax ratio

Experiments were designed as to allow Bcl2 and Bax staining in the same follicles in consecutive sections which then permitted the determination of the Bcl2/Bax ratio in individual follicles.

6.3.7 Statistical analysis

A minimum of 3 IHC experiments were done for all antigenic reactions presented (i.e. TUNEL, Bcl2 and Bax). Data are presented as mean ± SD. Statistical comparisons were performed using Prism GraphPad software version 6.0 (GraphPad Software, La Jolla, CA, USA). An unpaired *t*-test was

used for normally-distributed data. A Mann-Whitney test was used for non normally-distributed data. Differences were considered significant when $p<0.05$.

6.4 RESULTS

6.4.1 *C1galt1* Mutant follicles have lower levels of apoptosis compared to Controls at metestrus.

To investigate whether follicle atresia is altered in the hyperfertile *C1galt1* Mutant (Williams *et al*. 2007; Grasa *et al.* 2015), apoptosis was assessed by detection of DNA fragmentation (TUNEL assay) in granulosa cells (GCs). Ovarian sections that were not incubated with the terminal deoxynucleotidyl transferase enzyme (and therefore negative for TUNEL detection) showed no immunoreactivity (Fig. 6.1A) whereas sections incubated with the enzyme showed TUNEL staining (Fig. 6.1B).

Follicles with varied levels of TUNEL staining intensity were observed at all follicle stages analysed (Fig. 6.1C-F). Follicles with clear histological signs of atresia (e.g. oocyte membrane blebbing) had elevated TUNEL staining in GCs (Fig. 6.1F).

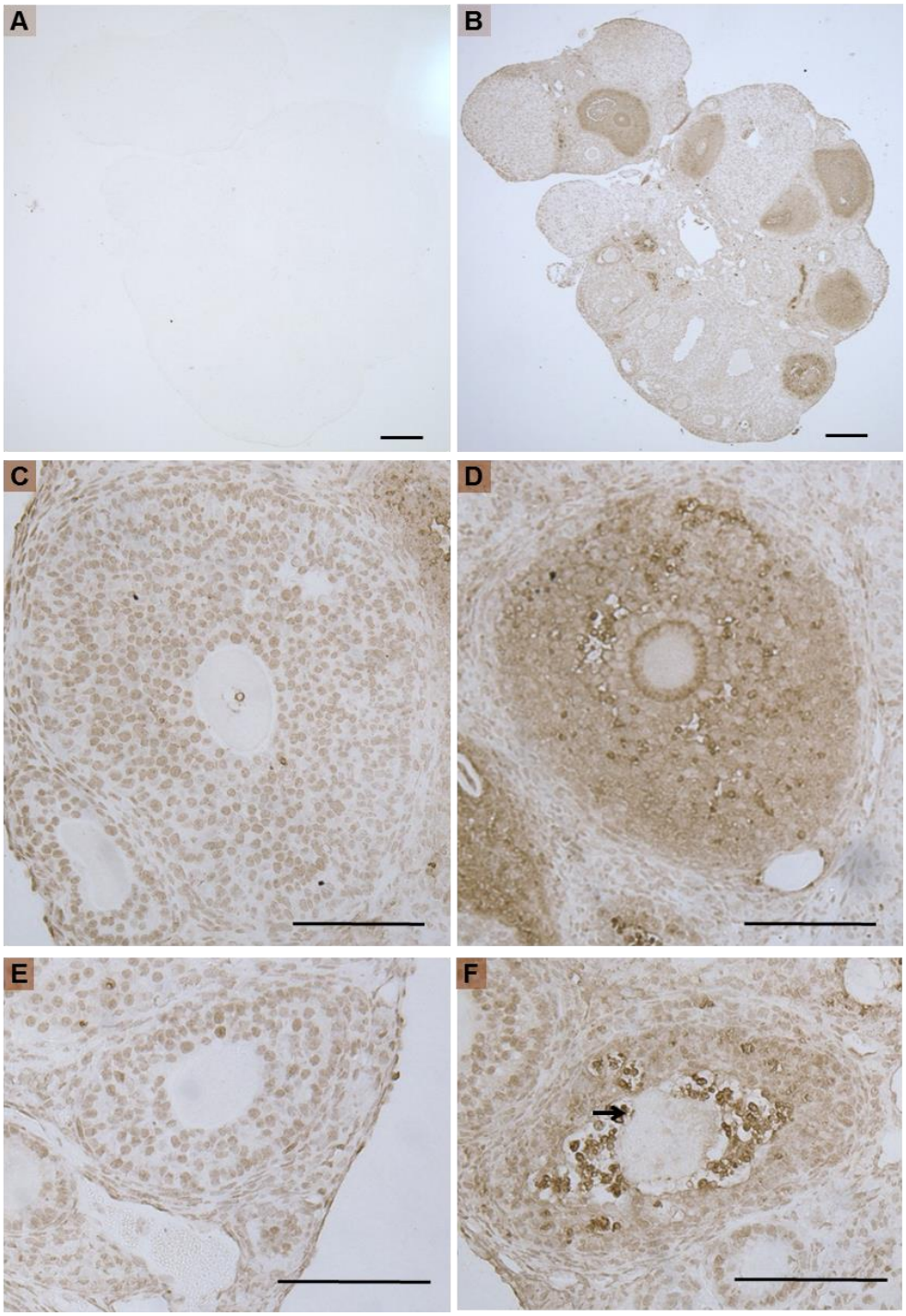

Figure 6.1. Ovarian sections from Control and Mutant mice showing follicles undergoing apoptosis as assessed by TUNEL. (A) Control (no enzyme) section. Scale bar: 200μm. (B) TUNEL enzyme- treated section. Scale bar: 200μm. Antral follicle with (C) undetected levels of apoptosis, and (D) elevated levels of apoptosis. Preantral follicle with (E) undetected levels of apoptosis, and (F) marked levels of apoptosis and oocyte membrane blebbing (arrow). For C-F scale bar: 100μm.

As post-pubertal mice are hormonally cycling and levels of apoptosis may fluctuate depending on the specific stage of the estrous cycle, apoptosis was assessed at 2 stages; proestrus (the day before ovulation) and metestrus (midway through 4-day cycle).

At proestrus, the levels of TUNEL staining were similar when comparing Control and Mutant follicles at each follicle stage (Fig. 6.2A). There was, however, an increase in TUNEL staining intensity in Early antral Control follicles compared to Preantral Controls, which was absent from Mutant follicles. At metestrus, Secondary Inc. and antral follicles (Early antral and Late antral) in the Mutant had lower levels of apoptosis compared to Controls (Fig. 6.2B).

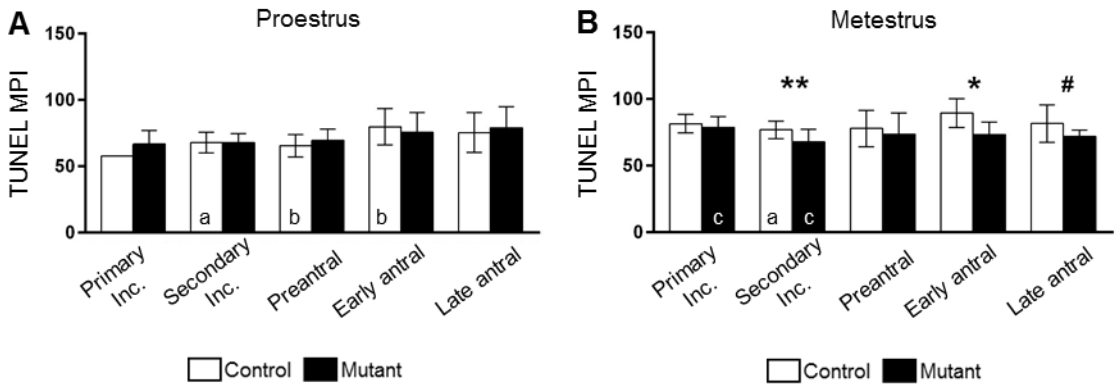

Figure 6.2. Assessment of apoptosis by the use of TUNEL assay at different stages of follicle development at proestrus and metestrus. Mean pixel intensity (MPI) of TUNEL staining in follicles of mice at (A) proestrus and (B) metestrus. Asterisks and hash indicate the following *p* values, between the Control and Mutant data at that stage of follicle development at that stage of the estrous cycle: **p*<0.05, ***p*<0.01, $^{\#}p$=0.06. Comparisons were made between follicle types both within each estrous stage and across the 2 stages. Columns with the same letter differed according to the following *p* values: a, b, c, *p*<0.05. Control, n=4 mice, n=47 follicles at proestrus and n=66 follicles at metestrus; Mutant, n=4 mice, n=49 follicles at proestrus and n=46 follicles at metestrus.

6.4.2 Oocyte-specific *C1galt1* deletion affects Bcl2 regulation in surrounding granulosa cells.

Having established that oocyte-specific *C1galt1* deletion affects follicle apoptosis, we next aimed to investigate the molecular basis for this alteration. The levels of the anti-apoptotic molecule Bcl2 were assessed in granulosa cells (GCs) (Fig. 6.3A-C), as increased Bcl2 levels promote growing follicle survival and reduce levels of apoptosis (Hsu *et al.* 1996, Morita *et al.* 1999).

The levels of Bcl2 detected in Control follicles were consistent at all stages of development at proestrus (Fig. 6.3D). The same was evident at metestrus (Fig. 6.3E), but surprisingly, the levels at metestrus were approximately twice those at proestrus ($p<0.0001$). In Mutant follicles, a similar rise in Bcl2 intensity from proestrus to metestrus was not observed. There was, however, decreased intensity detected at the Late antral follicles at metestrus compared to proestrus.

In addition, at proestrus, Mutant Primary Inc., Secondary Inc. and Late antral follicles had increased Bcl2 staining intensity compared to Controls (Fig. 6.3D) whereas this pattern was reversed at metestrus, where Mutant follicles had decreased Bcl2 levels compared to Controls (Fig. 6.3E). Fig. 6.3F compares Bcl2 levels for Control follicles at proestrus and metestrus.

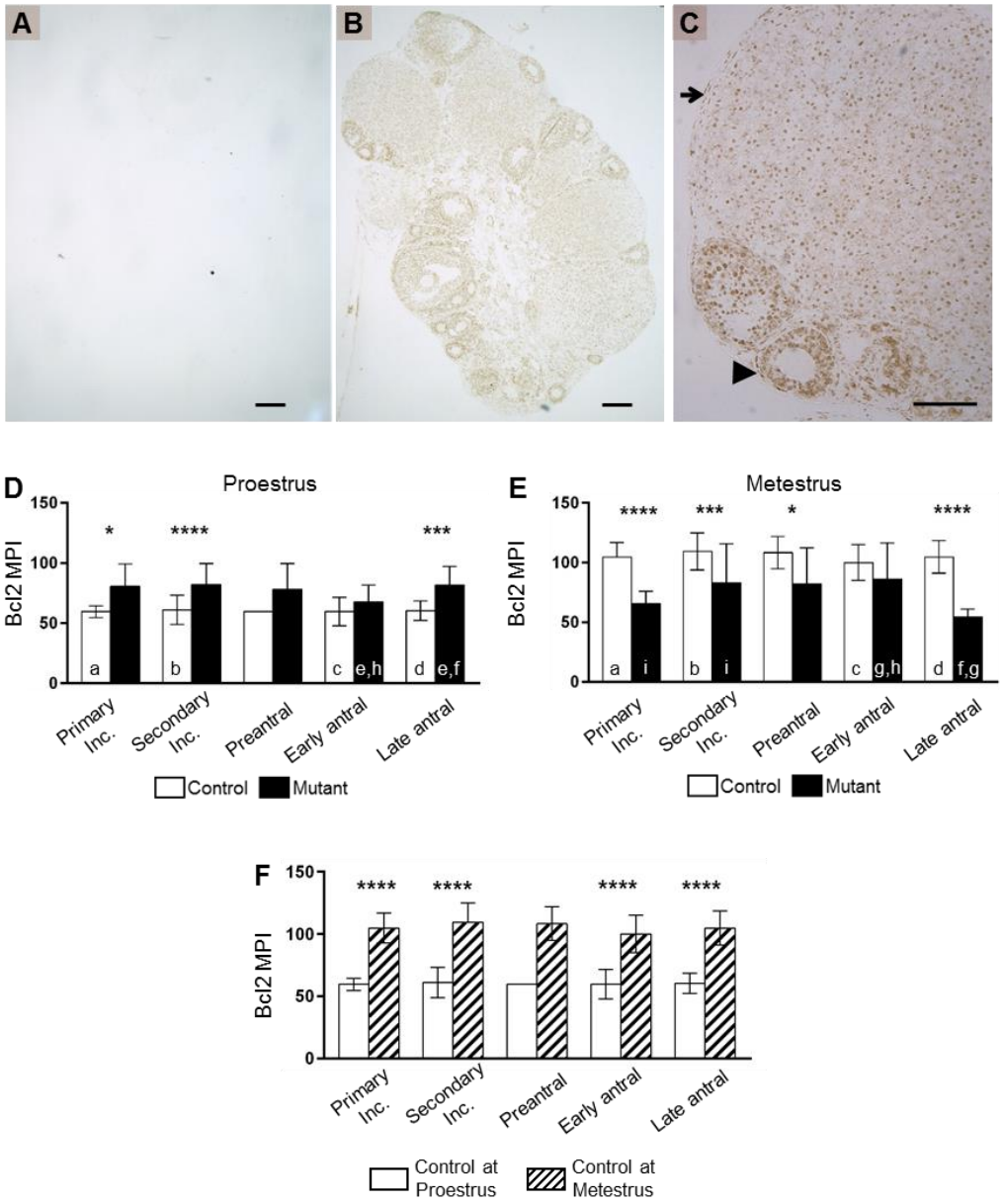

Figure 6.3. Analysis of Bcl2 levels at different stages of follicle development at proestrus and metestrus. (A) Control (no antibody) section. Scale bar: 200μm. (B) Bcl2 antibody-treated section. Scale bar: 200μm. (C) Higher magnification of a Bcl2 antibody-treated section. Note differential Bcl2 staining pattern between small growing follicles (arrowhead) and a corpus lutem (arrow). Scale bar: 100μm. Mean pixel intensity (MPI) of Bcl2 staining in follicles of mice at (D) proestrus, (E) metestrus and (F) Control follicles at proestrus and metestrus. Asterisks indicate the following *p* values, between the Control and Mutant data at that stage of follicle development at that stage of the estrous cycle: *p<0.05, ***p<0.001, ****p<0.0001. Comparisons were made between follicle types both within each estrous stage and across the 2 stages. Columns with the same letter differed according to the following *p* values: e, i, h, p<0.05; g, p<0.01; f, p<0.001; a, b, c, d, p<0.0001. Control, n=4 mice, n=44 follicles at proestrus and n=85 follicles at metestrus; Mutant, n=4 mice, n=81 follicles at proestrus and n=62 follicles at metestrus.

6.4.3 Oocyte-specific *C1galt1* deletion affects Bax regulation in surrounding granulosa cells.

Following the assessment of Bcl2 levels, we examined a pro-apoptotic member of the Bcl2 family proteins, Bax (Fig. 6.4A-C). Bax was selected due to reported Bax involvement in promoting follicle atresia (Perez *et al.* 1999).

Bax levels at proestrus in Control follicles at the Secondary Inc., Preantral and Early antral stages were lower compared to Mutant follicles at proestrus (Fig. 6.4D). They were also lower when compared to the same stage Control follicles at metestrus (Fig. 6.4E). The observed differences in Bcl2 levels in Control follicles between proestrus and metestrus suggest estrous stage-specific expression of Bcl2; the absence of such a pattern in Mutant follicles suggests altered Bcl2 expression, at least in the 2 stages of estrous studied.

Mutant Early antral follicles at metestrus exhibited lower levels of Bax staining both compared to Control Early antral follicles at metestrus, but also compared to Mutant Early antral follicles at proestrus (Fig. 6.4E).

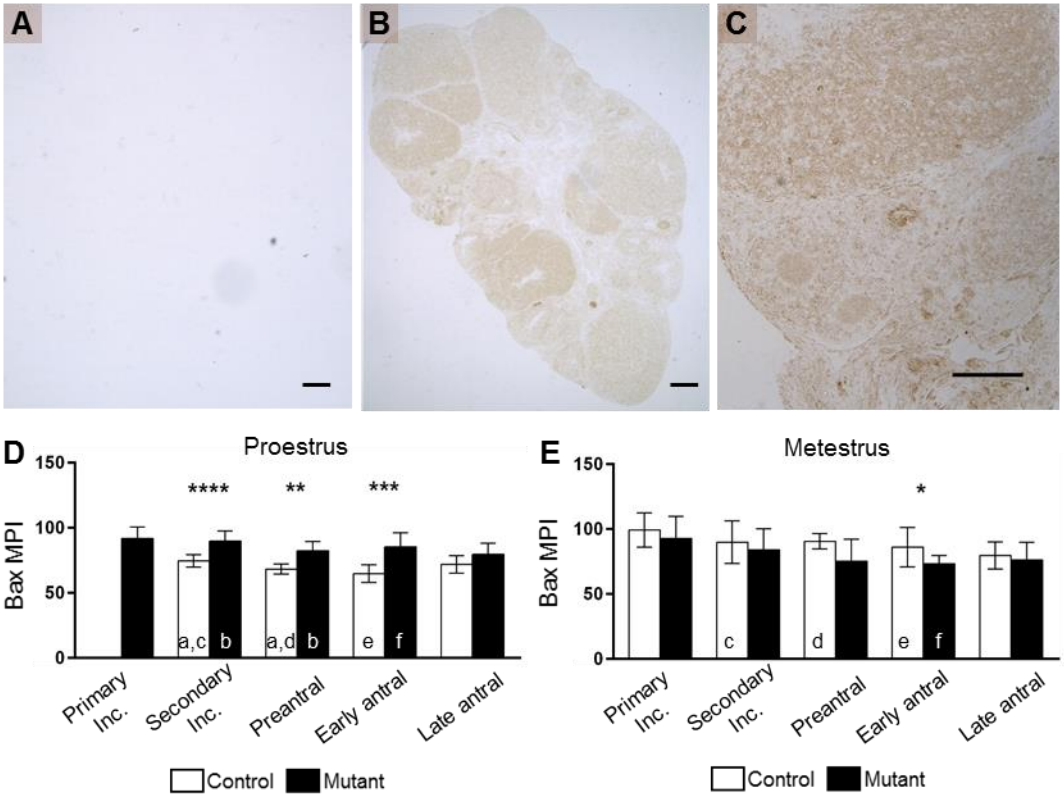

Figure 6.4. Analysis of Bax levels at different stages of follicle development at proestrus and metestrus. (A) Control (no antibody) section. Scale bar: 200μm. (B) Bax antibody-treated section. Scale bar: 200μm. (C) Higher magnification of a Bax antibody-treated section. Scale bar: 100μm. Mean pixel intensity (MPI) of Bax staining in follicles of mice at (D) proestrus and (E) metestrus. Asterisks indicate the following *p* values, between the Control and Mutant data at that stage of follicle development at that stage of the estrous cycle: **p*<0.05, ***p*<0.01, ****p*<0.001, *****p*<0.0001. Comparisons were made between follicle types both within each estrous stage and across the 2 stages. Columns with the same letter differed according to the following *p* values: a, b, f, *p*<0.05; d, e, *p*<0.01; c, *p*<0.0001. Control, n=4 mice, n=28 follicles at proestrus and n=62 follicles at metestrus; Mutant, n=4 mice, n=66 follicles at proestrus and n=52 follicles at metestrus.

6.4.4 *C1galt1* Mutant follicles have altered ratio of Bcl2 and Bax molecules, compared to Controls.

Although the patterns of anti-apoptotic Bcl2 and pro-apoptotic Bax detection indicate clear stage-specific regulation of both molecules in Controls and Mutants, the intracellular ratio between these 2 molecules has been shown to determine the vulnerability of cells to apoptosis (Yang & Korsmeyer 1996). A follicle stage-specific assessment of the Bcl2/Bax ratio in mouse ovaries has not been reported in literature, therefore here we aimed to investigate this relationship within Control mice and Mutant mice.

Analysis of the intrafollicular ratio of Bcl2/Bax was based on fewer numbers of follicles compared with follicles analyzed for Bcl-2 or Bax because not all follicles were present in consecutive sections, and thus Preantral, Primary Inc. and Secondary Inc. follicles were grouped together.

At proestrus, the individual levels of Bcl2 and Bax were similar for Control follicles at all stages (Fig. 6.3D and Fig 6.4D respectively), therefore it was unsurprising to find that the ratio of Bcl2/Bax in Controls did not differ between follicle stages at proestrus (Fig. 6.5A). The same pattern is observed at metestrus, where the Bcl2/Bax ratio is not different between follicle stages in Control (Fig. 6.5B). However, the Bcl2/Bax ratio is consistently elevated in all Control follicle stages at metestrus compared to proestrus.

At proestrus, a rise in Bcl2/Bax ratio was observed from the Early antral to Late antral Mutant follicles which supports their enhanced survival

prior to ovulation. In Mutant follicles, the Bcl2/Bax ratio did not differ between follicle stages at metestrus (Fig. 6.5B) similar to the pattern in Controls at metestrus, but the ratio was lower than Controls. Fig. 6.5C shows the comparison of the Bcl2/Bax ratio for Control follicles at proestrus and metestrus.

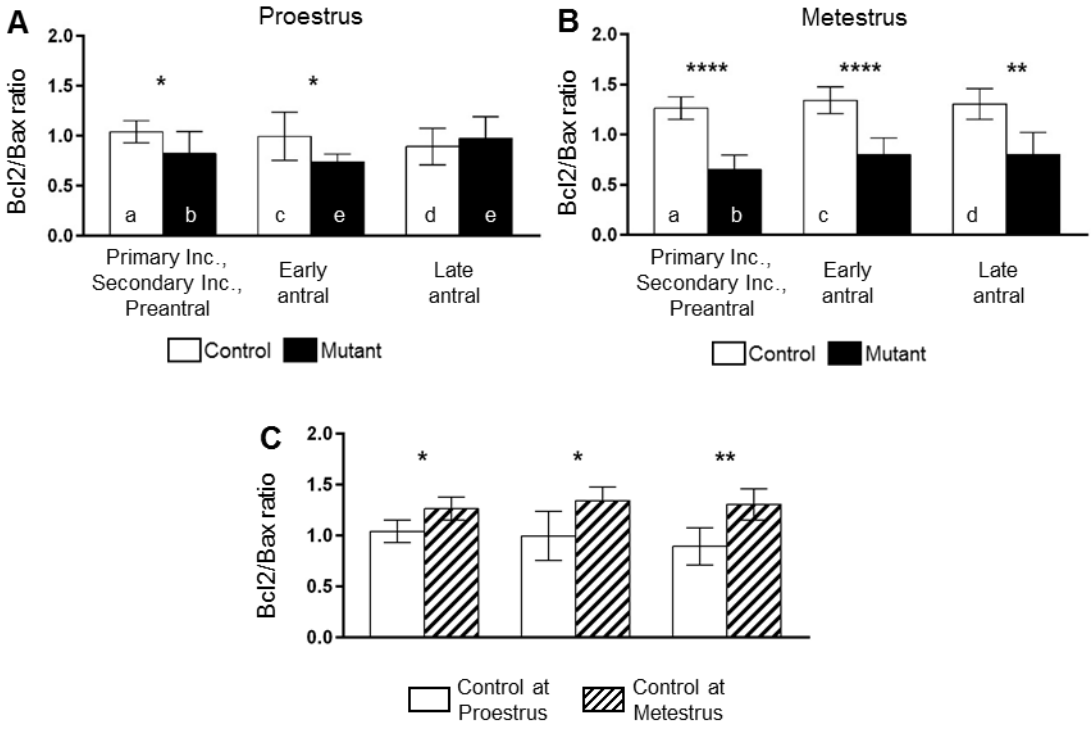

Figure 6.5. Ratio of Bcl2 to Bax detected in follicles of Control and Mutant mice at proestrus and metestrus. (A) Bcl2/Bax ratio at proestrus. (B) Bcl2/Bax ratio at metestrus. (C) Comparison of Bcl2/Bax ratio for Control follicles at proestrus and metestrus. Asterisks indicate the following *p* values, between the Control and Mutant data at that stage of follicle development at that stage of the estrous cycle: **p*<0.05, ***p*<0.01, *****p*<0.0001. Comparisons were made between follicle types both within each estrous stage and across the 2 stages. Columns with the same letter differed according to the following *p* values: a, b, c, e, *p*<0.05; d, *p*<0.01. Control, n=4 mice, n=16 follicles at proestrus and n=36 follicles at metestrus; Mutant, n=4 mice, n=17 follicles at proestrus and n=22 follicles at metestrus.

6.5 DISCUSSION

Mammalian ovarian follicle development is characterised by cell growth, proliferation and differentiation but also by high levels of follicle atresia as a result of cell apoptosis. Atresia is a characteristic of follicles at all stages of follicle development in mice (Gosden *et al.* 1983). The transition of Preantral follicles to an Early antral appears to be the critical point at which the fate of a follicle is decided, as the majority of growing follicles undergo atresia at this transition point (Hirshfield & Midgley 1978, Hirshfield 1988).

Although a lot of evidence exists regarding follicle-specific atresia at all stages of follicle development, the precise mechanisms and pathways involved in follicle apoptosis are unclear. Here, we hypothesised that the increased number of growing follicles in the post-pubertal Mutant is due to lower levels of apoptosis compared to Controls, therefore we investigated the role of oocyte produced *O*-glycans on granulosa cell (GC) apoptosis.

Assessment of follicle atresia

The study of follicular atresia is challenging due to (i) the number and (ii) the variety of follicles in the ovary at any given time, but also (iii) the hormonally cycling environment of the species studied.

Hirshfield and Midgley (1978) assessed the incidence of follicle atresia in cycling rats, however their experimental design was limited because even though rat ovaries were categorised based on their estrous stage, an n<3

samples per estrous stage (often n=1 per estrous stage) is not sufficient to draw convincing conclusions (Hirshfield & Midgley 1978). In addition, follicles were classified as atretic solely based on morphological criteria, with follicles of 2 or more pyknotic cells considered as atretic; however, the presence of a small number of pyknotic cells might not necessarily imply follicular atresia as cell pyknosis has been reported to be part of normal cellular homeostasis (Van Wezel *et al.* 1999, Rosales-Torres *et al.* 2000). Lastly, follicles were classified based on their diameter, whereas considering the complex and multi-dimensional nature of follicle development a more sophisticated classification system would be more appropriate.

Work from a different group reported the proportion of atretic to healthy follicles in 2-month old mice (Gosden *et al.* 1983). Even though follicles were classified based on the widely accepted Pedersen and Peters classification system (Pedersen & Peters 1968), numbers per follicle stage were from cycling mice of undefined estrous stage. Therefore, it is not possible to conclude estrous stage-specific changes in follicle atresia.

Conversely, a study with rat ovaries assessed the numbers of atretic follicles for each day of the estrous cycle (n=5 samples per group) but presented combined atretic follicle numbers without follicle classification according to stage (Hirshfield 1988).

In this Chapter, follicle atresia has been studied as a function of DNA fragmentation in the mouse in such a way as to consider all the abovementioned factors, i.e. in a follicle-specific manner at particular stages

of the estrous cycle. The detection of DNA fragmentation (by means of the TUNEL assay) was used to assess the incidence of follicle apoptosis, as the cleavage of genomic DNA is considered the hallmark of apoptosis (Wyllie, 1980; Duke *et al*. 1983).

In order for *C1galt1* Mutant mice to have more growing follicles post-pubertally (Williams & Stanley 2008) there has to be a decrease in apoptosis in the growing follicle pool. This is because expression of Cre recombinase (which deletes exons 1 and 2 of *C1galt1*) is under the ZP3 promoter; ZP3 is first expressed in primary follicles, and thus in *C1galt1* Mutants the number of follicles leaving the quiescent pool should remain unaltered. Indeed, TUNEL analysis did reveal a decrease in apoptosis levels in Mutant follicles compared to Controls at metestrus. The observed decrease in TUNEL levels at metestrus in the Mutant accompanies the increased number of healthy growing follicles (Williams & Stanley 2008).

Several studies show that the largest incidence of atresia in growing follicles takes place from the transition of FSH-independent Preantrals to FSH-dependent Early antral follicles (Hirshfield & Midgley 1978, Dorrington *et al.* 1983). Data from Control mice presented in this Chapter support this observation, as there are increased levels of TUNEL staining at Early antral follicles compared to Preantrals at proestrus. *C1galt1* Mutant follicles do not exhibit such elevation in TUNEL staining from Preantral to Early antral follicles. This could be due to increased sensitivity to FSH at the Preantral to Early antral transition that could rescue Mutant follicles from atresia and aid in becoming pre-ovulatory. Indeed, *C1galt1* Mutant follicles cultured *in vitro*

show increased FSH sensitivity following the Preantral to Early antral transition (Grasa *et al.* 2015).

Assessment of Bcl2 and Bax levels

Anti-apoptotic Bcl2 and pro-apoptotic Bax molecules have vital roles in ovarian follicle selection as demonstrated *in vivo* in rodent models (Ratts *et al.* 1995, Hsu *et al.* 1996, Morita *et al.* 1999). Several attempts have been made in the past to elucidate the spatio-temporal expression pattern of Bcl2 and Bax in the rodent ovary. Analysis of whole rat ovaries revealed changes in both Bcl2 and Bax protein levels according to estrous stage, but the nature of the experiment did not allow follicle stage-specific analysis of levels of these proteins (Slot *et al.* 2006). Other studies report immunohistochemical approaches to assess changes in Bcl2 and Bax levels in various follicle stages but their approach to measure staining intensity has the limitation of being semi-quantitative (Slot *et al.* 2006, Gursoy *et al.* 2008).

Here, levels of Bcl2 and Bax proteins have been quantified from immunohistochemical detection, in a follicle stage- and estrous stage-specific manner in Control and *C1galt1* Mutant ovaries. In Control follicles there is marked elevation in Bcl2 and Bax levels from proestrus to metestrus for all growing follicle stages studied, indicating estrous stage-dependent regulation of apoptosis molecules.

However, in Mutant follicles, such variations in Bcl2 and Bax between the 2 stages of the estrous cycle were almost entirely eliminated. This could be due to altered intra-follicular regulation which arises directly from oocyte-specific deletion of *C1galt1.* Alternatively, the effects observed in Bcl2 and Bax levels could be an indirect response to the altered endocrine profile observed in *C1galt1* Mutant mice (Grasa *et al*. 2015). What is evident nonetheless from comparisons between the Control and Mutant data, is that oocyte-secreted core 1-derived *O*-glycans affect the levels of Bcl2 and Bax in surrounding GCs.

The ratio of Bcl2/Bax which has been reported to be important for cell fate determination (Oltvai *et al.* 1993) has not been previously studied in mouse ovaries in a follicle stage-specific manner. Here, we explored the Bcl2/Bax relationship in all growing follicles at proestrus and metestrus.

An astonishing and novel finding of this study is how firmly the Bcl2/Bax ratio is maintained in Control follicles at all stages of development, within proestrus and metestrus. Interestingly, metestrus Bcl2/Bax levels are higher than proestrus in Control follicles, suggesting cycle stage-specific changes in the expressed ratio of these molecules.

Considering that *C1galt1* Mutant ovaries have more growing follicles, we hypothesised an elevation of the Bcl2/Bax ratio which would support enhanced follicle survival. However, the Bcl2/Bax ratio was not elevated in Mutant follicles compared to Controls. At proestrus, the day preceding ovulation, Mutant Late antral follicles had increased Bcl2/Bax ratio compared

to Mutant Early antral follicles, and this increase could make Mutant follicles at the last stages of development less susceptible to apoptosis.

Conclusion

In conclusion, even though TUNEL assessment confirmed reduced follicle apoptosis in the Mutant, the levels of Bcl2 and Bax detected were not in agreement with the decreased apoptosis phenotype as would be expected from the literature. Other apoptosis-inducing pathways (e.g. the Fas-Fas ligand system, (Jose de los Santos *et al.* 2000)) may be leading to decreased follicle apoptosis as observed through TUNEL assessment. Alternatively, apoptosis has been reported to result from depletion of cell survival factors (e.g. estradiol), therefore an alteration in cell survival factors in the Mutant could be contributing to the increased fertility phenotype.

Chapter 7: Investigating the mechanism of increased fertility in *C1galt1* Mutant mice: part II

Assessment of regulation of follicle development

7.1 INTRODUCTION

In mammals, the process of ovarian follicle development is the result of a highly regulated balance between follicle survival and follicle atresia. In particular, granulosa cells (GCs) have been demonstrated both *in vivo* and *in vitro* to secrete a wide array of proteins that act both on GCs themselves (autocrine) and on neighbouring follicular cells (paracrine) to determine the follicle's survival fate.

Roles of estrogen in follicle survival

Among the many GC-produced proteins that promote cell survival are growth factors, sex steroids and cytokines (Tilly *et al.* 1992). Estrogen in particular has been studied extensively for its mitogenic and anti-apoptotic effects on follicular cells. Estrogen has been shown to increase GC proliferation both *in vivo* (Goldenberg *et al.* 1972), and *in vitro* (Goldenberg *et al.* 1972, Rao *et al.* 1978).

GCs synthesise estrogen from thecal androgens (Dorrington *et al.* 1975, Hillier & De Zwart 1981) catalysed by the enzyme aromatase (also known as CYP19); secretion of estrogen is greatly stimulated by FSH *in vitro* and *in vivo* (Erickson & Hsueh 1978). Collectively, research into GC estrogen biosynthesis led to the '2-cell 2-gonadotrophin' model, whereby theca cells produce androgens in response to LH (Fortune & Armstrong 1977) and the androgens then diffuse through the follicle basal lamina and into GCs. FSH

stimulates aromatase in GCs, and aromatase catalyses the conversion of androgens to estrogens (Dorrington *et al.* 1975).

The aromatase enzyme in the mature ovary has a specific spatial expression pattern. Aromatase expression in rats is undetectable in small and medium-sized growing follicles, and it is only expressed in large antral and preovulatory follicles (Guigon *et al.* 2003). Particulary, the expression and localisation of aromatase in rats has been shown to be highest in mural GCs closest to the basal lamina compared to levels in mural GCs lining the antrum and is undetectable in cumulus cells (Sakurada *et al.* 2006).

Roles of AMH in follicle survival

The glycoprotein anti-mullerian hormone (AMH) is a member of the TGF-β superfamily. Despite its role in mammalian fetal development as an inhibitor of Mullerian duct development (Munsterberg & Lovell-Badge 1991), AMH has central roles in ovarian function and follicle development.

AMH expression is restricted to the GCs of growing follicles (Hirobe *et al.* 1992, Salmon *et al.* 2004). Specifically, in the immature rat ovary, AMH mRNA is found evenly distributed in the GC population of follicles from the primary stage to the multi-layered preantral stage (Ueno *et al.* 1989, Hirobe *et al.* 1992). However, in antral follicles AMH immunolocalisation becomes heterogeneous with the highest signal detected in GCs closest to the oocyte. AMH localisation in pre-ovulatory follicles is at low levels, predominantly from

the cumulus cells that are closest to the oocyte. Atretic follicles (assessed by morphological observation) do not show AMH presence (Ueno *et al.* 1989).

The role of AMH in the post-natal mammalian ovary became clear from studies of female $AMH^{-/-}$ mice and *in vitro* studies. AMH-deficient female mice have a severely depleted primordial follicle pool and more growing follicles at 4 months of age (Durlinger *et al.* 1999), indicating a role of AMH in inhibiting primordial follicle activation. Also, *in vivo* and *in vitro* studies reveal that AMH causes inhibition of the FSH-stimulated growth of preantral follicles to antral follicles (di Clemente *et al.* 1994, Durlinger *et al.* 1999).

Roles of the oocyte on estrogen and AMH production by GCs

Despite the hugely important involvement of GCs and GC-produced factors in follicle survival, the oocyte has been demonstrated to have a central role in GC development and function and therefore the oocyte actively participates in determining the follicle's survival status (for a wider discussion of the role of the oocyte on follicle development, see Chapter 1.1).

Particularly, the oocyte regulates the steroidogenic function of the follicle, despite the fact that the oocyte itself is not steroidogenic (Vanderhyden & Tonary 1995). *In vitro* studies show that oocytectomised complexes secrete less estradiol compared to intact oocyte-granulosa complexes, highlighting the role of the oocyte in inducing estradiol secretion (Vanderhyden & Tonary 1995). AMH production by GCs is also enhanced by

oocytes since cultured GCs produce more AMH in the presence of oocytes (Salmon *et al.* 2004).

Hypotheses and C1galt1 Mutant

Assessment of the follicle population in post-pubertal *C1galt1* Mutant mice revealed increased numbers of growing follicles compared to Controls (Grasa *et al*. 2015). In addition, work presented in Chapter 6 shows that Mutant follicles have lower levels of apoptosis. As estradiol has both pro-survival and anti-apoptotic roles, we first hypothesised that there is elevated estradiol in Mutant follicles compared to Controls.

Our second hypothesis is related to the elevated FSH sensitivity of follicles from *C1galt1* Mutant mice *in vitro* (Grasa *et al*. 2015). As AMH is thought to affect the FSH-induced growth in preantral follicles, we hypothesised that reduced AMH levels in Mutant follicles result in increased FSH-sensitivity permitting more follicles to progress to the antral stage.

7.2 AIMS

- To assess the effect of oocyte *C1galt1* deletion on estrogen synthesis in post-pubertal mice by detection of the aromatase enzyme in a follicle-specific and estrous-stage-specific manner.

- To investigate whether the oocyte *C1galt1* deletion affects AMH levels in Early and Late antral follicles by immunolocalisation and quantification of AMH.

7.3 MATERIALS AND METHODS

7.3.1 Tissue collection

Ovaries from 8- to 10-week-old Control and Mutant mice were collected at all 4 stages of the estrous cycle, fixed in 10% buffered formalin (Sigma-Aldrich, Dorset, UK) for 8 h, and washed in 70% ethanol. Ovaries were embedded in paraffin, sectioned at 5 μm and mounted on glass slides.

Estrous cycle evaluation (not performed by author)

As described in Chapter 6.3.1

7.3.2 Immunohistochemistry (IHC) for Aromatase and AMH detection.

The general protocol for IHC was followed as described in Chapter 2.3, with additional specific details provided in Table 7.1.

Table 7.1. Specific details of IHC protocol used for detection of AMH and Aromatase to complement the basic method described in Chapter 2.3.

	Molecule detected	
	AMH	**Aromatase**
Antigen retrieval	Heat-induced high pH solution	
Block agent	5% NGS, 2 h	
Primary antibody	mouse anti-human AMH monoclonal (MCA2246T; AbD Serotec, Kidlington, UK) at 1:100, 4^{o}C overnight	mouse anti-human Cytochrome P450 aromatase (MCA2077S, AbD Serotec) at 1:50, 4^{o}C overnight
Secondary antibody	Biotinylated goat anti-mouse IgG (BA-9200, Vector Laboratories), 1 h at RT	

7.3.3 Classification of follicles.

Only morphologically healthy follicles sectioned through the oocyte, to enable consistent follicle staging, were analyzed. Slides were counterstained with Hematoxylin (method described in Chapter 2.4) and re-imaged to enable visualization of follicle histology and cell boundaries. The criteria for classification of follicles up to the Preantral stage are described in Chapter 5.3.2. Classification of Early antral and Late antral follicles is based on the methodology outlined in Chapter 5.3.3.

7.3.4 Quantification of AMH and aromatase staining.

Assessment of GC staining for detection of AMH and aromatase was carried out. To quantify AMH and aromatase localisation, mean pixel intensity (MPI) of the GCs of individual follicles (excluding antrum and oocyte) was determined using ImageJ (National Institutes of Health, Bethesda, MD, USA).

7.3.5 Statistical analysis.

A minimum of three IHC experiments were done for all antigenic reactions presented (i.e. AMH and Aromatase). Data are presented as mean ± SD. Statistical comparisons were performed using Prism GraphPad software version 6.0 (GraphPad Software, La Jolla, CA, USA). An unpaired *t*-test was used to assess statistical differences for normally-distributed data, whereas a Mann-Whitney test was used for not normally-distributed data. Differences were considered significant when $p<0.05$.

Correlation between AMH and aromatase mean pixel intensity (MPI) was determined by using bivariate correlation statistics and is expressed as Spearman correlation coefficient, r^2. A strong correlation was considered when $r^2>0.8$

7.4 RESULTS

7.4.1 *C1galt1* Mutant follicles have higher levels of AMH compared to Controls at estrus and diestrus.

C1galt1 Mutant follicles show increased FSH-sensitivity when cultured *in vitro* (Grasa *et al*. 2015). As AMH secretion from GCs has been shown to attenuate the FSH-induced growth of follicles transitioning to the antral stage (di Clemente *et al.* 1994, Durlinger *et al.* 1999), we investigated AMH levels in growing follicles of mice at all 4 estrous stages; proestrus, estrus, metestrus and diestrus.

Ovarian sections that were not incubated with AMH antibody showed no immunoreactivity in GCs and oocytes, but showed non-specific staining of the antral fluid and zona pellucida (Fig. 7.1A). Sections incubated with the antibody showed GC-specific AMH staining (Fig. 7.1B).

The intensity and distribution of AMH staining varied according to follicle stage. All follicles at the Preantral stage or smaller showed homogeneous AMH staining throughout the entire GC population (Fig. 7.1 C, arrowhead). In contrast, follicles larger than Preantral showed heterogeneous pattern of AMH staining, with increased AMH intensity in the GCs close to the oocyte (Fig. 7.1 D). The theca cell layer did not show any immunoreactivity to the AMH antibody (Fig. 7.1 E-F).

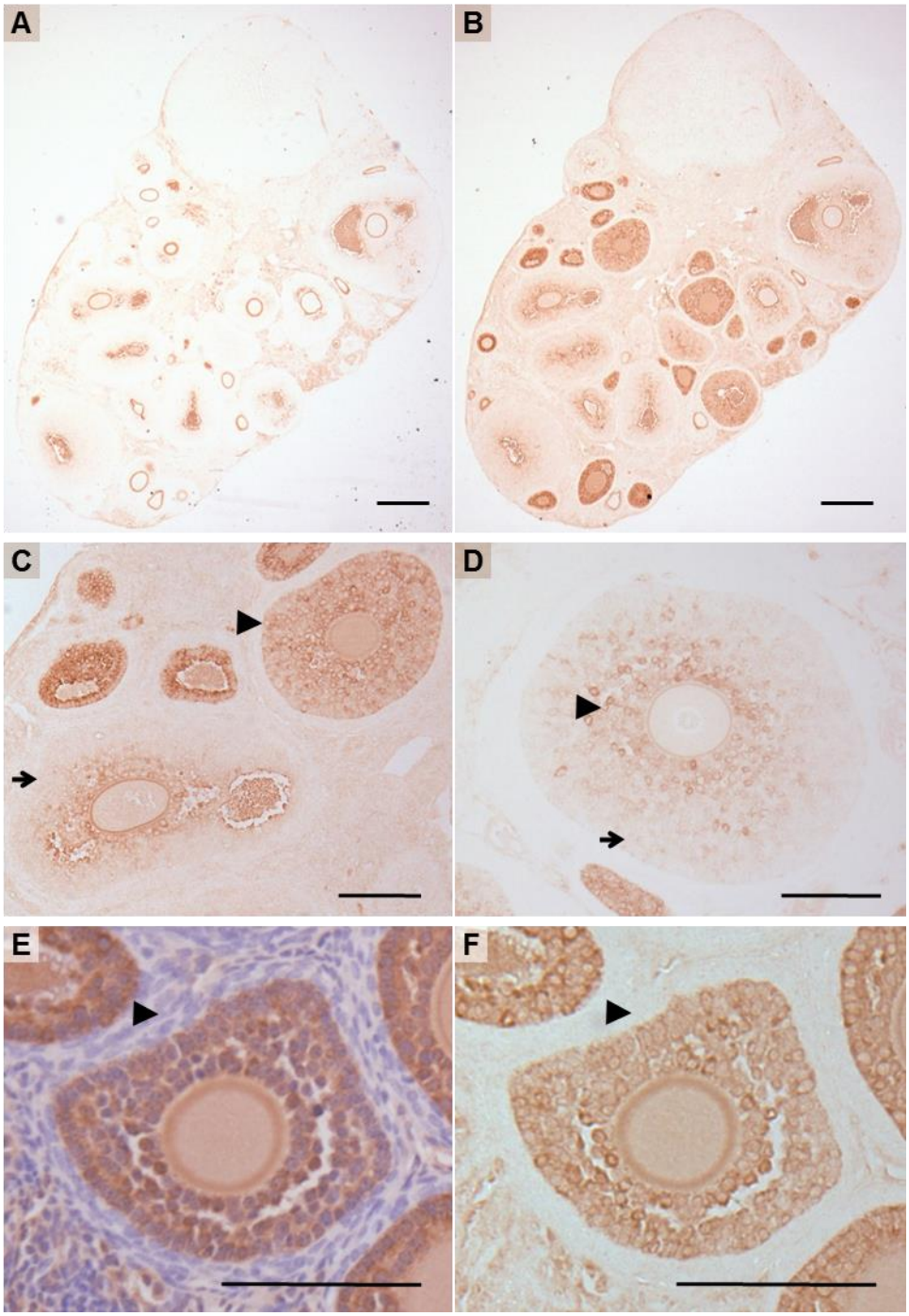

Figure 7.1 AMH immunohistochemical detection. (A) Control (no antibody) section. (B) AMH antibody-treated section. Scale bar for A and B: 200μm. (C) Differential AMH staining depending on follicle stage; follicles up to the preantral stage had homogeneous AMH staining throughout the GC population (arrowhead) whereas antral follicles had heterogeneous GC staining (arrow). (D) Antral follicles had high AMH immunoreactivity in the GC layers immediately surrounding the oocyte (arrowhead), but low immunoreactivity in the peripheral GCs (arrow). Hematoxylin staining shows the presence of the theca cell layer (E, arrowhead) which was AMH-negative for follicles at all stages (F, arrowhead). For C-F scale bar: 100μm.

At proestrus, the levels of AMH were similar when comparing Control and Mutant follicles at each follicle stage (Fig. 7.2A). However, there was a decrease in AMH staining intensity in Control Late antral follicles compared to less developed, Early antral follicles. The same pattern of AMH levels in Controls was also observed at estrus, metestrus and diestrus.

At estrus, Primary Inc., Secondary Inc. and Preantral follicles all had elevated levels of AMH intensity in Mutant mice compared to Controls (Fig. 7.2B). In addition, Secondary Inc. Mutant follicles had lower levels of AMH compared to Primary Inc. Mutant follicles, and Preantral Mutants had lower levels than Secondary Inc. Mutant follicles; these differences were not observed in Control follicles.

At metestrus, Mutant Early antral follicles had lower levels of AMH compared to Controls (Fig. 7.2C).

At diestrus, Mutant follicles at the Secondary Inc., Early antral and Late antral stages all had elevated AMH levels compared to Controls (Fig. 7.2D).

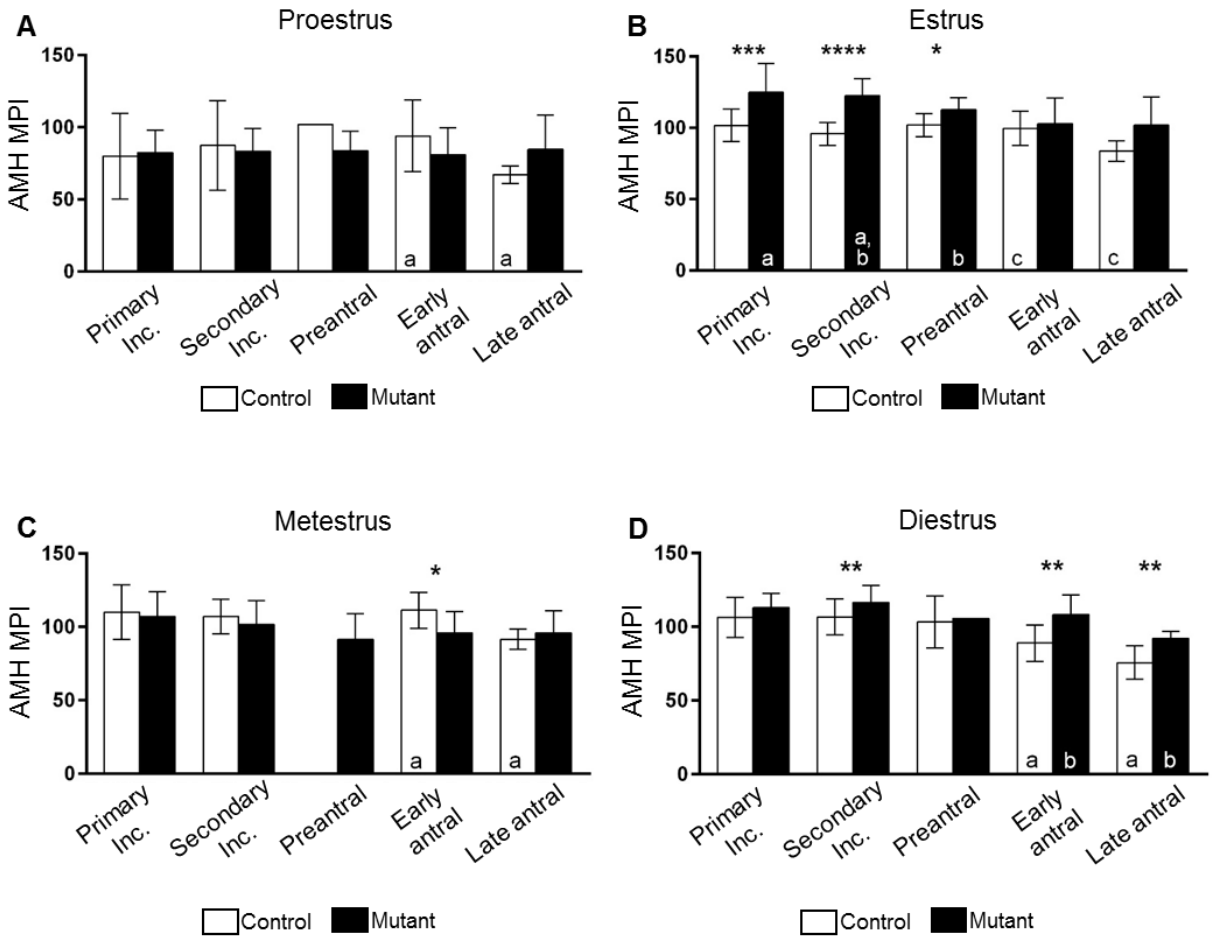

Figure 7.2. Assessment of AMH levels at each stage of the estrous cycle. (A) Mean pixel intensity (MPI) of AMH staining in follicles of mice at (A) proestrus, (B) estrus, (C) metestrus and (D) diestrus. For (A) to (D) asterisks indicate the following *p* values, between the Control and Mutant data at that stage of follicle development at that stage of the estrous cycle: *$p<0.05$, **$p<0.01$, ***$p<0.001$, ****$p<0.0001$. Comparisons were made between follicle types within each estrous stage. Columns with the same letter differed according to the following *p* values: For (A) a, $p<0.05$. For (B) a, c, $p<0.05$; b, $p<0.01$. For (C) a, $p<0.01$. For (D) a, b, $p<0.05$. Control, n=4 mice, n=48 follicles at proestrus, n=54 follicles at estrus, n=54 follicles at metestrus and n=86 follicles at diestrus. Mutant, n=4 mice, n=76 follicles at proestrus, n=83 follicles at estrus, n=70 follicles at metestrus and n=72 follicles at diestrus.

To assess the changes in AMH levels of follicle categories between the 4 stages of the estrous cycle, AMH levels were compared for each follicle stage at all estrous stages (Fig. 7.3). Sample number for Preantral follicles was low for the majority of the estrous stages, therefore comparison of Preantral follicles at each estrous stage is not provided.

Control Primary Inc. follicles show a cyclical fluctuation in AMH levels, whereby AMH levels increase from proestrus to estrus and decrease from diestrus to proestrus. Mutant Primary Inc. follicles also follow a similar cyclical variation in AMH levels. At estrus specifically, Mutant Primary Inc. follicles have higher AMH levels than Controls (Fig. 7.3A). Control and Mutant follicles at Secondary Inc., Early antral and Late antral stages also show a cyclical pattern of AMH detection, but the rise and fall of AMH levels occurs at different estrous stages for each follicle type.

Mutant Secondary Inc. follicles were found to have higher AMH levels compared to Controls at estrus and diestrus, and lower AMH levels compared to Controls at metestrus (Fig. 7.3B).

Mutant Early antral follicles have lower AMH levels at metestrus and higher levels at diestrus, compared to Controls (Fig. 7.3C).

Mutant Late antral follicles at diestrus have higher AMH levels than Controls (Fig. 7.3D).

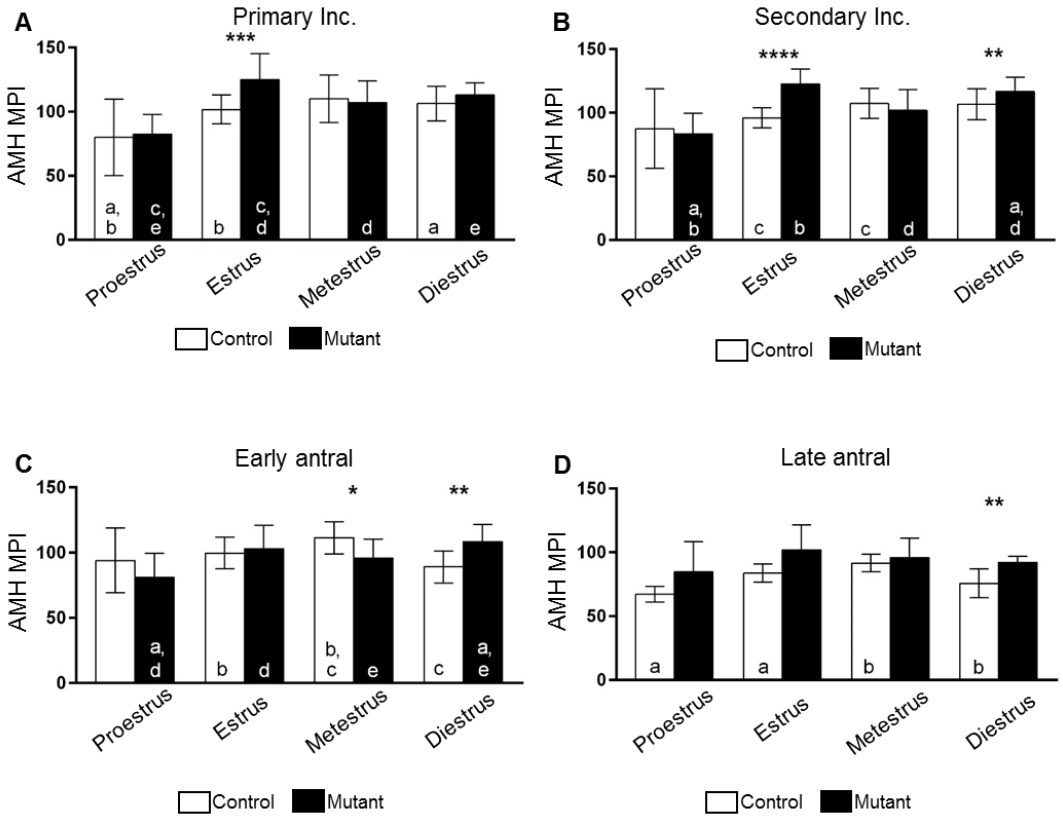

Figure 7.3. Assessment of AMH levels at each follicle stage. (A) Mean pixel intensity (MPI) of AMH staining in (A) Primary Inc., (B) Secondary Inc., (C) Early antral, and (D) Late antral follicles at all 4 stages of the estrous cycle. For (A) to (D) asterisks indicate the following *p* values, between the Control and Mutant data at that stage of follicle development at that stage of the estrous cycle: **p*<0.05, ***p*<0.01, ****p*<0.001, *****p*<0.0001.

Comparisons were made between estrous stage within each follicle stage. Columns with the same letter differed according to the following *p* values: For (A) b, *p*<0.05; a, *p*<0.01; d, *p*<0.001; c, e, *p*<0.0001. For (B) c, *p*<0.01; d, *p*<0.001; a, b, *p*<0.0001. For (C) b, d, e, *p*<0.05; a, c, *p*<0.01. For (D) a, b *p*<0.01. Control, n=4 mice, n=99 follicles at Primary Inc., n=62 follicles at Secondary Inc., n=37 follicles at Early antral and n=32 follicles at Late antral. Mutant, n=4 mice, n=89 follicles at Primary Inc., n=122 follicles at Secondary Inc., n=43 follicles at Early antral and n=21 follicles at Late antral.

7.4.2 Aromatase levels in *C1galt1* Mutant follicles at all stages of estrous are similar to Controls.

C1galt1 Mutant ovaries have increased number of growing follicles (Grasa *et al*. 2015) and reduced levels of follicle apoptosis (Chapter 6) resulting in larger litters (Grasa *et al*. 2015; Williams & Stanley 2008). As estrogen has been demonstrated to have mitogenic and anti-apoptotic effects on GCs (Goldenberg *et al.* 1972), we investigated the levels of the estrogen-producing aromatase enzyme in follicles at all stages of the estrous cycle.

Ovarian sections that were not incubated with aromatase antibody showed no immunoreactivity in GCs, theca and oocytes, but showed non-specific staining of the antral fluid and zona pellucida (Fig. 7.4A). Sections incubated with the antibody showed GC-specific aromatase staining in large antral follicles only (Fig. 7.4B, arrowheads).

The pattern of aromatase localisation in the large antral follicles was heterogeneous (Fig. 7.4C and D). The mural GCs lining the follicle basal lamina had more intense aromatase staining, whereas GCs closest to the oocyte and cumulus cells had undetectable aromatase levels. The theca cell layer did not show any immunoreactivity to the aromatase antibody (Fig. 7.4 C and D, arrowheads).

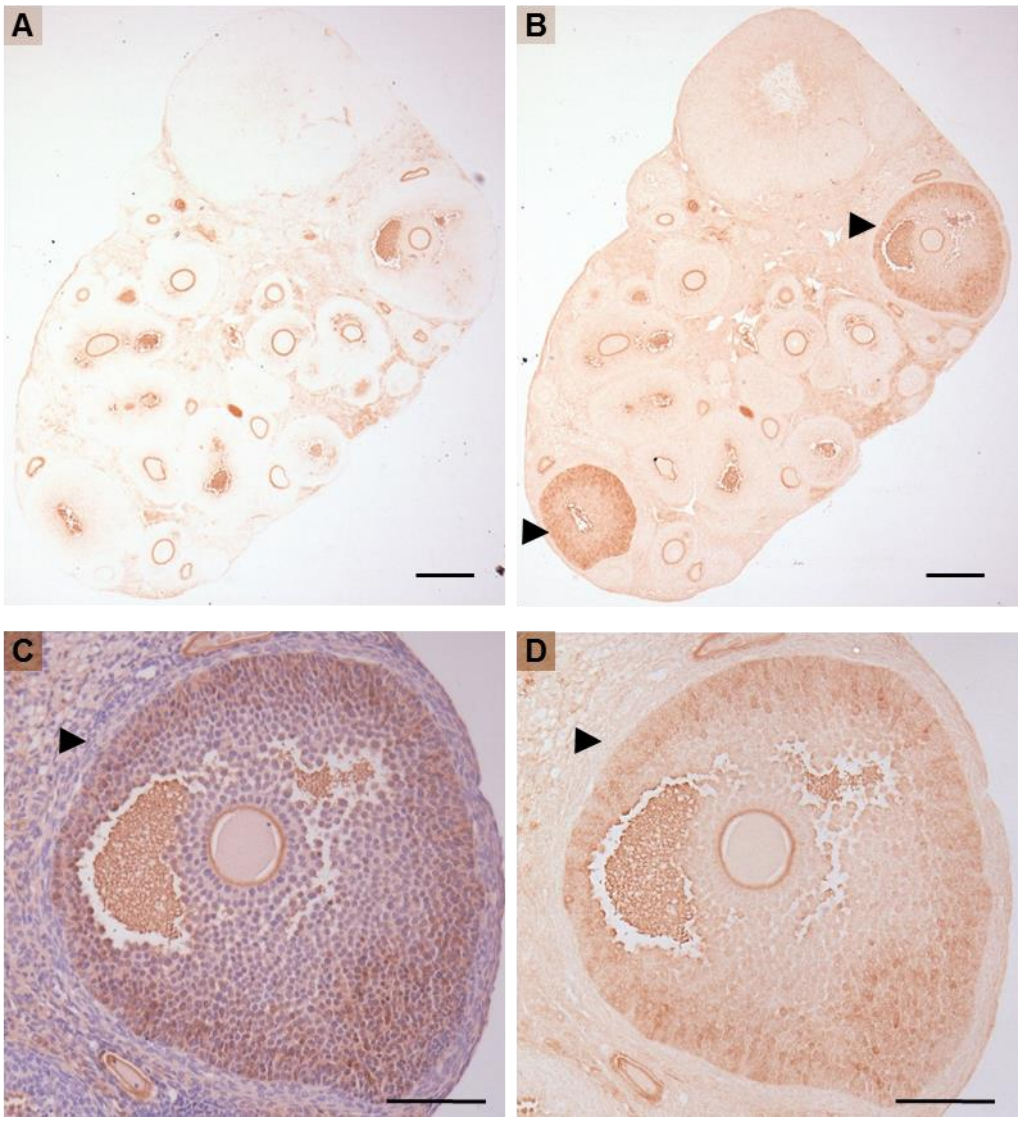

Figure 7.4. Aromatase immunohistochemical detection. (A) Control (no antibody) section. (B) Aromatase antibody-treated section. Note aromatase positive antral follicles (arrowheads). Scale bar for A and B: 200μm. (C) and (D) Differential aromatase staining in an antral follicle. Mural GCs near the basal lamina are more intensely stained compared to the rest of the mural GC population and cumulus cells. Hematoxylin staining shows the presence of the theca cell layer (C, arrowhead) which was AMH-negative for follicles stained with aromatase antibody (D, arrowhead). For C-D scale bar: 100μm.

Aromatase detection using IHC was only observed in Early antral and Late antral follicles, in both Control and Mutant ovaries. However, the sample size of Early antral follicles was less than 3 in all estrous stages in both Control and Mutant mice, therefore no statistical comparison could be performed.

The levels of aromatase in Late antral follicles were found to be similar in Control and Mutant, across the compared stages of the estrous cycle (Fig. 7.6)

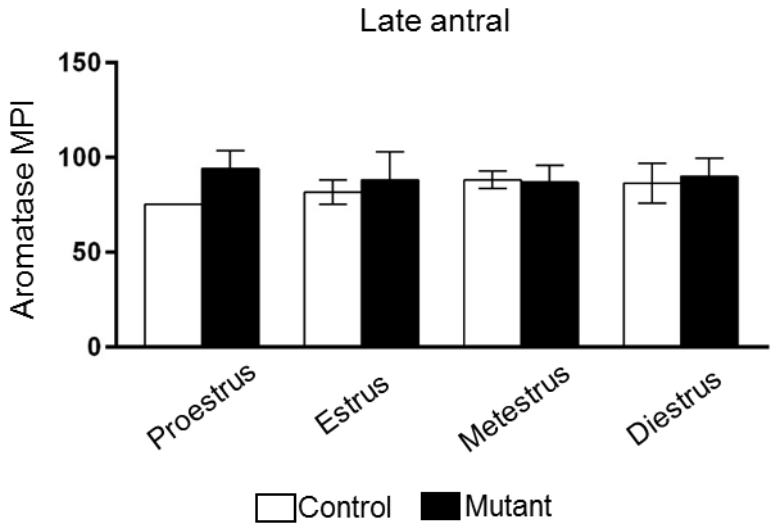

Figure 7.5. Assessment of aromatase levels in Late antral follicles at each estrous stage. Mean pixel intensity (MPI) of aromatase staining in at all 4 stages of the estrous cycle. Control, n=4 mice, n=24 follicles. Mutant, n=4 mice, n=24 follicles.

Immunolocalisation of aromatase and AMH in adjacent ovarian sections revealed the differential and specific presence of these molecules in different follicles. AMH predominantly is detected in growing follicles before the antral stage (Fig. 7.5A), whereas aromatase is detected in the large antral follicles (Fig. 7.5B)

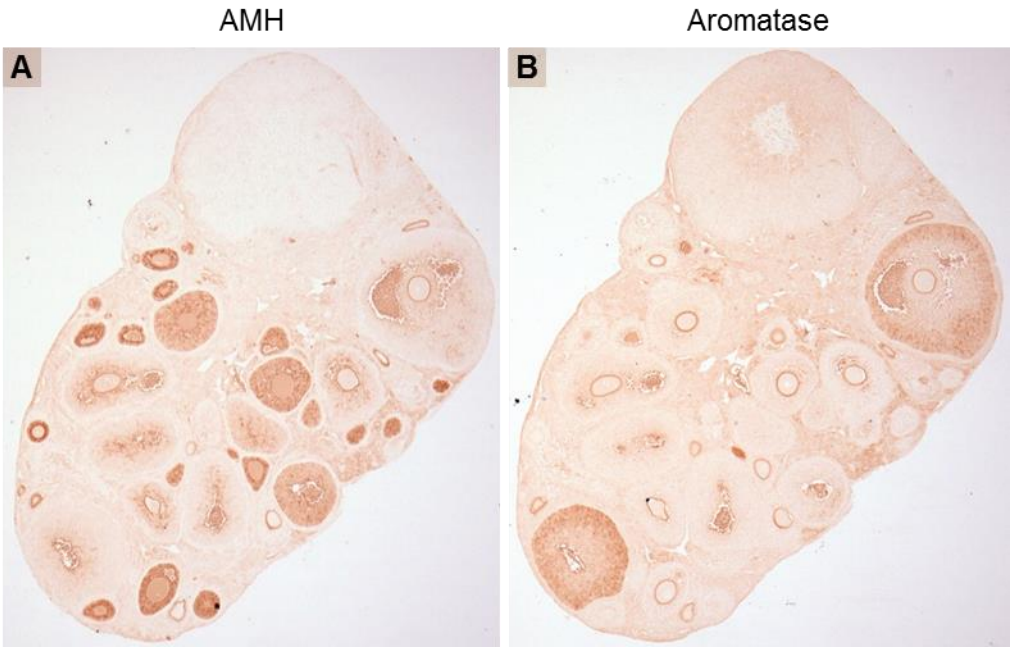

Figure 7.6. Comparison of Aromatase and AMH immunohistochemical detection. (A) AMH antibody- treated section and consecutive (B) aromatase antibody-treated section.

A subset of the follicles at the Early antral and Late antral stages were positive for both aromatase and AMH. Therefore, the levels of aromatase and AMH were correlated in a follicle-specific manner in Early antral and Late antral follicles (Fig. 7.7). The correlation between aromatase and AMH suggests a positive relationship between the two molecules, however the correlation coefficient (r^2<0.8) does not suggest a strong relationship between aromatase and AMH in either Control or Mutant follicles.

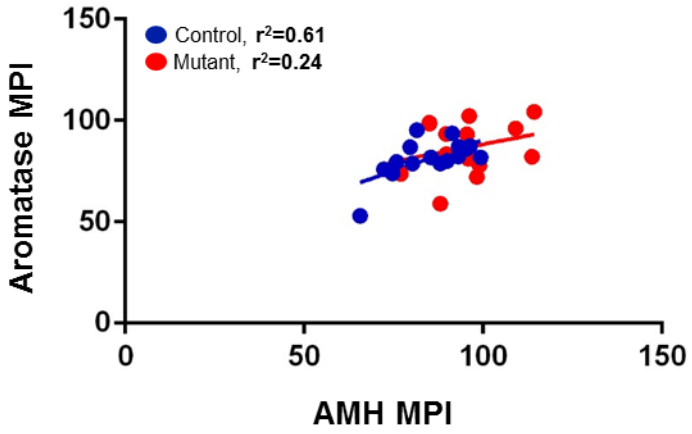

Figure 7.7. Correlation analysis between aromatase and AMH levels. Individual follicle analysis of correlation between aromatase and AMH levels in Early antral and Late antral follicles from all estrous stages, expressed as mean pixel intensity (MPI) per follicle. Control, n=9 mice and n=16 follicles. Mutant, n=11 mice and n=16 follicles.

7.5 DISCUSSION

Mammalian ovarian follicle development is characterised by cell growth, proliferation, differentiation and apoptosis. The transition from a preantral to an early antral follicle is FSH-dependent and is the critical point at which the fate of a follicle is decided as the majority of growing follicles undergo atresia at this transition (Hirshfield & Midgley 1978; Hirshfield 1988). The precise regulatory mechanisms that control the FSH-sensitivity of each preantral follicle are unclear, however both estradiol and AMH have been implicated as important players in this process.

Role of AMH in FSH sensitivity

In the $AMH^{-/-}$ female mouse, there are (i) increased numbers of small preantral and large preantral follicles at all stages of the estrous cycle, (ii) increased numbers of small antral follicles at the estrus stage and (iii) similar numbers of large antral follicles as Control mice (Visser *et al.* 2007). The role of AMH as an inhibitor of primordial follicle activation (Durlinger *et al.* 1999) explains the observed rise in small and large preantral follicles. For the observed increase in small antral follicles at estrus in $AMH^{-/-}$ ovaries compared to Controls, the authors provide 2 alternative hypotheses (Visser *et al*. 2007):

Hypothesis 1: The increased number of preantral follicles in $AMH^{-/-}$ mice compared to Controls allows more follicles to acquire FSH sensitivity to progress to the early antral stage.

Hypothesis 2: AMH attenuates FSH-induced growth to the early antral stage, therefore the absence of AMH in $AMH^{-/-}$ enables more follicles to progress through this crucial FSH-dependent growth.

The authors appear to favour the second hypothesis implicating AMH in FSH-induced follicle growth, with arguments used from *in vitro* studies as well (Durlinger *et al.* 2001). The observed rise in early antral follicles at estrus in $AMH^{-/-}$ is not observed in late antral follicles. Late antral follicles are found in similar numbers between control and $AMH^{-/-}$ mice, whereas it would be expected that late antrals would also be found at increased numbers compared to Controls. This observation suggests that even if AMH regulates FSH-sensitivity in preantral follicles, other ovarian mechanisms regulate the progression of early antral to late antral follicles.

However, the first hypothesis is not explored further, even though it is possible that the sole reason of increased early antral follicles in $AMH^{-/-}$ females compared to controls is due to increased preantral follicles. It can be argued that the larger growing follicle population, as a result of increased primordial follicle activation, cannot be supported to growth beyond the early antral stage due to the precise balance of intra- and extra-ovarian factors that tightly regulate ovulation number and that is why there is not an increase in late antral follicles in the Mutant compared to Controls.

In *C1galt1* Mutants, growing follicles at various estrous stages show raised levels of AMH compared to Controls. Based on the reported role of AMH as an inhibitor of the FSH-induced transition from preantral to the antral

stage, the *C1galt1* Mutant would be hypothesised to have a phenotype of reduced numbers of growing antral follicles. In contrast, the *C1galt1* Mutant has ~40% more preovulatory follicles at proestrus (Grasa *et al*. 2015), which leads to a similar rise in ovulation and litter size (Williams & Stanley 2008).

Therefore, the AMH data from analysis in *C1galt1* Mutant mice suggest 2 hypotheses: either the observed AMH rise in Mutant follicles is not sufficient to negatively impact their FSH-sensitivity or the reported role of AMH on FSH-sensitivity *in vivo* is not accurate. Nonetheless, the results presented in this Chapter show that oocyte core 1-derived *O*-glycans have an inhibitory effect on GC-produced AMH at estrus and diestrus, since deletion of core 1-derived *O*-glycans results in increased AMH levels.

Role of aromatase in follicle survival

The aromatase enzyme, expressed exclusively in the GCs of antral follicles, aromatises theca-produced androgens intro estrogen (Dorrington *et al.* 1975, Hillier & De Zwart 1981). Estrogen has a multitude of trophic effects on ovarian cells, including the support of follicle survival, increase in GC proliferation and a decrease in follicle apoptosis (Goldenberg *et al.* 1972).

The aromatase enzyme in the mature rodent ovary is expressed in large antral and preovulatory follicles (Guigon *et al.* 2003) and in particular, the expression of aromatase has been shown to be highest in mural GCs closest to the basal lamina, and lower in mural GCs lining the antrum and

undetectable in cumulus cells (Sakurada *et al.* 2006). Our immunohistochemical studies confirmed the abovementioned pattern of aromatase localisation, as both Control and Mutant follicles showed more intense staining on the peripheral mural GCs and lower staining in the inner mural GCs.

Interestingly, aromatase levels per Late antral follicle in the Mutant were similar to Controls at all stages of the estrous cycle. This observation suggests that *C1galt1* Mutant late antral follicles are functionally normal with respect to the steroidogenic abilities of cells. In addition, the presence of normal levels of aromatase in *C1galt1* Late antral follicles, in combination with increased numbers of large antral follicles in the Mutant (Grasa *et al*. 2015) suggests increased production of estradiol from the Mutant ovary. Indeed, endocrinology analysis from serum samples showed that the levels of estradiol approached a significant increase (p=0.08) in the Mutant compared to Controls at the proestrus stage (Grasa *et al*. 2015). Collectively, these results show that *C1galt1* Mutant females have (i) more large antral follicles, (ii) each capable of normal estradiol production resulting in (iii) elevated total estradiol production in the ovary.

Importance of proposed elevated aromatase levels per *C1galt1* Mutant ovary:

(i) Intra-follicular communication

Estradiol production in follicles has trophic and anti-apoptotic effects on cells producing the estradiol (autocrine action) but also on other cells within the follicle as well (paracrine action), supported by the presence of the estrogen receptor (ER) in theca cells (Billig *et al.* 1993, Revelli *et al.* 1996). Late antral follicles in *C1galt1* Mutant mice have normal levels of aromatase, indicating normal estradiol production per follicle *in vivo*. Therefore, we hypothesise that maintenance of normal estradiol levels within Late antral follicles contributes to the survival of these follicles through the last stages of follicle development, to enable successful ovulation.

(ii) Inter-follicular communication

The estrogen receptor (ER) is present in rat ovaries 4 days after birth (Drummond & Findlay 1999). During this early post-natal period, the rodent ovary is only inhabited by primordial and primary follicles, suggesting ER expression in quiescent and/or small growing follicles. Immunohistochemical studies confirmed that ER is indeed expressed in primary follicles but not in primordial follicles (Sar & Welsch 1999). As estrogen production is a function of large antral follicles, the presence of estrogen receptor on small growing

follicles suggests an inter-follicular effect of estrogen, e.g. produced by large antral follicles and acting on small growing follicles.

Therefore, the overall increase in estradiol production in *C1galt1* Mutant ovaries could be contributing to the elevated numbers of growing follicles in the Mutant ovary, resulting in increased fertility.

Chapter 8: Conclusions

Conclusions

This thesis explored the effects of oocyte-produced core 1-derived *O*-glycans on the process of follicle development and function. Through the work presented here, novel findings have been made regarding (i) the normal physiology of follicle development in mice (from data of Control mice), and (ii) the role of oocyte-produced core 1-derived *O*-glycans in primary follicles onward, on various aspects of follicle development by use of the *C1galt1* Mutant mouse.

8.1 Novel findings on follicle development physiology

Although the primary aim of this thesis was the exploration of the *C1galt1* Mutant mouse and subsequent comparison between Control and Mutant, consideration of data solely from Control mice is of great interest as it reveals novel insights into follicle development.

In Chapter 3, analysis of the central section of cumulus-oocyte complexes (COC) (9 h post-hCG injection) revealed details on dynamics of cumulus formation. Characteristics of the COC such as cell density and cumulus size were quantified and describe the COC just prior to ovulation. A novel approach was taken to assess levels of various cumulus extracellular matrix (ECM) proteins within individual follicles, thereby providing information on the relationship between the different molecular. Surprisingly, correlations

between molecules, and between molecules and cumulus expansion did not reveal strong relationships (Ploutarchou *et al.* 2015), despite the reported importance of each individual molecule in the formation of a stable cumulus complex (Sato *et al.* 2001, Zhuo *et al.* 2001, Fulop *et al.* 2003, Salustri *et al.* 2004, Scarchilli *et al.* 2007). This finding reveals that the cumulus ECM proteins exist in varying levels, above a set threshold, without compromising the process of cumulus expansion. When levels fall below the threshold (as in the case of the various ECM protein knockout mouse models) cumulus expansion is negatively compromised and subsequently affects other processes like ovulation and fertilisation.

Note should be made of the differences in the size of the cumulus between hormonally-injected and naturally ovulated cumulus-egg complexes (CECs). Exogenous hormone induction of ovulation results in cumulus complexes which are smaller in terms of diameter in comparison to naturally ovulated complexes. Despite extensive research in literature, it appears that the effect of hormone injection on cumulus expansion has not been reported before. Therefore, when aiming to investigate the normal physiology of follicle development in the mouse, other experimental animals and human, the results obtained through hormone injection should not be considered as an exact representation of natural processes.

The growth and atresia of follicles are associated with major structural and functional changes, therefore classifying follicles (based on morphology) with the aim of investigating individual follicle stages needs to be as precise and inclusive of various follicle factors as possible. A widely used

classification system was proposed by Pedersen and Peters (Pedersen & Peters 1968) based on GC number in the follicle's central section. However, I believe that other follicle characteristics in addition to GC number need to be incorporated into the classification method to more closely resemble the functional status of the follicle. For instance, the Pedersen system classifies all follicles with 20 or less GCs as type 3a. However, a follicle with less than 20 cells could be a transitional follicle (transitioning from primordial to primary) or a primary follicle, depending on the extent of GC cuboidalisation, a feature which is readily distinguishable morphologically. In addition, the Pedersen and Peters system classifies follicles of 201-400 cells as type 5b. Through personal experience during this DPhil, it became apparent that follicles with 201-400 cells may or may not have a small antrum – a feature which is likely central in determining the functional properties of the particular follicle. Therefore, these additional features to GC number were taken into consideration to classify follicles in a more precise manner (Chapter 5).

Using our enhanced follicle classification system, an in-depth analysis of oocyte nuclei sizes measured from follicles at all stages is provided in Chapter 5. Although not an aim of this thesis, it would be interesting to correlate the growth dynamics of oocyte nucleus size with whole oocyte size. In addition, the detailed analysis of various follicle characteristics at all follicle stages (Chapter 5) provides the dynamics of follicle growth at 3 weeks of age in the mouse. Indeed, such data could be used beyond this thesis for correlations with functional properties of the follicle to further understand follicle growth.

In Chapter 6, follicle stage-specific and estrous-stage specific quantification of DNA fragmentation (TUNEL assay), Bcl2 and Bax levels in ovaries was performed. Such analysis of apoptosis and apoptosis-related proteins has not been done before; previous research reports do not explore apoptosis changes at (i) different estrous stages, and/or (ii) different follicle stages (Gosden *et al.* 1983, Slot *et al.* 2006). The hormonal environment indeed affects the survival of follicles, suggesting changes in apoptosis levels through the estrous cycle, and also follicles at different stages have varying susceptibility to apoptosis. Therefore, both factors (estrous stage and follicle stage) were taken into consideration when assessing apoptosis in this thesis.

Assessment of Bcl2:Bax ratio revealed 2 novel findings: (i) the consistency of the ratio at all follicle stages within proestrus and metestrus and (ii) the increase of the ratio from proestrus to metestrus for all follicle stages. The increase of Bcl2:Bax ratio from proestrus to metestrus could be due to (i) increased Bcl2, (ii) decreased Bax or (iii) both. Individual analysis of Bcl2 and Bax levels revealed that both molecules increased from proestrus to metestrus, but Bcl2 increased more than Bax therefore leading to a higher ratio at metestrus.

The observed changes in Bcl2:Bax ratio between proestrus and metestrus highlight direct or indirect regulation of these molecules by hormones. Considering the anti-apoptotic roles of Bcl2 and pro-apoptotic roles of Bax, the rise in Bcl2:Bax ratio at metestrus suggests varying susceptibility of follicle to apoptosis depending on estrous stage.

To conclude, despite the fact that investigation in the *C1galt1* Mutant mouse was the primary aim of this thesis, new findings have furthered our knowledge into the physiology of Control mice.

8.2 Novel findings on the roles of oocyte derived *O*-glycans in follicle development

The oocyte-specific mutation of *C1galt1* in mice resulted in modified cumulus expansion without negatively affecting fertility (Williams *et al.* 2007). The central role of cumulus expansion in ovulation and fertilisation has been emphasized numerous times in the past (Chen *et al.* 1993, Tanghe *et al.* 2002) (Ng *et al.* 1999), therefore the *C1galt1* Mutant provided a unique model for studying cumulus expansion.

In Chapter 3, the modified cumulus matrix of *C1galt1* Mutant COCs was investigated and shown to result predominantly by fewer CCs with additional minor changes in cumulus ECM proteins. It has been suggested that cumulus complex assessment can be an informative predictor of oocyte developmental potential, since CC number and proliferarion is positively correlated with oocyte maturation and fertilisation potential (Gregory 1998, Khurana & Niemann 2000). The results presented in this thesis indicate that a ~23% decrease in CC number associated with oocytes in *C1galt1* Mutants is not detrimental to ovulation or oocyte quality as determined by live births.

Therefore a reduction of CC number of this magnitude is not a reliable assessment to predict oocyte developmental potential. As a result, a partially expanded cumulus complex may not be the best indicator of oocyte quality.

These data have wider implications in the field of Assisted Reproductive Technologies (ARTs) since selection of developmentally competent eggs should not be judged solely by the size of the cumulus complex and the number of CCs surrounding an egg. In addition, using a novel method of correlating the levels of cumulus ECM molecules within individual cumulus complexes, evidence is provided that considerable variation exists in the composition of the cumulus ECM, which are tolerated without adverse effects on fertility in both the Control and the Mutant, as long as all components are present above a threshold level.

Furthermore, the abovementioned results support the well-known role of oocyte-produced factors in cumulus expansion, shown both *in vivo* and *in vitro* (Su *et al.* 2004, Dragovic *et al.* 2005, Peng *et al.* 2013). The individual oocyte glycoproteins that are affected by the *C1galt1* deletion cannot be identified at this point in time due to the absence of reports on the *O*-glycosylation status of all oocyte proteins. Recombinant human BMP15 (an oocyte growth factor) has been shown to be *O*-glycosylated (Saito *et al.* 2008). However, the specific structure of *O*-glycosylation (e.g. core 1 to 8) on BMP15 is not known, therefore it remains to be identified whether BMP15 has core 1-derived *O*-glycans and also if these exist on native mouse BMP15. In $BMP15^{-/-}$ female mice the process of cumulus expansion is compromised to the extent that some oocytes in preovulatory follicles are not associated

with any cumulus cells therefore preventing ovulation (Yan *et al.* 2001). In the case that BMP15 has core 1-derived *O*-glycans, the absence of these glycans in *C1galt1* Mutant oocytes could be altering BMP15's function so that cumulus expansion is compromised but to a lesser extent than BMP15$^{-/-}$ mice.

A very intriguing aspect of *C1galt1* Mutant mouse has always been its sustained increased fertility (Williams & Stanley 2007). Therefore, one of the primary aims of this thesis was to investigate this phenotype further, and try to elucidate the changes in follicle development that result in increased numbers of growing follicles in the Mutant compared to Controls (Grasa *et al*. 2015).

An early model proposed for the increased fertility in *C1galt1* Mutant mice, hypothesised that follicles take longer to develop, therefore accumulating at the gonadotrophin-responsive stages and increasing the number of follicles available for ovulation (Williams & Stanley 2008). The results presented in Chapter 5 reveal that antral follicles are found in similar numbers between Control and Mutant mice. Furthermore, according to recent studies on the dynamics of follicle development, primordial follicles in prepubertal mice take ~23 days to become antral (Zheng *et al.* 2014). Therefore, the Late antral follicles observed at 3 weeks (Chapter 5) are presumably the very first antral follicles formed in the mouse ovary. If the model on accumulation of slower growing Mutant follicles was valid, it would

be expected that less antral follicles are observed in the Mutant ovary. However, as this is not the case, the model is flawed.

One of the most important findings in this thesis was reduced follicle apoptosis in the Mutant at metestrus. The reduced follicle apoptosis in the Mutant provides a mechanism for the elevated number of growing follicles. An alternative or supplementary hypothesis for the increased number of growing follicles in the Mutant is the activation of more primordial follicles, leading to a larger growing pool. However, this seems unlikely as (i) oocyte gene deletion only occurs at the primary follicle stage, therefore the primordial follicle is unaffected, and (ii) follicle counts of Mutant transitional and primary follicles are similar to Control at both 3 weeks (Chapter 5) and 6 weeks (Grasa *et al.* 2015) indicating that primordial follicle activation is unchanged. Therefore, the reduction in apoptosis presented here provides a probable explanation for the increased follicle numbers phenotype in *C1galt1* Mutants.

Another aspect of post-pubertal mice investigated were the levels of aromatase; aromatase levels in Late antral follicles from *C1galt1* Mutants were similar to Controls (Chapter 7), suggesting similar estradiol production by each Late antral follicle in the Mutant. *C1galt1* Mutants have increased numbers of antral follicles (Grasa *et al*. 2015) therefore the overall production of estradiol from the Mutant is expected to increase. Indeed, estradiol levels in serum in the Mutant are 25% higher than Controls (Grasa *et al*. 2015). Estradiol has been shown to have both pro-survival and anti-apoptotic effects on follicles (Goldenberg *et al.* 1972, Lund *et al.* 1999). Therefore, the overall

increase in estradiol production in the Mutant could be contributing to both the increased numbers of growing follicles and the decreased levels of apoptosis observed in the Mutant compared to the Control. However, this hypothesis creates a paradox: even if increased estradiol supports the growth of more follicles, there had to be more follicles there in the first place to produce more estradiol. Therefore, the elevated estradiol levels in Mutant ovaries could be acting as a secondary supportive mechanism in follicle survival, but the original cause of increased follicle numbers is likely a factor other than estradiol.

In addition, estradiol induces an increase in GC proliferation (Goldenberg *et al.* 1972, Rao *et al.* 1978). Interestingly, Mutant Late antral follicles at 3 weeks of age have more GCs compared to Controls (Chapter 5), further supporting the role of estradiol in GC proliferation. It should be noted that GC counts were done in 3 week old mice, whereas estradiol levels were assessed in post-pubertal mice; even though the results from the two studies are not directly related, inferences can be made about the biological importance of the results.

Molecular origin of increased fertility in *C1galt1* mice

The specific oocyte protein(s) responsible for increased fertility and reduced apoptosis in *C1galt1* are currently unknown. Heterozygous mutations in GDF9 or BMP15 result in increased ovulation rates in ewes (Galloway *et al.* 2000, Souza *et al.* 2014), however increased fertility in mice as a result of GDF9 or BMP15 mutations has not been shown. Interestingly,

the ratio of levels of *GDF9* and *BMP15* expression has been shown to be highly correlated within various species studied (Sheep, pig, cow, rat, mouse, deer) and the ratio is different between species (Crawford & McNatty 2012). Poly-ovulatory animals have an increased GDF9:BMP15 ratio compared to mono-ovulatory animals. Indeed, *C1galt1* Mutant mice have been shown to have an increased ratio of GDF9:BMP15 expression levels from whole ovary analysis (Grasa *et al*. 2015). However, it was unclear whether this is purely due to increased numbers of growing follicles in the Mutant ovary (whereby the increase in GDF9 is larger than the increase in BMP15), or due to more GDF9 and/or less BMP15 secreted by each growing oocyte. Results presented in Chapter 5 with relation to the growth characteristics of small and large growing follicles, suggest that each follicle is under the effect of elevated GDF9 levels or more active GDF9, therefore providing a possible explanation for the origin of elevated GDF9:BMP15 levels in the serum.

Mechanism of increased fertility in *C1galt1* mice

The presence of multiple sheep strains with genetic mutations that lead to increased fertility (Galloway *et al.* 2000, Wilson *et al.* 2001) has fascinated reproductive researchers for decades. In an effort to explain the increased fertility in sheep, Scaramuzzi *et al.* presented 2 alternative mechanisms by which sheep become poly-ovulatory (Fig. 8.1) (Scaramuzzi *et al.* 1993). One mechanism favours the temporal widening of the 'window' during which follicles can respond to gonadotrophins, i.e. if growing follicles are exposed to FSH for longer, then a greater number of preantral follicles

will become FSH-dependent and proceed to the preovulatory stage. A second mechanism favours an increased activation of primordial follicles, therefore increased numbers of all growing follicles, leading to more ovulations.

C1galt1 Mutant mice have similar numbers of small growing follicles (Chapter 5 and Grasa *et al.* 2015) but more follicles at the preantral and subsequent stages. *C1galt1* Mutant follicles also exhibit increased FSH-sensitivity *in vitro* (Grasa *et al.* 2015). Therefore, the mechanism by which *C1galt1* Mutant mice have increased fertility more likely matches mechanism A (Fig. 8.1). However, it should be noted that the models in Fig. 8.1 refer to sheep mechanisms, and mechanisms may vary between species. An alternative mechanism by which *C1galt1* Mutant follicles have increased sensitivity allowing more follicles to reach the pre-ovulatory stage (not proposed in Fig. 8.1), could be elevated FSH-R in growing follicles, which again makes the growing follicle population more sensitive to FSH. FSH-R expression was assessed in whole ovaries from *C1galt1* Mutants, revealing no differences between Control and Mutant at any estrus stage (Grasa *et al*. 2015). However, as such levels are representative of whole ovary expression, it remains to be elucidated whether FSH-R in individual follicles are elevated.

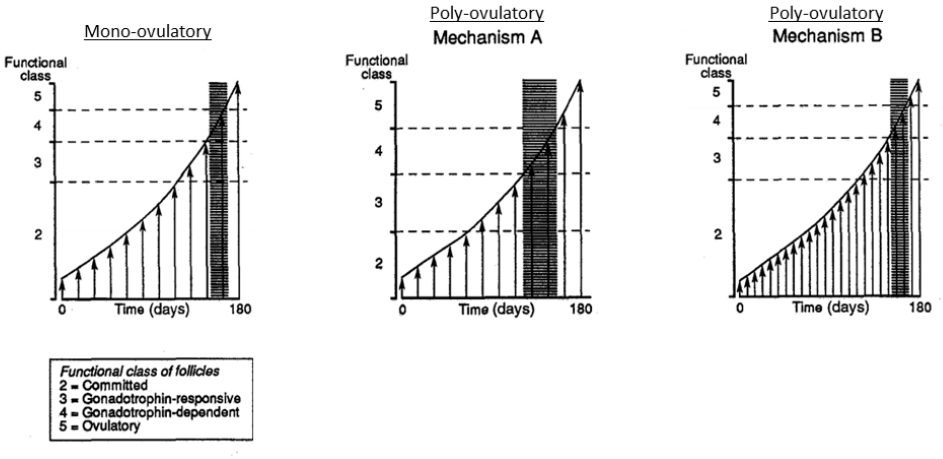

Figure 8.1. Mechanisms for increased ovulation rate in sheep. Developing follicles are shown by the vertical arrows. The shaded vertical area is the 'window' during which growing follicles become FSH-dependent and progress to the antral stage. Multiple ovulations in sheep are proposed to result either as a result of mechanism A, whereby follicles have a wider 'window' of opportunity to become FSH-dependent, or mechanism B, whereby recruitment of more follicles from the primordial follicle pool results in more follicles available for further development. Adapted from Scaramuzzi *et al*. 1993.

To conclude, investigations into the *C1galt1* Mutant mouse revealed novel insights into the roles of oocyte-produced core 1-derived *O*-glycans in cumulus expansion, follicle development and follicle survival. Detailed structural and molecular analysis of cumulus expansion showed that modifications in cumulus expansion are not always detrimental to ovulation or fertilisation. In addition, *C1galt1* Mutants have altered (i) follicle growth characteristics, (ii) levels of apoptosis-related molecules and (iii) levels of AMH, all of which could be directly or indirectly contributing to the increased fertility phenotype.

References

Abel MH, Wootton AN, Wilkins V, Huhtaniemi I, Knight PG & Charlton HM 2000 The effect of a null mutation in the follicle-stimulating hormone receptor gene on mouse reproduction. *Endocrinology* **141** 1795-1803.

Abercrombie M 1946 Estimation of nuclear population from microtome sections. *Anatomical Record* **94** 239-247.

Allen WM 1935 THE ISOLATION OF CRYSTALLINE PROGESTIN. *Science* **82** 89-93.

Almeida AP, Saraiva MVA, Araújo VR, Magalhães DM, Duarte ABG, Frota IMA, Lopes CAP, Campello CC, Silva JRV & Figueiredo JR 2011 Expression of growth and differentiation factor 9 (GDF-9) and its effect on the in vitro culture of caprine preantral ovarian follicles. *Small Ruminant Research* **100** 169-176.

Antunes JL, Carmel PW, Housepian EM & Ferin M 1978 Luteinizing hormone-releasing hormone in human pituitary blood. *Journal of Neurosurgery* **49** 382-386.

Armstrong DT & Papkoff H 1976 Stimulation of aromatization of exogenous and endogenous androgens in ovaries of hypophysectomized rats in vivo by follicle-stimulating hormone. *Endocrinology* **99** 1144-1151.

Baenziger JU & Green ED 1988 Pituitary glycoprotein hormone oligosaccharides: structure, synthesis and function of the asparagine-linked oligosaccharides on lutropin, follitropin and thyrotropin. *Biochimica et Biophysica Acta* **947** 287-306.

Baker TG 1963 A QUANTITATIVE AND CYTOLOGICAL STUDY OF GERM CELLS IN HUMAN OVARIES. *Proceedings of the Royal Society of London. Series B: Biological Sciences* **158** 417-433.

Ball GD, Leibfried ML, Lenz RW, Ax RL, Bavister BD & First NL 1983 Factors affecting successful in vitro fertilization of bovine follicular oocytes. *Biology of Reproduction* **28** 717-725.

Baranova NS, Inforzato A, Briggs DC, Tilakaratna V, Enghild JJ, Thakar D, Milner CM, Day AJ & Richter RP 2014 Incorporation of Pentraxin 3 into Hyaluronan

Matrices is Tightly Regulated and Promotes Matrix Cross-Linking. *Journal of Biological Chemistry*.

Batista F, Lu L, Williams SA & Stanley P 2012 Complex N-glycans are essential, but core 1 and 2 mucin O-glycans, O-fucose glycans, and NOTCH1 are dispensable, for mammalian spermatogenesis. *Biology of Reproduction* **86** 179.

Beaumont HM & Mandl AM 1962 *A Quantitative and Cytological Study of Oogonia and Oocytes in the Foetal and Neonatal Rat*.

Bedford JM & Kim HH 1993 Cumulus oophorus as a sperm sequestering device, in vivo. *Journal of Experimental Zoology* **265** 321-328.

Belchetz PE, Plant TM, Nakai Y, Keogh EJ & Knobil E 1978 Hypophysial responses to continuous and intermittent delivery of hypopthalamic gonadotropin-releasing hormone. *Science* **202** 631-633.

Billig H, Furuta I & Hsueh AJ 1993 Estrogens inhibit and androgens enhance ovarian granulosa cell apoptosis. *Endocrinology* **133** 2204-2212.

Bleil JD & Wassarman PM 1980 Structure and function of the zona pellucida: identification and characterization of the proteins of the mouse oocyte's zona pellucida. *Developmental Biology* **76** 185-202.

Borum K 1961 Oogenesis in the mouse. A study of the meiotic prophase. *Experimental Cell Research* **24** 495-507.

Braw-Tal R, McNatty KP, Smith P, Heath DA, Hudson NL, Phillips DJ, McLeod BJ & Davis GH 1993 Ovaries of ewes homozygous for the X-linked Inverdale gene (FecXI) are devoid of secondary and tertiary follicles but contain many abnormal structures. *Biology of Reproduction* **49** 895-907.

Buccione R, Vanderhyden BC, Caron PJ & Eppig JJ 1990 FSH-induced expansion of the mouse cumulus oophorus in vitro is dependent upon a specific factor(s) secreted by the oocyte. *Developmental Biology* **138** 16-25.

Burden S & Yarden Y 1997 Neuregulins and their receptors: a versatile signaling module in organogenesis and oncogenesis. *Neuron* **18** 847-855.

Camp TA, Rahal JO & Mayo KE 1991 Cellular localization and hormonal regulation of follicle-stimulating hormone and luteinizing hormone receptor messenger RNAs in the rat ovary. *Molecular Endocrinology* **5** 1405-1417.

Carabatsos MJ, Elvin J, Matzuk MM & Albertini DF 1998 Characterization of oocyte and follicle development in growth differentiation factor-9-deficient mice. *Developmental Biology* **204** 373-384.

Carrette O, Nemade RV, Day AJ, Brickner A & Larsen WJ 2001 TSG-6 is concentrated in the extracellular matrix of mouse cumulus oocyte complexes through hyaluronan and inter-alpha-inhibitor binding. *Biology of Reproduction* **65** 301-308.

Chen L, Russell PT & Larsen WJ 1993 Functional significance of cumulus expansion in the mouse: roles for the preovulatory synthesis of hyaluronic acid within the cumulus mass. *Molecular Reproduction and Development* **34** 87-93.

Chen L, Zhang H, Powers RW, Russell PT & Larsen WJ 1996 Covalent linkage between proteins of the inter-alpha-inhibitor family and hyaluronic acid is mediated by a factor produced by granulosa cells. *Journal of Biological Chemistry* **271** 19409-19414.

Chian RC, Okuda K & Niwa K 1995 Influence of cumulus cells on in vitro fertilization of bovine oocytes derived from in vitro maturation. *Animal Reproduction Science* **38** 37-48.

Christensen AP, Patel SH, Grasa P, Christian HC & Williams SA 2015 Oocyte glycoproteins regulate the form and function of the follicle basal lamina and theca cells. *Developmental Biology* **401** 287-298.

Clarke IJ, Cummins JT, Findlay JK, Burman KJ & Doughton BW 1984 Effects on plasma luteinizing hormone and follicle-stimulating hormone of varying the frequency and amplitude of gonadotropin-releasing hormone pulses in ovariectomized ewes with hypothalamo-pituitary disconnection. *Neuroendocrinology* **39** 214-221.

Collins TJ, Parkening TA & Smith ER 1981 Plasma and pituitary concentrations of LH, FSH and prolactin after injection of GnRH in aged female C57BL/6 mice. *Neurobiology of Aging* **2** 125-131.

Conti M, Hsieh M, Park JY & Su YQ 2006 Role of the epidermal growth factor network in ovarian follicles. *Molecular Endocrinology* **20** 715-723.

Crawford JL & McNatty KP 2012 The ratio of growth differentiation factor 9: bone morphogenetic protein 15 mRNA expression is tightly co-regulated and differs between species over a wide range of ovulation rates. *Molecular and Cellular Endocrinology* **348** 339-343.

D'Alessandris C, Andreozzi F, Federici M, Cardellini M, Brunetti A, Ranalli M, Del Guerra S, Lauro D, Del Prato S, Marchetti P, Lauro R & Sesti G 2004 Increased O-glycosylation of insulin signaling proteins results in their impaired activation and enhanced susceptibility to apoptosis in pancreatic beta-cells. *FASEB Journal* **18** 959-961.

Da Silva-Buttkus P, Jayasooriya GS, Mora JM, Mobberley M, Ryder TA, Baithun M, Stark J, Franks S & Hardy K 2008 Effect of cell shape and packing density on granulosa cell proliferation and formation of multiple layers during early follicle development in the ovary. *Journal of Cell Science* **121** 3890-3900.

Daniel SA & Armstrong DT 1980 Enhancement of follicle-stimulating hormone-induced aromatase activity by androgens in cultured rat granulosa cells. *Endocrinology* **107** 1027-1033.

Davis GH, McEwan JC, Fennessy PF, Dodds KG, McNatty KP & O WS 1992 Infertility due to bilateral ovarian hypoplasia in sheep homozygous (FecXI FecXI) for the Inverdale prolificacy gene located on the X chromosome. *Biology of Reproduction* **46** 636-640.

Day AJ & Prestwich GD 2002 Hyaluronan-binding proteins: tying up the giant. *Journal of Biological Chemistry* **277** 4585-4588.

Dekel N 1988 Regulation of oocyte maturation. The role of cAMP. *Annals of the New York Academy of Sciences* **541** 211-216.

Dekel N & Sherizly I 1985 Epidermal growth factor induces maturation of rat follicle-enclosed oocytes. *Endocrinology* **116** 406-409.

di Clemente N, Wilson C, Faure E, Boussin L, Carmillo P, Tizard R, Picard JY, Vigier B, Josso N & Cate R 1994 Cloning, expression, and alternative splicing of the receptor for anti-Mullerian hormone. *Molecular Endocrinology* **8** 1006-1020.

Di Pasquale E, Beck-Peccoz P & Persani L 2004 Hypergonadotropic Ovarian Failure Associated with an Inherited Mutation of Human Bone Morphogenetic Protein-15 (BMP15) Gene. *American Journal of Human Genetics* **75** 106-111.

Diaz FJ, Wigglesworth K & Eppig JJ 2007 Oocytes determine cumulus cell lineage in mouse ovarian follicles. *Journal of Cell Science* **120** 1330-1340.

Dierich A, Sairam MR, Monaco L, Fimia GM, Gansmuller A, LeMeur M & Sassone-Corsi P 1998 Impairing follicle-stimulating hormone (FSH) signaling in vivo: targeted disruption of the FSH receptor leads to aberrant gametogenesis and hormonal imbalance. *Proc Natl Acad Sci U S A* **95** 13612-13617.

Dong J, Albertini DF, Nishimori K, Kumar TR, Lu N & Matzuk MM 1996 Growth differentiation factor-9 is required during early ovarian folliculogenesis. *Nature* **383** 531-535.

Dorrington JH, McKeracher HL, Chan AK & Gore-Langton RE 1983 Hormonal interactions in the control of granulosa cell differentiation. *J Steroid Biochem* **19** 17-32.

Dorrington JH, Moon YS & Armstrong DT 1975 Estradiol-17beta biosynthesis in cultured granulosa cells from hypophysectomized immature rats; stimulation by follicle-stimulating hormone. *Endocrinology* **97** 1328-1331.

Downs SM 1989 Specificity of epidermal growth factor action on maturation of the murine oocyte and cumulus oophorus in vitro. *Biology of Reproduction* **41** 371-379.

Dragovic RA, Ritter LJ, Schulz SJ, Amato F, Armstrong DT & Gilchrist RB 2005 Role of oocyte-secreted growth differentiation factor 9 in the regulation of mouse cumulus expansion. *Endocrinology* **146** 2798-2806.

Dragovic RA, Ritter LJ, Schulz SJ, Amato F, Thompson JG, Armstrong DT & Gilchrist RB 2007 Oocyte-secreted factor activation of SMAD 2/3 signaling enables initiation of mouse cumulus cell expansion. *Biology of Reproduction* **76** 848-857.

Drummond AE & Findlay JK 1999 The role of estrogen in folliculogenesis. *Molecular and Cellular Endocrinology* **151** 57-64.

Dube JL, Wang P, Elvin J, Lyons KM, Celeste AJ & Matzuk MM 1998 The bone morphogenetic protein 15 gene is X-linked and expressed in oocytes. *Molecular Endocrinology* **12** 1809-1817.

Duke RC, Chervenak R & Cohen JJ 1983 Endogenous endonuclease-induced DNA fragmentation: an early event in cell-mediated cytolysis. *Proc Natl Acad Sci U S A* **80** 6361-6365.

Durlinger AL, Gruijters MJ, Kramer P, Karels B, Kumar TR, Matzuk MM, Rose UM, de Jong FH, Uilenbroek JT, Grootegoed JA & Themmen AP 2001 Anti-Mullerian hormone attenuates the effects of FSH on follicle development in the mouse ovary. *Endocrinology* **142** 4891-4899.

Durlinger AL, Kramer P, Karels B, de Jong FH, Uilenbroek JT, Grootegoed JA & Themmen AP 1999 Control of primordial follicle recruitment by anti-Mullerian hormone in the mouse ovary. *Endocrinology* **140** 5789-5796.

Ebner R, Chen RH, Shum L, Lawler S, Zioncheck TF, Lee A, Lopez AR & Derynck R 1993 Cloning of a type I TGF-beta receptor and its effect on TGF-beta binding to the type II receptor. *Science* **260** 1344-1348.

Edson MA, Lin YN & Matzuk MM 2010 Deletion of the novel oocyte-enriched gene, Gpr149, leads to increased fertility in mice. *Endocrinology* **151** 358-368.

Ellenbogen A, Shavit T & Shalom-Paz E 2014 IVM results are comparable and may have advantages over standard IVF. *Facts Views Vis Obgyn* **6** 77-80.

Elvin JA, Yan C, Wang P, Nishimori K & Matzuk MM 1999 Molecular characterization of the follicle defects in the growth differentiation factor 9-deficient ovary. *Molecular Endocrinology* **13** 1018-1034.

Eppig JJ 1979 FSH stimulates hyaluronic acid synthesis by oocyte-cumulus cell complexes from mouse preovulatory follicles. *Nature* **281** 483-484.

Eppig JJ 1991 Maintenance of meiotic arrest and the induction of oocyte maturation in mouse oocyte-granulosa cell complexes developed in vitro from preantral follicles. *Biology of Reproduction* **45** 824-830.

Eppig JJ & Downs SM 1984 Chemical signals that regulate mammalian oocyte maturation. *Biology of Reproduction* **30** 1-11.

Erickson GF & Hsueh AJ 1978 Stimulation of aromatase activity by follicle stimulating hormone in rat granulosa cells in vivo and in vitro. *Endocrinology* **102** 1275-1282.

Fortune JE & Armstrong DT 1977 Androgen production by theca and granulosa isolated from proestrous rat follicles. *Endocrinology* **100** 1341-1347.

Fulop C, Kamath RV, Li Y, Otto JM, Salustri A, Olsen BR, Glant TT & Hascall VC 1997a Coding sequence, exon-intron structure and chromosomal localization of murine TNF-stimulated gene 6 that is specifically expressed by expanding cumulus cell-oocyte complexes. *Gene* **202** 95-102.

Fulop C, Salustri A & Hascall VC 1997b Coding sequence of a hyaluronan synthase homologue expressed during expansion of the mouse cumulus-oocyte complex. *Archives of Biochemistry and Biophysics* **337** 261-266.

Fulop C, Szanto S, Mukhopadhyay D, Bardos T, Kamath RV, Rugg MS, Day AJ, Salustri A, Hascall VC, Glant TT & Mikecz K 2003 Impaired cumulus mucification and female sterility in tumor necrosis factor-induced protein-6 deficient mice. *Development* **130** 2253-2261.

Galloway SM, McNatty KP, Cambridge LM, Laitinen MP, Juengel JL, Jokiranta TS, McLaren RJ, Luiro K, Dodds KG, Montgomery GW, Beattie AE, Davis GH & Ritvos O 2000 Mutations in an oocyte-derived growth factor gene (BMP15) cause increased ovulation rate and infertility in a dosage-sensitive manner. *Nature Genetics* **25** 279-283.

Garlanda C, Bottazzi B, Bastone A & Mantovani A 2005 Pentraxins at the crossroads between innate immunity, inflammation, matrix deposition, and female fertility. *Annual Review of Immunology* **23** 337-366.

Gilchrist RB, Lane M & Thompson JG 2008 Oocyte-secreted factors: regulators of cumulus cell function and oocyte quality. *Hum Reprod Update* **14** 159-177.

Goldenberg RL, Vaitukaitis JL & Ross GT 1972 Estrogen and follicle stimulation hormone interactions on follicle growth in rats. *Endocrinology* **90** 1492-1498.

Gosden RG, Hunter RH, Telfer E, Torrance C & Brown N 1988 Physiological factors underlying the formation of ovarian follicular fluid. *Journal of Reproduction and Fertility* **82** 813-825.

Gosden RG, Laing SC, Felicio LS, Nelson JF & Finch CE 1983 Imminent oocyte exhaustion and reduced follicular recruitment mark the transition to acyclicity in aging C57BL/6J mice. *Biology of Reproduction* **28** 255-260.

Grasa P, Ploutarchou P & Williams SA 2015 Oocytes lacking O-glycans alter follicle development and increase fertility by increasing follicle FSH sensitivity, decreasing apoptosis, and modifying GDF9:BMP15 expression. *FASEB Journal* **29** 525-539.

Gregory L 1998 Ovarian markers of implantation potential in assisted reproduction. *Human Reproduction* **13 Suppl 4** 117-132.

Guigon CJ, Mazaud S, Forest MG, Brailly-Tabard S, Coudouel N & Magre S 2003 Unaltered development of the initial follicular waves and normal pubertal onset in female rats after neonatal deletion of the follicular reserve. *Endocrinology* **144** 3651-3662.

Gursoy E, Ergin K, Basaloglu H, Koca Y & Seyrek K 2008 Expression and localisation of Bcl-2 and Bax proteins in developing rat ovary. *Research in Veterinary Science* **84** 56-61.

Haisenleder DJ, Ortolano GA, Jolly D, Dalkin AC, Landefeld TD, Vale WW & Marshall JC 1990 Inhibin secretion during the rat estrous cycle: relationships to FSH secretion and FSH beta subunit mRNA concentrations. *Life Sciences* **47** 1769-1773.

Hashimoto O, Takagi R, Yanuma F, Doi S, Shindo J, Endo H, Hasegawa Y & Shimasaki S 2012 Identification and characterization of canine growth differentiation factor-9 and its splicing variant. *Gene* **499** 266-272.

Hayashi M, McGee EA, Min G, Klein C, Rose UM, van Duin M & Hsueh AJ 1999 Recombinant growth differentiation factor-9 (GDF-9) enhances growth and differentiation of cultured early ovarian follicles. *Endocrinology* **140** 1236-1244.

Heldin CH, Miyazono K & ten Dijke P 1997 TGF-beta signalling from cell membrane to nucleus through SMAD proteins. *Nature* **390** 465-471.

Hess KA, Chen L & Larsen WJ 1998 The ovarian blood follicle barrier is both charge- and size-selective in mice. *Biology of Reproduction* **58** 705-711.

Higman VA, Briggs DC, Mahoney DJ, Blundell CD, Sattelle BM, Dyer DP, Green DE, DeAngelis PL, Almond A, Milner CM & Day AJ 2014 A refined model for the TSG-6 link module in complex with hyaluronan: use of defined oligosaccharides to probe structure and function. *Journal of Biological Chemistry* **289** 5619-5634.

Hillier SG & De Zwart FA 1981 Evidence that granulosa cell aromatase induction/activation by follicle-stimulating hormone is an androgen receptor-regulated process in-vitro. *Endocrinology* **109** 1303-1305.

Hirobe S, He WW, Lee MM & Donahoe PK 1992 Mullerian inhibiting substance messenger ribonucleic acid expression in granulosa and Sertoli cells coincides with their mitotic activity. *Endocrinology* **131** 854-862.

Hirshfield AN 1988 Size-frequency analysis of atresia in cycling rats. *Biology of Reproduction* **38** 1181-1188.

Hirshfield AN & Midgley AR, Jr. 1978 Morphometric analysis of follicular development in the rat. *Biology of Reproduction* **19** 597-605.

Hizaki H, Segi E, Sugimoto Y, Hirose M, Saji T, Ushikubi F, Matsuoka T, Noda Y, Tanaka T, Yoshida N, Narumiya S & Ichikawa A 1999 Abortive expansion of the cumulus and impaired fertility in mice lacking the prostaglandin E receptor subtype EP(2). *Proc Natl Acad Sci U S A* **96** 10501-10506.

Hogue CJ 2002 Successful assisted reproductive technology: the beauty of one. *Obstetrics and Gynecology* **100** 1017-1019.

Hoodbhoy T, Joshi S, Boja ES, Williams SA, Stanley P & Dean J 2005 Human sperm do not bind to rat zonae pellucidae despite the presence of four homologous glycoproteins. *Journal of Biological Chemistry* **280** 12721-12731.

Hsu CJ, Holmes SD & Hammond JM 1987 Ovarian epidermal growth factor-like activity. Concentrations in porcine follicular fluid during follicular enlargement. *Biochemical and Biophysical Research Communications* **147** 242-247.

Hsu SY, Lai RJ, Finegold M & Hsueh AJ 1996 Targeted overexpression of Bcl-2 in ovaries of transgenic mice leads to decreased follicle apoptosis, enhanced folliculogenesis, and increased germ cell tumorigenesis. *Endocrinology* **137** 4837-4843.

Hsueh AJ, Billig H & Tsafriri A 1994 Ovarian follicle atresia: a hormonally controlled apoptotic process. *Endocrine Reviews* **15** 707-724.

Ievoli E, Lindstedt R, Inforzato A, Camaioni A, Palone F, Day AJ, Mantovani A, Salvatori G & Salustri A 2011 Implication of the oligomeric state of the N-terminal PTX3 domain in cumulus matrix assembly. *Matrix Biology* **30** 330-337.

Inforzato A, Baldock C, Jowitt TA, Holmes DF, Lindstedt R, Marcellini M, Rivieccio V, Briggs DC, Kadler KE, Verdoliva A, Bottazzi B, Mantovani A, Salvatori G & Day AJ 2010 The angiogenic inhibitor long pentraxin PTX3 forms an asymmetric octamer with two binding sites for FGF2. *Journal of Biological Chemistry* **285** 17681-17692.

Irving-Rodgers HF, Mussard ML, Kinder JE & Rodgers RJ 2002 Composition and morphology of the follicular basal lamina during atresia of bovine antral follicles. *Reproduction* **123** 97-106.

Izquierdo-Rico MJ, Jimenez-Movilla M, Llop E, Perez-Oliva AB, Ballesta J, Gutierrez-Gallego R, Jimenez-Cervantes C & Aviles M 2009 Hamster zona pellucida is formed by four glycoproteins: ZP1, ZP2, ZP3, and ZP4. *J Proteome Res* **8** 926-941.

Jose de los Santos M, Anderson DJ, Racowsky C & Hill JA 2000 Presence of Fas-Fas ligand system and bcl-2 gene products in cells and fluids from gonadotropin-stimulated human ovaries. *Biology of Reproduction* **63** 1811-1816.

Ju T, Brewer K, D'Souza A, Cummings RD & Canfield WM 2002 Cloning and expression of human core 1 beta1,3-galactosyltransferase. *Journal of Biological Chemistry* **277** 178-186.

Kaivo-Oja N, Bondestam J, Kamarainen M, Koskimies J, Vitt U, Cranfield M, Vuojolainen K, Kallio JP, Olkkonen VM, Hayashi M, Moustakas A, Groome NP, ten Dijke P, Hsueh AJ & Ritvos O 2003 Growth differentiation factor-9 induces Smad2 activation and inhibin B production in cultured human granulosa-luteal cells. *Journal of Clinical Endocrinology and Metabolism* **88** 755-762.

Khurana NK & Niemann H 2000 Effects of oocyte quality, oxygen tension, embryo density, cumulus cells and energy substrates on cleavage and morula/blastocyst formation of bovine embryos. *Theriogenology* **54** 741-756.

Knight PG & Glister C 2006 TGF-beta superfamily members and ovarian follicle development. *Reproduction* **132** 191-206.

Kohda D, Morton CJ, Parkar AA, Hatanaka H, Inagaki FM, Campbell ID & Day AJ 1996 Solution structure of the link module: a hyaluronan-binding domain involved in extracellular matrix stability and cell migration. *Cell* **86** 767-775.

Kumar TR, Wang Y, Lu N & Matzuk MM 1997 Follicle stimulating hormone is required for ovarian follicle maturation but not male fertility. *Nature Genetics* **15** 201-204.

Lefievre L, Conner SJ, Salpekar A, Olufowobi O, Ashton P, Pavlovic B, Lenton W, Afnan M, Brewis IA, Monk M, Hughes DC & Barratt CL 2004 Four zona pellucida glycoproteins are expressed in the human. *Human Reproduction* **19** 1580-1586.

Levine JE & Ramirez VD 1982 Luteinizing hormone-releasing hormone release during the rat estrous cycle and after ovariectomy, as estimated with push-pull cannulae. *Endocrinology* **111** 1439-1448.

Lintern-Moore S & Moore GP 1979 The initiation of follicle and oocyte growth in the mouse ovary. *Biology of Reproduction* **20** 773-778.

Lund SA, Murdoch J, Van Kirk EA & Murdoch WJ 1999 Mitogenic and antioxidant mechanisms of estradiol action in preovulatory ovine follicles: relevance to luteal function. *Biology of Reproduction* **61** 388-392.

Matzuk MM & Lamb DJ 2008 The biology of infertility: research advances and clinical challenges. *Nature Medicine* **14** 1197-1213.

McClure N, Macpherson AM, Healy DL, Wreford N & Rogers PA 1994 An immunohistochemical study of the vascularization of the human Graafian follicle. *Human Reproduction* **9** 1401-1405.

McNatty KP & Henderson KM 1987 Gonadotrophins, fecundity genes and ovarian follicular function. *J Steroid Biochem* **27** 365-373.

McNeilly JR, Watson EA, White YA, Murray AA, Spears N & McNeilly AS 2011 Decreased oocyte DAZL expression in mice results in increased litter size by modulating follicle-stimulating hormone-induced follicular growth. *Biology of Reproduction* **85** 584-593.

McPherron AC & Lee SJ 1993 GDF-3 and GDF-9: two new members of the transforming growth factor-beta superfamily containing a novel pattern of cysteines. *Journal of Biological Chemistry* **268** 3444-3449.

Milner CM & Day AJ 2003 TSG-6: a multifunctional protein associated with inflammation. *Journal of Cell Science* **116** 1863-1873.

Milner CM, Higman VA & Day AJ 2006 TSG-6: a pluripotent inflammatory mediator? *Biochemical Society Transactions* **34** 446-450.

Moon YS, Dorrington JH & Armstrong DT 1975 Stimulatory action of follice-stimulating hormone on estradiol-17 beta secretion by hypophysectomized rat ovaries in organ culture. *Endocrinology* **97** 244-247.

Moore RK, Otsuka F & Shimasaki S 2003 Molecular basis of bone morphogenetic protein-15 signaling in granulosa cells. *Journal of Biological Chemistry* **278** 304-310.

Moremen KW, Tiemeyer M & Nairn AV 2012 Vertebrate protein glycosylation: diversity, synthesis and function. *Nat Rev Mol Cell Biol* **13** 448-462.

Morita Y, Perez GI, Maravei DV, Tilly KI & Tilly JL 1999 Targeted expression of Bcl-2 in mouse oocytes inhibits ovarian follicle atresia and prevents spontaneous and chemotherapy-induced oocyte apoptosis in vitro. *Molecular Endocrinology* **13** 841-850.

Mottershead DG, Harrison CA, Mueller TD, Stanton PG, Gilchrist RB & McNatty KP 2013 Growth differentiation factor 9:bone morphogenetic protein 15 (GDF9:BMP15) synergism and protein heterodimerization. *Proc Natl Acad Sci U S A* **110** E2257.

Mukhopadhyay D, Hascall VC, Day AJ, Salustri A & Fulop C 2001 Two distinct populations of tumor necrosis factor-stimulated gene-6 protein in the extracellular matrix of expanded mouse cumulus cell-oocyte complexes. *Archives of Biochemistry and Biophysics* **394** 173-181.

Munsterberg A & Lovell-Badge R 1991 Expression of the mouse anti-mullerian hormone gene suggests a role in both male and female sexual differentiation. *Development* **113** 613-624.

Murr SM, Geschwind, II & Bradford GE 1973 Plasma LH and FSH during different oestrous cycle conditions in mice. *Journal of Reproduction and Fertility* **32** 221-230.

Natraj U & Richards JS 1993 Hormonal regulation, localization, and functional activity of the progesterone receptor in granulosa cells of rat preovulatory follicles. *Endocrinology* **133** 761-769.

Nelson JF, Felicio LS, Randall PK, Sims C & Finch CE 1982 A longitudinal study of estrous cyclicity in aging C57BL/6J mice: I. Cycle frequency, length and vaginal cytology. *Biology of Reproduction* **27** 327-339.

Ng ST, Chang TH & Wu TC 1999 Prediction of the rates of fertilization, cleavage, and pregnancy success by cumulus-coronal morphology in an in vitro fertilization program. *Fertility and Sterility* **72** 412-417.

Oltvai ZN, Milliman CL & Korsmeyer SJ 1993 Bcl-2 heterodimerizes in vivo with a conserved homolog, Bax, that accelerates programmed cell death. *Cell* **74** 609-619.

Orisaka M, Tajima K, Mizutani T, Miyamoto K, Tsang BK, Fukuda S, Yoshida Y & Kotsuji F 2006 Granulosa cells promote differentiation of cortical stromal cells into theca cells in the bovine ovary. *Biology of Reproduction* **75** 734-740.

Pan Y, Yago T, Fu J, Herzog B, McDaniel JM, Mehta-D'Souza P, Cai X, Ruan C, McEver RP, West C, Dai K, Chen H & Xia L 2014 Podoplanin requires sialylated O-glycans for stable expression on lymphatic endothelial cells and for interaction with platelets. *Blood* **124** 3656-3665.

Panigone S, Hsieh M, Fu M, Persani L & Conti M 2008 Luteinizing hormone signaling in preovulatory follicles involves early activation of the epidermal growth factor receptor pathway. *Molecular Endocrinology* **22** 924-936.

Park JY, Su YQ, Ariga M, Law E, Jin SL & Conti M 2004 EGF-like growth factors as mediators of LH action in the ovulatory follicle. *Science* **303** 682-684.

Pedersen T & Peters H 1968 Proposal for a classification of oocytes and follicles in the mouse ovary. *Journal of Reproduction and Fertility* **17** 555-557.

Pelosi E, Omari S, Michel M, Ding J, Amano T, Forabosco A, Schlessinger D & Ottolenghi C 2013 Constitutively active Foxo3 in oocytes preserves ovarian reserve in mice. *Nat Commun* **4** 1843.

Peng J, Li Q, Wigglesworth K, Rangarajan A, Kattamuri C, Peterson RT, Eppig JJ, Thompson TB & Matzuk MM 2013 Growth differentiation factor 9:bone morphogenetic protein 15 heterodimers are potent regulators of ovarian functions. *Proc Natl Acad Sci U S A* **110** E776-785.

Peng XR, Hsueh AJ, LaPolt PS, Bjersing L & Ny T 1991 Localization of luteinizing hormone receptor messenger ribonucleic acid expression in ovarian cell types during follicle development and ovulation. *Endocrinology* **129** 3200-3207.

Pepling ME & Spradling AC 2001 Mouse ovarian germ cell cysts undergo programmed breakdown to form primordial follicles. *Developmental Biology* **234** 339-351.

Perez GI, Robles R, Knudson CM, Flaws JA, Korsmeyer SJ & Tilly JL 1999 Prolongation of ovarian lifespan into advanced chronological age by Bax-deficiency. *Nature Genetics* **21** 200-203.

Peters H 1969 The development of the mouse ovary from birth to maturity. *Acta Endocrinol (Copenh)* **62** 98-116.

Philpott CC, Ringuette MJ & Dean J 1987 Oocyte-specific expression and developmental regulation of ZP3, the sperm receptor of the mouse zona pellucida. *Developmental Biology* **121** 568-575.

Picton HM 2001 Activation of follicle development: the primordial follicle. *Theriogenology* **55** 1193-1210.

Ploutarchou P, Melo P, Day AJ, Milner CM & Williams SA 2015 Molecular analysis of the cumulus matrix: insights from mice with O-glycan-deficient oocytes. *Reproduction* **149** 533-543.

Qvist R, Blackwell LF, Bourne H & Brown JB 1990 Development of mouse ovarian follicles from primary to preovulatory stages in vitro. *Journal of Reproduction and Fertility* **89** 169-180.

Rabinovici J & Jaffe RB 1990 Development and regulation of growth and differentiated function in human and subhuman primate fetal gonads. *Endocrine Reviews* **11** 532-557.

Raisova M, Hossini AM, Eberle J, Riebeling C, Wieder T, Sturm I, Daniel PT, Orfanos CE & Geilen CC 2001 The Bax//Bcl-2 Ratio Determines the Susceptibility of Human Melanoma Cells to CD95//Fas-Mediated Apoptosis. **117** 333-340.

Rankin T, Familari M, Lee E, Ginsberg A, Dwyer N, Blanchette-Mackie J, Drago J, Westphal H & Dean J 1996 Mice homozygous for an insertional mutation in the Zp3 gene lack a zona pellucida and are infertile. *Development* **122** 2903-2910.

Rao MC, Midgley AR, Jr. & Richards JS 1978 Hormonal regulation of ovarian cellular proliferation. *Cell* **14** 71-78.

Ratts VS, Flaws JA, Kolp R, Sorenson CM & Tilly JL 1995 Ablation of bcl-2 gene expression decreases the numbers of oocytes and primordial follicles established in the post-natal female mouse gonad. *Endocrinology* **136** 3665-3668.

Revelli A, Pacchioni D, Cassoni P, Bussolati G & Massobrio M 1996 In situ hybridization study of messenger RNA for estrogen receptor and immunohistochemical detection of estrogen and progesterone receptors in the human ovary. *Gynecological Endocrinology* **10** 177-186.

Richardson SJ, Senikas V & Nelson JF 1987 Follicular depletion during the menopausal transition: evidence for accelerated loss and ultimate exhaustion. *Journal of Clinical Endocrinology and Metabolism* **65** 1231-1237.

Rodgers RJ & Irving-Rodgers HF 2010 Formation of the ovarian follicular antrum and follicular fluid. *Biology of Reproduction* **82** 1021-1029.

Roh JS, Bondestam J, Mazerbourg S, Kaivo-Oja N, Groome N, Ritvos O & Hsueh AJ 2003 Growth differentiation factor-9 stimulates inhibin production and activates Smad2 in cultured rat granulosa cells. *Endocrinology* **144** 172-178.

Rosales-Torres AM, Avalos-Rodriguez A, Vergara-Onofre M, Hernandez-Perez O, Ballesteros LM, Garcia-Macedo R, Ortiz-Navarrete V & Rosado A 2000 Multiparametric study of atresia in ewe antral follicles: histology, flow cytometry, internucleosomal DNA fragmentation, and lysosomal enzyme activities in granulosa cells and follicular fluid. *Molecular Reproduction and Development* **55** 270-281.

Rottger S, White J, Wandall HH, Olivo JC, Stark A, Bennett EP, Whitehouse C, Berger EG, Clausen H & Nilsson T 1998 Localization of three human polypeptide GalNAc-transferases in HeLa cells suggests initiation of O-linked

glycosylation throughout the Golgi apparatus. *Journal of Cell Science* **111 (Pt 1)** 45-60.

Rugg MS, Willis AC, Mukhopadhyay D, Hascall VC, Fries E, Fulop C, Milner CM & Day AJ 2005 Characterization of complexes formed between TSG-6 and inter-alpha-inhibitor that act as intermediates in the covalent transfer of heavy chains onto hyaluronan. *Journal of Biological Chemistry* **280** 25674-25686.

Saito S, Yano K, Sharma S, McMahon HE & Shimasaki S 2008 Characterization of the post-translational modification of recombinant human BMP-15 mature protein. *Protein Science* **17** 362-370.

Sakurada Y, Shirota M, Inoue K, Uchida N & Shirota K 2006 New approach to in situ quantification of ovarian gene expression in rat using a laser microdissection technique: relationship between follicle types and regulation of inhibin-alpha and cytochrome P450aromatase genes in the rat ovary. *Histochemistry and Cell Biology* **126** 735-741.

Salakou S, Kardamakis D, Tsamandas AC, Zolota V, Apostolakis E, Tzelepi V, Papathanasopoulos P, Bonikos DS, Papapetropoulos T, Petsas T & Dougenis D 2007 Increased Bax/Bcl-2 ratio up-regulates caspase-3 and increases apoptosis in the thymus of patients with myasthenia gravis. *In Vivo* **21** 123-132.

Salmon NA, Handyside AH & Joyce IM 2004 Oocyte regulation of anti-Mullerian hormone expression in granulosa cells during ovarian follicle development in mice. *Developmental Biology* **266** 201-208.

Salustri A, Garlanda C, Hirsch E, De Acetis M, Maccagno A, Bottazzi B, Doni A, Bastone A, Mantovani G, Beck Peccoz P, Salvatori G, Mahoney DJ, Day AJ, Siracusa G, Romani L & Mantovani A 2004 PTX3 plays a key role in the organization of the cumulus oophorus extracellular matrix and in in vivo fertilization. *Development* **131** 1577-1586.

Salustri A, Yanagishita M & Hascall VC 1989 Synthesis and accumulation of hyaluronic acid and proteoglycans in the mouse cumulus cell-oocyte complex during follicle-stimulating hormone-induced mucification. *Journal of Biological Chemistry* **264** 13840-13847.

Salustri A, Yanagishita M & Hascall VC 1990 Mouse oocytes regulate hyaluronic acid synthesis and mucification by FSH-stimulated cumulus cells. *Developmental Biology* **138** 26-32.

Sanggaard KW, Karring H, Valnickova Z, Thogersen IB & Enghild JJ 2005 The TSG-6 and I alpha I interaction promotes a transesterification cleaving the protein-glycosaminoglycan-protein (PGP) cross-link. *Journal of Biological Chemistry* **280** 11936-11942.

Sanggaard KW, Sonne-Schmidt CS, Krogager TP, Lorentzen KA, Wisniewski HG, Thogersen IB & Enghild JJ 2008 The transfer of heavy chains from bikunin proteins to hyaluronan requires both TSG-6 and HC2. *Journal of Biological Chemistry* **283** 18530-18537.

Sar M & Welsch F 1999 Differential expression of estrogen receptor-beta and estrogen receptor-alpha in the rat ovary. *Endocrinology* **140** 963-971.

Sato H, Kajikawa S, Kuroda S, Horisawa Y, Nakamura N, Kaga N, Kakinuma C, Kato K, Morishita H, Niwa H & Miyazaki J 2001 Impaired fertility in female mice lacking urinary trypsin inhibitor. *Biochemical and Biophysical Research Communications* **281** 1154-1160.

Scaramuzzi RJ, Adams NR, Baird DT, Campbell BK, Downing JA, Findlay JK, Henderson KM, Martin GB, McNatty KP, McNeilly AS & et al. 1993 A model for follicle selection and the determination of ovulation rate in the ewe. *Reproduction, Fertility, and Development* **5** 459-478.

Scarchilli L, Camaioni A, Bottazzi B, Negri V, Doni A, Deban L, Bastone A, Salvatori G, Mantovani A, Siracusa G & Salustri A 2007 PTX3 interacts with inter-alpha-trypsin inhibitor: implications for hyaluronan organization and cumulus oophorus expansion. *Journal of Biological Chemistry* **282** 30161-30170.

Shalgi R, Kraicer PF & Soferman N 1972 Gases and electrolytes of human follicular fluid. *Journal of Reproduction and Fertility* **28** 335-340.

Shi S, Williams SA, Seppo A, Kurniawan H, Chen W, Ye Z, Marth JD & Stanley P 2004 Inactivation of the Mgat1 gene in oocytes impairs oogenesis, but embryos lacking complex and hybrid N-glycans develop and implant. *Molecular and Cellular Biology* **24** 9920-9929.

Shur BD & Hall NG 1982 A role for mouse sperm surface galactosyltransferase in sperm binding to the egg zona pellucida. *Journal of Cell Biology* **95** 574-579.

Slot KA, Voorendt M, de Boer-Brouwer M, van Vugt HH & Teerds KJ 2006 Estrous cycle dependent changes in expression and distribution of Fas, Fas ligand, Bcl-2, Bax, and pro- and active caspase-3 in the rat ovary. *Journal of Endocrinology* **188** 179-192.

Sola RJ & Griebenow K 2010 Glycosylation of therapeutic proteins: an effective strategy to optimize efficacy. *BioDrugs* **24** 9-21.

Souchelnytskyi S, ten Dijke P, Miyazono K & Heldin CH 1996 Phosphorylation of Ser165 in TGF-beta type I receptor modulates TGF-beta1-induced cellular responses. *The EMBO Journal* **15** 6231-6240.

Souza CJ, McNeilly AS, Benavides MV, Melo EO & Moraes JC 2014 Mutation in the protease cleavage site of GDF9 increases ovulation rate and litter size in heterozygous ewes and causes infertility in homozygous ewes. *Animal Genetics* **45** 732-739.

Stanley P 2011 Golgi glycosylation. *Cold Spring Harb Perspect Biol* **3**.

Su YQ, Wu X, O'Brien MJ, Pendola FL, Denegre JN, Matzuk MM & Eppig JJ 2004 Synergistic roles of BMP15 and GDF9 in the development and function of the oocyte-cumulus cell complex in mice: genetic evidence for an oocyte-granulosa cell regulatory loop. *Developmental Biology* **276** 64-73.

Tanghe S, Van Soom A, Nauwynck H, Coryn M & de Kruif A 2002 Minireview: Functions of the cumulus oophorus during oocyte maturation, ovulation, and fertilization. *Molecular Reproduction and Development* **61** 414-424.

Taylor RC, Cullen SP & Martin SJ 2008 Apoptosis: controlled demolition at the cellular level. *Nat Rev Mol Cell Biol* **9** 231-241.

Tian E, Hoffman MP & Ten Hagen KG 2012 O-glycosylation modulates integrin and FGF signalling by influencing the secretion of basement membrane components. *Nat Commun* **3** 869.

Tilly JL, Billig H, Kowalski KI & Hsueh AJ 1992 Epidermal growth factor and basic fibroblast growth factor suppress the spontaneous onset of apoptosis in cultured rat ovarian granulosa cells and follicles by a tyrosine kinase-dependent mechanism. *Molecular Endocrinology* **6** 1942-1950.

Tsujimoto H, Takeshita S, Nakatani K, Kawamura Y, Tokutomi T & Sekine I 2001a Delayed apoptosis of circulating neutrophils in Kawasaki disease. *Clinical and Experimental Immunology* **126** 355-364.

Tsujimoto H, Takeshita S, Nakatani K, Kawamura Y, Tokutomi T & Sekine I 2001b Delayed apoptosis of circulating neutrophils in Kawasaki disease. *Clinical and Experimental Immunology* **126** 355-364.

Ueno S, Kuroda T, Maclaughlin DT, Ragin RC, Manganaro TF & Donahoe PK 1989 Mullerian inhibiting substance in the adult rat ovary during various stages of the estrous cycle. *Endocrinology* **125** 1060-1066.

van Delft MF & Huang DC 2006 How the Bcl-2 family of proteins interact to regulate apoptosis. *Cell Res* **16** 203-213.

Van Soom A, Tanghe S, De Pauw I, Maes D & de Kruif A 2002 Function of the cumulus oophorus before and during mammalian fertilization. *Reprod Domest Anim* **37** 144-151.

Van Wezel IL, Dharmarajan AM, Lavranos TC & Rodgers RJ 1999 Evidence for alternative pathways of granulosa cell death in healthy and slightly atretic bovine antral follicles. *Endocrinology* **140** 2602-2612.

Vanderhyden BC & Armstrong DT 1989 Role of cumulus cells and serum on the in vitro maturation, fertilization, and subsequent development of rat oocytes. *Biology of Reproduction* **40** 720-728.

Vanderhyden BC, Caron PJ, Buccione R & Eppig JJ 1990 Developmental pattern of the secretion of cumulus expansion-enabling factor by mouse oocytes and the role of oocytes in promoting granulosa cell differentiation. *Developmental Biology* **140** 307-317.

Vanderhyden BC & Tonary AM 1995 Differential regulation of progesterone and estradiol production by mouse cumulus and mural granulosa cells by A factor(s) secreted by the oocyte. *Biology of Reproduction* **53** 1243-1250.

Varani S, Elvin JA, Yan C, DeMayo J, DeMayo FJ, Horton HF, Byrne MC & Matzuk MM 2002 Knockout of pentraxin 3, a downstream target of growth differentiation factor-9, causes female subfertility. *Molecular Endocrinology* **16** 1154-1167.

Varnosfaderani Sh R, Ostadhosseini S, Hajian M, Hosseini SM, Khashouei EA, Abbasi H, Hosseinnia P & Nasr-Esfahani MH 2013 Importance of the GDF9 signaling pathway on cumulus cell expansion and oocyte competency in sheep. *Theriogenology* **80** 470-478.

Visser JA, Durlinger AL, Peters IJ, van den Heuvel ER, Rose UM, Kramer P, de Jong FH & Themmen AP 2007 Increased oocyte degeneration and follicular atresia during the estrous cycle in anti-Mullerian hormone null mice. *Endocrinology* **148** 2301-2308.

Williams SA & Stanley P 2008 Mouse fertility is enhanced by oocyte-specific loss of core 1-derived O-glycans. *FASEB Journal* **22** 2273-2284.

Williams SA, Xia L, Cummings RD, McEver RP & Stanley P 2007 Fertilization in mouse does not require terminal galactose or N-acetylglucosamine on the zona pellucida glycans. *Journal of Cell Science* **120** 1341-1349.

Wilson T, Wu XY, Juengel JL, Ross IK, Lumsden JM, Lord EA, Dodds KG, Walling GA, McEwan JC, O'Connell AR, McNatty KP & Montgomery GW 2001 Highly prolific Booroola sheep have a mutation in the intracellular kinase domain of bone morphogenetic protein IB receptor (ALK-6) that is expressed in both oocytes and granulosa cells. *Biology of Reproduction* **64** 1225-1235.

Wrana JL, Attisano L, Wieser R, Ventura F & Massague J 1994 Mechanism of activation of the TGF-beta receptor. *Nature* **370** 341-347.

Wu X, Chen L, Brown CA, Yan C & Matzuk MM 2004 Interrelationship of growth differentiation factor 9 and inhibin in early folliculogenesis and ovarian tumorigenesis in mice. *Molecular Endocrinology* **18** 1509-1519.

Wyllie AH, Kerr JF & Currie AR 1980 Cell death: the significance of apoptosis. *International Review of Cytology* **68** 251-306.

Xia L, Ju T, Westmuckett A, An G, Ivanciu L, McDaniel JM, Lupu F, Cummings RD & McEver RP 2004 Defective angiogenesis and fatal embryonic hemorrhage in mice lacking core 1-derived O-glycans. *Journal of Cell Biology* **164** 451-459.

Yago T, Fu J, McDaniel JM, Miner JJ, McEver RP & Xia L 2010 Core 1-derived O-glycans are essential E-selectin ligands on neutrophils. *Proc Natl Acad Sci U S A* **107** 9204-9209.

Yan C, Wang P, DeMayo J, DeMayo FJ, Elvin JA, Carino C, Prasad SV, Skinner SS, Dunbar BS, Dube JL, Celeste AJ & Matzuk MM 2001 Synergistic roles of bone morphogenetic protein 15 and growth differentiation factor 9 in ovarian function. *Molecular Endocrinology* **15** 854-866.

Yang E & Korsmeyer SJ 1996 Molecular thanatopsis: a discourse on the BCL2 family and cell death. *Blood* **88** 386-401.

Yoshioka S, Ochsner S, Russell DL, Ujioka T, Fujii S, Richards JS & Espey LL 2000 Expression of tumor necrosis factor-stimulated gene-6 in the rat ovary in response to an ovulatory dose of gonadotropin. *Endocrinology* **141** 4114-4119.

Young JD, Tsuchiya D, Sandlin DE & Holroyde MJ 1979 Enzymic O-glycosylation of synthetic peptides from sequences in basic myelin protein. *Biochemistry* **18** 4444-4448.

Young JM & McNeilly AS 2010 Theca: the forgotten cell of the ovarian follicle. *Reproduction* **140** 489-504.

Zheng W, Zhang H, Gorre N, Risal S, Shen Y & Liu K 2014 Two classes of ovarian primordial follicles exhibit distinct developmental dynamics and physiological functions. *Human Molecular Genetics* **23** 920-928.

Zhuo L, Yoneda M, Zhao M, Yingsung W, Yoshida N, Kitagawa Y, Kawamura K, Suzuki T & Kimata K 2001 Defect in SHAP-hyaluronan complex causes severe female infertility. A study by inactivation of the bikunin gene in mice. *Journal of Biological Chemistry* **276** 7693-7696.

APPENDIX A

Published article: Molecular analysis of the cumulus matrix: insights from mice with O-glycan-deficient oocytes.

Authors: Panayiota Ploutarchou, Pedro Melo, Anthony J Day, Caroline M Milner and Suzannah A Williams.

REPRODUCTION
RESEARCH

Molecular analysis of the cumulus matrix: insights from mice with *O*-glycan-deficient oocytes

Panayiota Ploutarchou, Pedro Melo, Anthony J Day[1,2], Caroline M Milner[1] and Suzannah A Williams

Nuffield Department of Obstetrics and Gynaecology, Women's Centre, Level 3, John Radcliffe Hospital, University of Oxford, Oxford OX3 9DU, UK, [1]Faculty of Life Sciences, University of Manchester, Michael Smith Building, Oxford Road, Manchester M13 9PT, UK and [2]Wellcome Trust Centre for Cell-Matrix Research, Faculty of Life Sciences, University of Manchester, Michael Smith Building, Oxford Road, Manchester M13 9PT, UK

Correspondence should be addressed to S A Williams; Email: suzannah.williams@obs-gyn.ox.ac.uk

Abstract

During follicle development, oocytes secrete factors that influence the development of granulosa and cumulus cells (CCs). In response to oocyte and somatic cell signals, CCs produce extracellular matrix (ECM) molecules resulting in cumulus expansion, which is essential for ovulation, fertilisation, and is predictive of oocyte quality. The cumulus ECM is largely made up of hyaluronan (HA), TNF-stimulated gene-6 (TSG-6, also known as TNFAIP6), pentraxin-3 (PTX3), and the heavy chains (HCs) of serum-derived inter-α-inhibitor proteins. In contrast to other *in vivo* models where modified expansion impairs fertility, the cumulus mass of *C1galt1* Mutants, which have oocyte-specific deletion of core 1-derived *O*-glycans, is modified without impairing fertility. In this report, we used *C1galt1* Mutant (*C1galt1*^{FF}:ZP3*Cre*) and Control (*C1galt1*^{FF}) mice to investigate how cumulus expansion is affected by oocyte-specific deletion of core 1-derived *O*-glycans without adversely affecting oocyte quality. Mutant cumulus–oocyte complexes (COCs) are smaller than Controls, with fewer CCs. Interestingly, the CCs in Mutant mice are functionally normal as each cell produced normal levels of the ECM molecules HA, TSG-6, and PTX3. However, HC levels were elevated in Mutant COCs. These data reveal that oocyte glycoproteins carrying core 1-derived *O*-glycans have a regulatory role in COC development. In addition, our study of Controls indicates that a functional COC can form provided all essential components are present above a minimum threshold level, and thus some variation in ECM composition does not adversely affect oocyte development, ovulation or fertilisation. These data have important implications for IVF and the use of cumulus expansion as a criterion for oocyte assessment.

Reproduction (2015) **149** 533–543

Introduction

The process of follicle development begins with the activation of a quiescent primordial follicle and culminates with the ovulation of a single fertilisable egg. During the early stages of follicle development, the granulosa cells that surround the oocyte proliferate to form multiple layers of cells. As the follicle develops, antral fluid is deposited between the granulosa cells which facilitates the physical separation and differentiation of the granulosa cell population into mural granulosa cells (mGCs; which line the wall of the follicle) and cumulus cells (CCs) that are associated with the oocyte.

Prior to ovulation, an extracellular matrix (ECM) is assembled between the CCs leading to expansion of the cumulus mass that surrounds the oocyte. The expanded cumulus mass is believed to facilitate efficient capture of an ovulated egg by the oviductal fimbriae and transport into the oviduct (Chen *et al*. 1993, Tanghe *et al*. 2002). Furthermore, oocyte quality has been linked to the degree of cumulus expansion in humans (Ng *et al*. 1999). Therefore, ECM deposition and cumulus expansion are important for ovulation, fertilisation and implantation.

Ovulation is stimulated by the release of luteinising hormone (LH), which initiates two signalling events. First, mGCs secrete epidermal growth factor-like (EGF-L) peptides that bind to EGF receptors on CCs (Park *et al*. 2004). Secondly, also acting on CCs, the oocyte produces soluble growth factors termed as oocyte-secreted factors (OSFs) that are required for cumulus expansion in mice; these include members of the transforming growth factor beta (TGF-β) superfamily (e.g. GDF9 and BMP15) (Su *et al*. 2004, Dragovic *et al*. 2005, Peng *et al*. 2013). Binding of TGF-β ligands to cognate receptors on CCs results in the activation of

© 2015 The authors
ISSN 1470–1626 (paper) 1741–7899 (online)
DOI: 10.1530/REP-14-0503
Online version via www.reproduction-online.org

This work is licensed under a Creative Commons Attribution 3.0 Unported License.

signal transduction pathways mediated via either SMAD2/3 or SMAD1/5/8 (Knight & Glister 2006). Although OSFs have a central role in cumulus expansion in mice, a similar role has not been shown in mono-ovulatory species. Cow and ovine cumulus–oocyte complexes (COCs) undergo follicle-stimulating hormone-induced cumulus expansion *in vitro* in the absence of the oocyte, suggesting that OSFs are not vital for cumulus expansion in all species (Gilchrist *et al.* 2008, Varnosfaderani Sh *et al.* 2013). The role of OSFs in COC expansion in humans is currently unclear (Gilchrist *et al.* 2008).

Following the LH surge, the activation of EGF- and OSF-mediated signalling pathways induces CCs to express hyaluronan synthase 2 (HAS2) and synthesise the glycosaminoglycan hyaluronan (HA) (Fulop *et al.* 1997*a*), the major structural component of the viscoelastic cumulus ECM (Salustri *et al.* 1989). The organisation and stability of the cumulus matrix are dependent on cross linking of the HA polysaccharide, which is mediated by several proteins, including pentraxin-3 (PTX3), TSG-6 (which is the secreted protein product of TNFAIP6, hereafter referred to as TSG-6) and the heavy chains (HCs) of inter-α-inhibitor (IαI) and pre-α-inhibitor (PαI) (Sato *et al.* 2001, Zhuo *et al.* 2001, Fulop *et al.* 2003, Salustri *et al.* 2004, Scarchilli *et al.* 2007).

IαI and PαI are synthesised in the liver and transported in serum, but their size and charge cause them to be excluded from the follicle by the basal lamina (Hess *et al.* 1998). At ovulation, the LH surge initiates the breakdown of the blood–follicle barrier (McClure *et al.* 1994, Irving-Rodgers *et al.* 2002), allowing IαI and PαI to diffuse into pre-ovulatory follicles where the HC components are incorporated into the cumulus ECM (Chen *et al.* 1996). In cumulus expansion, the HCs are transferred from IαI and PαI onto HA to form covalent HC·HA complexes; this process is catalysed by TSG-6 and occurs via TSG-6·HC intermediates (Rugg *et al.* 2005, Sanggaard *et al.* 2008). Mice that are deficient in the expression of either *bikunin* (and hence unable to assemble IαI) or *Tnfaip6* fail to support COC expansion (Sato *et al.* 2001, Zhuo *et al.* 2001, Fulop *et al.* 2003), indicating that the covalent modification of HA with HCs is essential for the assembly and cross linking of a stable cumulus ECM.

TSG-6 participates in multiple ECM remodelling processes (Milner & Day 2003, Milner *et al.* 2006) and is secreted by CCs and mGCs in response to ovulatory stimuli (Fulop *et al.* 1997*b*, Yoshioka *et al.* 2000, Carrette *et al.* 2001, Mukhopadhyay *et al.* 2001). As noted above, TSG-6 binds covalently to HCs during the catalysis of HC·HA formation (Rugg *et al.* 2005, Sanggaard *et al.* 2005, 2008). TSG-6-deficient female mice lack HC·HA complexes and are severely sub-fertile, which has been attributed to an unstable cumulus ECM leading to an absence of cumulus expansion (Fulop *et al.* 2003). Although TSG-6 contains a link module domain (in common with most other HA-binding proteins (Day & Prestwich 2002, Higman *et al.* 2014)) and binds directly to HA (Kohda *et al.* 1996), it is unclear whether TSG-6 is incorporated into the cumulus ECM.

PTX3, which is also secreted by CCs and required for ECM formation, is a multimeric protein, belonging to the pentraxin superfamily (Garlanda *et al.* 2005, Inforzato *et al.* 2010). COCs of PTX3-deficient mice have disorganised CC layers and females are sterile (Salustri *et al.* 2004). PTX3 has been found to interact with HCs (Scarchilli *et al.* 2007, Ievoli *et al.* 2011) and to play a key role in the organisation and cross-linking of HC·HA (Baranova *et al.* 2014).

As described previously, compromised COC expansion negatively affects female fertility in mice; in human IVF, the degree of cumulus expansion has been shown to be positively correlated with oocyte quality and thus fertilisation and implantation rates (Ng *et al.* 1999). However, the *C1galt1* mouse model is unique since it exhibits defective cumulus expansion, but fertility is not compromised (Williams & Stanley 2008, Grasa *et al.* 2014). These observations suggest that some aspects of cumulus expansion are redundant to successful fertilisation and the aim of this study was to identify these aspect(s).

Eggs ovulated from *C1galt1* Mutant mice are surrounded by a cumulus mass that is denser and more resistant to hyaluronidase treatment compared with Control, indicating altered structure and function (Williams & Stanley 2008). Interestingly, *C1galt1* Mutant mice exhibit increased fertility due to more follicles reaching the pre-ovulatory stage (Williams & Stanley 2008, Grasa *et al.* 2014). *C1galt1* encodes the glycosyltransferase T-synthase, also known as core 1 β1, 3-galactosyltransferase (C1galt1), which is responsible for the synthesis of core 1-derived *O*-glycans (Fig. 1). *O*-glycosylation is a common post-translational modification and has important implications in determining the structure and function of glycoproteins. *O*-glycans have

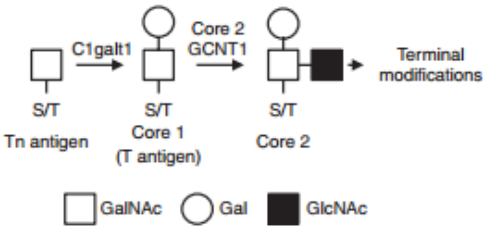

Figure 1 Action of C1galt1 in *O*-glycosylation. Core 1 β1,3-galactosyltransferase 1 (C1galt1) catalyses the addition of a galactose molecule to the Tn-antigen (*N*-acetylgalactosamine – serine/threonine) to form core 1 *O*-glycans, which are precursors to more complex *O*-glycans. Core 2 GCNT1 (β-1,6-*N*-acetylglucosaminyltransferase) extends core 1 *O*-glycans by the addition of *N*-acetylglucosamine to form core 2 *O*-glycans. In the *C1galt1* Mutant mice, oocytes do not produce C1galt1 and thus core 1-derived *O*-glycans are no longer synthesised on oocyte glycoproteins.

been shown to be important in receptor signalling (Stanley 2011), cell–cell interaction (Yago *et al.* 2010), cell–matrix interaction (Tian *et al.* 2012), and can provide protective roles for glycoproteins against proteolytic degradation (Pan *et al.* 2014). In the *C1galt1* Mutant, use of the ZP3*Cre* transgene enables deletion of *C1galt1* (and hence a lack of core 1-derived *O*-glycans on glycoproteins) specifically in oocytes from the primary follicle stage onwards (Philpott *et al.* 1987). The effects of oocyte-generated core 1-derived *O*-glycans, including those of OSFs, on surrounding CCs have not been investigated and therefore the *C1galt1* Mutant mouse provides a good model to investigate the role of these glycans on cumulus function.

Therefore, on the basis that the cumulus expansion defect in *C1galt1* Mutant mice does not lead to a respective compromise in subsequent fertility (as opposed to other mouse models with cumulus defects), our first hypothesis was that the altered cumulus mass was due to molecular changes in the cumulus ECM. Changes in any of the cumulus molecules would indicate either redundancy or plasticity in the function of the cumulus complex. In addition, considering the importance of the different cumulus ECM molecules (evident from the knock-out mouse models described previously) our novel intra-follicular approach, comparing ECM molecules of individual COCs, enabled us to determine the degree of correlation between these molecules in Control cumulus complexes.

In this study, we demonstrate that the modified cumulus matrix of *C1galt1* Mutant COCs results predominantly from the reduced Mutant cumulus size brought about by fewer CCs with additional minor changes in cumulus ECM proteins. These data have wider implications in the field of assisted reproductive technologies (ARTs) since selection of developmentally competent eggs should not be judged solely by the size of the cumulus complex and the number of CCs surrounding an egg. In addition, using this novel method of correlating the levels of cumulus ECM molecules within individual cumulus complexes, we provide evidence that considerable variations exist in the composition of the cumulus ECM, which are tolerated without adverse effects on fertility in both the Control and the Mutant, as long as all components are present above a threshold level.

Materials and methods

Animals and hormone treatments

C1galt1^{FF}:ZP3*Cre* male mice (*Mus musculus*) were mated with *C1galt1*^{FF} female mice to generate *C1galt1*^{FF}:ZP3*Cre* (Mutant) and *C1galt1*^{FF} (Control) female mice (Williams *et al.* 2007). Mice were kept in a 12 h light:12 h darkness cycle with lights on at 0700 h. For superovulation, mice were injected intraperitoneally with 5 IU of pregnant mare serum gonadotrophin (PMSG, Biosupply, Bradford, UK) at 1600 h and, 48 h later, with 5 IU of human chorionic gonadotrophin (hCG; Chorulon, Biosupply). All experiments were approved by the Home Office and the Clinical Medical Local Ethical Review Committee.

Genotyping

Mice were genotyped using protocols adapted from Williams *et al.* (2007). Each 25 µl PCR contained 2.5 µl of 10× PCR buffer (Bioline, London, UK), 0.75 µl of 50 mM $MgCl_2$ solution (Bioline), 0.5 µl of 10 mM dNTP (Roche, Mannheim, Germany), 0.5 µl of each primer (Eurogentec, Liege Science Park, Seraing, Belgium), 1 µl of genomic DNA (ear) and 0.15 µl of Taq polymerase (Bioline) for the detection of floxed *C1galt1* or 0.5 µl of Taq polymerase for the detection of the *Cre* transgene. The primers used to detect the *C1galt1* floxed allele were either TS1 (Williams *et al.* 2007) and TS8 (TCTGCATTGAAGTT-CATCTGT) or FB33 and FB34 (Batista *et al.* 2012) and the *Cre* transgene was detected using primers PS502 and PS607 (Shi *et al.* 2004).

Ovary collection and histology

Ovaries from 8- to 9-week-old mice were dissected 9 h post-hCG, fixed in 10% buffered formalin (Sigma–Aldrich, Dorset, UK) for 8 h and washed in 70% ethanol. The ovaries were embedded in paraffin, sectioned at 5 µm and mounted on glass slides.

Histochemistry and immunohistochemistry

The sections were deparaffinised and rehydrated. Antigen retrieval was performed to enable detection of TSG-6, Ki-67 and pSMAD2 (low pH solution, Vector Labs, Peterborough, UK) and pSMAD1/5/8 (0.01 M citrate buffer). Endogenous peroxidase was blocked with 3% H_2O_2 (Fisher Scientific, Loughborough, UK) in PBS for 5 min. The sections were blocked with 2% FCS (Sigma–Aldrich) in PBS for 1 h before HA detection, or with 1.5% normal goat serum (NGS, Vectastain ABC Kit, Vector Labs) in TBS for 1 h before TSG-6, Ki-67 and pSMAD2 detection, or with 10% dry milk (Alcafe, Reading, UK) in PBS for 1 h before PTX detection, or with 5% dry milk in PBS for 2 h before HC detection, or with 5% BSA (Fisher Scientific) in PBS for 1 h before pSMAD1/5/8 detection. The sections were then incubated with either 0.25 mg/ml biotinylated HA binding protein (bHABP (Clark *et al.* 2011), Seikagaku, Tokyo, Japan) at 1:50, or rabbit anti-mouse TSG-6 polyclonal anti-sera (Carrette *et al.* 2001) at 1:150, or 1 mg/ml rabbit anti-human PTX3 polyclonal antibody ((Scarchilli *et al.* 2007), generously supplied by Dr Antonio Inforzato) at 1:200, or 7.6 mg/ml rabbit anti-human Iαl/Pαl polyclonal antibody at 1:100 (to detect HCs) ((Carrette *et al.* 2001, Mukhopadhyay *et al.* 2001); Dako, Glostrup, Denmark), or rabbit anti-Ki-67 antibody (Abcam, Cambridge, UK) at 1:100, or rabbit anti-pSMAD2 polyclonal antibody (0.25 mg/ml; Life Technologies, Invitrogen, Paisley, UK) at 1:100, or anti-pSMAD1/5/8 polyclonal antibody (Cell Signalling, Beverly, MA, USA) at 1:250; all reagents were diluted in their respective blocking

solution and incubated for 2 h at room temperature (HA, Ki-67 and pSMAD2) or at 4 °C overnight (TSG-6, PTX3, HC and pSMAD1/5/8). The specificity of anti-pSMAD1/5/8 was determined by western blot analysis of BMP2-treated HeLa and MEF cells (Cell Signalling), anti-pSMAD2 was shown to be specific by western blot analysis of TGF-β-stimulated HepG2 cells (Life Technologies), immunogen affinity-purified anti-Ki-67 was assessed using immunohistochemistry with positive control tissue (Abcam; Chen *et al.* 2014, Nenicu *et al.* 2014). The specifities of the anti-IαI (Carrette *et al.* 2001, Mukhopadhyay *et al.* 2001, Salustri *et al.* 2004), anti-TSG-6 (Carrette *et al.* 2001, Mukhopadhyay *et al.* 2001) and anti-PTX3 reagents (Salustri *et al.* 2004) have all been demonstrated by western blot analysis in the context of murine COC extracts.

All immunohistochemistry slides were incubated with biotinylated anti-rabbit IgG secondary antibody (Vectastain ABC Elite Kit, Vector Labs) for 1 h at room temperature, followed by ABC solution (Vectastain ABC Elite Kit) for 30 min at room temperature. Antigen-specific detection was revealed using a DAB Kit (Vector Labs). The slides were then dehydrated and mounted with Depex (VWR, Leicestershire, UK) and imaged using the same light microscope (Leica DM 2500, Microscope services Ltd, Woodstock, UK). Experiments to detect HA and protein antigens using bHABP or antibodies, respectively, were all performed a minimum of three times.

Characterisation of cumulus complex

Molecules detected in CCs and cumulus ECM were quantified using ImageJ Software (National Institutes of Health, Bethesda, MD, USA). In ImageJ, each pixel is given an intensity value from 0 (black) to 255 (white); based on this, total pixel intensity and mean pixel intensity are calculated. The values for total pixel intensity, number of pixels, and mean pixel intensity for each cumulus complex were all calculated and exported from ImageJ. The pixel values were then inverted, therefore 0=white and 255=black, to facilitate data interpretation. Finally, mean pixel intensity was expressed as a percentage (i.e. scale 0–100). To normalise to CC numbers, the value of total pixel intensity was simply divided by CC numbers.

To analyse the size of cumulus complexes, the section closest to the centre of the oocyte was chosen. Cumulus area was quantified by selecting the space occupied by CCs (Fig. 2A), and average cumulus diameter was determined by

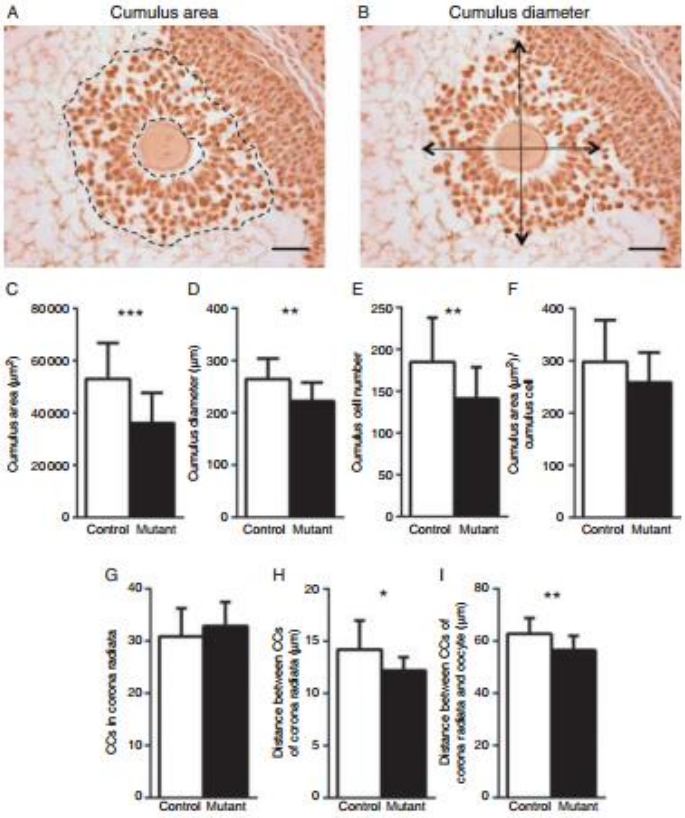

Figure 2 Oocyte-derived *O*-glycans modify cumulus expansion. The central section through each oocyte was selected and the size of the cumulus complex assessed by determining the area occupied by the CCs (A) and by averaging the two largest perpendicular diameters of the COC (B). The following values were determined for Control and Mutant COCs: size of the cumulus area in COCs (C), average diameter of COCs (D), total CC number making up the cumulus complex (E), density of CC distribution in COCs (F), number of CCs making up corona radiata (G), average distance between adjacent CCs in the corona radiata (H) and average distance between corona radiata CCs and the centre of the oocyte (I). Data are presented as mean values±s.d. (C, D, E and F): $n=16$ Control and $n=22$ Mutant COCs. (G, H and I): $n=13$ Control and $n=29$ Mutant COCs. *$P<0.05$; **$P<0.01$ and ***$P<0.001$. Scale bar: 50 µm.

averaging the two largest perpendicular diameters in the cumulus complex (Fig. 2B). To count the total number of CCs in each COC and the number of CCs in the corona radiata, the centremost section of the COC was counterstained with haematoxylin (Shandon Gill 2 Haematoxylin, Fisher Scientific) and the number of CCs was determined using the count tool in ImageJ. To measure the distance between each corona radiata CC and the distance between corona radiata CCs and the oocyte, the straight-line tool in ImageJ was used. The numbers of complexes analysed are given in respective figure legends.

Statistical analysis

All bar graphs values are presented as mean±s.d. and data were analysed using Student's *t*-test (GraphPad Prism Software, Inc., San Diego, CA, USA). A P value of <0.05 was considered to be statistically significant. For correlations of ECM molecules and cumulus expansion, the coefficient of determination (r^2) was calculated (GraphPad Prism) to establish the degree of association between the variables. An r^2 value of >0.8 was considered to indicate a strong association.

Results

Cumulus expansion in the C1galt1 *Mutant is reduced*

Eggs from superovulated *C1galt1* Mutant female mice are surrounded by modified cumulus masses compared with Controls (Williams & Stanley 2008). To characterise and quantify the Mutant phenotype in expanded COCs, *C1galt1* Mutant and Control females were induced to ovulate using exogenous gonadotrophins. Ovaries were collected 9 h post-hCG and sections through the centre of each oocyte were selected for subsequent analysis (oocyte diameter did not differ between Control and Mutant follicles, data not shown). Analysis of these sections revealed that cumulus mass area (Fig. 2A) and diameter (Fig. 2B) were both significantly decreased in Mutant follicles (~32% decrease; Fig. 2C and ~16% decrease; Fig. 2D respectively). Cumulus cell (CC) counts further revealed that the reduced cumulus mass area contained a significantly smaller number of CCs in the Mutant (~24% fewer) compared with Controls (Fig. 2E). Therefore, although the amount of space occupied by each CC (i.e. density) did not differ in Controls and Mutants, there was a ~13% decrease in average area per CC in the Mutant, reflecting a non-significant increase in density (Fig. 2F).

The innermost layer of the cumulus mass is known as the corona radiata. The number of CCs in the corona radiata was similar in Mutant and Control (Fig. 2G). However, the distance between each corona radiata CC and the distance between corona radiata CCs and the oocyte were both decreased in the Mutant (Fig. 2H and I respectively).

Cumulus ECM composition is altered in the C1galt1 *Mutant*

Having determined that *C1galt1* Mutant COCs have smaller cumulus masses, we investigated the molecular origin of this phenotype by analysing the cumulus ECM composition. HA was detected throughout the cumulus ECM and also around the peripheral mGCs closest to the CCs (Fig. 3Ai). Quantification revealed that even though the mean intensity of HA staining in the COC was increased in the Mutant (Fig. 3Aii), when normalised to CC number the stain density was similar in Control and Mutant COCs (Fig. 3Aiii). PTX3 was also detected (Fig. 3Bi) and although mean staining intensity was increased in the Mutant (Fig. 3Bii), intensities per CC were similar in Control and Mutant (Fig. 3Biii). TSG-6 was detected surrounding the CCs (Fig. 3Ci), and the staining intensities were comparable in Mutants and Controls (Fig. 3Cii and iii). IαI and PαI enter ovarian follicles from serum and the HC components become covalently attached to HA. The presence of HCs in the cumulus mass was assessed using an antibody which detects bikunin and the HCs of IαI and PαI; this analysis is hereafter referred to as HC (Fig. 3Di). HC detection revealed a similar pattern to that seen for HA, with an increase in staining intensity in Mutants compared with Controls (Fig. 3Dii). However, in contrast to the other matrix components investigated here, HCs were found to be more densely distributed in Mutant cumulus ECM compared with Controls (Fig. 3Diii). Overall, these results indicate that the CCs surrounding the Mutant oocytes are not functionally different compared with Controls, as they produce normal levels of ECM components. However, there is evidence of molecular and therefore structural differences between the cumulus matrix in Mutant and Control mice.

Quantification of cumulus intracellular molecules

Cumulus expansion requires OSF action on the CCs. As the *C1galt1* Mutant has an oocyte-specific deletion which affects secreted core 1-derived *O*-glycoproteins, we hypothesised that this mutation might directly or indirectly affect the function of one or more OSFs. To assess the function of the OSF involved in cumulus expansion, we examined intracellular signalling pathways activated in response to TGF-β ligands (key OSFs are members of the TGF-β superfamily); i.e., the SMAD2 and SMAD1/5/8 pathways. Localisation of pSMAD2 was cell-associated as expected (Fig. 4A) and normalisation of the stain to CC numbers revealed similar levels in Controls and Mutants (Fig. 4B). In addition, the levels of pSMAD1/5/8, which was also cell-associated (Fig. 4C), did not differ between Controls and Mutants (Fig. 4D).

As modified cumulus expansion in the *C1galt1* Mutant is not associated with changes in the ability

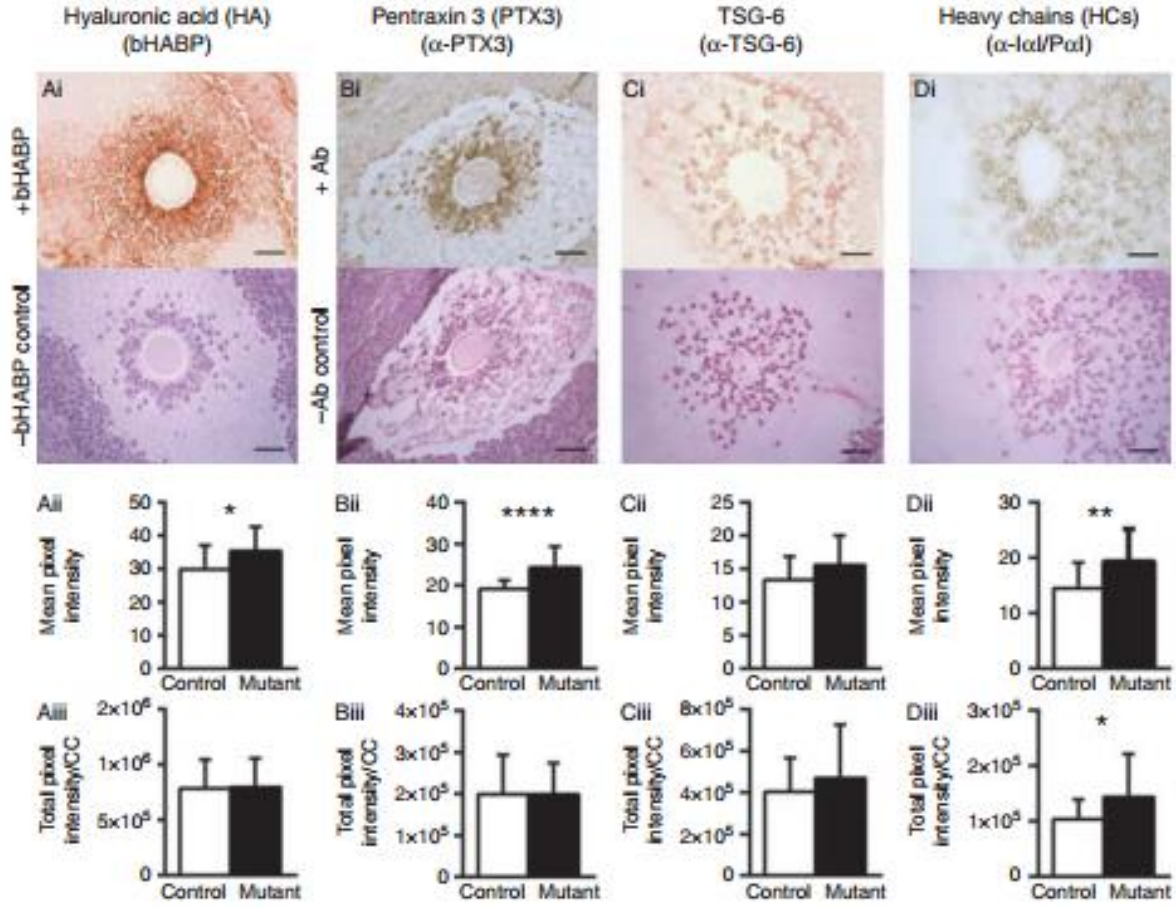

Figure 3 Localisation and quantification of HA, PTX3, TSG-6 and Iαl in preovulatory cumulus masses. Localisations of (Ai) HA, (Bi) PTX3, (Ci) TSG-6, (Di) HCs were determined in preovulatory follicles (molecule used for detection in brackets). Respective mean pixel intensities (Aii), (Bii), (Cii), (Dii) and total pixel intensities normalised to CC number (Aiii), (Biii), (Ciii) and (Diii) were determined for each of the matrix components. The upper panels of (Ai), (Bi), (Ci) and (Di) show representative images from COCs stained with bHABP or a protein-specific antibody; lower panels show sections counterstained with haematoxylin in the absence of any bHABP or primary antibody (i.e. only secondary detection reagents were applied). Data are presented as mean values ± s.d. (Aii and Aiii): $n=17$ Control and $n=21$ Mutant. (Bii and Biii): $n=17$ Control and $n=23$ Mutant. (Cii and Ciii): $n=20$ Control and $n=20$ Mutant. (Dii and Diii): $n=16$ Control and $n=21$ Mutant. *$P<0.05$; **$P<0.01$ and ****$P<0.0001$. Scale bar: 50 μm. Ab, antibody.

of CCs to deposit ECM, we investigated whether the proliferative potential of CCs was altered in the Mutant leading to changes in CC counts. Localisation and quantification of Ki-67, a nuclear marker of proliferation (Fig. 4E), revealed that levels of Ki-67 were similar in Control and Mutant CCs (Fig. 4F) indicating that cell proliferation was unaltered at 9 h post-hCG.

Correlations between cumulus expansion and cumulus molecules

Although the requirement for HA, PTX3, TSG-6 and HCs in cumulus expansion and their inter-dependence during ECM deposition are well described, the relationship between the available concentrations of these molecules and the extent of expansion have not been analysed in detail. In this study, we tested whether there was any correlation between the amount of each molecule present in the cumulus mass (as determined by staining intensity) and the cumulus area (Supplementary Figure 1, see section on supplementary data given at the end of this article). Surprisingly, in Controls, the extent of cumulus expansion did not correlate with the quantity per CC of HA, TSG-6, PTX3 or HCs (Supplementary Figure 1A, B, C and D) nor did levels of OSF-induced pSMAD2 per CC correlate with cumulus size (Supplementary Figure 1E). Furthermore, in *C1galt1* Mutant mice, the lack of oocyte glycoproteins with core 1-derived *O*-glycans did not alter the relationship between ECM molecules or pSMAD2

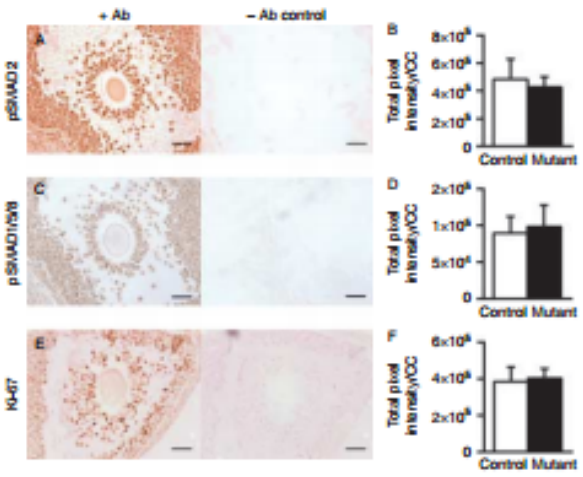

Figure 4 Localisation and quantification of pSMAD2, pSMAD1/5/8 and Ki-67 in preovulatory cumulus masses. Localisations of (A) pSMAD2, (C) pSMAD1/5/8, (E) Ki-67 and respective total pixel intensity normalised to CC number (B), (D) and (F) were determined for Mutant and Control preovulatory follicles. Left panels of (A), (C) and (E) show representative images from COCs stained with each of the protein-specific antibodies; right panels show sections without addition of primary antibody, showing no visible DAB staining. Data are presented as mean values ± s.d. (B): $n=15$ Control and $n=18$ Mutant COCs. (D): $n=19$ Control and $n=20$ Mutant COCs. (F): $n=16$ Control and $n=19$ Mutant COCs. Scale bar: 50 μm.

with cumulus size, as no correlations were observed (Supplementary Figure 1F, G, H, I and J) similar to Controls.

Correlations between different cumulus molecules

In light of the interdependencies between ECM components during cumulus expansion (Fulop *et al.* 2003, Salustri *et al.* 2004, Scarchilli *et al.* 2007), the relationships between the quantities of these molecules within individual COCs were also investigated (Supplementary Figure 2, see section on supplementary data given at the end of this article). Somewhat surprisingly, no correlation was found between any combination of cumulus ECM proteins in either Control or Mutant revealing unexpected flexibility in the system. As activation of the SMAD2/3 pathway in CCs is essential for cumulus expansion, we also investigated the relationship between the levels of CC-derived ECM components and the levels of pSMAD2 in CCs. Again, no correlations were observed in either Controls (Supplementary Figure 3A, B and C) or Mutants (Supplementary Figure 3D, E and F).

Discussion

Cumulus mass expansion has important roles in oocyte development, ovulation and is believed to facilitate the transfer of ovulated eggs to the oviduct. Indeed, historically, CC numbers surrounding eggs for human IVF have been thought to be a useful marker of implantation potential (Gregory 1998). Cumulus expansion in the preovulatory follicles of mice requires paracrine signals from the oocyte, which act on CCs to promote the formation of a HA-rich ECM. Even though the programming of the granulosa cells surrounding the oocyte to differentiate into CCs is understood to be dependent on OSFs, the specific OSF(s) critical for regulating cumulus expansion in mice have not yet been determined.

Our results reveal that reduced cumulus size does not prevent ovulation and subsequent fertilisation, as these processes are not compromised in the *C1galt1* Mutant despite a ~32% decrease in cumulus size compared with Controls. These data suggest that there is a minimum size of cumulus required, below which ovulation and fertilisation are negatively affected. If this is the case, then the extent of cumulus matrix expansion within *C1galt1* Mutant follicles is sufficient to support ovulation and fertilisation. We also present novel analysis of the associations between the different cumulus ECM molecules by determining the levels of essential cumulus matrix molecules (i.e. HA, HCs, TSG-6 and PTX3) within individual COCs. These analyses reveal that there are no strong correlations either between the amount of any one of these ECM molecules and the size of the cumulus mass or between the relative levels of any of the matrix components in both Control and Mutant COCs. This suggests a highly flexible system whereby the relative amounts of HA, HCs, TSG-6 and PTX3 can vary quite substantially but can still form a functional matrix provided that they are all present at, or above, the minimum level required. Furthermore, the degree of cumulus expansion does not predict the respective levels of cumulus ECM molecules.

The role of the cumulus complex in supporting oocyte maturation (De Matos *et al.* 2008, Lu *et al.* 2013) has been identified as an important factor in determining the success of some human-ART methods (e.g. *in vitro* maturation (IVM)). The low success rate of ARTs (IVM <35% (Ellenbogen *et al.* 2014) and IVF <40% (Hogue 2002)) is partly attributed to the selection of eggs that, despite possessing a normal complement of chromosomes, have other impairments. Therefore, the development of objective criteria to define oocyte quality is of great importance. It has been suggested that CC assessment can be an informative predictor of oocyte developmental potential, because CC proliferative potential has been positively correlated with pregnancy rates (Gregory 1998, Khurana & Niemann 2000). The results presented in this report indicate that the ~23% decrease in CC number associated with oocytes in *C1galt1* Mutants is not detrimental to fertilisation and implantation and therefore a reduction in this magnitude

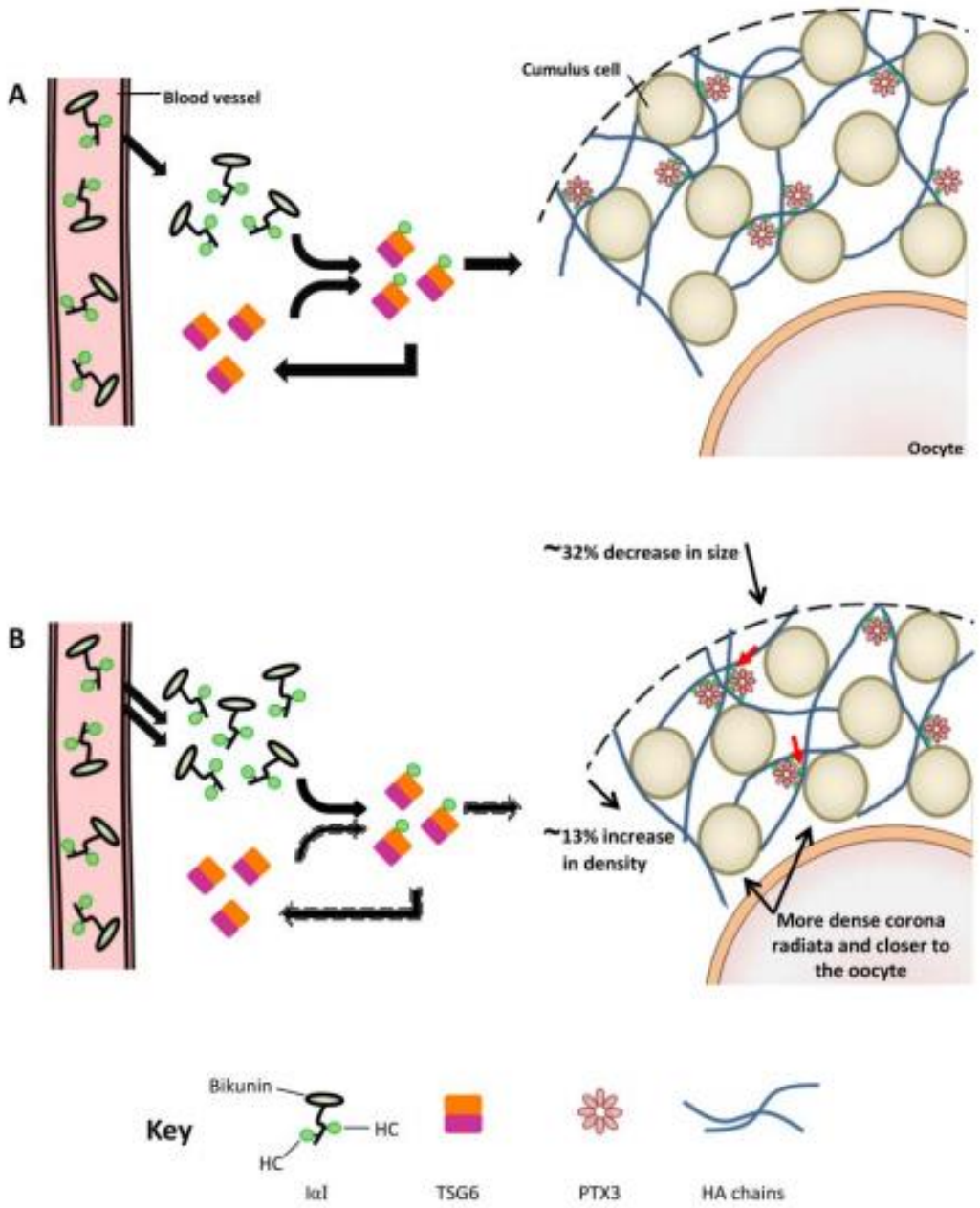

Figure 5 Proposed model of modified cumulus expansion in *C1galt1* Mutant mice. (A) Schematic model of the interactions between HA and HA-binding proteins in ECM from Control COCs. IαI family proteins are transported by blood and following the ovulatory LH surge, they diffuse into the preovulatory follicle. TSG-6 molecules, secreted by cumulus cells, act as catalysts in the transfer of the heavy chains (HCs) components of IαI onto HA chains. HA is the structural backbone of cumulus ECM and interactions with the multimeric PTX3 and HC enable HA chain cross linking. (B) The cumulus mass of Mutant COCs occupies ~32% less area compared with the Control (Fig. 2C), and also contains fewer CCs (Fig. 2E). In addition, the area per CC in the Mutant is ~13% less than Controls (Fig. 2F). The cumulus ECM of the Mutant contains increased amounts of HCs per CC (red arrows; Fig. 3Diii), while levels of HA, PTX3 and TSG-6 per CC remain similar to Controls (Fig. 3Aiii, Biii and Ciii). The modified basal lamina of Mutant follicles (Christensen *et al.* 2014) may allow the influx of more IαI molecules during follicle development and the periovulatory period (double arrows from blood vessel); this could result in increased transfer of HCs onto HA (arrows with broken border), resulting in a higher degree of HA chain cross linking. As a result, the Mutant develops a smaller, denser, cumulus mass compared with Controls. The relative sizes of the molecules and cells and the relative sizes of each of the components of IαI are not to scale, as HCs are bigger compared with the Bikunin component.

in CC number is not a reliable assessment to predict oocyte developmental potential. As a result, a partially expanded cumulus complex in human ARTs may not be the best indicator of oocyte quality.

To investigate the origin of the reduced cumulus size observed in the *C1galt1* Mutant, we examined two parameters that underlie the formation of the cumulus matrix during the periovulatory period: i) the number of CCs that make up the CC complex and ii) the ability of each individual CC to produce cumulus ECM molecules. Mutant COCs were shown to occupy ~32% less area compared with the Control, which is accompanied by fewer CCs in the entire complex. Furthermore, the corona radiata CCs in the Mutant were more tightly packed and were also closer to the oocyte compared with Control indicating aberrant expansion. In addition, the area occupied per CC in the Mutant is ~13% less than Controls, making the Mutant COC ~13% more dense. As a result of this, the mean intensity of HA and PTX3 molecules was higher in the Mutant COC, although when analysed per CC, the intensity of these two molecules was similar between Control and Mutant, indicating that each individual CC in the Mutant functions as Control. Interestingly, the levels of HCs detected, which are the only cumulus ECM component not produced within the follicle, were increased in Mutants compared with Controls. An increased production of IαI, and thus HC, by the liver due to the oocyte modification is unlikely. However, it has been observed that the basal lamina of Mutant follicles is altered during follicle development (Christensen *et al.* 2014). Therefore, in these mice the basal lamina may be permeable to IαI even in the absence of an ovulatory stimulus, such that the intrafollicular presence of IαI, and hence HCs, is elevated compared with Controls during the periovulatory period. Increased levels of HCs could result in more extensive HA cross linking (Baranova *et al.* 2014) and hence a more compact cumulus matrix. Therefore, although CCs in *C1galt1* Mutant mice appear functionally normal, as demonstrated by cumulus intracellular signalling pathways and the ability of CCs to produce ECM components, the combined effects of fewer CCs and more HCs could result in the production of a cumulus matrix with altered organisation in *C1galt1* Mutant mice (see proposed model in Fig. 5).

The decreased number of CCs in Mutant preovulatory follicles suggests that these cells have an altered proliferative potential, but there was no difference in Ki-67 levels between Control and Mutant. However, the reduced CC number in Mutant follicles suggests that: i) there was altered proliferation of CCs in earlier stages of cumulus expansion, or ii) there were fewer somatic cells associated with the oocyte from the outset, or iii) CC apoptosis is elevated in the Mutant resulting in fewer CCs at 9 h post-hCG. The second hypothesis is consistent with the characteristics of Booroola sheep that exhibit increased fertility (similar to *C1galt1* Mutant mice) resulting from heterozygosity of a mutation in bone morphogenetic protein receptor 1B (BMPR1B; a receptor for TGF-β superfamily molecules). In these sheep, the increased number of preovulatory follicles is accompanied by a smaller number of granulosa cells per follicle, resulting in fewer cells contributing to the cumulus complex (McNatty & Henderson 1987). However, as SMAD signalling (activated by TGF-β superfamily molecules) was unaltered in *C1galt1* Mutant mice, it is unlikely that TGF-β signalling is modified at this stage by the oocyte-generated core 1-derived *O*-glycans, including those of OSFs. This does not rule out changes in COC signalling at earlier stages of Mutant follicle development which may be the origin of the reduced number of CCs.

In conclusion, the absence of core 1-derived *O*-glycans from oocyte-expressed glycoproteins has effects on the whole follicle that are evident from i) greater levels of HCs of IαI and PαI in the follicle and ii) altered numbers of CCs. This highlights the critical role of the oocyte in follicle development. The effects of *C1galt1* deletion on the cumulus mass surrounding the oocyte could be a direct result of changes in the OSFs that determine the proliferative potential of CCs or an indirect outcome relating to the effects of OSFs on EGF-ligands/EGF-receptors, whereby if these are altered, the LH signal is not properly transmitted to CCs. The observation that mouse COCs with reduced CC numbers can function normally without compromising the developmental potential of oocytes is intriguing and raises the question of why do Control COCs have an apparent excess of CCs? In addition, it will be interesting to investigate whether this observed CC redundancy in mouse COCs applies to human COCs, in which case, assessment of the cumulus complex as an indication of oocyte quality for IVF needs to be used with caution. Finally, the lack of any strong correlations between the levels of different ECM molecules relative to each other or to the size of the cumulus mass indicates that, providing the minimum requirements for matrix formation are met, this system possesses a high degree of flexibility. It remains to be determined whether the specific expression patterns of individual ECM molecules by human CCs might be predictive of oocyte quality.

Supplementary data

This is linked to the online version of the paper at http://dx.doi.org/10.1530/REP-14-0503.

Declaration of interest

The authors declare that there is no conflict of interest that could be perceived as prejudicing the impartiality of the research reported.

Funding

This research was supported by the John Fell OUP Fund (grant 073/582 to S A Williams). C M Milner and A J Day would like to acknowledge the support of the Medical Research Council (grant G0701180).

Acknowledgements

The authors would like to thank Dr Antonio Inforzato for generously supplying the anti-PTX3 antibody. They would also like to thank Dr Patricia Grasa Molina and Joel Ward for technical assistance in tissue collection and development of analysis method respectively, and Prof. Graeme Martin, Dr Rebecca Dragovic and Mrs Heidy Kaune Galaz for their input on this manuscript.

References

Baranova NS, Inforzato A, Briggs DC, Tilakaratna V, Enghild JJ, Thakar D, Milner CM, Day AJ & Richter RP 2014 Incorporation of pentraxin 3 into hyaluronan matrices is tightly regulated and promotes matrix cross-linking. *Journal of Biological Chemistry* **289** 30481–30498. (doi:10.1074/jbc.M114.568154)

Batista F, Lu L, Williams SA & Stanley P 2012 Complex *N*-glycans are essential, but core 1 and 2 mucin *O*-glycans, *O*-fucose glycans, and NOTCH1 are dispensable, for mammalian spermatogenesis. *Biology of Reproduction* **86** 179. (doi:10.1095/biolreprod.111.098103)

Carrette O, Nemade RV, Day AJ, Brickner A & Larsen WJ 2001 TSG-6 is concentrated in the extracellular matrix of mouse cumulus oocyte complexes through hyaluronan and inter-α-inhibitor binding. *Biology of Reproduction* **65** 301–308. (doi:10.1095/biolreprod65.1.301)

Chen L, Russell PT & Larsen WJ 1993 Functional significance of cumulus expansion in the mouse: roles for the preovulatory synthesis of hyaluronic acid within the cumulus mass. *Molecular Reproduction and Development* **34** 87–93. (doi:10.1002/mrd.1080340114)

Chen L, Zhang H, Powers RW, Russell PT & Larsen WJ 1996 Covalent linkage between proteins of the inter-α-inhibitor family and hyaluronic acid is mediated by a factor produced by granulosa cells. *Journal of Biological Chemistry* **271** 19409–19414. (doi:10.1074/jbc.271.32.19409)

Chen F, Marquez H, Kim YK, Qian J, Shao F, Fine A, Cruikshank WW, Quadro L & Cardoso WV 2014 Prenatal retinoid deficiency leads to airway hyperresponsiveness in adult mice. *Journal of Clinical Investigation* **124** 801–811. (doi:10.1172/JCI70291)

Christensen AP, Patel SH, Grasa P, Christian HC & Williams SA 2014 Oocyte glycoproteins regulate the form and function of the follicle basal lamina and theca cells. *Developmental Biology*. pii: S0012-1606(14)00654-X. (doi:10.1016/j.ydbio.2014.12.024)

Clark SJ, Keenan TD, Fielder HL, Collinson LJ, Holley RJ, Merry CL, van Kuppevelt TH, Day AJ & Bishop PN 2011 Mapping the differential distribution of glycosaminoglycans in the adult human retina, choroid, and sclera. *Investigative Ophthalmology & Visual Science* **52** 6511–6521. (doi:10.1167/iovs.11-7909)

Day AJ & Prestwich GD 2002 Hyaluronan-binding proteins: tying up the giant. *Journal of Biological Chemistry* **277** 4585–4588. (doi:10.1074/jbc.R100036200)

De Matos DG, Miller K, Scott R, Tran CA, Kagan D, Nataraja SG, Clark A & Palmer S 2008 Leukemia inhibitory factor induces cumulus expansion in immature human and mouse oocytes and improves mouse two-cell rate and delivery rates when it is present during mouse *in vitro* oocyte maturation. *Fertility and Sterility* **90** 2367–2375. (doi:10.1016/j.fertnstert.2007.10.061)

Dragovic RA, Ritter LJ, Schulz SJ, Amato F, Armstrong DT & Gilchrist RB 2005 Role of oocyte-secreted growth differentiation factor 9 in the regulation of mouse cumulus expansion. *Endocrinology* **146** 2798–2806. (doi:10.1210/en.2005-0098)

Ellenbogen A, Shavit T & Shalom-Paz E 2014 IVM results are comparable and may have advantages over standard IVF. *Facts, Views & Vision in ObGyn* **6** 77–80.

Fulop C, Salustri A & Hascall VC 1997*a* Coding sequence of a hyaluronan synthase homologue expressed during expansion of the mouse cumulus–oocyte complex. *Archives of Biochemistry and Biophysics* **337** 261–266. (doi:10.1006/abbi.1996.9793)

Fulop C, Kamath RV, Li Y, Otto JM, Salustri A, Olsen BR, Glant TT & Hascall VC 1997*b* Coding sequence, exon–intron structure and chromosomal localization of murine TNF-stimulated gene 6 that is specifically expressed by expanding cumulus cell–oocyte complexes. *Gene* **202** 95–102. (doi:10.1016/S0378-1119(97)00459-9)

Fulop C, Szanto S, Mukhopadhyay D, Bardos T, Kamath RV, Rugg MS, Day AJ, Salustri A, Hascall VC, Glant TT *et al.* 2003 Impaired cumulus mucification and female sterility in tumor necrosis factor-induced protein-6 deficient mice. *Development* **130** 2253–2261. (doi:10.1242/dev.00422)

Garlanda C, Bottazzi B, Bastone A & Mantovani A 2005 Pentraxins at the crossroads between innate immunity, inflammation, matrix deposition, and female fertility. *Annual Review of Immunology* **23** 337–366. (doi:10.1146/annurev.immunol.23.021704.115756)

Gilchrist RB, Lane M & Thompson JG 2008 Oocyte-secreted factors: regulators of cumulus cell function and oocyte quality. *Human Reproduction Update* **14** 159–177. (doi:10.1093/humupd/dmm040)

Grasa P, Ploutarchou P & Williams SA 2014 Oocytes lacking *O*-glycans alter follicle development and increase fertility by increasing follicle FSH sensitivity, decreasing apoptosis, and modifying GDF9:BMP15 expression. *FASEB Journal* **29** 525–539. (doi:10.1096/fj.14-253757)

Gregory L 1998 Ovarian markers of implantation potential in assisted reproduction. *Human Reproduction* **13** (Suppl 4) 117–132. (doi:10.1093/humrep/13.suppl_4.117)

Hess KA, Chen L & Larsen WJ 1998 The ovarian blood follicle barrier is both charge- and size-selective in mice. *Biology of Reproduction* **58** 705–711. (doi:10.1095/biolreprod58.3.705)

Higman VA, Briggs DC, Mahoney DJ, Blundell CD, Sattelle BM, Dyer DP, Green DE, DeAngelis PL, Almond A, Milner CM *et al.* 2014 A refined model for the TSG-6 link module in complex with hyaluronan: use of defined oligosaccharides to probe structure and function. *Journal of Biological Chemistry* **289** 5619–5634. (doi:10.1074/jbc.M113.542357)

Hogue CJ 2002 Successful assisted reproductive technology: the beauty of one. *Obstetrics and Gynecology* **100** 1017–1019. (doi:10.1016/S0029-7844(02)02327-X)

Ievoli E, Lindstedt R, Inforzato A, Camaioni A, Palone F, Day AJ, Mantovani A, Salvatori G & Salustri A 2011 Implication of the oligomeric state of the N-terminal PTX3 domain in cumulus matrix assembly. *Matrix Biology* **30** 330–337. (doi:10.1016/j.matbio.2011.05.002)

Inforzato A, Baldock C, Jowitt TA, Holmes DF, Lindstedt R, Marcellini M, Rivieccio V, Briggs DC, Kadler KE, Verdoliva A *et al.* 2010 The angiogenic inhibitor long pentraxin PTX3 forms an asymmetric octamer with two binding sites for FGF2. *Journal of Biological Chemistry* **285** 17681–17692. (doi:10.1074/jbc.M109.085639)

Irving-Rodgers HF, Mussard ML, Kinder JE & Rodgers RJ 2002 Composition and morphology of the follicular basal lamina during atresia of bovine antral follicles. *Reproduction* **123** 97–106. (doi:10.1530/rep.0.1230097)

Khurana NK & Niemann H 2000 Effects of oocyte quality, oxygen tension, embryo density, cumulus cells and energy substrates on cleavage and morula/blastocyst formation of bovine embryos. *Theriogenology* **54** 741–756. (doi:10.1016/S0093-691X(00)00387-3)

Knight PG & Glister C 2006 TGF-β superfamily members and ovarian follicle development. *Reproduction* **132** 191–206. (doi:10.1530/rep.1.01074)

Kohda D, Morton CJ, Parkar AA, Hatanaka H, Inagaki FM, Campbell ID & Day AJ 1996 Solution structure of the link module: a hyaluronan-binding domain involved in extracellular matrix stability and cell migration. *Cell* **86** 767–775.

Lu CH, Lee RK, Hwu YM, Lin MH, Yeh LY, Chen YJ, Lin SP & Li SH 2013 Involvement of the serine protease inhibitor, SERPINE2, and the urokinase plasminogen activator in cumulus expansion and oocyte maturation. *PLoS ONE* **8** e74602. (doi:10.1371/journal.pone.0074602)

McClure N, Macpherson AM, Healy DL, Wreford N & Rogers PA 1994 An immunohistochemical study of the vascularization of the human Graafian follicle. *Human Reproduction* **9** 1401–1405.

McNatty KP & Henderson KM 1987 Gonadotrophins, fecundity genes and ovarian follicular function. *Journal of Steroid Biochemistry* **27** 365–373. (doi:10.1016/0022-4731(87)90329-3)

Milner CM & Day AJ 2003 TSG-6: a multifunctional protein associated with inflammation. *Journal of Cell Science* **116** 1863–1873. (doi:10.1242/jcs.00407)

Milner CM, Higman VA & Day AJ 2006 TSG-6: a pluripotent inflammatory mediator? *Biochemical Society Transactions* **34** 446–450. (doi:10.1042/BST0341261)

Mukhopadhyay D, Hascall VC, Day AJ, Salustri A & Fulop C 2001 Two distinct populations of tumor necrosis factor-stimulated gene-6 protein in the extracellular matrix of expanded mouse cumulus cell–oocyte complexes. *Archives of Biochemistry and Biophysics* **394** 173–181. (doi:10.1006/abbi.2001.2552)

Nenicu A, Körbel C, Gu Y, Menger MD & Laschke MW 2014 Combined blockade of angiotensin II type 1 receptor and activation of peroxisome proliferator-activated receptor-γ by telmisartan effectively inhibits vascularization and growth of murine endometriosis-like lesions. *Human Reproduction* **29** 1011–1024. (doi:10.1093/humrep/deu035)

Ng ST, Chang TH & Wu TC 1999 Prediction of the rates of fertilization, cleavage, and pregnancy success by cumulus–coronal morphology in an *in vitro* fertilization program. *Fertility and Sterility* **72** 412–417. (doi:10.1016/S0015-0282(99)00290-3)

Pan Y, Yago T, Fu J, Herzog B, McDaniel JM, Mehta-D'Souza P, Cai X, Ruan C, McEver RP, West C *et al.* 2014 Podoplanin requires sialylated *O*-glycans for stable expression on lymphatic endothelial cells and for interaction with platelets. *Blood* **124** 3656–3665. (doi:10.1182/blood-2014-04-572107)

Park JY, Su YQ, Ariga M, Law E, Jin SL & Conti M 2004 EGF-like growth factors as mediators of LH action in the ovulatory follicle. *Science* **303** 682–684. (doi:10.1126/science.1092463)

Peng J, Li Q, Wigglesworth K, Rangarajan A, Kattamuri C, Peterson RT, Eppig JJ, Thompson TB & Matzuk MM 2013 Growth differentiation factor 9:bone morphogenetic protein 15 heterodimers are potent regulators of ovarian functions. *PNAS* **110** E776–E785. (doi:10.1073/pnas.1218020110)

Philpott CC, Ringuette MJ & Dean J 1987 Oocyte-specific expression and developmental regulation of ZP3, the sperm receptor of the mouse zona pellucida. *Developmental Biology* **121** 568–575. (doi:10.1016/0012-1606(87)90192-8)

Rugg MS, Willis AC, Mukhopadhyay D, Hascall VC, Fries E, Fulop C, Milner CM & Day AJ 2005 Characterization of complexes formed between TSG-6 and inter-α-inhibitor that act as intermediates in the covalent transfer of heavy chains onto hyaluronan. *Journal of Biological Chemistry* **280** 25674–25686. (doi:10.1074/jbc.M501332200)

Salustri A, Yanagishita M & Hascall VC 1989 Synthesis and accumulation of hyaluronic acid and proteoglycans in the mouse cumulus cell–oocyte complex during follicle-stimulating hormone-induced mucification. *Journal of Biological Chemistry* **264** 13840–13847.

Salustri A, Garlanda C, Hirsch E, De Acetis M, Maccagno A, Bottazzi B, Doni A, Bastone A, Mantovani G, Beck Peccoz P *et al.* 2004 PTX3 plays a key role in the organization of the cumulus oophorus extracellular matrix and in *in vivo* fertilization. *Development* **131** 1577–1586. (doi:10.1242/dev.01056)

Sanggaard KW, Karring H, Valnickova Z, Thogersen IB & Enghild JJ 2005 The TSG-6 and Inl interaction promotes a transesterification cleaving the protein-glycosaminoglycan-protein (PGP) cross-link. *Journal of Biological Chemistry* **280** 11936–11942. (doi:10.1074/jbc.M409016200)

Sanggaard KW, Sonne-Schmidt CS, Krogager TP, Lorentzen KA, Wisniewski HG, Thogersen IB & Enghild JJ 2008 The transfer of heavy chains from bikunin proteins to hyaluronan requires both TSG-6 and HC2. *Journal of Biological Chemistry* **283** 18530–18537. (doi:10.1074/jbc.M800874200)

Sato H, Kajikawa S, Kuroda S, Horisawa Y, Nakamura N, Kaga N, Kakinuma C, Kato K, Morishita H, Niwa H *et al.* 2001 Impaired fertility in female mice lacking urinary trypsin inhibitor. *Biochemical and Biophysical Research Communications* **281** 1154–1160. (doi:10.1006/bbrc.2001.4475)

Scarchilli L, Camaioni A, Bottazzi B, Negri V, Doni A, Deban L, Bastone A, Salvatori G, Mantovani A, Siracusa G *et al.* 2007 PTX3 interacts with inter-α-trypsin inhibitor: implications for hyaluronan organization and cumulus oophorus expansion. *Journal of Biological Chemistry* **282** 30161–30170. (doi:10.1074/jbc.M703738200)

Shi S, Williams SA, Seppo A, Kurniawan H, Chen W, Ye Z, Marth JD & Stanley P 2004 Inactivation of the Mgat1 gene in oocytes impairs oogenesis, but embryos lacking complex and hybrid *N*-glycans develop and implant. *Molecular and Cellular Biology* **24** 9920–9929. (doi:10.1128/MCB.24.22.9920-9929.2004)

Stanley P 2011 Golgi glycosylation. *Cold Spring Harbor Perspectives in Biology* **3** a005199. (doi:10.1101/cshperspect.a005199)

Su YQ, Wu X, O'Brien MJ, Pendola FL, Denegre JN, Matzuk MM & Eppig JJ 2004 Synergistic roles of BMP15 and GDF9 in the development and function of the oocyte–cumulus cell complex in mice: genetic evidence for an oocyte-granulosa cell regulatory loop. *Developmental Biology* **276** 64–73. (doi:10.1016/j.ydbio.2004.08.020)

Tanghe S, Van Soom A, Nauwynck H, Coryn M & de Kruif A 2002 Minireview: Functions of the cumulus oophorus during oocyte maturation, ovulation, and fertilization. *Molecular Reproduction and Development* **61** 414–424. (doi:10.1002/mrd.10102)

Tian E, Hoffman MP & Ten Hagen KG 2012 *O*-glycosylation modulates integrin and FGF signalling by influencing the secretion of basement membrane components. *Nature Communications* **3** 869. (doi:10.1038/ncomms1874)

Varnosfaderani Sh R, Ostadhosseini S, Hajian M, Hosseini SM, Khashouei EA, Abbasi H, Hosseinnia P & Nasr-Esfahani MH 2013 Importance of the GDF9 signaling pathway on cumulus cell expansion and oocyte competency in sheep. *Theriogenology* **80** 470–478. (doi:10.1016/j.theriogenology.2013.05.009)

Williams SA & Stanley P 2008 Mouse fertility is enhanced by oocyte-specific loss of core 1-derived *O*-glycans. *FASEB Journal* **22** 2273–2284. (doi:10.1096/fj.07-101709)

Williams SA, Xia L, Cummings RD, McEver RP & Stanley P 2007 Fertilization in mouse does not require terminal galactose or *N*-acetylglucosamine on the zona pellucida glycans. *Journal of Cell Science* **120** 1341–1349. (doi:10.1242/jcs.004291)

Yago T, Fu J, McDaniel JM, Miner JJ, McEver RP & Xia L 2010 Core 1-derived *O*-glycans are essential E-selectin ligands on neutrophils. *PNAS* **107** 9204–9209. (doi:10.1073/pnas.1003110107)

Yoshioka S, Ochsner S, Russell DL, Ujioka T, Fujii S, Richards JS & Espey LL 2000 Expression of tumor necrosis factor-stimulated gene-6 in the rat ovary in response to an ovulatory dose of gonadotropin. *Endocrinology* **141** 4114–4119. (doi:10.1210/en.141.11.4114)

Zhuo L, Yoneda M, Zhao M, Yingsung W, Yoshida N, Kitagawa Y, Kawamura K, Suzuki T & Kimata K 2001 Defect in SHAP–hyaluronan complex causes severe female infertility. A study by inactivation of the bikunin gene in mice. *Journal of Biological Chemistry* **276** 7693–7696. (doi:10.1074/jbc.C000899200)

Received 26 September 2014
First decision 5 November 2014
Revised manuscript received 5 February 2015
Accepted 12 February 2015

APPENDIX B

Published article: Oocytes lacking O-glycans alter follicle development and increase fertility by increasing follicle FSH sensitivity, decreasing apoptosis, and modifying GDF9:BMP15 expression

Authors: Patricia Grasa, Panayiota Ploutarchou, and Suzannah A. Williams

The FASEB Journal • Research Communication

Oocytes lacking *O*-glycans alter follicle development and increase fertility by increasing follicle FSH sensitivity, decreasing apoptosis, and modifying GDF9:BMP15 expression

Patricia Grasa, Panayiota Ploutarchou, and Suzannah A. Williams[1]

Nuffield Department of Obstetrics and Gynaecology, University of Oxford, Women's Centre, John Radcliffe Hospital, Oxford, United Kingdom

ABSTRACT **The number of eggs ovulated varies within and between species and is influenced by many variables. However, the regulatory mechanisms remain poorly understood. We previously demonstrated a key role for the oocyte because mice generating oocytes deficient in core 1-derived *O*-glycans ovulate ~40–50% more eggs than Controls. Here we analyze the basis of this phenotype using Mutant [core 1 β1,3-galactosyltransferase 1 (*C1galt1*)^{FF}: zona pellucida glycoprotein 3 *Cre* (ZP3Cre)] and Control (*C1galt1*^{FF}) female mice. In culture, Mutant follicles exhibited delayed antrum formation [indicative of follicle stimulant hormone (FSH) dependence] and increased sensitivity to FSH. Although the Mutant estrous cycle was extended, comprehensive endocrine changes were not observed; rather FSH, LH, inhibin B, and anti-Mullerian hormone were temporally altered, revealing estrous cycle stage-specific modifications to the hypothalamic-pituitary-gonadal axis. At proestrus, when FSH levels were decreased in Mutants, ovaries contained more, smaller, preantral follicles. Mutant follicles exhibited reduced levels of apoptosis, and both B-cell lymphoma 2 (Bcl-2) and BCL-2–associated X protein (Bax) were altered compared with Controls. Mutant ovaries also had an increase in the expression ratio of growth differentiation factor 9 (*GDF9*): bone morphogenetic protein 15 (*BMP15*) at diestrus. On the basis of these data, we propose that modified oocyte glycoproteins alter *GDF9:BMP15* expression modifying follicle development resulting in the generation of more follicles. Thus, the oocyte is a key regulator of follicle development and has a crucial role in determining ovulation rate.—Grasa, P., Ploutarchou, P., Williams, S. A. Oocytes lacking *O*-glycans alter follicle development and increase fertility by increasing follicle FSH sensitivity, decreasing apoptosis, and modifying GDF9:BMP15 expression. *FASEB J.* 29, 525–539 (2015). www.fasebj.org**

Key Words: *ovary · C1galt1 · T-syn · ovulation rate · endocrine profile*

THE UPPER LIMIT OF FEMALE fertility in mammals is limited by the number of eggs ovulated. However, the mechanisms that regulate the ovulation rate (OR) of each species remain unclear (1). Each egg develops within an ovarian follicle and because follicle development takes multiple estrous cycles, the ovary contains many follicles at all different stages of development. Follicle development is a complex and highly regulated process and has many different developmental stages that are both morphologically and molecularly distinct. The process of follicle development starts when a primordial follicle, containing a meiotically arrested oocyte, is recruited and begins to grow. Each follicle that enters the growing pool has 1 of 2 outcomes: either full development accompanied by proliferation and differentiation of granulosa and theca cells until the follicle reaches the preovulatory stage or death (2). Follicle death occurs via programmed cell death known as apoptosis, which is regulated by distinct protein families such as the B-cell lymphoma 2 (Bcl-2) family (3–5). Bcl-2 is antiapoptotic, promoting cell survival (6), whereas BCL-2–associated X protein (Bax) is proapoptotic (7), and both have been shown to be important in ovarian follicle apoptosis (8, 9). Although the levels of the different pro- and anti-apoptotic molecules are important, it is the ratio of Bcl-2 to Bax that determines cell susceptibility to apoptosis; a lower ratio, and thus dominance of Bax over Bcl-2, denotes accelerated apoptosis (10). Initial follicle development does not require gonadotropins although follicles are able to respond to follicle stimulant hormone (FSH) (11–13), whereas antral follicles are dependent on FSH (12, 14, 15). The transition of preantral to antral follicles also requires FSH and involves morphological separation and differentiation of preantral granulosa cells into the cumulus cells, which surround the oocyte, and mural granulosa cells, which line the follicle, by the formation of a fluid-filled cavity known as the antrum (16). The ability of a follicle

Abbreviations: ALK6, activin-like kinase 6; AMH, anti-Mullerian hormone; Bax, BCL-2–associated X protein; Bcl-2, B-cell lymphoma 2; BMP15, bone morphogenetic protein 15; BSA, bovine serum albumin; C1galt1, core 1 β1,3-galactosyltransferase 1; CL, corpora lutea; CV, coefficient of variation; DAZL, deleted in azoospermia-like; FOXO3, Forkhead box O3;

(*continued on next page*)

[1] Correspondence: Nuffield Department of Obstetrics & Gynaecology, University of Oxford, Women's Centre, Level 3, John Radcliffe Hospital, Oxford, OX3 9DU United Kingdom. E-mail: suzannah.williams@obs-gyn.ox.ac.uk

doi: 10.1096/fj.14-253757

0892-6638/15/0029-0525 © FASEB

to develop from the late preantral to the preovulatory stage depends on the sensitivity of the follicle to FSH, as well as serum concentrations of this gonadotropin (17, 18).

Follicle development is regulated by endocrine signals but is also modulated by a number of locally produced intra-ovarian factors that act in both paracrine and autocrine ways (19, 20). The oocyte itself plays an active role in this regulation through oocyte secreted factors that act on granulosa and theca cells (21–25). Many of these intra-ovarian regulators belong to the TGF-β superfamily (20, 27). Some of these factors including inhibins, activins, and anti-Mullerian hormone (AMH, also known as Mullerian inhibiting substance) are secreted by granulosa cells and modulate the response of the follicle to gonadotropins. AMH inhibits both primordial follicle growth *in vitro* (28, 29) and FSH-stimulated follicle growth *in vitro* and *in vivo* (30). Among the oocyte-specific factors, growth differentiation factor 9 (GDF9) is required for primary follicle progression, because GDF9-null mice are infertile due to an arrest at this stage of follicle development (21, 31). Bone morphogenetic protein 15 (BMP15), also oocyte-specific, induces granulosa cell proliferation *in vitro* (32, 33); however, its action varies between species (34). Mice deficient in BMP15 are subfertile, whereas sheep heterozygous for BMP15 exhibit an increased OR and sheep lacking BMP15 are completely infertile (35). GDF9 and BMP15 also act synergistically to regulate follicle development (36–38). Furthermore, the ratio of these growth factors to each other has been implicated in the species-specific regulation of OR (39).

Ovulation rate in mice is relatively consistent within each strain, and studies investigating the regulation of follicle development in transgenic knock-out/-in or mutant mice have resulted almost without exception in decreased female fertility as reviewed by Barnett (40). However, since that review was published, we described a transgenic mouse model that exhibits a sustained increase in OR and fertility (41). This phenotype results from oocyte-specific ablation of core 1 β1,3-galactosyltransferase 1 (also known as T-synthase, *C1galt1*), which is required for the generation of core 1–derived *O*-glycans. Ovaries from *C1galt1* Mutant mice generate oocytes that lack T-synthase from the primary follicle stage onward by deletion of floxed alleles by *Cre* recombinase under the control of a zona pellucida glycoprotein 3 (ZP3) promoter. *C1galt1* Mutant ovaries generating oocytes lacking core 1 β1,3-galactosyltransferase contain higher numbers of developing follicles; this is not caused by altered recruitment of primordial follicles because gene deletion occurs after this stage (41). Since we first described this Mutant in 2008, a few other mouse models have been described with increased fertility (42–46). Mice lacking GPCR 149 (Gpr149), an oocyte enriched transcript, have higher numbers of developing follicles and exhibit an enhanced OR, which is associated with an increase in GDF9 and FSH receptor expression (42). Tumor necrosis factor (TNF-α)–deficient mice have increased fertility, likely resulting from altered follicle development because ovaries contain more developing follicles (45). A decrease in granulosa cell apoptosis could be the cause of the increased fertility of aquaporin-8–deficient females (43), whereas mice heterozygous for deleted in azoospermia-like (DAZL) exhibit an increased OR associated with an increase in sensitivity of the follicle to FSH in culture (44). Overexpression of Forkhead box O3 (FOXO3) in oocytes attenuates the postnatal decline of primordial follicles resulting in enhanced fertility (46). Using a different approach, outbred mice lines with high fertility have been obtained by selective breeding for more than 40 y (47).

The aim of this study was to determine the mechanism of the increased fertility phenotype in females with oocyte-specific deletion of *C1galt1* by evaluating follicular development, apoptosis, the endocrinology, and expression levels of ovarian regulators of female fertility.

MATERIALS AND METHODS

Mice

Female mice with floxed *C1galt1* alleles (*C1galt1*^{FF}) were mated with males *C1galt1*^{FF} carrying a ZP3*Cre* recombinase transgene, to obtain Control *C1galt1*^{FF} and Mutant *C1galt1*^{FF}:ZP3*Cre* females (41). The ZP3*Cre* transgene does not affect fertility (48, 49). Mice were maintained in individually ventilated cages (IVC) in 12:12 h light-dark cycles. Bedding from male cages was added to female stock cages weekly to ensure females maintained normal estrous cycles in the absence of males (50, 51). All experiments were approved by the Home Office and the Local Ethical Review Committee.

Genotyping

Mice were genotyped using protocols adapted from Williams *et al.* (49). Each 25 μl PCR reaction contained 2.5 μl of 10× PCR buffer (Bioline, London, United Kingdom), 0.75 μl of 50 mM $MgCl_2$ solution (Bioline), 0.5 μl of 10 mM deoxyribonucleotide triphosphates (Roche, Mannheim, Germany), 0.5 μl of each primer (Eurogentec, Liege Science Park, Belgium), 1 μl of genomic DNA (ear), and 0.15 μl of Taq polymerase (Bioline) for the detection of floxed *C1galt1* or 0.5 μl of Taq polymerase for the detection of the *Cre* transgene. The primers used to detect the *C1galt1* floxed allele were either TS1 (49) and TS8 (TCTGCATTGAAGTTCATCTGT) or FB33 and FB34 (52), and the *Cre* transgene was detected using primers PS502 and PS607 (48).

Estrous cycle evaluation

The estrous cycle of female mice has 4 distinct stages (proestrus, estrus, metestrus, and diestrus) identified by the analysis of the cell types present in the vagina (53). Estrus cyclicity was evaluated in 8- to 10-wk-old Control and Mutant females by daily analysis of vaginal smears collected between 8:00 and 10:00 AM. Vaginal cell smears were obtained by rinsing the vagina with 100 μl of 0.9% sodium chloride, which was placed on a glass slide, air dried, and stained with Giemsa (Sigma-Aldrich, Dorset, United Kingdom). Cell type was evaluated, and the stage of the estrous cycle was determined. During diestrus, vaginal washes were characterized by high leukocyte content, whereas during proestrus nucleated

(*continued from previous page*)

FSH, follicle stimulating hormone; FSHR, follicle stimulating hormone receptor; GDF9, growth differentiation factor 9; Gpr149, GPCR 149; IVC, individually ventilated cages; LH, luteinizing hormone; LHR, LH receptor; OR, ovulation rate; PpiB, peptidylprolyl isomerase B (cyclophilin B); RIA, radioimmunoassay; TNFα, tumor necrosis factor α; T-synthase, core 1 β3galactosyltransferase; ZP3, zona pellucida glycoprotein 3

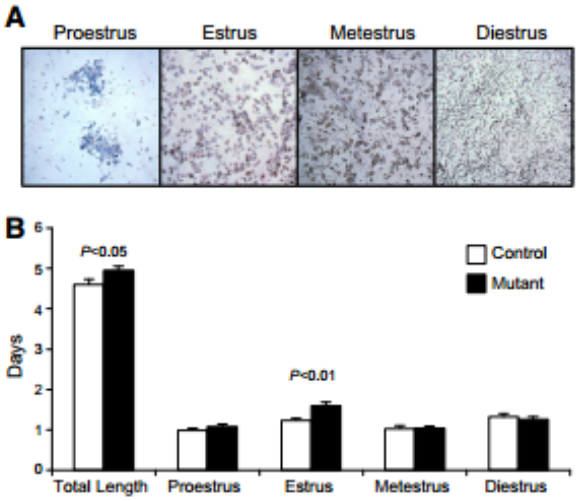

Figure 1. Estrous cycle evaluation. *A*) Representative images of Giemsa-stained vaginal smears at proestrus, estrus, metestrus, and diestrus. Estrous cycle was evaluated by cytologic examination of Giemsa-stained vaginal smears. During diestrus, vaginal washes were characterized by high leukocyte content, whereas during proestrus clusters of nucleated epithelial cells appear. Estrus was identified by the presence of cornified enucleate epithelial cells present in densely packed clusters, and in metestrus cornified epithelial cells and polimorphonuclear leukocytes are seen. *B*) Graph showing the total length of estrous cycle in Control (white) and Mutant (black) females and the time spent in each stage of the cycle. Control, $n = 63$; Mutant, $n = 59$.

epithelial cells appear. Estrus was identified by the presence of cornified enucleate epithelial cells, and in metestrus leukocyte infiltration starts (**Fig. 1*A***). Smears were used to establish that an animal was having regular cycles, as evidenced by at least 2 complete estrous cycles, before death and sample collection.

The onset of puberty was determined as the day of vaginal opening. Control and Mutant females were examined daily from 3 wk of age.

Tissue and serum collection

Control and Mutant 8- to 10-wk-old females were anesthetized by intraperitoneal injection of 50 μl of pentobarbitone sodium 20% (w/v) (Animalcare Ltd, York, United Kingdom), and blood was collected by cardiac puncture between 10:00 AM and 2:00 PM. Blood samples were kept at room temperature for 90 min to coagulate and then centrifuged at 2000 *g* for 15 min. The serum was collected and samples stored at −70°C until analysis. The right ovary was fixed in 10% buffered formalin (Sigma-Aldrich) for 8 h, whereas the left ovary was snap frozen in liquid nitrogen and kept at −70°C until RNA extraction.

Follicle culture

Ovaries from 3- to 4-wk-old Control and Mutant females were dissected in Leibovitz L-15 medium (Hyclone; Thermo Fisher Scientific, Loughborough, United Kingdom) supplemented with 3 mg/ml bovine serum albumin (BSA; Sigma-Aldrich), under a stereomicroscope on a heated stage (Leica M125; Microscope Services Ltd., Woodstock, United Kingdom). Preantral follicles with a diameter of 200 ± 10 μm were placed individually into a well of a 96-well plate each containing 30 μl α-minimal essential medium (Hyclone; Thermo Fisher Scientific) enriched with 5% fetal bovine serum (Biosera, Ringmer, United Kingdom), 25 μg/ml (142 μM) ascorbic acid (Sigma-Aldrich), and 0.1–5 IU/ml recombinant human FSH (Gonal-F; Merck Serono, Feltham, United Kingdom), and covered with 75 μl of silicone oil (Dow Corning fluid; VWR International Ltd., Lutterworth, United Kingdom) (54). The 96-well plates containing the culture medium overlaid with oil were placed in the incubator to equilibrate at 37°C with air containing 5% CO_2, for at least 2 h. Follicles were cultured for up to 6 d with transfer to a new well with fresh pre-equilibrated medium every day. Follicle diameter was measured using a pre-calibrated ocular micrometer. Morphology, follicle survival, and the presence of an antral cavity were also evaluated. A total of 44 mice were used for the study: 22 Control and 22 Mutant. Only viable follicles that grew beyond day 2 were included in the analysis.

Serum analysis

Serum levels of FSH, LH, estradiol, inhibin A, inhibin B, AMH, progesterone, and testosterone were determined by the Center for Research in Reproduction at the University of Virginia (Ligand Assay and Analysis Core Laboratories, Charlottesville, VA, USA). Wherever possible, the same sample was analyzed for multiple hormones with LH, FSH, estradiol, inhibin A, and inhibin B assessed in the same sample for 84 of 101 samples. Gonadotropin levels were assayed with a FSH/LH Multiplex assay. The reportable range for FSH was 2.4–300.0 ng/ml, with an intra-assay coefficient of variation (CV) of 7.9% and 3.5% for low and high control samples, respectively. Mouse LH had a readable range of 0.24–30.0 ng/ml, with a CV of 2.4% and 4.0% for low and high control samples, respectively. Progesterone and testosterone serum concentrations were measured by radioimmunoassay (RIA), with a reportable range of 0.09–13.9 ng/ml and 1.06–94.74 ng/ml, respectively. The CV for the low and high controls assayed for testosterone was 6.8% and 0.6%, respectively. The CV for progesterone was 2.7% and 4.2% for low and high control samples, respectively. Estradiol, AMH, inhibin A, and inhibin B were assayed by ELISA. The readable range for estradiol was 3–300 pg/ml and had a CV of 1.3% and 12.8% for low and high control samples, respectively. The CV of AMH was 16.1% and 4.4% for low and high control samples, respectively, and had a reportable range of 0.17–24.0 ng/ml. The inhibin A assay had a CV of 4.1% and 1.6% for low and high control samples, respectively, and a reportable range of 10–1000 pg/ml. The readable range of inhibin B assay was 9.4–951.0 pg/ml, and the CV was 13.2% and 3.2% for low and high control samples, respectively.

Ovarian histology

Formalin-fixed ovaries were paraffin embedded and sectioned (5 μm). Every 10th serial section was counterstained with hematoxylin (Shandon Gill 2 hematoxylin; Thermo Fisher Scientific) and eosin (Sigma-Aldrich), mounted, and photographed using a DM 2500 Leica microscope (Microscope Services Ltd.) and a MicroPublisher 5.0 RTV camera (Qimaging; Microscope Services Ltd.). Ovaries at proestrus and metestrus were assessed, and follicles were classified according to Pedersen and Peters (55) based on the number of granulosa cells in a central section through the oocyte nucleus. Primary follicles have a single layer of cuboidal granulosa cells and include types 3a (≤20 granulosa cells) and 3b (21–60 granulosa cells). Type 4, also known as secondary follicles, corresponds to follicles with 2 layers of granulosa cells (61–100 granulosa cells). Preantral follicles contain multiple layers of granulosa cells and include type 5a (101–200 granulosa cells) and type 5b (201–400 granulosa cells). Types 6 (401–600 granulosa cells) and 7 (≥600 granulosa cells) were grouped as antral follicles; type 6 contains

areas of antral fluid, whereas type 7 has a larger single antral cavity. To discriminate follicles showing an early antral cavity, 2 new types, 5a+antrum (5a+A) and 5b+antrum (5b+A), have been introduced in this study. Where follicles were combined to a group known as antral follicles, types 5a+A, 5b+A, 6, and 7 were included. Only morphologically healthy follicles sectioned through the center of the oocyte with a visible nucleus were analyzed. The number of granulosa cells present in small follicles (3a, 3b, 4, and 5a) were counted twice using microscopy at ×40 magnification. To determine the number of granulosa cells from larger follicles (5b, 6, and 7), high magnification images were used. The presence of a small antrum was recorded, and antrum size was expressed as the number of granulosa cells that would be required to fill the antral space. The number of corpora lutea (CL) in each ovary was recorded, and CL area was determined in the largest cross section using ImageJ (National Institutes of Health, Bethesda, MD, USA).

Immunohistochemistry

Ovaries from 8- to 10-wk-old mice were dissected, and the stage of the estrous cycle of the mice was determined as described above. The ovaries were fixed in 10% buffered formalin (Sigma-Aldrich) for 8 h and washed in 70% ethanol. Ovaries were embedded in paraffin, sectioned at 5 μm, and mounted on glass slides.

Sections were deparaffinized and rehydrated. Endogenous peroxidase was blocked with 3% H_2O_2 (Thermo Fisher Scientific) in PBS for 5 min. Sections were blocked with 10% dry milk (Alcafe, Reading, UK) in PBS for 1 h prior to Bcl-2 detection or with 5% BSA (Thermo Fisher Scientific) in PBS for 1 h prior to Bax detection. Sections were then incubated with either rabbit anti-mouse Bcl-2 polyclonal antibody (PRS3335; Sigma-Aldrich) at 1:50 or rabbit anti-mouse Bax polyclonal antibody (SAB4502549; Sigma-Aldrich) at 1:100. Both antibodies were diluted in their respective blocking solution, and incubations were at 4°C overnight.

All immunohistochemistry slides were incubated with biotinylated anti-rabbit IgG secondary antibody (Vectastain ABC Elite Kit; Vector Laboratories, Peterborough, United Kingdom) for 1 h at room temperature, followed by ABC solution (Vectastain ABC Elite Kit; Vector Laboratories) for 30 min at room temperature. Antigen-specific detection was revealed using a DAB kit (Vector Laboratories). Slides were then dehydrated, mounted with Depex (VWR, Leicestershire, United Kingdom), and imaged using the same light microscope (Leica DM 2500; Microscope Services Ltd.).

TUNEL assay

Apoptosis was detected using TUNEL staining (Apoptag kit; Watford, Hertfordshire, United Kingdom) on 10% buffered formalin-fixed ovary sections. Sections were deparaffinized, rehydrated, and incubated with 20 μg/ml of Proteinase K (Roche Diagnostics, Welwyn Garden City, Hertfordshire, United Kingdom) for 15 min at room temperature. Endogenous peroxidase was blocked with 3% H_2O_2 (Thermo Fisher Scientific) in PBS for 5 min. Equilibration buffer was added to the sections for 10 min at room temperature. Sections were then incubated with 30% terminal deoxynucleotidyl transferase enzyme in reaction buffer for 1 h at 37°C. Control sections were incubated with reaction buffer only. All sections were then incubated with Stop/Wash buffer for 10 min at room temperature, and then anti-digoxigenin conjugate was added to the sections for 30 min at room temperature. Antigen-specific detection was revealed using a DAB kit (Vector Laboratories). Slides were then dehydrated, mounted with Depex, and imaged using the same light microscope (Leica DM 2500; Microscope Services Ltd.).

Characterization of follicles assessed for apoptosis

Only morphologically healthy follicles sectioned through the oocyte were analyzed. Slides were counterstained with hematoxylin (Shandon Gill 2 Hematoxylin; Thermo Fisher Scientific) to enable visualization of follicle histology and cell boundaries. The number of granulosa cells was counted (using the count tool of Image J software) to classify follicles as type 4, 5a, 5a+A, 5b, 5b+A, and 6 (described above). To quantify Bcl-2, Bax, and TUNEL assay in follicles, mean pixel intensity of the granulosa cells of individual follicles (excluding antrum and oocyte) was determined using ImageJ.

RNA extraction and real-time PCR

RNA extraction and cDNA synthesis

Total RNA was extracted and purified from ovaries at each stage of the estrous cycle, using the NucleoSpin RNA II kit (Thermo Fisher Scientific), and the quality and quantity of extracted RNA were then assessed using Nanodrop. First-strand cDNA was synthesized using the SuperScript kit (Life Technologies Limited, Paisley, United Kingdom). Random primers were used at a concentration of 250 ng/μl, and 0.5 μg of total RNA was used in each reaction. Samples were made in triplicate, and 2 controls were synthesized: 1 devoid of RNA and 1 without reverse transcriptase enzyme.

Quantitative PCR

The expression levels of GDF9, BMP15, FSH receptor (FSHR), LH receptor (LHR), and cyclophilin B [peptidylprolyl isomerase B (*PpiB*); as a reference gene] (56, 57) were quantified by SYBR Green quantitative PCR (MESA Green qPCR kit; Eurogentec). Primers were synthesized from the 5′ to 3′ end, and the sequences were as follows: *GDF9* forward, TAC CGT CCG GCT CTT CAG T; *GDF9* reverse, TTA AAC AGC AGG TCC ACC ATC; *BMP15* forward, CAG TAA GGC CTC CCA GAG GT; *BMP15* reverse, AAG TTG ATG GCG GTA AAC CA; *FSHR* forward, CGC AAA GGC AAA GGC CCA GC; *FSHR* reverse, ACA GGA GCA GGC TGC GAT GC; *LHR* forward, TAG TCG GGC GAG GCC AGC TC; *LHR* reverse, CGG GTC CCG GCT CTG AGA CA; *PpiB* forward, TGG AGA GCA CCA AGA CAG ACA; *PpiB* reverse, TGC CGG AGT CGA CAA TGA T. All primers were tested by PCR to evaluate their specificity. Several dilutions of cDNA samples were tested, and a 1:5 dilution was selected for amplification. The total volumes of reagents used per well were 10 μl of 2× reaction buffer, 0.5 μl of the forward primer, 0.5 μl of the reverse primer, 8 μl of water, and 1 μl of the cDNA sample. Experiments were performed using an ABI Prism 7500 real-time PCR instrument (Applied Biosystems, Life Technologies Ltd., Paisley, United Kingdom). Gene expression data were normalized using *PpiB* as the reference gene for the ovary (56, 57).

Statistical analysis

All data are presented as mean ± SEM. Control and Mutant data were compared using *t* tests. For data that did not have a normal distribution or if the sample size was small, a Mann-Whitney *U* test was performed. The Pearson correlation coefficient was calculated to assess correlations between 2 variables (*i.e.*, follicle diameter and day of culture *in vitro*, and number of granulosa cells and antrum size *in vivo*), with an R^2 value of 1 indicating a perfect correlation and a value of 0 indicating no correlation. All statistical analyses were performed using Prism GraphPad software version 4.0b (version 4.0b, 2004; GraphPad Software, La Jolla, CA, USA). $P \leq 0.05$ was considered significant; however, if the *P* value approaches significance, it is provided in the figures.

RESULTS

C1galt1 Mutant females have longer cycles due to an increased time in estrus

The increased fertility phenotype of *C1galt1* Mutant mice was proposed to result from prolonged follicle development (41). To assess whether the proposed prolonged follicle development is related to cycle length, the stage of cycle was determined daily by analysis of vaginal smears (Fig. 1*A*). Analyses confirmed that Mutant females have longer cycles (4.95 ± 0.10 d) than Control females (4.60 ± 0.04 d, $P < 0.05$) due to an increased time at the estrus stage ($P < 0.01$; Fig. 1*B*). However, the onset of puberty did not differ between Control (31.4 ± 1.0 d of age, $n = 18$) and Mutant females (31.8 ± 1.0 d, $n = 24$).

Follicles with oocytes lacking *C1galt1* are more sensitive to FSH *in vitro*

Since the estrous cycle is determined by follicles growing in the ovary, follicle development was assessed *in vitro* in different concentrations of FSH (5, 2.5, 0.5, and 0.1 IU/ml). In excess FSH (5 and 2.5 IU/ml), Control and Mutant follicles showed similar growth rates (**Fig. 2*A***). In contrast, the growth of Control follicles cultured with 0.5 IU/ml FSH was retarded from day 3 onward. On day 6, the mean diameter of Control follicles (315.4 ± 47.7 μm) was less than Mutant follicles (337.7 ± 7.2; $P < 0.05$). In the lowest concentration of FSH analyzed, 0.1 IU/ml, Mutant follicles grew larger than Controls from day 4 to day 6 of culture (Fig. 2*A*).

Follicles with oocytes lacking *C1galt1* exhibit delayed antrum formation

A crucial aspect of follicle development is antrum formation, and therefore, the day the antrum was first observed in cultured follicles was assessed by image analysis (Fig. 2*B*) in excess FSH (5 IU/ml; Fig. 2*C*). Although Mutant follicles demonstrated a greater sensitivity to FSH *in vitro* (Fig. 2*A*), when growth was equivalent in excess FSH, antrum development was delayed (3.6 ± 0.2 d) compared with Control follicles (2.7 ± 0.2 d, $P < 0.01$; Fig. 2*C*). However, the follicle size at which an antral cavity is first detected *in vitro* did not differ between both Control (302.9 ± 4.5 μm) and Mutant follicles (300.9 ± 3.8 μm) (Fig. 2*D*). There were no correlations between the size of early antral follicles and the day of culture in Control ($R^2 = 0.332$) and Mutant follicles ($R^2 = 0.007$; Fig. 2*E*).

Endocrine profile of *C1galt1* Mutant females is modified

To investigate whether the changes in Mutant follicle development are reflected in changes in the endocrine profile, the serum levels of FSH, LH, estradiol, inhibins A and B, AMH, progesterone, and testosterone were measured at each stage of the estrous cycle. None of the hormones analyzed showed a uniform increase or decrease at all 4

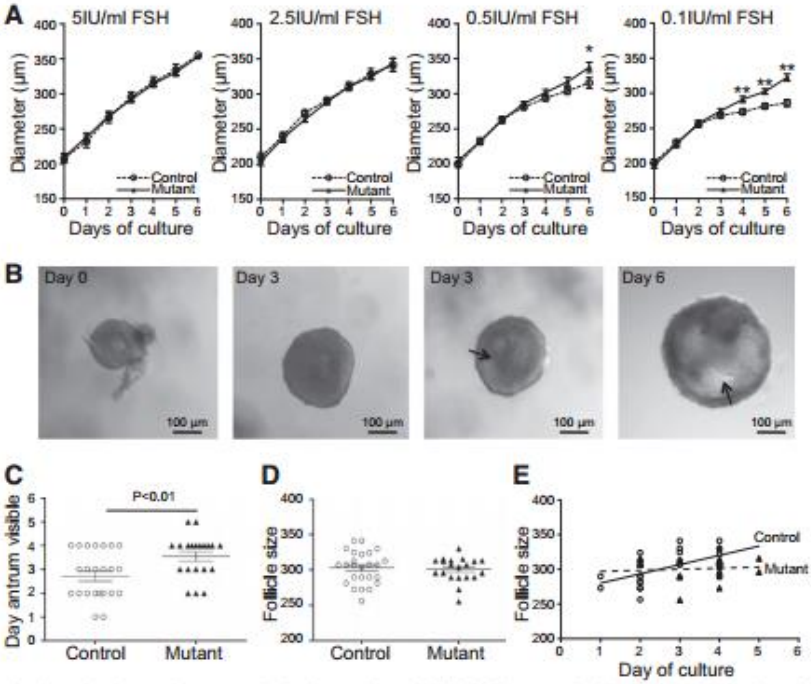

Figure 2. *In vitro* follicle growth and antrum development. *A*) Follicle growth during 6 d of culture with 5, 2.5, 0.5, and 0.1 IU/ml of FSH (Control, open circles; n = 27, 19, 26, and 17 follicles; Mutant, black triangles; n = 29, 24, 24, and 24 follicles for 5, 2.5, 0.5, and 0.1 IU FSH, respectively. Follicles with a diameter of 200 ± 10 μm were obtained by dissection of ovaries from 3- to 4-wk-old females. Follicles were placed in individual wells of a 96-well plate, cultured for 6 d in the presence of FSH, and transferred daily to a new well with fresh medium. Follicle diameter was measured daily using a precalibrated ocular micrometer. *B*) Representative images of follicles at days 0, 3, and 6 of culture with 5 IU FSH. Black arrows indicate antral spaces. *C*) Day of culture when an antral cavity is first observed in follicles cultured with 5 IU FSH. *D*) Follicle size when the antrum is first observed. *E*) Relationship between the day of culture when a cavity is detected and follicle diameter in Control (solid line) and Mutant (broken line). Control, n = 25; Mutant, n = 20. $^*P < 0.05$, $^{**}P < 0.01$.

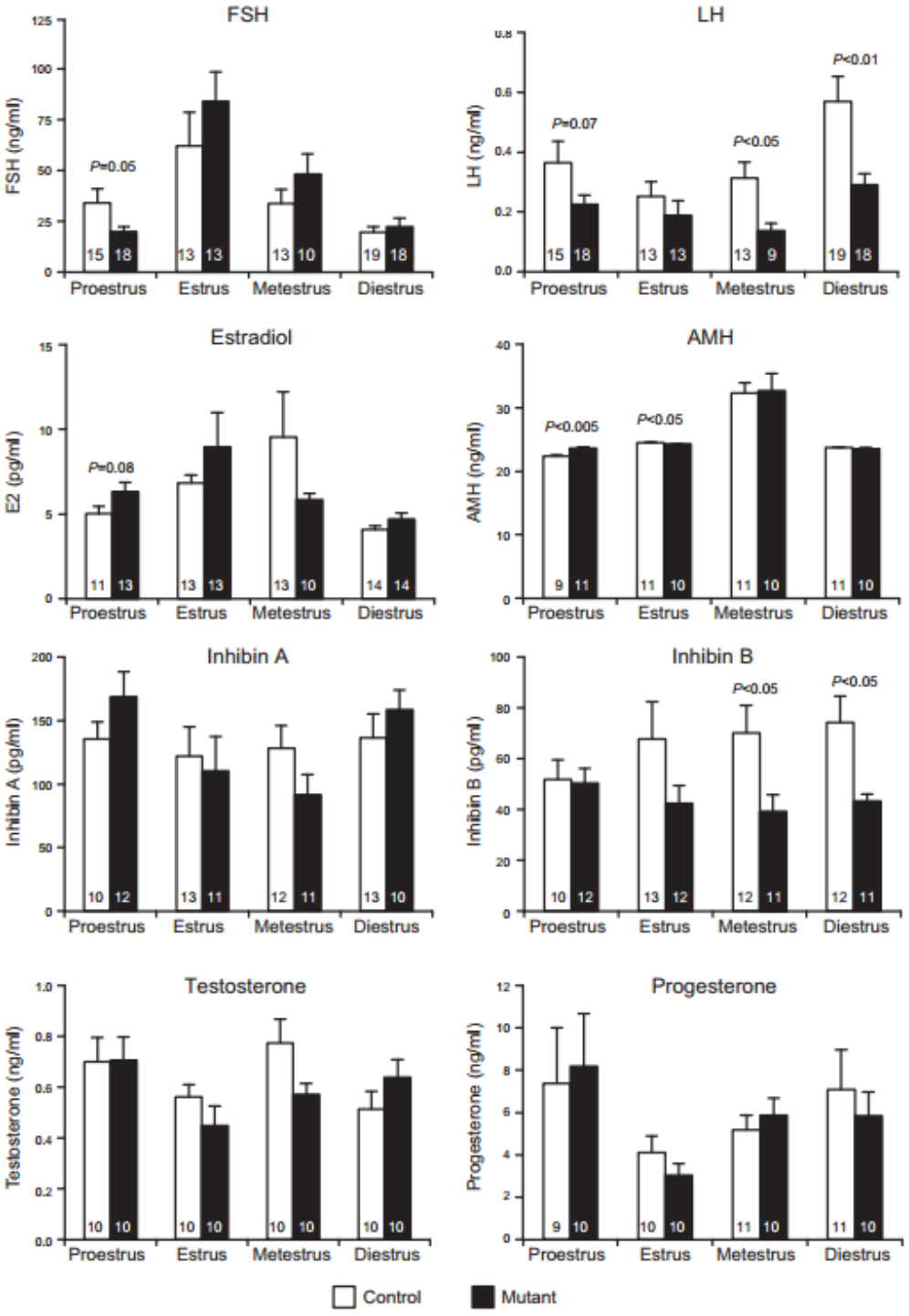

Figure 3. Endocrinology of Control and Mutant females at each stage of the estrous cycle. Blood samples were collected, serum was obtained by centrifugation, and the levels of FSH, LH, estradiol, inhibin A, inhibin B, AMH, progesterone, and testosterone were determined. Gonadotropin levels were assayed with a FSH/LH Multiplex assay. Progesterone and testosterone serum concentrations were measured by RIA. Estradiol, AMH, inhibin A, and inhibin B were assayed by ELISA. White bars correspond to Control samples and black bars to Mutant samples. The numbers in each column indicate the sample size.

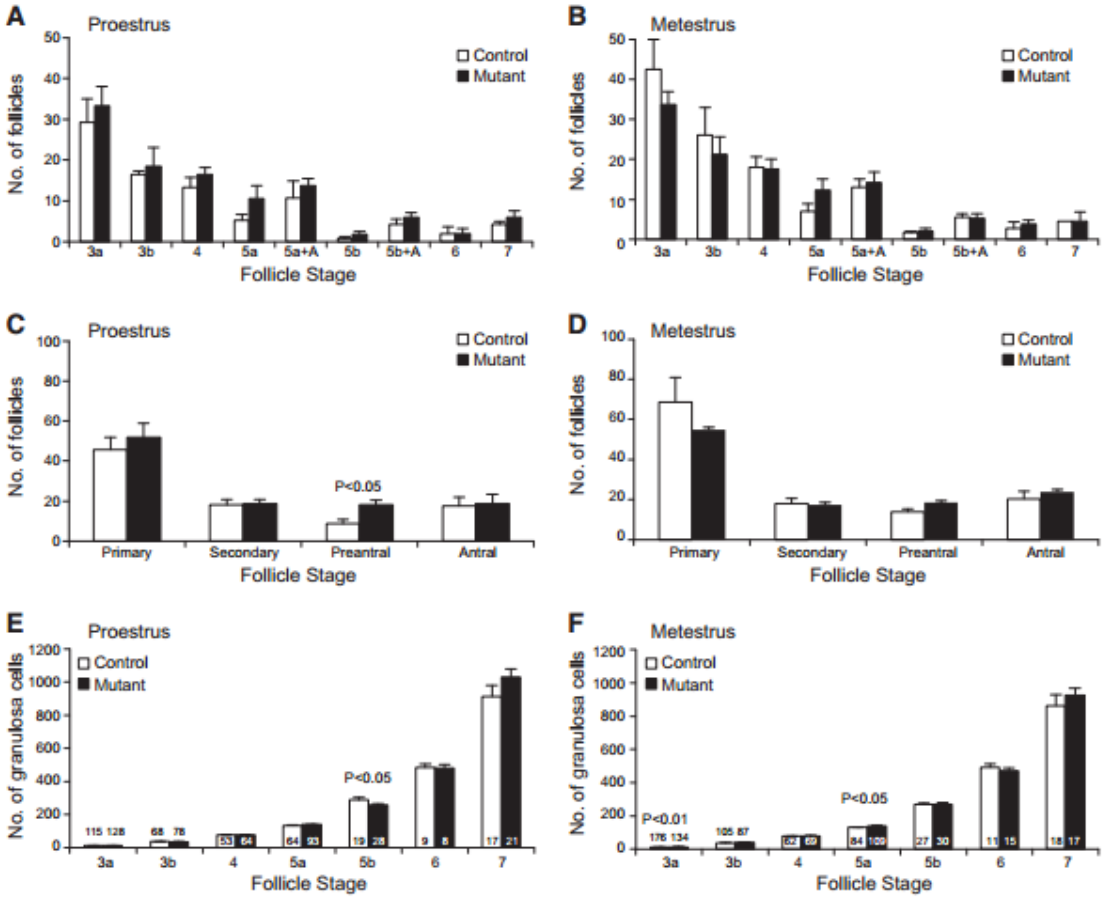

Figure 4. *In vivo* follicle development. *A–B*) Number of follicles at each stage of development in Control (white bars) and Mutant (black bars) right ovaries at proestrus (*A*) and metestrus (*B*) according to Pedersen and Peters (55), which is based on the number of granulosa cells in a single central section. Primary follicles include types 3a (≤20 granulosa cells) and 3b (21–60 granulosa cells). Type 4 follicles contain 61–100 granulosa cells. Type 5a follicles contain 101–200 granulosa cells, and 5b follicles have 201–400 granulosa cells. Types 5a and 5b follicles that contained an incipient antrum were also identified: 5a+A and 5b+A. Antral follicles include type 6 (401–600 granulosa cells with areas of fluid) and type 7 (>600 granulosa cells and a single antral cavity). *C–D*) Number of primary (3a and 3b), secondary (4), preantral (5a and 5b), and antral follicles (5a+A, 5b+A, 6, and 7) at proestrus (*C*) and metestrus (*D*). Control, $n = 4$; Mutant, $n = 4$. *E–F*) Number of granulosa cells at each follicle stage in ovaries at proestrus and metestrus, respectively. The numbers in each column indicate the number of follicles analyzed per ovary at each developmental stage.

stages of the estrous cycle in Mutants compared with Controls. However, FSH concentrations were lower in Mutant females at the proestrus stage (**Fig. 3**), whereas LH was also decreased at diestrus and metestrus. Despite the decrease in FSH concentrations in Mutant females at proestrus, neither estradiol nor inhibin A or B concentrations were significantly increased. However, inhibin A and estradiol were non-significantly elevated, and therefore, the combined influence of these 2 hormones most likely led to the decrease in FSH during proestrus. In contrast, inhibin B levels were significantly decreased during the luteal phase. Granulosa cell generated AMH levels were higher in Mutants at proestrus and lower at estrus. Concentrations of testosterone and progesterone in Mutants were unaltered at all 4 stages of the estrous cycle.

C1galt1 Mutant ovaries contain increased numbers of preantral follicles at proestrus containing fewer granulosa cells

To relate the changes in endocrinology to follicle development, the number of follicles at each stage of development in postpubertal Control and Mutant females was evaluated at 2 stages of the estrous cycle. Proestrus and metestrus were selected because they represent the first day of the follicular and luteal phase, respectively. No differences were found between the number of Control and Mutant follicles at any of the developmental stages (**Fig. 4*A*, *B***). However when follicles were grouped in primary (3a–3b), secondary (4), preantral (5a–5b), and antral [5a and 5b with precocious antrum (5a+A, 5b+A)

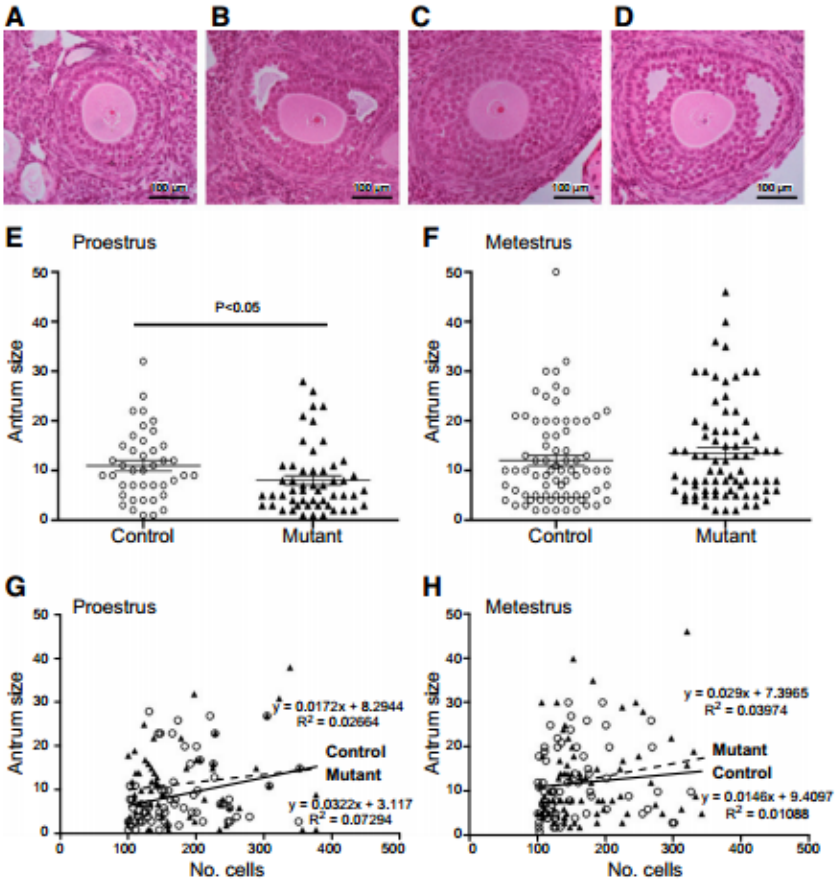

Figure 5. Analysis of *in vivo* antrum development in Control and Mutant mice. Representative images of 5a, 5a+A (*A–B*), 5b and 5b+A (*C–D*) follicles: (*A, C*) preantral and (*B, D*) early antral follicles. The presence of a small antrum in 5a and 5b follicles was recorded, and antrum size was expressed as the number of granulosa cells that would be required to fill the antral space. *E–F*) Antrum size in 5a–5b follicles at proestrus and metestrus, respectively. Correlation analysis between antrum size and number of granulosa cells at (*G*) proestrus and (*H*) metestrus. Control, open circles and solid line; Mutant, black triangles and broken line.

and 6–7] Mutant ovaries contained more preantral follicles at proestrus ($P < 0.05$; Fig. 4*C*) compared with Controls. However, this increase in Mutant preantral follicles was not evident at metestrus (Fig. 4*D*). The number of follicles at each developmental stage, compared between the 2 stages of the estrous cycle, did not differ in Controls or Mutants.

To determine whether follicle size was altered by oocytes lacking core 1-derived *O*-glycans, the number of granulosa cells present in follicles at each development stage was evaluated. At proestrus, large preantral (5b) follicles in Mutant ovaries contained less granulosa cells (258.3 ± 9.1) than Control follicles (289.5 ± 14.5; Fig. 4*E*). In contrast, 3a and 5a Mutant follicles contained more granulosa cells than Controls at metestrus (Fig. 4*F*).

Some follicles classified as 5a and 5b according to the number of granulosa cells (55) also exhibited an incipient or small antral cavity (5a+A and 5b+A; **Fig. 5*A–D***). At proestrus, the antral cavity of 5a and 5b follicles was smaller in Mutant follicles than Control follicles (Fig. 5*E*); however, 2 d later at metestrus, follicles did not exhibit this difference (Fig. 5*F*).

The number of granulosa cells in a follicle and the size of the antrum in Control or Mutant follicles at proestrus or metestrus were not correlated (Fig. 5*G, H*).

The decrease in the number of granulosa cells was reflected in CL size (**Fig. 6**), with Mutant CL smaller than control CL (0.37 ± 0.01 mm^2 and 0.28 ± 0.01 mm^2, respectively; $P < 0.001$). However, as expected based on the increased OR of Mutant mice (41), Mutant ovaries contained double the number of CL than Controls at proestrus, but this increase did not quite achieve significance, most likely due to the assessment of only 1 ovary per mouse, resulting in more variability in CL number per ovary (7.25 ± 1.5 per Mutant ovary and 3.75 ± 0.5 per Control ovary; $P = 0.06$; Fig. 6).

Analysis of apoptosis

An important aspect of follicle selection is the programmed apoptosis of follicles. To determine whether a decrease in follicle apoptosis was a factor in the increased number of follicles observed in Mutant ovaries, we analyzed ovarian sections at the proestrus and metestrus stages of the cycle (**Fig. 7*A–C***). These analyses revealed a decrease in TUNEL staining of Mutant antral follicles, including those with an incipient antrum, at metestrus (Fig. 7*D*).

To investigate the molecular basis for this alteration in follicle apoptosis, the anti-apoptotic molecule Bcl-2 and the pro-apoptotic molecule Bax were investigated (**Fig. 7*E, F***).

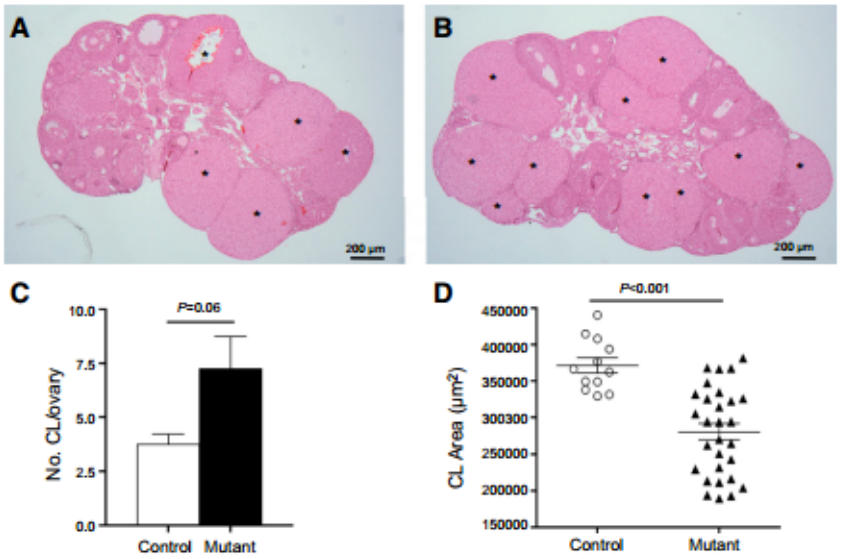

Figure 6. CL evaluation. Representative images of (*A*) Control and (*B*) Mutant ovaries at proestrus, stained with hematoxylin and eosin. Asterisks indicate CL. *C*) Number of CL present in Control (white bars) and Mutant (black bars) ovaries (one ovary only counted per mouse). *D*) Areas of the CL found in Control (open circles) and Mutant (black triangles) ovaries. CL areas were measured in the biggest cross section of each CL.

The levels of Bcl-2 detected in Control follicles were consistent at all stages of development at proestrus, and the same was evident at metestrus, but surprisingly, the levels at proestrus were approximately half those at metestrus ($P < 0.0001$). In Mutant follicles, the levels of Bcl-2 only differed between the 2 d of the estrous cycle in stage 4 follicles, whereas the levels in the remainder of the follicle stages remained constant at metestrus and proestrus (Fig. 7*E*). Furthermore, within each stage of the cycle, the levels of Bcl-2 in Mutant follicles were consistent except when comparing stage 5+A to stage 6 in proestrus ($P < 0.05$). Therefore, when comparing the levels of Bcl-2 between Mutants and Controls, the levels of Bcl-2 in the Mutants are higher at all stages of follicle development at proestrus, whereas at metestrus, Mutant levels are lower than Controls at stages 4, 5+A, and 6 because of the changes in Control levels at the 2 stages of the estrous cycle.

When examining the pro-apoptotic factor Bax (Fig. 7*F*), a similar profile to Bcl-2 was observed in Control follicles with consistent levels of Bax at all stages of development at proestrus or at metestrus. However, the levels of Bax in Control follicles during proestrus are lower than those at metestrus ($P < 0.05$). In Mutant follicles, both 5+A and 6 follicles had increased levels of Bax at proestrus compared with metestrous ($P < 0.01$ and $P < 0.05$, respectively). Interestingly, similar to Bcl-2 (Fig. 7*E*), the levels of Bax for 5+A follicles were higher than stage 6 but only at proestrus (Fig. 7*F*). Therefore, again similar to Bcl-2, Bax levels in Mutant follicles were higher than Control follicles at all stages of development ($P < 0.001$) at proestrus, whereas at metestrus, Mutant follicle levels of Bax were lower than Control at stages 4 ($P < 0.05$) and 6 ($P < 0.01$).

Although these patterns indicate clear regulation of both Bcl-2 and Bax in both Controls and Mutants, the intracellular ratio between these 2 molecules has been shown to be important for induction of apoptosis. Analysis of the intrafollicular ratio of Bcl-2:Bax was based on fewer numbers of follicles compared with follicles analyzed for Bcl-2 or Bax because not all follicles were present in consecutive sections, and thus follicles 4 and 5 were grouped together (Fig. 7*G*). Based on the Bcl-2 and Bax data described above, it was unsurprising to find that the ratio of Bcl-2:Bax in Control follicles was consistent at either proestrus or metestrus but was increased in metestrus compared with proestrus ($P < 0.01$ for 4 and 5 follicles and $P < 0.0001$ for 6 follicles; Fig. 7*G*). In Mutant follicles, this ratio did not differ between follicle stages at proestrus but was increased in metestrus, when comparing type 6 follicles to 4 and 5 ($P < 0.01$). Therefore, when comparing the ratios between Mutants and Controls within each estrous stage, because both Bcl-2 and Bax levels were higher in Mutant follicles at proestrus, no difference in the ratio of Bcl-2:Bax was observed at proestrus. However, at metestrus, the ratio of Bcl-2:Bax was lower in Mutant follicles compared with Controls at both stages 4 and 5 ($P < 0.001$) and stage 6 ($P < 0.0001$; Fig. 7*G*).

C1galt1 ovaries have a higher ratio of *GDF9:BMP15* expression

To investigate regulators of follicle development that may be altered due to oocyte-specific deletion of *C1galt1*, ovarian expression of gonadotropin receptors and 2 oocyte-specific genes *GDF9* and *BMP15* was determined for the 4 stages of the estrous cycle (**Fig. 8**). Although there were no significant differences in mRNA level for any of the genes studied, Mutant *GDF9* was increased at diestrus 1.7-fold compared with Controls. To analyze gene expression further, the ratio of *GDF9* to *BMP15* was assessed because changes in this ratio have been linked to the different ORs of different mammalian species (39). Analysis of Mutants revealed the ratio of expression of *GDF9* to *BMP15* was higher ($P = 0.05$) compared with Controls at diestrus. This increased ratio is consistent with the elevated ratio in mammals with higher ORs (39).

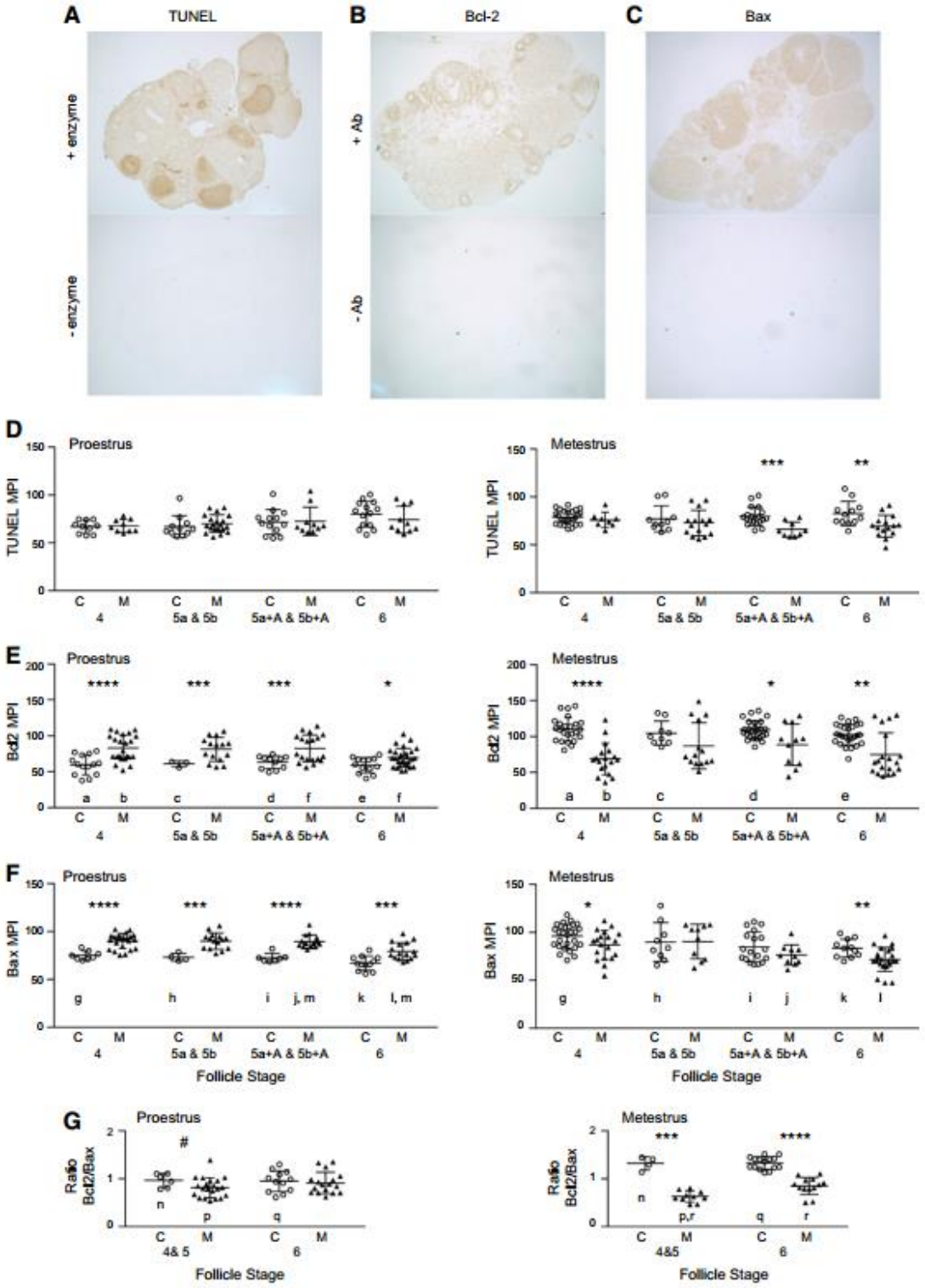

Figure 7. Assessment of apoptosis at different stages of follicle development at proestrus and metestrus. Follicles were defined based on the number of granulosa cells in a single central section according to Pedersen and Peters (55). Type 4 follicles contain

(*continued on next page*)

DISCUSSION

Female mice with oocyte-specific deletion of *C1galt1* have modified follicle development that results in a sustained increase in OR and fertility that is non-pathological (41). We reveal here that the lack of oocyte core 1-derived *O*-glycans results in multiple changes in follicle development including enhanced sensitivity of follicles to FSH *in vitro*, a decrease in the degree of apoptosis, and an altered *GDF9* to *BMP15* expression ratio. *C1galt1* Mutant females have longer estrous cycles than Controls because of an increase in the length of the estrus phase. The endocrine profile of Mutant females is also modified with decreased levels of gonadotropins, inhibin B, and AMH at specific stages of the estrous cycle and higher levels of AMH at proestrus. The hormonal changes most likely reflect the modified follicle development in Mutant ovaries. Moreover, the size of the cavity of early antral follicles in Mutants at this stage of the cycle is smaller than in Control follicles, and *in vitro* antrum development in Mutant follicles is delayed. Mutant follicles also develop a higher sensitivity to FSH by the third day of culture that may well contribute to an increase in follicle survival. Indeed, analysis revealed a decrease in apoptotic follicles in Mutant ovaries, which likely contributes to the resulting increased number of follicles. Finally, as a result of oocyte glycoprotein modification in Mutant females, an increase in the ratio of *GDF9:BMP15* expression was found at diestrus.

Follicle development is modified in prepubertal *C1galt1* Mutant females with ovaries containing increased numbers of preantral and antral follicles (41); however, the critical point in Mutant follicle development was unclear. In this study, we investigated follicle development in postpubertal females. At proestrus, Mutant females contained higher numbers of preantral follicles than Controls, but these follicles contained less granulosa cells resulting in smaller CL. The smaller CL size most likely reflects the reduced size of Mutant follicles. Smaller CL have also been observed in ewes with a natural mutation in the BMP15 receptor activin-like kinase 6 (ALK6; also known as BMPRIB type 1 receptor). Like the *C1galt1* Mutant mice, these females have a higher OR than wild-type females (58). This decrease in follicle size at ovulation accompanying an overall increase in OR in both species implies that there may be a common molecular mechanism.

During the transition from a preantral to an antral stage, follicles are highly susceptible to atresia, and FSH can be considered a survival factor (59, 60). This transition is a critical point and unless follicles are provided with the FSH they require, they will undergo atresia (59, 61). *In vitro*, *C1galt1* Mutant follicles are more sensitive to lower FSH concentrations after transition to an FSH-dependent antral follicle and grow larger than Controls. Therefore, it is likely that *in vivo* more Mutant follicles would be more resistant to the decrease of FSH in the late follicular phase, escape atresia, and continue to develop. However, the expression of the FSH receptor appears to be unmodified in Mutant ovaries, but only whole ovaries were analyzed in this instance. Therefore because the modifications in mutant follicle development are very much stage specific, analysis of the whole ovary may have masked subtle changes in the FSH receptors of individual follicles.

For there to be an increase in the number of developing follicles, there has to be a decrease in apoptosis. This is because the genetic modification in Mutants only occurs in the oocyte after this point, and thus the number of follicles leaving the quiescent pool should remain unaltered. TUNEL analysis did indeed reveal a decrease in apoptotic follicles in Mutant ovaries at metestrus. Analysis of follicular levels of the pro-apoptotic Bax (7) and the anti-apoptotic Bcl-2 (6) revealed striking observations in both Control and Mutant ovaries. In Control follicles, marked differences were observed between the proestrus and metestrus stages of the estrous cycle for both Bcl-2 and Bax, indicating estrous cycle-dependent regulation of apoptosis molecules. Estrous cycle-specific changes in these molecules have been previously observed by analysis of whole rat ovaries (62); however, our analyses reveal that in Control ovaries these changes occur in follicles at all stages of development rather than those more susceptible to apoptosis. However, in Mutant follicles, the variations in Bcl-2 and Bax between the 2 stages of the estrous cycle were almost entirely eliminated. There are various possible explanations for this observation, including altered intra-follicular regulation or a response to the altered endocrine profile (for example, AMH has been proposed as an inhibitor of follicular atresia) (63). However, because follicle development is a continuous process, we cannot be certain on which day the modifications are initiated, and thus what mechanisms are involved, versus the day we are observing the differences. Furthermore, the ratio of Bcl-2:Bax, which has been reported to be important for cell fate determination (10) was not elevated in Mutant follicles, which was surprising considering that Mutant ovaries contain more healthy follicles. Although other factors, including GDF9, can modify the function of members of the Bcl-2 family (64), overall levels of Bcl-2 or Bax may not reflect function. It is also possible that other members of the Bcl-2 family are involved in the regulation of apoptosis in Mutant follicles. Clearly, the *in vivo* influences regulating follicular apoptosis are complex. Our current understanding is that follicles are selected from a pool subjected to a careful balance of

61–100 granulosa cells, type 5a follicles have 101–200 granulosa cells, and 5b follicles have 201–400 granulosa cells. Types 5a and 5b follicles were classified as 5a+A and 5b+A if an incipient antrum was present. Type 6 follicles contain 401–600 granulosa cells with antral fluid. Representative images of TUNEL staining (*A*) and detection of Bcl-2 (*B*) and Bax (*C*). Mean pixel intensity of TUNEL staining in follicles of mice at proestrus and metestrus (*D*). Mean pixel intensity of Bcl-2 detection in follicles of mice at proestrus and metestrus (*E*). Mean pixel intensity of Bax detection in follicles of mice at proestrus and metestrus (*F*). Ratio of Bcl-2 to Bax detected in follicles of mice at proestrus and metestrus (*G*). Asterisks indicate significant differences between the Control and Mutant data at that stage of follicle development at that stage of the estrous cycle: *$P < 0.05$, **$P < 0.01$, ***$P < 0.001$, ****$P < 0.0001$. Letters below the data points within a panel indicate a significant difference for either Control or Mutant follicles between the 2 stages of the estrous cycle or between different stages of follicle development at the same stage of the estrous cycle: b, f, h, l, and m, $P < 0.05$; i, j, n, p, and r, $P < 0.01$; k, $P < 0.001$; a, c, d, e, g, and q, $P < 0.0001$. Control, $n = 4$; Mutant, $n = 4$.

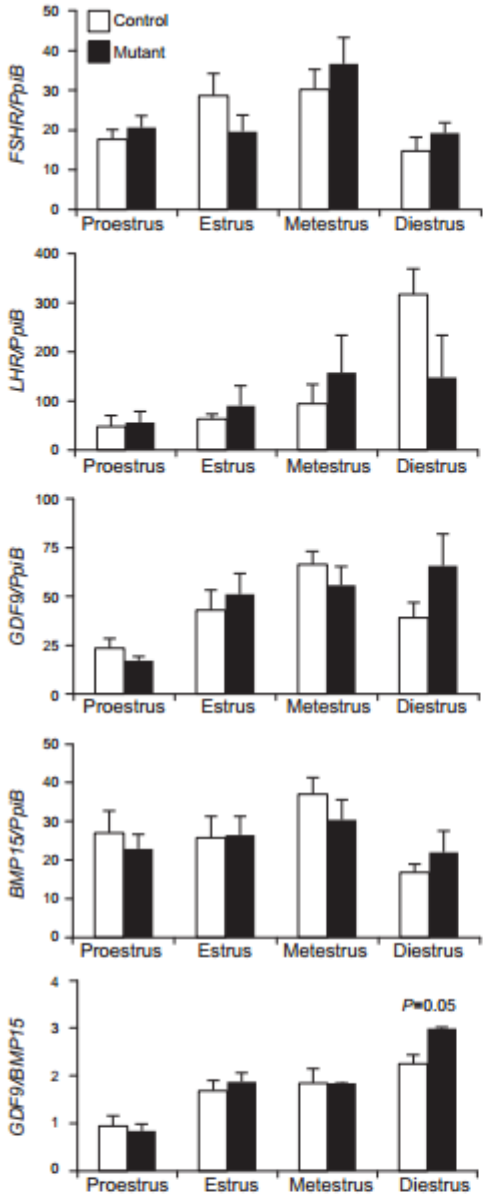

Figure 8. Ovarian expression of follicle development regulators. mRNA levels of (*A*) *FSHR*, (*B*) *LHR*, (*C*) *GDF9*, and (*D*) *BMP15* expressed relative to *PpiB* expression. *E*) Ratio between *GDF9* and *BMP15* expression. Total RNA was extracted and purified from frozen ovaries using the NucleoSpin RNA II kit. First-strand cDNA was synthesized using the SuperScript kit. Gene expression was quantified by SYBR Green qPCR, using *PpiB* as a reference gene. Control: proestrus and estrus, $n = 6$; metestrus, $n = 3$; and diestrus, $n = 4$. Mutant: proestrus and estrus, $n = 6$; metestrus and diestrus, $n = 3$.

intra- and extra-ovarian hormonal support of follicles at specific stages of development (65), and therefore, although follicle apoptosis in the Mutant is reduced, the specific molecular mechanisms are not clear.

Among the intra-ovarian factors that regulate follicular growth, oocyte-specific factors play an essential role (22). Two major factors, GDF9 and BMP15, are important regulators of female fertility through modulation of proliferation and differentiation of granulosa cells (32, 66, 67). Mice lacking *GDF9* are sterile, whereas *BMP15*$^{-/-}$ mice have decreased fertility (21, 36). Both are members of the TGF-β family, have synergic actions on granulosa cells (38, 68), and can form heterodimers enhancing their activity (37, 69, 70). In *C1galt1* Mutant females, the expression levels of *BMP15* and *GDF9* are not modified; however, there is an increase in the *GDF9:BMP15* ratio. A recent study has shown that the ratio of *GDF9:BMP15* differs between species and is related to the species-specific regulation of OR (39). This ratio is higher in mice compared with species with low ORs such as sheep, cows, or deer (39). However, the simple change in ratio of GDF9 to BMP15 cannot be the only OR regulating factor because mice heterozygous for BMP15 would have a higher GDF9: BMP15 ratio, but fertility is not increased in *BMP15*$^{+/-}$ mice (36). Furthermore, sheep heterozygous for *BMP15* or the receptor, *ALK6*, have increased fertility (35). Therefore, the increase in *GDF9:BMP15* ratio in Mutant females at diestrus is unlikely to be the sole mechanism behind the increased OR. However, since GDF9 suppresses granulosa cell apoptosis during the transition from the preantral to early antral stage and stimulates *FSHR* expression (71), whereas BMP15 inhibits *FSHR* expression (72), the increased ratio of *GDF9:BMP15* most likely contributes to the Mutant phenotype.

Antrum development both *in vivo* and *in vitro* is delayed in Mutant females, consistent with the proposed model of prolonged development of Mutant follicles (41). Likewise, the lower circulating levels of FSH are consistent with the slower preantral development and a delay in antrum formation (15). This "delay" in Mutant follicle development and the higher FSH sensitivity of antral follicles could lead to a higher number of follicles that are able to progress beyond the critical point, and continue to grow and ovulate. The decrease in FSH is likely due to elevated negative feedback from the increased numbers of Mutant follicles producing estradiol and inhibin.

As a result of the altered follicle development, the endocrine profile of *C1galt1* females is modified. The decrease in FSH concentration observed in our model also occurs in females heterozygous for DAZL, which also exhibit increased FSH sensitivity and increased fertility like the *C1galt1* Mutants. However, in *DAZL*$^{+/-}$ females, the decreased FSH levels were modulated by an increase in inhibin B production by larger follicles (44), whereas in our Mutant, inhibin B concentrations were not elevated at any stage of the cycle but were actually reduced at metestrus and diestrus. Without measuring inhibin production by individual Mutant follicles, one explanation for the decrease in inhibin B might be the reduced size of the preantral follicles because inhibin B is generated by granulosa cells of preantral and small antral follicles (73). Estrogens are also modulators of FSH levels and considering the estrogen and inhibin A levels in Mutant females were both 25% higher than Controls, although these increases did not attain significance, it would not be inappropriate to propose that the combined negative feedback of these 2 hormones is primarily responsible for the decrease in FSH at proestrus. AMH is another intra-ovarian molecule secreted by granulosa cells and modulates FSH

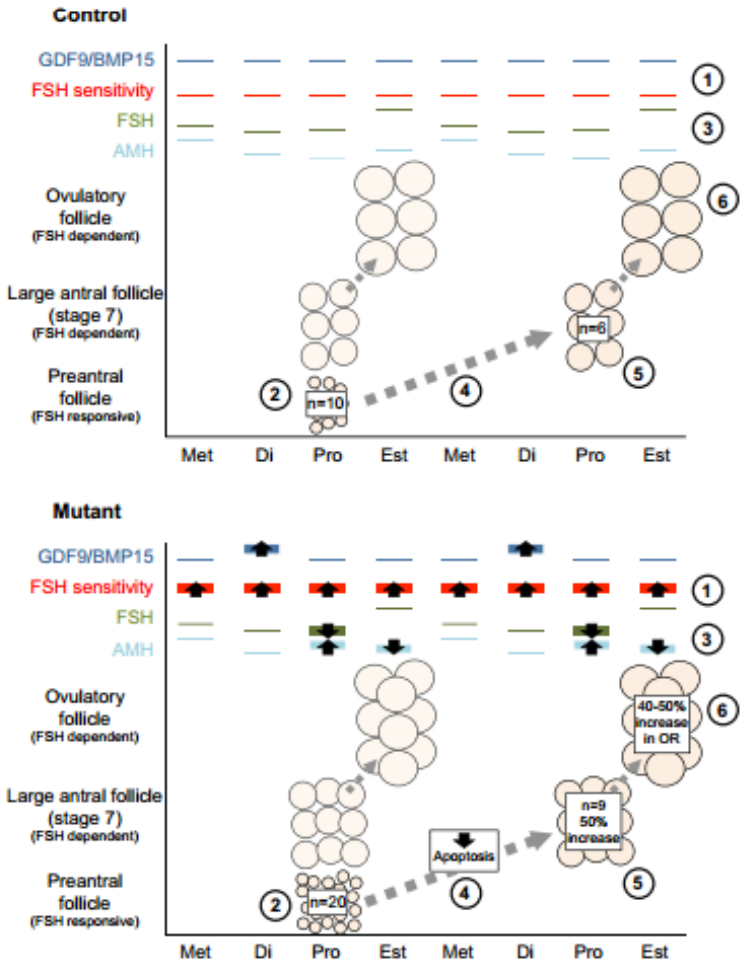

Figure 9. Proposed model of the modified follicle development in *C1galt1* Mutant females. [1] The ratio of *GDF9:BMP15* is modified in Mutant ovaries compared with Controls at the diestrus stage of the cycle and affects follicle function leading to an increase in follicle sensitivity to FSH. [2] These changes result in increased numbers of viable preantral follicles present at the proestrus stage in Mutant ovaries (data from Fig. 4*C*). [3] The increased number of preantral follicles at proestrus in Mutants results in an increase in AMH and also a decline in FSH most likely due to combined negative feedback by the elevated estradiol and inhibin A (data from Fig. 3). For clarity, only FSH and AMH are represented in this figure. [4] The preantral follicles at the proestrus stage develop to become large antral follicles at proestrus of the next cycle and are more resistant to apoptosis. [5] At proestrus of the next estrous cycle, more large antral Mutant follicles are available to undergo selection for ovulation than Controls (data from Fig. 4*A*). [6] Due to the increase in number of large antral follicles and increased FSH sensitivity (data from Fig. 2*A*), more follicles are able to become ovulatory in Mutant ovaries leading to a 50% increase in OR (41).

responsiveness of the follicles (28–30). In our Mutant, AMH levels are increased at proestrus, most likely due to the increased number of preantral follicles, and decreased at estrus after the ovulation of the large antral follicles. The lower levels of AMH found at estrus could be responsible for the increased FSH sensitivity of the new batch of growing follicles (29). Surprisingly, progesterone concentrations were unaltered in Mutant females despite the fact that Mutant ovaries contain double the number of CL than Controls. Since Mutant CL are smaller than Controls, it is likely that the lack of a real change in serum progesterone concentrations is at least due in part to the decrease in CL size. Therefore, the increase in estrus cycle length found, in combination with the altered gonadotropins and ovarian hormone levels, suggests the involvement of the hypothalamic-pituitary-gonadal axis in the phenotype developed by Mutant females.

We propose a model based on the data described in this paper to explain the mechanism for the increased fertility phenotype (**Fig. 9**). Since the origin of the phenotype is the oocyte as this is where the genetic modification occurs, this is the starting point for the proposed mechanism. The ratio of *GDF9:BMP15* is modified in Mutant ovaries compared with Controls at the diestrus stage of the cycle affecting follicle function, leading to an increase in follicle sensitivity to FSH and decreased apoptosis at the metestrus stage of the cycle. These changes result in increased numbers of viable preantral follicles present at the proestrus stage in Mutant ovaries resulting in an increase in AMH and also a decline in FSH, most likely because of combined negative feedback by the elevated estradiol and inhibin A. The preantral follicles at the proestrus stage develop to become large antral follicles at proestrus of the next cycle, and thus more Mutant follicles are available to undergo selection for ovulation than Controls, leading to a 50% increase in OR (41).

In conclusion, the modification of oocyte-specific glycoproteins by deletion of *C1galt1* increase the ratio of *GDF9:BMP15* expression, which most likely alters follicle development leading to changes in hormonal profile resulting in increased fertility. Determining the mechanisms that regulate OR is critical to further our understanding of how follicles, and thus individual eggs, are selected for ovulation. FJ

The authors thank Dr. Norah Spears, Dr. Tamara Sirey, Charlotte Holdsworth, Sophie Robin, and members of the animal house facility for technical assistance and Heidy Kaune for critical reading of the manuscript. This work was supported by the John Fell Fund Oxford University Press (University of Oxford).

REFERENCES

1. Fortune, J. E. (1994) Ovarian follicular growth and development in mammals. *Biol. Reprod.* **50**, 225–232
2. Matsuda, F., Inoue, N., Manabe, N., and Ohkura, S. (2012) Follicular growth and atresia in mammalian ovaries: regulation by survival and death of granulosa cells. *J. Reprod. Dev.* **58**, 44–50
3. Tsujimoto, H., Takeshita, S., Nakatani, K., Kawamura, Y., Tokutomi, T., and Sekine, I. (2001) Delayed apoptosis of circulating neutrophils in Kawasaki disease. *Clin. Exp. Immunol.* **126**, 355–364
4. van Delft, M. F., and Huang, D. C. (2006) How the Bcl-2 family of proteins interact to regulate apoptosis. *Cell Res.* **16**, 203–213
5. Taylor, R. C., Cullen, S. P., and Martin, S. J. (2008) Apoptosis: controlled demolition at the cellular level. *Nat. Rev. Mol. Cell Biol.* **9**, 231–241
6. Vaux, D. L., Cory, S., and Adams, J. M. (1988) Bcl-2 gene promotes haemopoietic cell survival and cooperates with c-myc to immortalize pre-B cells. *Nature* **335**, 440–442
7. Pawlowski, J., and Kraft, A. S. (2000) Bax-induced apoptotic cell death. *Proc. Natl. Acad. Sci. USA* **97**, 529–531
8. Gosden, R., and Spears, N. (1997) Programmed cell death in the reproductive system. *Br. Med. Bull.* **53**, 644–661
9. Hussein, M. R. (2005) Apoptosis in the ovary: molecular mechanisms. *Hum. Reprod. Update* **11**, 162–177
10. Oltvai, Z. N., Milliman, C. L., and Korsmeyer, S. J. (1993) Bcl-2 heterodimerizes in vivo with a conserved homolog, Bax, that accelerates programmed cell death. *Cell* **74**, 609–619
11. Cortvrindt, R., Smitz, J., and Van Steirteghem, A. C. (1997) Assessment of the need for follicle stimulating hormone in early preantral mouse follicle culture in vitro. *Hum. Reprod.* **12**, 759–768
12. Kumar, T. R., Wang, Y., Lu, N., and Matzuk, M. M. (1997) Follicle stimulating hormone is required for ovarian follicle maturation but not male fertility. *Nat. Genet.* **15**, 201–204
13. McGee, E. A., Perlas, E., LaPolt, P. S., Tsafriri, A., and Hsueh, A. J. (1997) Follicle-stimulating hormone enhances the development of preantral follicles in juvenile rats. *Biol. Reprod.* **57**, 990–998
14. Hartshorne, G. M., Sargent, I. L., and Barlow, D. H. (1994) Growth rates and antrum formation of mouse ovarian follicles in vitro in response to follicle-stimulating hormone, relaxin, cyclic AMP and hypoxanthine. *Hum. Reprod.* **9**, 1003–1012
15. Hillier, S. G. (1994) Current concepts of the roles of follicle stimulating hormone and luteinizing hormone in folliculogenesis. *Hum. Reprod.* **9**, 188–191
16. Rodgers, R. J., and Irving-Rodgers, H. F. (2010) Formation of the ovarian follicular antrum and follicular fluid. *Biol. Reprod.* **82**, 1021–1029
17. Hirshfield, A. N., and De Paolo, L. V. (1981) Effect of suppression of the surge of follicle-stimulating hormone with porcine follicular fluid on follicular development in the rat. *J. Endocrinol.* **88**, 67–71
18. McGee, E. A., and Hsueh, A. J. (2000) Initial and cyclic recruitment of ovarian follicles. *Endocr. Rev.* **21**, 200–214
19. Adashi, E. Y. (1992) Intraovarian peptides. Stimulators and inhibitors of follicular growth and differentiation. *Endocrinol. Metab. Clin. North Am.* **21**, 1–17
20. Knight, P. G., and Glister, C. (2006) TGF-beta superfamily members and ovarian follicle development. *Reproduction* **132**, 191–206
21. Dong, J., Albertini, D. F., Nishimori, K., Kumar, T. R., Lu, N., and Matzuk, M. M. (1996) Growth differentiation factor-9 is required during early ovarian folliculogenesis. *Nature* **383**, 531–535
22. Eppig, J. J. (2001) Oocyte control of ovarian follicular development and function in mammals. *Reproduction* **122**, 829–838
23. Matzuk, M. M., Burns, K. H., Viveiros, M. M., and Eppig, J. J. (2002) Intercellular communication in the mammalian ovary: oocytes carry the conversation. *Science* **296**, 2178–2180
24. Wu, X., Chen, L., Brown, C. A., Yan, C., and Matzuk, M. M. (2004) Interrelationship of growth differentiation factor 9 and inhibin in early folliculogenesis and ovarian tumorigenesis in mice. *Mol. Endocrinol.* **18**, 1509–1519
25. Gilchrist, R. B., Lane, M., and Thompson, J. G. (2008) Oocyte-secreted factors: regulators of cumulus cell function and oocyte quality. *Hum. Reprod. Update* **14**, 159–177
26. Findlay, J. K. (1993) An update on the roles of inhibin, activin, and follistatin as local regulators of folliculogenesis. *Biol. Reprod.* **48**, 15–23
27. Matzuk, M. M., Kumar, T. R., Shou, W., Coerver, K. A., Lau, A. L., Behringer, R. R., and Finegold, M. J. (1996) Transgenic models to study the roles of inhibins and activins in reproduction, oncogenesis, and development. *Recent Prog. Horm. Res.* **51**, 123–154
28. Durlinger, A. L., Kramer, P., Karels, B., de Jong, F. H., Uilenbroek, J. T., Grootegoed, J. A., and Themmen, A. P. (1999) Control of primordial follicle recruitment by anti-Müllerian hormone in the mouse ovary. *Endocrinology* **140**, 5789–5796
29. Durlinger, A. L. L., Gruijters, M. J. G., Kramer, P., Karels, B., Kumar, T. R., Matzuk, M. M., Rose, U. M., de Jong, F. H., Uilenbroek, J. T. J., Grootegoed, J. A., and Themmen, A. P. N. (2001) Anti-Müllerian hormone attenuates the effects of FSH on follicle development in the mouse ovary. *Endocrinology* **142**, 4891–4899
30. Durlinger, A. L., Gruijters, M. J., Kramer, P., Karels, B., Ingraham, H. A., Nachtigal, M. W., Uilenbroek, J. T., Grootegoed, J. A., and Themmen, A. P. (2002) Anti-Müllerian hormone inhibits initiation of primordial follicle growth in the mouse ovary. *Endocrinology* **143**, 1076–1084
31. Carabatsos, M. J., Elvin, J., Matzuk, M. M., and Albertini, D. F. (1998) Characterization of oocyte and follicle development in growth differentiation factor-9-deficient mice. *Dev. Biol.* **204**, 373–384
32. Otsuka, F., Yao, Z., Lee, T., Yamamoto, S., Erickson, G. F., and Shimasaki, S. (2000) Bone morphogenetic protein-15. Identification of target cells and biological functions. *J. Biol. Chem.* **275**, 39523–39528
33. McMahon, H. E., Hashimoto, O., Mellon, P. L., and Shimasaki, S. (2008) Oocyte-specific overexpression of mouse bone morphogenetic protein-15 leads to accelerated folliculogenesis and an early onset of acyclicity in transgenic mice. *Endocrinology* **149**, 2807–2815
34. Lin, J. Y., Pitman-Crawford, J. L., Bibby, A. H., Hudson, N. L., McIntosh, C. J., Juengel, J. L., and McNatty, K. P. (2012) Effects of species differences on oocyte regulation of granulosa cell function. *Reproduction* **144**, 557–567
35. Galloway, S. M., McNatty, K. P., Cambridge, L. M., Laitinen, M. P., Juengel, J. L., Jokiranta, T. S., McLaren, R. J., Luiro, K., Dodds, K. G., Montgomery, G. W., Beattie, A. E., Davis, G. H., and Ritvos, O. (2000) Mutations in an oocyte-derived growth factor gene (BMP15) cause increased ovulation rate and infertility in a dosage-sensitive manner. *Nat. Genet.* **25**, 279–283
36. Yan, C., Wang, P., DeMayo, J., DeMayo, F. J., Elvin, J. A., Carino, C., Prasad, S. V., Skinner, S. S., Dunbar, B. S., Dube, J. L., Celeste, A. J., and Matzuk, M. M. (2001) Synergistic roles of bone morphogenetic protein 15 and growth differentiation factor 9 in ovarian function. *Mol. Endocrinol.* **15**, 854–866
37. McIntosh, C. J., Lun, S., Lawrence, S., Western, A. H., McNatty, K. P., and Juengel, J. L. (2008) The proregion of mouse BMP15 regulates the cooperative interactions of BMP15 and GDF9. *Biol. Reprod.* **79**, 889–896
38. Mottershead, D. G., Ritter, L. J., and Gilchrist, R. B. (2012) Signalling pathways mediating specific synergistic interactions between GDF9 and BMP15. *Mol. Hum. Reprod.* **18**, 121–128
39. Crawford, J. L., and McNatty, K. P. (2012) The ratio of growth differentiation factor 9: bone morphogenetic protein 15 mRNA expression is tightly co-regulated and differs between species over a wide range of ovulation rates. *Mol. Cell. Endocrinol.* **348**, 339–343
40. Barnett, K. R., Schilling, C., Greenfeld, C. R., Tomic, D., and Flaws, J. A. (2006) Ovarian follicle development and transgenic mouse models. *Hum. Reprod. Update* **12**, 537–555
41. Williams, S. A., and Stanley, P. (2008) Mouse fertility is enhanced by oocyte-specific loss of core 1-derived O-glycans. *FASEB J.* **22**, 2273–2284
42. Edson, M. A., Lin, Y. N., and Matzuk, M. M. (2010) Deletion of the novel oocyte-enriched gene, Gpr149, leads to increased fertility in mice. *Endocrinology* **151**, 358–368
43. Su, W., Qiao, Y., Yi, F., Guan, X., Zhang, D., Zhang, S., Hao, F., Xiao, Y., Zhang, H., Guo, L., et al. (2010) Increased female fertility in aquaporin 8-deficient mice. *IUBMB Life* **62**, 852–857

44. McNeilly, J. R., Watson, E. A., White, Y. A., Murray, A. A., Spears, N., and McNeilly, A. S. (2011) Decreased oocyte DAZL expression in mice results in increased litter size by modulating follicle-stimulating hormone-induced follicular growth. *Biol. Reprod.* **85**, 584–593
45. Cui, L. L., Yang, G., Pan, J., and Zhang, C. (2011) Tumor necrosis factor α knockout increases fertility of mice. *Theriogenology* **75**, 867–876
46. Pelosi, E., Omari, S., Michel, M., Ding, J., Amano, T., Forabosco, A., Schlessinger, D., and Ottolenghi, C. (2013) Constitutively active Foxo3 in oocytes preserves ovarian reserve in mice. *Nat. Commun.* **4**, 1843
47. Langhammer, M., Michaelis, M., Hoeflich, A., Sobczak, A., Schoen, J., and Weitzel, J. M. (2014) High-fertility phenotypes: two outbred mouse models exhibit substantially different molecular and physiological strategies warranting improved fertility. *Reproduction* **147**, 427–433
48. Shi, S., Williams, S. A., Seppo, A., Kurniawan, H., Chen, W., Ye, Z., Marth, J. D., and Stanley, P. (2004) Inactivation of the Mgat1 gene in oocytes impairs oogenesis, but embryos lacking complex and hybrid N-glycans develop and implant. *Mol. Cell. Biol.* **24**, 9920–9929
49. Williams, S. A., Xia, L., Cummings, R. D., McEver, R. P., and Stanley, P. (2007) Fertilization in mouse does not require terminal galactose or N-acetylglucosamine on the zona pellucida glycans. *J. Cell Sci.* **120**, 1341–1349
50. Whitten, W. K. (1956) Modification of the oestrous cycle of the mouse by external stimuli associated with the male. *J. Endocrinol.* **13**, 399–404
51. Whitten, W. K. (1959) Occurrence of anoestrus in mice caged in groups. *J. Endocrinol.* **18**, 102–107
52. Batista, F., Lu, L., Williams, S. A., and Stanley, P. (2012) Complex N-glycans are essential, but core 1 and 2 mucin O-glycans, O-fucose glycans, and NOTCH1 are dispensable, for mammalian spermatogenesis. *Biol. Reprod.* **86**, 179
53. Nelson, J. F., Felicio, L. S., Randall, P. K., Sims, C., and Finch, C. E. (1982) A longitudinal study of estrous cyclicity in aging C57BL/6J mice: I. Cycle frequency, length and vaginal cytology. *Biol. Reprod.* **27**, 327–339
54. Murray, A. A., Swales, A. K., Smith, R. E., Molinek, M. D., Hillier, S. G., and Spears, N. (2008) Follicular growth and oocyte competence in the in vitro cultured mouse follicle: effects of gonadotrophins and steroids. *Mol. Hum. Reprod.* **14**, 75–83
55. Pedersen, T., and Peters, H. (1968) Proposal for a classification of oocytes and follicles in the mouse ovary. *J. Reprod. Fertil.* **17**, 555–557
56. Cai, J. H., Deng, S., Kumpf, S. W., Lee, P. A., Zagouras, P., Ryan, A., and Gallagher, D. S. (2007) Validation of rat reference genes for improved quantitative gene expression analysis using low density arrays. *Biotechniques* **42**, 503–512
57. Hernandez Gifford, J. A., Hunzicker-Dunn, M. E., and Nilson, J. H. (2009) Conditional deletion of beta-catenin mediated by Amhr2cre in mice causes female infertility. *Biol. Reprod.* **80**, 1282–1292
58. McNatty, K. P., Galloway, S. M., Wilson, T., Smith, P., Hudson, N. L., O'Connell, A., Bibby, A. H., Heath, D. A., Davis, G. H., Hanrahan, J. P., and Juengel, J. L. (2005) Physiological effects of major genes affecting ovulation rate in sheep. *Genet. Sel. Evol.* **37** (Suppl 1), S25–S38
59. Schwartz, N. B. (1974) The role of FSH and LH and of their antibodies on follicle growth and on ovulation. *Biol. Reprod.* **10**, 236–272
60. Dorrington, J. H., McKeracher, H. L., Chan, A. K., and Gore-Langton, R. E. (1983) Hormonal interactions in the control of granulosa cell differentiation. *J. Steroid Biochem.* **19**(1A), 17–32
61. Hirshfield, A. N., and Midgley, A. R., Jr. (1978) Morphometric analysis of follicular development in the rat. *Biol. Reprod.* **19**, 597–605
62. Slot, K. A., Voorendt, M., de Boer-Brouwer, M., van Vugt, H. H., and Teerds, K. J. (2006) Estrous cycle dependent changes in expression and distribution of Fas, Fas ligand, Bcl-2, Bax, and pro- and active caspase-3 in the rat ovary. *J. Endocrinol.* **188**, 179–192
63. Seifer, D. B., and Merhi, Z. (2014) Is AMH a regulator of follicular atresia? [E-pub ahead of print] *J. Assist. Reprod. Genet.*
64. Wang, X. L., Wang, K., Zhao, S., Wu, Y., Gao, H., and Zeng, S. M. (2013) Oocyte-secreted growth differentiation factor 9 inhibits BCL-2-interacting mediator of cell death-extra long expression in porcine cumulus cell. *Biol. Reprod.* **89**, 56
65. Baker, S. J., and Spears, N. (1999) The role of intra-ovarian interactions in the regulation of follicle dominance. *Hum. Reprod. Update* **5**, 153–165
66. Vitt, U. A., Hayashi, M., Klein, C., and Hsueh, A. J. (2000) Growth differentiation factor-9 stimulates proliferation but suppresses the follicle-stimulating hormone-induced differentiation of cultured granulosa cells from small antral and preovulatory rat follicles. *Biol. Reprod.* **62**, 370–377
67. Otsuka, F., McTavish, K. J., and Shimasaki, S. (2011) Integral role of GDF-9 and BMP-15 in ovarian function. *Mol. Reprod. Dev.* **78**, 9–21
68. Reader, K. L., Heath, D. A., Lun, S., McIntosh, C. J., Western, A. H., Littlejohn, R. P., McNatty, K. P., and Juengel, J. L. (2011) Signalling pathways involved in the cooperative effects of ovine and murine GDF9+BMP15-stimulated thymidine uptake by rat granulosa cells. *Reproduction* **142**, 123–131
69. McIntosh, C. J., Lawrence, S., Smith, P., Juengel, J. L., and McNatty, K. P. (2012) Active immunization against the pro-regions of GDF9 or BMP15 alters ovulation rate and litter size in mice. *Reproduction* **143**, 195–201
70. Peng, J., Li, Q., Wigglesworth, K., Rangarajan, A., Kattamuri, C., Peterson, R. T., Eppig, J. J., Thompson, T. B., and Matzuk, M. M. (2013) Growth differentiation factor 9:bone morphogenetic protein 15 heterodimers are potent regulators of ovarian functions. *Proc. Natl. Acad. Sci. USA* **110**, E776–E785
71. Orisaka, M., Orisaka, S., Jiang, J. Y., Craig, J., Wang, Y., Kotsuji, F., and Tsang, B. K. (2006) Growth differentiation factor 9 is anti-apoptotic during follicular development from preantral to early antral stage. *Mol. Endocrinol.* **20**, 2456–2468
72. Otsuka, F., Yamamoto, S., Erickson, G. F., and Shimasaki, S. (2001) Bone morphogenetic protein-15 inhibits follicle-stimulating hormone (FSH) action by suppressing FSH receptor expression. *J. Biol. Chem.* **276**, 11387–11392
73. Welt, C. K., and Schneyer, A. L. (2001) Differential regulation of inhibin B and inhibin a by follicle-stimulating hormone and local growth factors in human granulosa cells from small antral follicles. *J. Clin. Endocrinol. Metab.* **86**, 330–336

Received for publication April 10, 2014.
Accepted for publication September 24, 2014.